



The University of
Nottingham

KINETIC STUDIES OF COPPER-CATALYSED
CONJUGATE ADDITION REACTIONS WITH
ORGANOALUMINIUM REAGENTS AND THEIR
IMPLEMENTATION TOWARDS ENANTIOSELECTIVE
SYNTHESIS OF QUINOLONE DERIVATIVES

A thesis submitted to The University of Nottingham for the degree of
Doctor of Philosophy
in the Faculty of Science

2018

Alexander Kingsbury
School of Chemistry

Contents

| | |
|--|------------|
| Abstract | 3 |
| Acknowledgements | 4 |
| Abbreviations | 5 |
| SECTION 1 | 9 |
| 1.1 Introduction | 10 |
| 1.1.1 Introduction to Conjugate Addition Chemistry | 10 |
| 1.1.2 Organometallic Reagents in Conjugate Addition Chemistry | 12 |
| 1.1.3 Analysis of Catalytic Systems Using Copper Catalysts and Kinetic Studies into Conjugate Addition Chemistry | 17 |
| 1.2 Project Aims | 36 |
| 1.3 Results and Discussion | 37 |
| 1.3.1 Methodology Development | 37 |
| 1.3.2 Establishing the Rate Equation | 45 |
| 1.3.3 Proposal of the Mechanistic Pathway | 49 |
| 1.4 Conclusions..... | 55 |
| 1.5 Future Work | 57 |
| SECTION 2 | 59 |
| 2.1 Introduction | 60 |
| 2.1.1 Introduction to Quinolones | 60 |
| 2.1.2 The Synthesis of Quinolones and Their Derivatives..... | 62 |
| 2.1.3 General Synthetic Routes to Racemic and Enantioenriched sp^3 -Hybridised Quinolone Derivatives..... | 68 |
| 2.1.4 Synthetic Routes to Racemic and Enantioenriched sp^3 -Hybridised Quinolone Derivatives Using Conjugate Addition Chemistry | 74 |
| 2.2 Project Aims | 81 |
| 2.3 Results and Discussion | 82 |
| 2.3.1 Synthesis of Unsubstituted Quinolone Substrate Cores and Organometallic Addition..... | 82 |
| 2.3.2 Synthesis of Quinolone Carboxylate Substrate and Organometallic Addition. | 91 |
| 2.3.3 Ligand optimisation and Scope Analysis..... | 96 |
| 2.3.4 Diversification of Enantioenriched Products | 104 |
| 2.4 Conclusions..... | 108 |
| 2.5 Future Work | 110 |
| 3.1 Supplementary Information | 114 |
| 3.1.1 General Information and Specifications for Kinetic Studies | 114 |
| 3.1.2 Reagent Order Determination in Kinetic Studies | 115 |

| | | |
|----------|--|------------|
| 3.1.3 | General Information and Specifications for Quinolone Conjugate Addition Reactions..... | 117 |
| 3.1.4 | Experimental Data..... | 118 |
| 4 | References..... | 195 |

Abstract

Conjugate addition reactions with organometallic reagents have been extensively utilised in the synthesis of a wide range of diverse molecules. Despite this, certain phenomena regarding the mechanistic pathway of the reaction remain unexplored. As such, challenges associated with certain synthetic transformations involving this class of reaction require extensive research to expand our understanding on a molecular level and implement this understanding in a functional capacity.

Here we present studies involving the elucidation of the mechanistic pathway for copper-catalysed conjugate reactions of organoaluminium reagents. This involved detailed kinetic studies concerning the formation of an active complex between an α,β -unsaturated enone and triethylaluminium, its involvement in the formation of a proposed transition state for the conjugate addition reaction and discovering the stoichiometry of this transition state.

Additionally, the development of a methodology towards the enantioselective copper-catalysed conjugate addition of organoaluminium reagents to quinolone substrates was performed in efforts to access a series of diverse, biologically-active scaffolds. The primary aim was to perform addition with alkyl- and alkenylaluminium reagents to these quinolone substrates; these would afford novel products which have not been synthesised with existing methodology.

Acknowledgements

First and foremost, I would like to thank Simon, for his continuous advice and support during my studies. The enthusiasm for the project and for chemistry as a discipline in itself was infectious and inspiring and has left its indelible mark upon me.

I would also like to thank the members of the Woodward research group, past and present, for providing a warm and pleasant atmosphere in which to work. Particular thanks go to John, Lee and Ryan who collectively and individually helped me through numerous challenges with support, warmth, but mostly puns. Without these people being there each day, the journey would have been considerably more difficult and far less enjoyable.

I would like to thank my family for their love and support. Even from a distance, they still managed to be a constant, reassuring presence in times of hardship as well as sharing my happiness in times of success. I will forever be grateful for the time and opportunities their efforts have afforded me.

My secondary school chemistry teachers, Dr. Taylor and Dr. Neave, your encouragement was not for nought! Frustrating as I am sure it was to teach me at times, it was your combined patience and enthusiasm that set me on the path I took.

Lastly, I would like to thank my fiancée, Becky. At what was possibly my lowest ebb, you and the boys came into my life and transformed it beyond all recognition. I never could have hoped for such a ray of sunshine to illuminate my world at its darkest. I can only hope that the rest of our lives are filled with the same bliss and wonder that have filled every moment we have spent together so far.

To these people, and many more, I owe so much. Thank you.

Abbreviations

| | |
|--------------------|---|
| \propto | ...is directly proportionate to... |
| 1D | One-dimensional |
| 2D | Two-dimensional |
| 5-HT | 5-Hydroxytryptamine |
| Å | Ångström (10^{-10} m) |
| A.U. | Absorbance Units |
| ACA | Asymmetric conjugate addition |
| Alloc | Allyloxycarbonyl |
| Ar | Aryl |
| BINAP | 2,2'-Bis(diphenylphosphino)-1,1'-binaphthyl |
| BINOL | 1,1'-Bi-2-naphthol |
| BMIM | 1-Butyl-3-methylimidazolium |
| Bn | Benzyl |
| Boc | Tertiary Butyloxycarbonyl |
| Bu | Butyl |
| Cbz | Benzyloxycarbonyl |
| Chirasil dex-CB | Cyclodextrin column bound to dimethylpolysiloxane |
| cm^{-1} | Wavenumber |
| Conv. | Conversion |
| Cp | Cyclopentadiene |
| cp* | Oxidised ferrocene-cyclopentadiene |
| Cp* | Pentamethylcyclopentadiene |
| Cy | Cyclohexyl |
| dba | Dibenzylideneacetone |

| | |
|------------------|---|
| DFT | Density functional theory |
| dm | Decimetre(s) |
| DMEDA | <i>N,N</i> -Dimethylethylenediamine |
| DMF | <i>N,N</i> -Dimethylformamide |
| DMSO | Dimethyl sulfoxide |
| DNA | Deoxyribosenucleic acid |
| dr | Diastereomeric ratio |
| ee | Enantiomeric excess |
| EPR | Electron Paramagnetic Resonance |
| Et | Ethyl |
| EWG | Electron-withdrawing group |
| GC | Gas chromatography |
| h | Hour(s) |
| HMBC | Heteronuclear Multiple Bond Correlation |
| HPLC | High performance liquid chromatography |
| Hz | Hertz |
| iBu | Isobutyl |
| IC ₅₀ | Half maximum inhibitory concentration |
| iPr | Isopropyl |
| IR | Infrared (spectroscopy) |
| <i>J</i> | Coupling constant |
| JosiPhos | (2 <i>R</i>)-1-[(1 <i>R</i>)-1-(Dicyclohexylphosphino)ethyl]-2-(diphenylphosphino)ferrocene |
| <i>K</i> | Equilibrium constant |
| <i>k</i> | Rate constant |
| kcal | Kilocalorie(s) |

| | |
|--------|-------------------------------|
| kJ | Kilojoule(s) |
| Me | Methyl |
| min. | Minute(s) |
| mM | Millimolar |
| mmol | Millimole(s) |
| mol | Mole(s) |
| mT | Millitesla |
| MW | Microwave |
| nBu | Linear butyl |
| NMR | Nuclear Magnetic Resonance |
| Np | Naphthyl |
| nPr | Linear propyl |
| OAc | Acetate |
| OTf | Trifluoromethanesulfonate |
| Ph | Phenyl |
| Pn | Pentyl |
| PPA | Polyphosphoric acid |
| ppm | Parts per million |
| Pr | Propyl |
| R | Alkyl |
| r.d.s. | Rate-determining step |
| r.t. | Room temperature |
| R^2 | Co-efficient of determination |
| RTIL | Room temperature ionic liquid |
| s | Second(s) |

| | |
|-------------|---|
| <i>t</i> | Time |
| <i>T</i> | Temperature |
| TADDOL | $\alpha,\alpha,\alpha',\alpha'$ -Tetramethyl-2,2-disubstituted 1,3-dioxolane-4,5-dimethanol |
| TaniaPhos | (<i>R_P</i>)-1-Dicyclohexylphosphino-2-[(<i>R</i>)- α -(dimethylamino)-2-(dicyclohexylphosphine)benzyl]ferrocene |
| TBA | Tetrabutylammonium |
| tBu | Tertiary Butyl |
| TC | Thiophene-2-carboxylate |
| TEMPO | 2,2,6,6-Tetramethyl-1-piperidinyloxy free radical |
| <i>tert</i> | Tertiary |
| THF | Tetrahydrofuran |
| TIPS | Triisopropylsilyl |
| TM | Trademark |
| TMS | Trimethylsilyl |
| ΔG | Gibbs' free energy |
| μ | Bridging (ligand) |

SECTION 1

KINETIC STUDIES OF COPPER-CATALYSED CONJUGATE ADDITION REACTION WITH ORGANOALUMINIUM REAGENTS

This work has been published in a peer-reviewed journal:

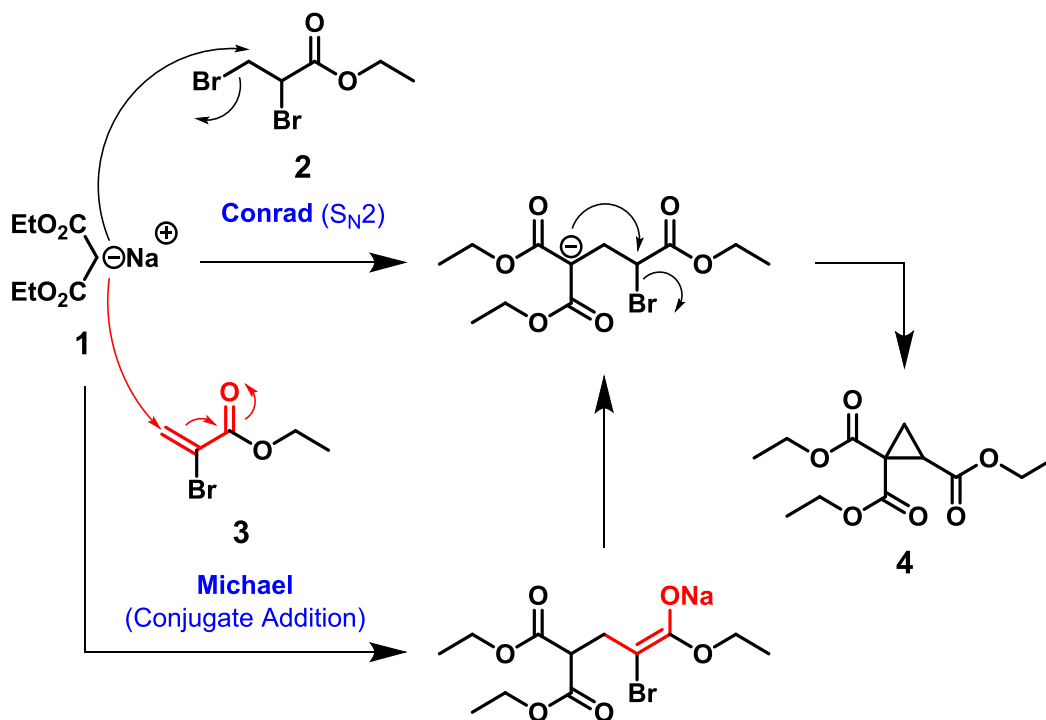
“Kinetic Analysis of Copper(I)/Feringa-Phosphoramidite Catalysed AlEt_3 1,4-Addition to Cyclohex-2-en-1-one”

Willcox, D., Nouch, R., Kingsbury, A., Robinson, D., Carey, J., Brough, S., Woodward, S., *ACS Catal.* **2017**, 7, 6901

1.1 Introduction

1.1.1 Introduction to Conjugate Addition Chemistry

Conjugate addition chemistry was originally discovered by Michael and co-workers in 1887.¹ This discovery was based on an observation he made concerning a reaction performed three years earlier by Conrad *et al.* which afforded triethyl cyclopropane-1,1,2-tricarboxylate **4** (Scheme 1).²



Scheme 1 Conrad and Michael's synthetic routes and proposed mechanistic pathways for the formation of compound **4**

The reaction of ethyl 2,3-dibromopropionate **2** with sodium diethyl malonate salt **1** proceeded as expected via S_N2 displacement of the primary alkyl bromide followed by a second S_N2 displacement of the secondary alkyl bromide on the adjacent carbon atom; the subsequent ring closure formed compound **4** as predicted. Michael's observation was that the same product was afforded when ethyl 2-bromoacrylate **3** was incorporated in the reaction in place of the dibromide. Michael's rationale was that a different mechanistic pathway must be followed for this reaction based on the conjugated system within compound **3**. The reaction of an enolate species with the conjugated α,β-unsaturated enone system now bears his name; it represents the first example of a reaction within the broader conjugate addition – or 1,4-addition – reaction class.

Naturally, numerous developments and modifications were made to this reaction; as well as enolate nucleophiles, a wide range of heteroatomic and organometallic nucleophiles were also available for similar transformations. As such, the scope for this reaction increased at an astonishing rate and the array of novel molecules now available *via* this methodology expanded exponentially over the following years. This was further accentuated by the facile synthetic incorporation of the necessary functional group required for this reaction accompanied by its existence in various compounds in nature.

1.1.2 Organometallic Reagents in Conjugate Addition Chemistry

While enolates used in Michael addition reactions are popular nucleophiles due to their capacity for forming carbon-carbon bonds, organometallic reagents can also carry out this process and function as a more variable source of alkyl, alkenyl, alkynyl and aryl nucleophiles. The initial syntheses and subsequent development of these reagents occurred over a time period during which Michael's discovery was made with the discovery and utilisation of organozinc, organoaluminium, organoindium and organomagnesium reagents by various researchers.³⁻⁶ The primary issue that was encountered for this transformation was the regioselectivity of the reaction between the α,β -unsaturated enone and the organometallic reagent (Figure 1).

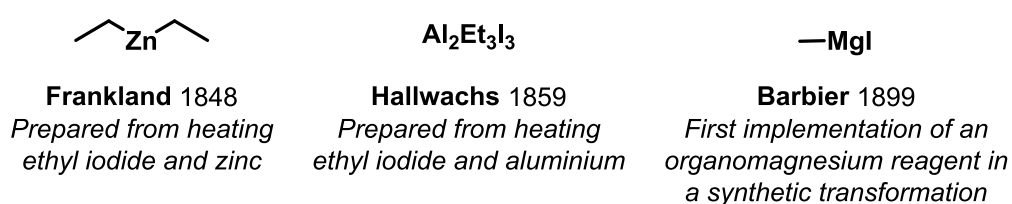


Figure 1 Preparation and utilisation of organometallic reagents

Kharasch and co-workers found that the incorporation of various Lewis acids within the reaction between methylmagnesium bromide and isophorone **5** drastically affected the yields of the isolated products as well as the proportions of the products afforded (Table 1).⁷

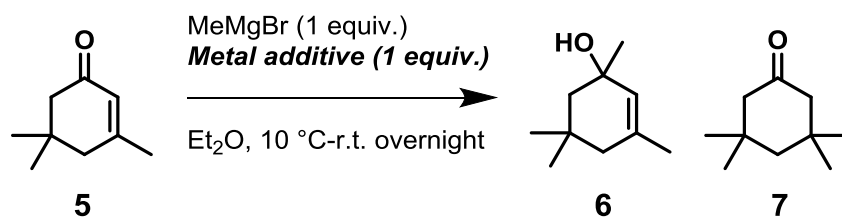


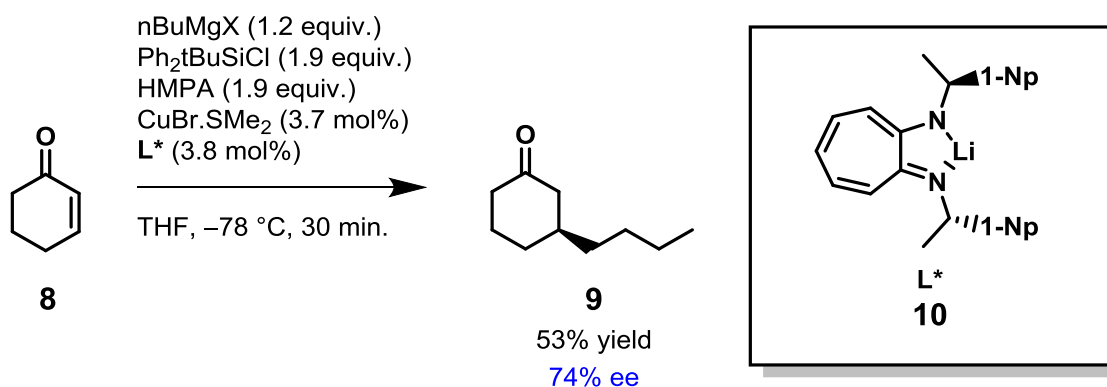
Table 1 Kharasch *et al.* yields of afforded products for metal-catalysed Grignard additions to isophorone 5

| Entry | Metal additive | Yield of 6 (%) (1,2-addition) | Yield of 7 (%) (1,4-addition) |
|-------|-------------------|----------------------------------|----------------------------------|
| 1 | None | 43 | - |
| 2 | NiCl ₂ | 23 | 5 |
| 3 | AgCl | 35 | - |
| 4 | CrCl ₃ | 27 | - |
| 5 | VCl ₂ | 57 | - |
| 6 | MnCl ₂ | 29 | - |
| 7 | CuCl | - | 83 |

Addition of a stoichiometric amount of copper (I) chloride to the reaction mixture saw a shift in the regioselectivity of the nucleophilic addition (Entry 7, Table 1); where no conversion to compound 7 via 1,4-addition was observed in the majority of examples and only negligible conversion in this manner for a select few cases, 1,4-addition overwhelmingly predominated with a copper catalyst. Further investigations by Gilman and co-workers led to the discovery of organocuprates; these alkylcopper species were softer nucleophiles and the transmetalation of hydrocarbon functional groups from a pre-existing organometallic species to catalytic copper enabled consistent regioselective 1,4-addition to α,β -unsaturated enones.⁸ Consequently, these reagents have also been implemented in this class of reaction with remarkable success, highlighted in many reviews describing their reactivity.⁹

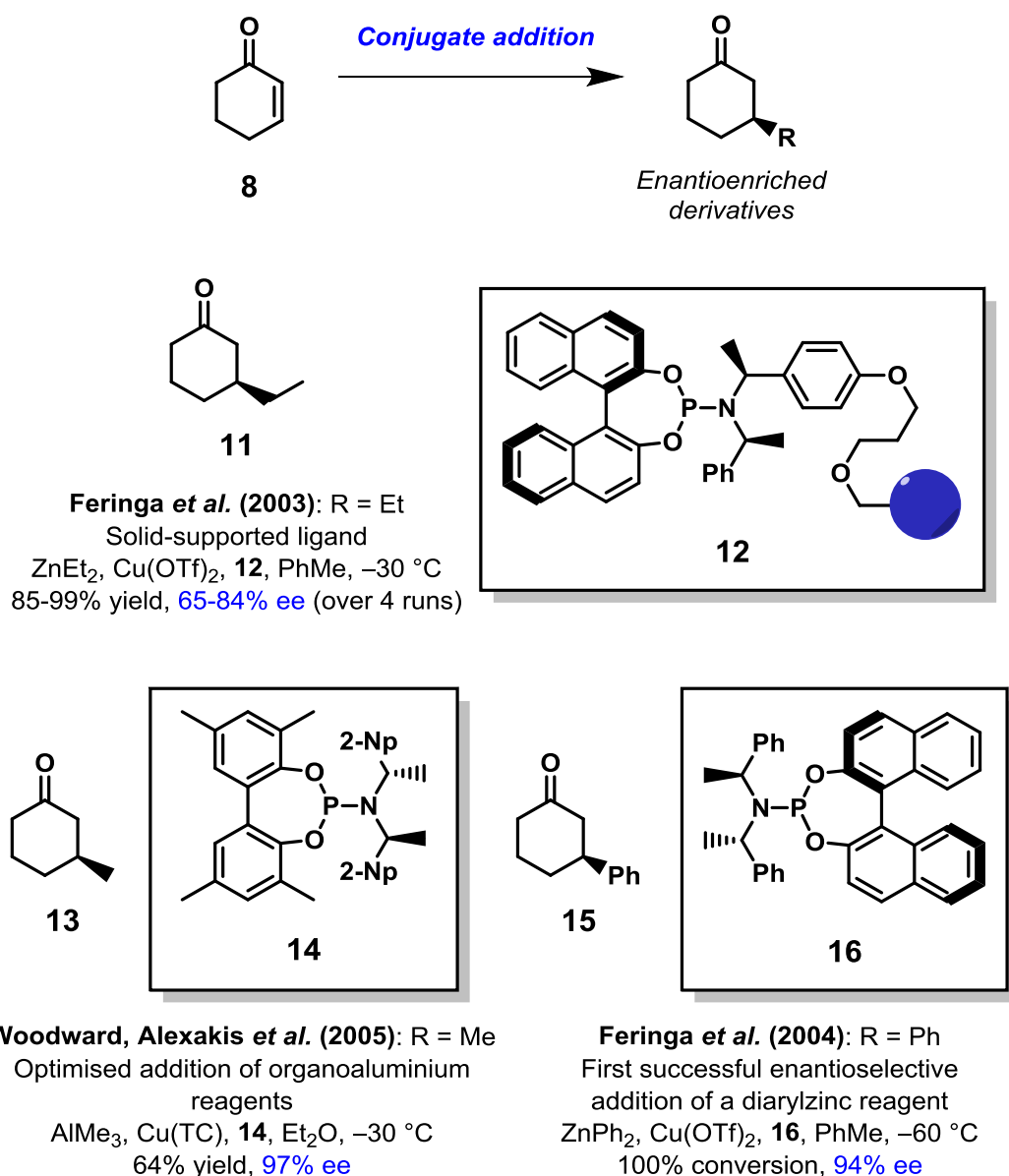
The prochiral nature of the reactive centre for conjugate addition chemistry within the α,β -unsaturated enone functional group lends itself to the development of methodology towards enantioselective elaboration of these molecules. The first example of this transformation was conducted by Lippard and co-workers in 1990 where successful

addition of *n*-butylmagnesium chloride to 2-cyclohexenone **8** was performed enantioselectively forming (*S*)-3-*n*-butylcyclohexanone **9** in 74% ee (Scheme 2).¹⁰



Scheme 2 Lippard *et al.* the first enantioselective metal catalysed conjugate addition reaction

Numerous examples of complementary enantioselective adaptations to this reaction with differing substrates, organometallics, copper catalysts and ligands have been performed in the wake of this discovery, highlighting not only the versatility of the reaction itself, but the breadth in application for a range of different reagents. 2-Cyclohexenone **8** is a commonly used substrate for the study of enantioselective conjugate additions of organometallics, with many different classes of organometallic reagents used for its successful enantioselective elaboration (Scheme 3).^{11–13}



Scheme 3 Examples of successful enantioselective conjugate additions with organometallic reagents; blue circle in compound **12** represents solid supported reagent

While the reaction itself has been implemented on many occasions affording desirable enantioenriched derivatives of compound **8** amongst countless others, knowledge regarding the reaction on a kinetic level has not been studied in great depth; only a small number examples exist in the literature at the time this thesis was written. With the growing number of successful developments to the methodology in this area, research into the reaction itself and its mechanistic pathway may illuminate factors that have previously inhibited the efficacy of the reaction whilst also elucidating aspects that can improve the transformation. Continuing studies into copper catalysed organometallic conjugate addition reactions – with which the described work is

associated – hope to elucidate certain phenomena regarding the reaction profile and hence improve future reaction optimisations based on an established foundation of research.

1.1.3 Analysis of Catalytic Systems Using Copper Catalysts and Kinetic Studies into Conjugate Addition Chemistry

Kinetic analysis of reactions is a heavily researched discipline; indeed, investigations into optimising the method in which this research area is explored have been examined, critically evaluated and developed to improve the quality of research.¹⁴ The ability to dissect the minutiae of a reaction and deconstruct it such that each fundamental step of a mechanism can be understood affords the possibility of potentially boundless exploitation of the studied reaction. With developments in computational studies and capabilities for the evaluation of theoretical molecular ground states and transition states over the years, perceived axiomatic truths can be reinforced, scrutinised or even debunked to the benefit of both the chemical and scientific communities.

Developments in copper catalysis and the unceasing exploration of its potential lead to the inevitable need to understand the complexities of the transformations. As such, a vast array of different methodologies to decipher the mysteries of copper on both structural and reactive levels have been performed to better comprehend its chemical processes. Copper catalysed reactions using organometallics exhibit unique features due to the nature of these reagents such as their intrinsic reductive properties or their tendency to behave as Lewis acids. However, the sensitivity of these reagents to air, moisture and heat means vigilance must be exercised to ensure their stability during any undertaken analysis; this inhibits the scope of analytical methods available for studying them, though studies can be both thorough in their exploration and fruitful in the knowledge acquired.

The combination of organometallic reagents and stoichiometric copper salts is known to form organocuprates, as described in the aforementioned work by Gilman, though catalytic copper also encourages the same reactivity.⁸ The use of copper appeals due to its tolerance for a broad range of functional groups and demonstrably high regio- and stereoselectivity of the reactions in which it is used. These features have made this class of reagents highly popular in enantioselective carbon-carbon bond formation.^{15,16} The interaction between organocuprates and various substrates will affect the reactivity of these species; successful reactions require the binding of the organocuprate species to a π -system within the substrate molecule. While these transition states were believed to be short-lived as well as extremely sensitive to external stimuli, isolation and characterisation of these systems has been successfully performed. One notable example was the isolation and recrystallisation of a cuprate-

carbonyl π -complex **18** of lithium dimethylcuprate and 9-fluorenone **17** by Ogle and co-workers in 2013; while NMR spectroscopic studies suggested this structure existed within the reaction mixture, its unusual stability facilitated the production of high quality crystals enabling X-ray crystallographic data to be obtained (Figure 2).¹⁷

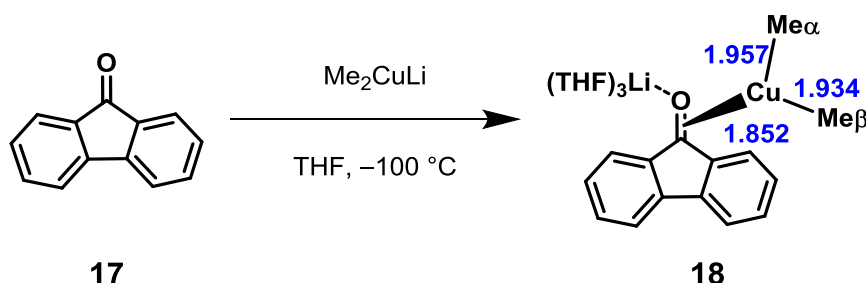


Figure 2 Ogle *et al.* isolated cuprate-carbonyl π -complex

This was the first and only (as of the commencement of writing this thesis) example of an isolated copper-carbonyl π -complex; copper π -complexes with carbon-carbon double bonds in conjugate addition reaction systems form the predominant number of those that have been studied and described. Characterised examples showing unequivocal evidence of copper-alkene binding of organocuprates have been performed by Krause and co-workers; the first example used low temperature NMR spectroscopic studies of ^{13}C -labelled enoates and 2-en-4-ynoates to analyse J -coupling constants between atoms and elucidate the copper binding site (Figure 3).¹⁸

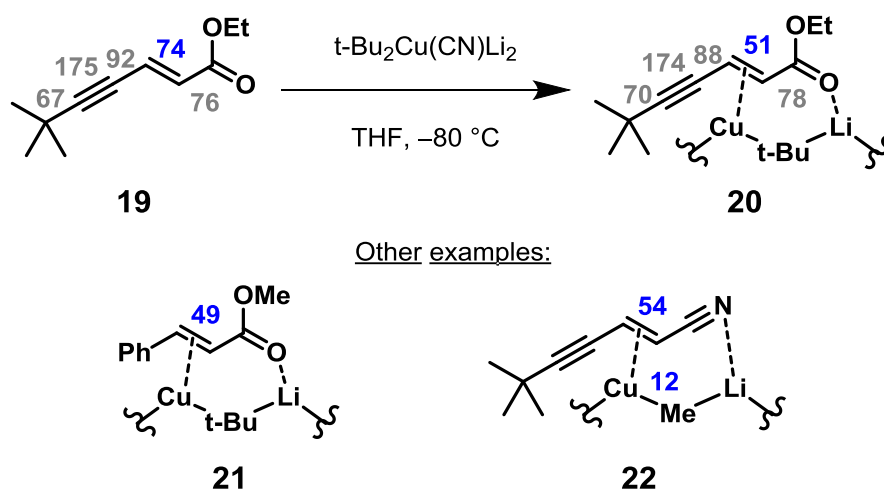


Figure 3 Krause *et al.* copper-alkene binding of organocuprates; $^1J_{CC}$ coupling constants (in Hz) of ^{13}C labelled compounds shown on respective bonds

The decrease in the J -coupling constant between C-2 and C-3 from approximately 70 Hz to approximately 50 Hz – indicative of a single bond between two sp^2 -hybridised carbon atoms - in complexes **20**, **21** and **22** accompanied by the lack of meaningful change in any other J -coupling constants within the respective molecules are indicative of co-ordination of the π -bond between the atoms to the copper centre. This was particularly interesting in the examples of complexes **20** and **22** as it also implied selective binding to the π -system at the alkene in preference to the adjacent alkyne moiety; the proximal nature of the carbonyl group to the alkene is the most likely reason for the selectivity over alkyne binding as it forms a transition state with considerably reduced strain. Another observation that was made was the presence of two distinct methyl-metal carbon species in the ^{13}C NMR spectrum of complex **22** at upfield frequencies of -5.1 and -10.7 ppm; the former was expressed as a singlet whilst the latter displayed a coupling constant of $^2J_{CC} = 12$ Hz to the labelled carbon atom at C-3. The conclusion drawn from this is while two methyl groups are bound to the copper atom in the cuprate species, only one of them is in close enough proximity for addition to occur; this in itself was a momentous step in elucidating structural features of bound organocuprates within reaction systems.

Krause's second success develops on the hypotheses formulated in his first study; dienone **23** was subjected to similar NMR spectroscopic studies in an effort to explain why, in spite of clear evidence to suggest binding to the most proximal double bond in the structure is preferable, 1,6-addition product **24** is formed in almost quantitative yield (Figure 4).¹⁹

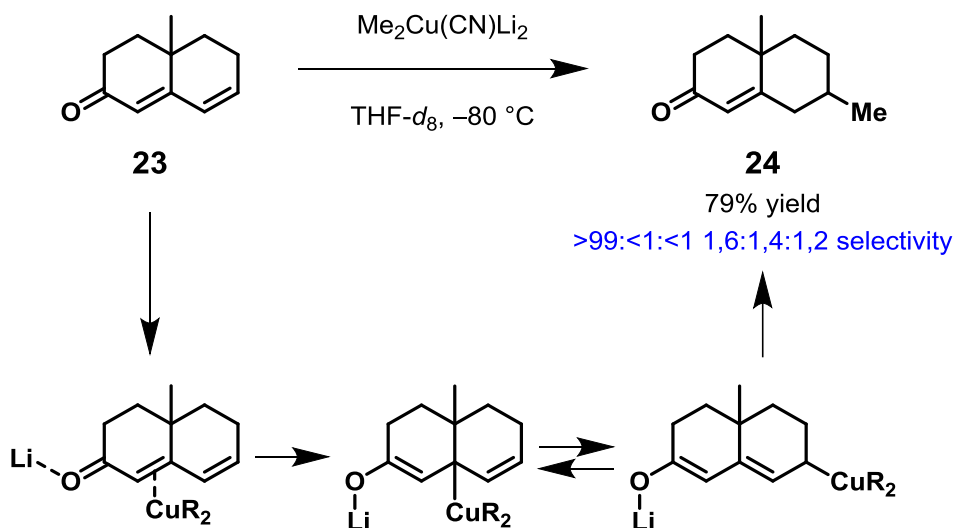


Figure 4 Krause *et al.* 1,6-addition and proposed shuffling mechanism

The proposition made was a shuffling of the conjugated system so that the expected intermediate is converted reversibly to a σ -species which further rearranges to form compound **24** on heating of the sample. Expectations for signals in the ^{13}C NMR spectrum were for unambiguous evidence of a bound copper species as well as the starting material and product peaks; the comparative stability of the intermediate reinforces the notion that this π -complex acts as a key intermediate for addition of organocuprates to conjugated systems. Additionally, the σ -species also acts as a plausible Cu(III) intermediate in the reaction. Subsequent conjugate addition reaction methodology has thus used this structure to rationalise similar reactions undergoing this transformation.

The detection and characterisation of Cu(III) complexes has been achieved using a variety of techniques. Numerous NMR spectroscopic studies attesting to the existence of these species have been performed by Ogle and co-workers regarding cross-coupling reactions involving copper as well as conjugate addition reactions; many different complexes were synthesised and detected within the undertaken experiments.^{20–25} Examples in which Cu(III) complexes were isolated and characterised have also been achieved; Lee and co-workers successfully isolated compound **25** – a trigonal bipyramidal complex – accompanied by extensive computational analysis of the binding of different ligands to the copper centre (Figure 5).²⁶

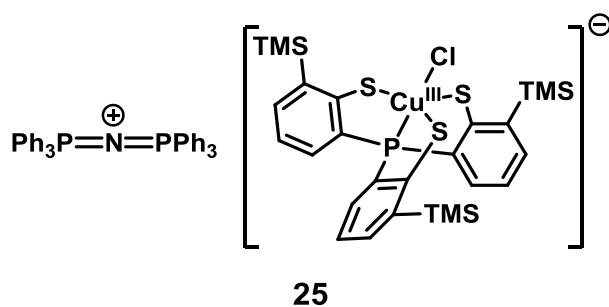


Figure 5 Stable isolable Cu^{III} complex isolated by Lee *et al.*

Further examples of isolated Cu-(III) complexes include compound **26** by Doerrner *et al.* as well as compound **27** by Ribas and co-workers; both of these complexes demonstrate copper centres with square planar geometry (Figure 6).^{27,28}

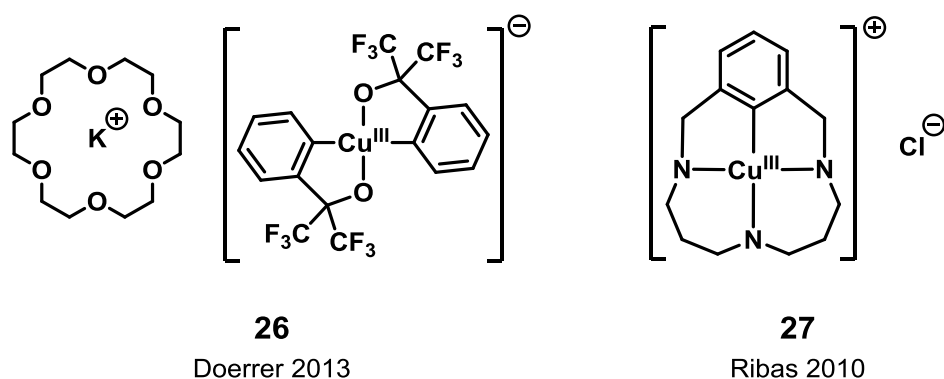
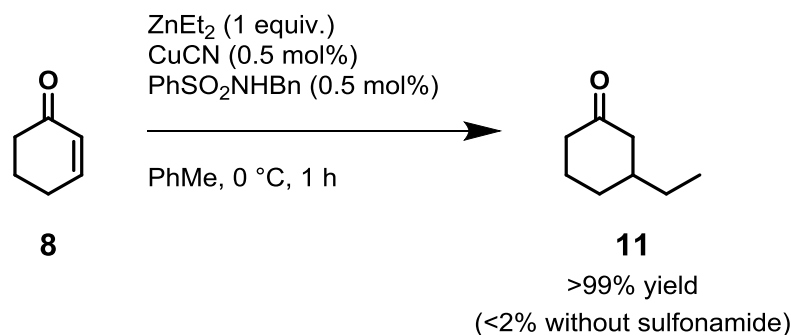


Figure 6 Isolated Cu^{III} complexes

The evidence provided in these bodies of work regarding Cu-(III) species further solidifies the notion that this oxidation state can exist within the conjugate addition pathway, particularly with the results Ogle obtained. With this in mind, experimentally derived mechanisms for this transformation incorporating this species at some stage provide a logical platform from which to develop an understanding of the reaction coordinate.

The solid foundations for kinetic studies to be performed were first explored by Noyori and co-workers in 2000; preliminary kinetic studies on the addition of diethylzinc to 2-cyclohexenone **8** were able to elucidate the order of the reaction with respect to the catalyst and the organometallic reagent, both of which were first order (Scheme 4).²⁹



Scheme 4 Noyori *et al.* reaction scheme for kinetic studies

This study was one of the first of its kind to attempt to unveil the route which conjugate addition reactions follow as well as a rationalisation of its catalytic nature. Unfortunately, only a rudimentary catalytic cycle was proposed based on the findings of this study; further investigation was needed in order to identify the mechanistic pathway (Figure 7). The cycle begins with the transmetalation of one of the alkyl groups on the zinc atom to the copper catalyst bridged by the sulfonamide counteranion forming the catalytic species. This is followed by co-ordination of the enone and a second dialkylzinc species, addition of the alkyl group to the enone substrate and subsequent elimination of the conjugate addition enolate product and reformation of the original copper-zinc bridged catalytic species.

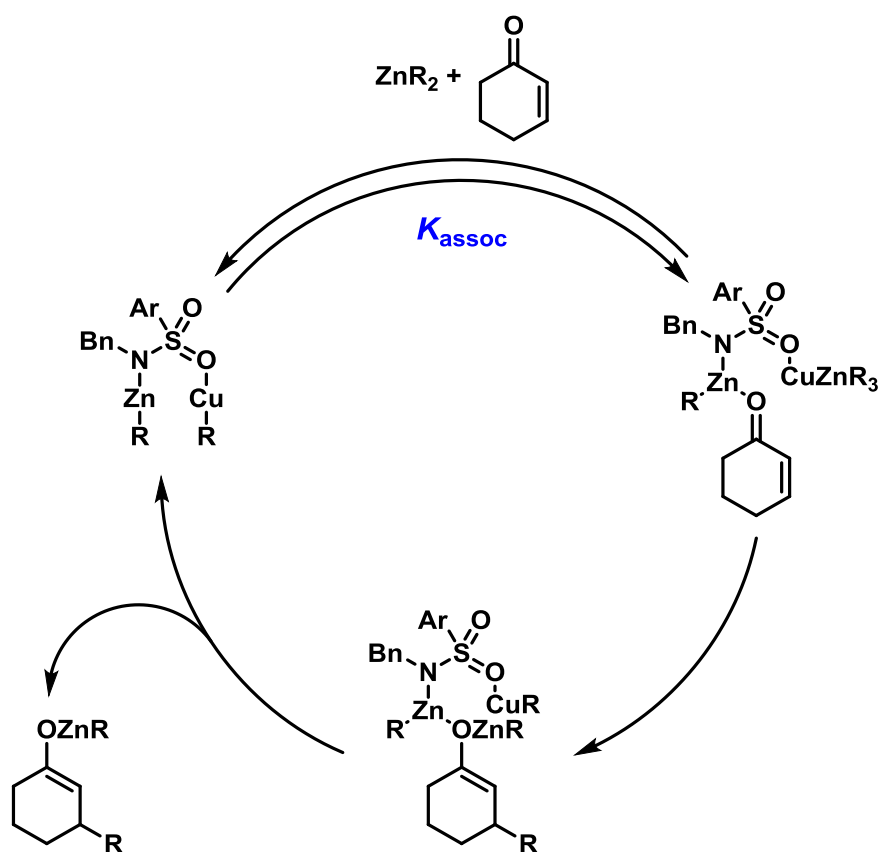


Figure 7 Noyori *et al.* proposed catalytic cycle based on kinetic studies

Developing on the ideas postulated by Noyori, Schrader examined the role which phosphorus-based ligands perform in the same conjugate addition reaction between diethylzinc and 2-cyclohexenone **8**.³⁰ EPR spectra that were obtained for mixtures of Cu(OTf)₂, diethylzinc and a collection of prolinamine based phosphorus-based ligands synthesised for the project as well as others ubiquitous to the field showed the formation of a diamagnetic copper centre over time signified by the disappearances of signals in the spectra; this was believed to be the Cu-(I) species. Addition of the ligand altered the signals, followed by formation of a diamagnetic species over time and disappearance of all signals upon addition of the organometallic reagent. This Cu-(I) species was subsequently used as a focal point around which the mechanistic studies were performed.

In the resulting experimentation, GC analysis was used to show concentrations of the product over the course of the reaction. This method showed the reaction exhibited the same kinetic profile as suggested by Noyori with both the organometallic reagent and copper-ligand species exhibiting first order kinetic behaviour; it also demonstrated a clear effect based on the class of ligand used in the reaction where the reaction rate can be affected by as much as two orders of magnitude based on the ligand structure.

The synthesised ligand from Schrader's research was compared with TADDOL and BINOL based ligands. It should also be noted, however, that numerous issues can be associated with Schrader's work. For example, the internal standard used within the reaction mixture – compound **8** – is known to react with the zinc enolate product from generated in the reaction. This is accompanied by the technical difficulties faced during experimentation involving the failure to adequately quench the extracted aliquot at low temperature. Consequently, further reaction within the aliquot resulting in the generation of spurious results with poor reproducibility. Thus, the collected data, although is able to be fitted to first order behaviour, could easily accommodate a wide range of kinetic rate laws and even reactant orders.

With further evidence of the copper-alkene π -complex being seen in NMR spectroscopic analysis of the reaction, the Cu-(III) intermediate was suggested as an intermediate through which the reaction pathway progressed *via* co-ordination of the catalyst to enone **8** to form species **I** oxidative addition at the reactive centre on species **II** followed by reductive elimination to form the desired product species **III** and regenerate the Cu-(I) catalyst. The final reductive elimination of copper and regeneration of the Cu-(I) catalyst was believed by Schrader to be the rate limiting step in the conjugate addition reaction and was henceforth used to rationalise his conclusions. This is based on literature precedent for preliminary kinetic studies testifying in favour of this pathway for stoichiometric organocuprates (Figure 8).^{31,32}

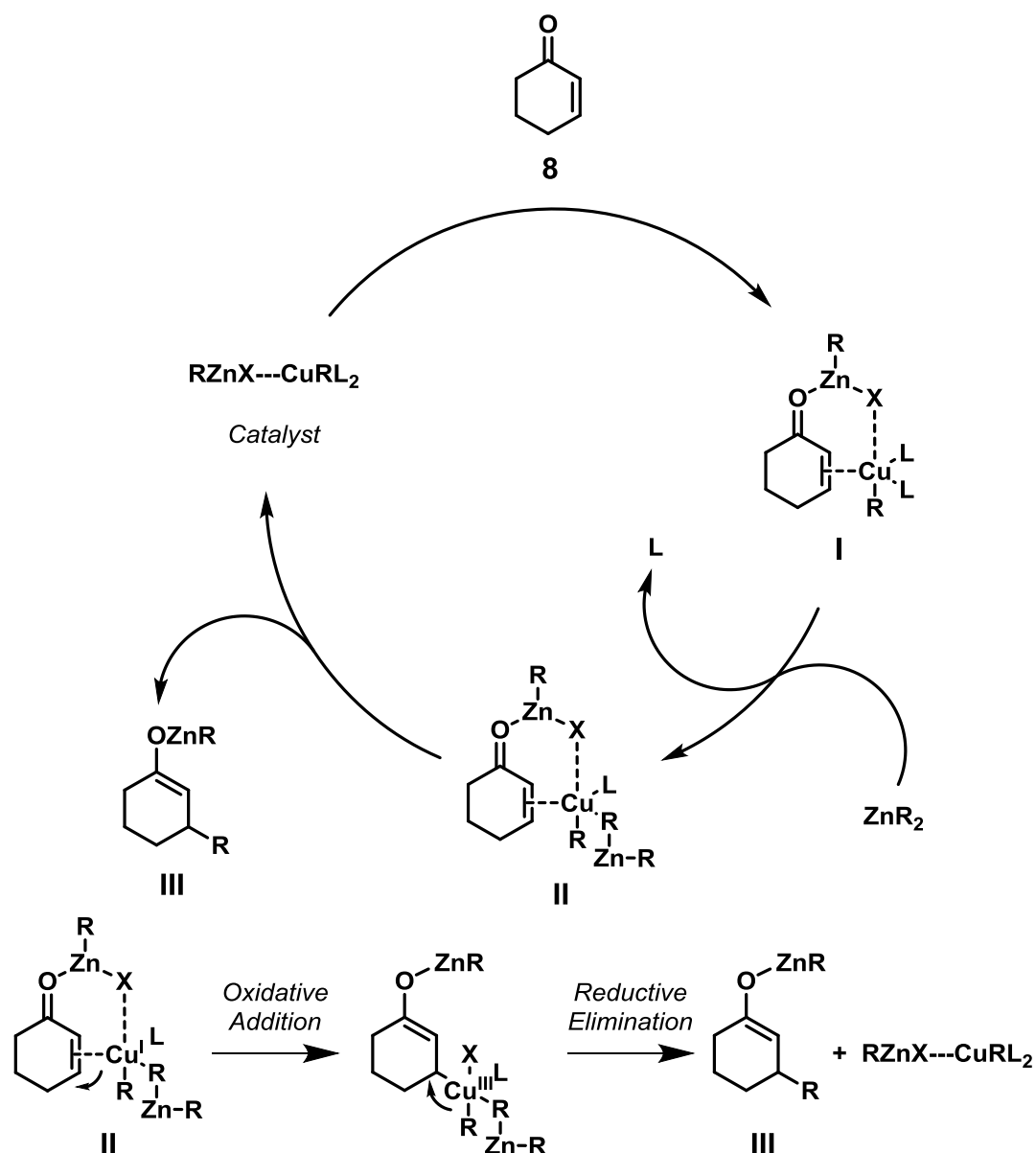
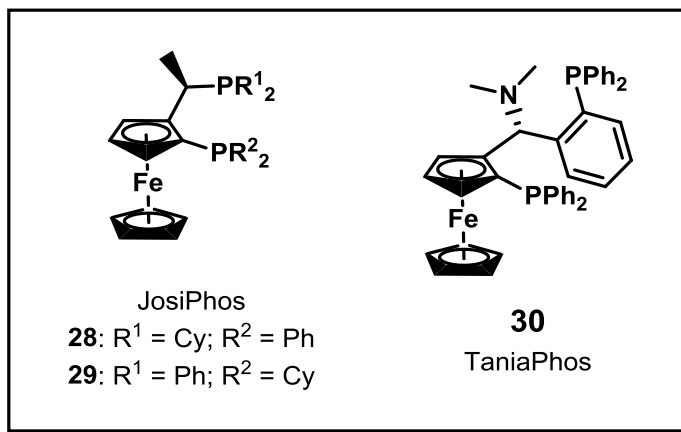
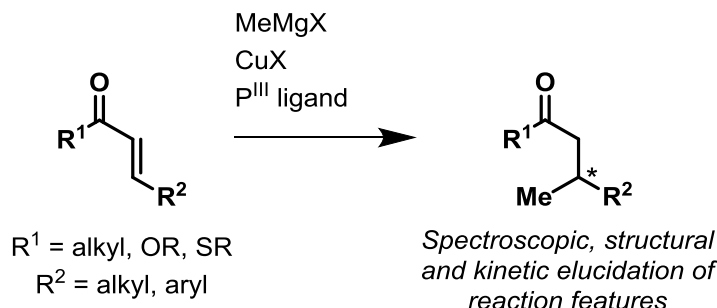


Figure 8 Proposed catalytic cycle and rationale for Cu-(III) intermediate during conjugate addition process

The results obtained in these experiments, despite their deficiencies, became the cornerstone for understanding the kinetic profile of copper catalysed conjugate reactions and acted as a springboard for further investigation. Subsequent studies used many of Schrader's postulated ideas as foundations upon which to build and develop new hypotheses regarding the reaction.

Following on from Schrader's work, Feringa and co-workers conducted profound research into an analogous reaction using methylmagnesium bromide as the organometallic reagent; despite the versatility and ubiquity of these reagents, research into the kinetic profile of conjugate addition reactions involving organomagnesiums and

other organometallic reagents apart from alkylzincs was conspicuous in its absence.³³ Air stable Josiphos-ligands **28** and **29** as well as TaniaPhos ligand **30** were used in conjunction with copper bromide-dimethyl sulphide complex to elucidate structural details of the pre-catalyst alongside its role within the catalytic cycle (Scheme 5).



Scheme 5 Feringa *et al.* reaction scheme for kinetic studies

The effect of the solvent on the formation of the pre-catalyst was examined. X-ray crystallographic data of material isolated from mixtures of the copper salt and Josiphos ligand displayed clear structural differences: highly polar solvents favoured a mononuclear complex structure **31**, while halogenated and ethereal solvents – generally more conducive to successful organometallic conjugate reactions – exhibited a dinuclear structure **32** (Figure 9). Interconversion between the two structures was also observed by Feringa and co-workers upon addition of a solvent different polarity to either mixture.

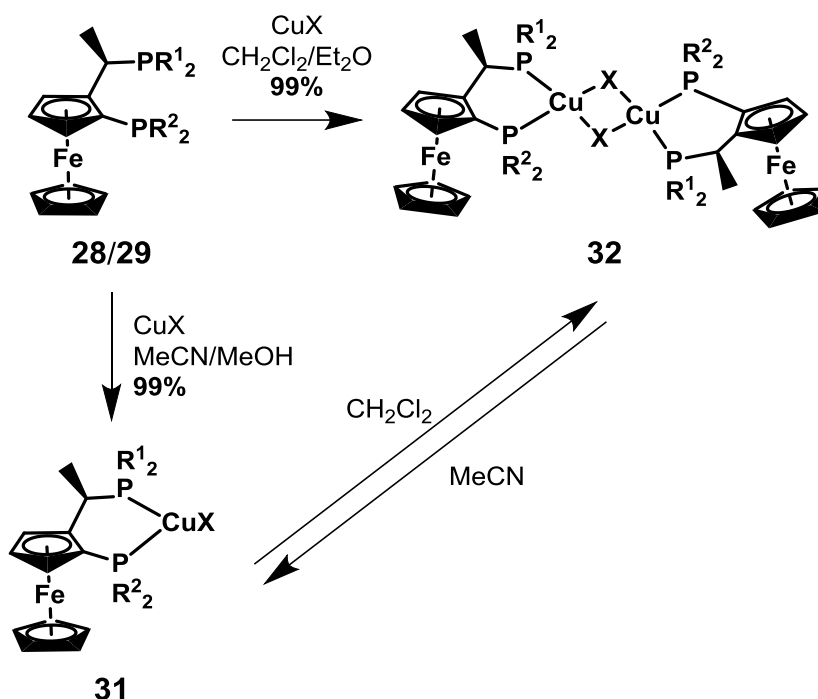


Figure 9 Solvent influence on ligand-copper complex structures

The structure of the pre-catalyst may have a monumental effect on the transformation considering different solvent systems noticeably alter yield and enantioselectivity of the reaction. As such, structural elucidation of the pre-catalyst gives potential insight into the transition states for reaction to progress effectively. Oxidative electrochemical studies gave further information regarding the redox properties of the complexes. While room temperature studies could not provide conclusive evidence of the dinuclear structure confirmed by X-ray crystallography, low temperature electrochemical studies demonstrate two distinct single-electron Cu(II)-Cu(I) processes at highly anodic potentials further confirming the active dinuclear structure within solution.

An interesting observation was that although a severe reduction in enantioselectivity was observed when chloride or iodide anions were used in place of bromide, the alteration of the halide counteranion exhibited negligible effects on the redox reactions related to Cu(II)-Cu(I) transitions. However, the effect of ligand variation was noticeable and significant as different electronic properties of the ligand changed the redox properties of the copper centre; this goes some way to explain the differing specificity of copper catalysed conjugate addition reactions with respect to the ligand incorporated in the reaction conditions.

Further investigation of the solvent effect showed a clear trend based on the coordination properties of the solvent molecules; the conjugate addition reaction between

3-octen-2-one **33** and methylmagnesium bromide was studied in various solvent systems (Table 2).

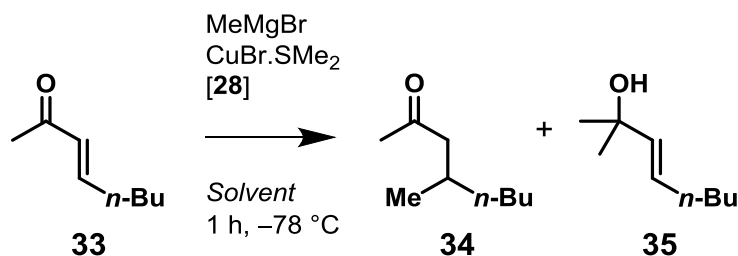


Table 2 Solvent effects on conjugate addition reaction

| Entry ^[a] | Solvent | Conversion (%) ^[b] | 34:35 ^[b] | ee (%) ^[c] |
|----------------------|---------------------------------|-------------------------------|----------------------|-----------------------|
| 1 | CH ₂ Cl ₂ | 88 | 86:14 | 92 |
| 2 | PhMe | 89 | 88:12 | 91 |
| 3 | ^t BuOMe | 90 | 97:3 | 96 |
| 4 | Et ₂ O | 87 | 83:17 | 87 |
| 5 | THF | 65 | 2:98 | 2 |
| 6 ^[d] | CH ₂ Cl ₂ | 35 | 75:25 | 80 |
| 7 ^[e] | CH ₂ Cl ₂ | 25 | 42:58 | 75 |

^[a] Reaction conditions: 0.35 M solution of **33**, 1.5 equiv. MeMgBr, 5 mol% CuBr-**28** complex, -78 °C, 1 h. ^[b] Conversion and regioselectivity determined by GC. ^[c] Determined by Chiral-GC (Chirasil dex-CB column). ^[d] 1 equiv. 1,4-dioxane added to reaction mixture prior to addition of **33**. ^[e] Me₂Mg used in place of MeMgBr

Co-ordinating solvents such as THF and 1,4-dioxane (used as an additive, see Entry 6, Table 2) had a severely deleterious effect on not only the enantioselectivity of the transformation, but also the regioselectivity. The shift in the position of the Schlenk equilibrium for more co-ordinating solvents is well-documented.^{34,35} The use of dimethylmagnesium – the more populous structure in the position of the Schlenk equilibrium in co-ordinating solvents – in place of methylmagnesium bromide demonstrated the same reduction in enantio- and regioselectivity as those containing THF and dioxane suggesting the active species in the transformation is the monoalkylmagnesium halide rather than the dialkylmagnesium species (Figure 10).

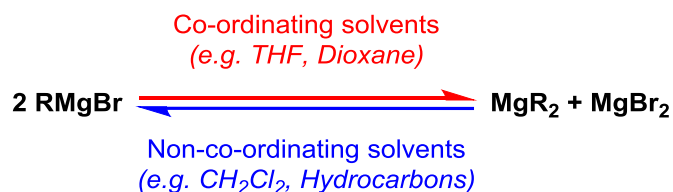


Figure 10 Schlenk equilibrium and solvent effects

NMR spectroscopic studies were able to elucidate details regarding the copper-ligand-organometallic complex which is formed prior to the commencement of the conjugate addition reaction. ^{31}P NMR spectroscopic data for the copper-ligand complex **32** in the absence of the organomagnesium reagent showed a $^2J_{\text{PP}}$ coupling constant of 186 Hz; this value decreased to 143 Hz upon addition of methylmagnesium bromide suggesting a new species has been formed. The new species was identified as compound **36** by ^1H NMR spectroscopy as a peak at -0.3 ppm (characteristic of CuMe species) became visible in the spectrum; this peak size did not increase in excess concentration of methylmagnesium bromide. When methyllithium was used in place of the Grignard reagent, an alternative structure **37** was observed; decomplexation of the ligand occurred at higher organometallic concentrations as the coupling between the ligand phosphorus atoms disappeared and formation of lithium dimethylcuprate dominated (Figure 11).

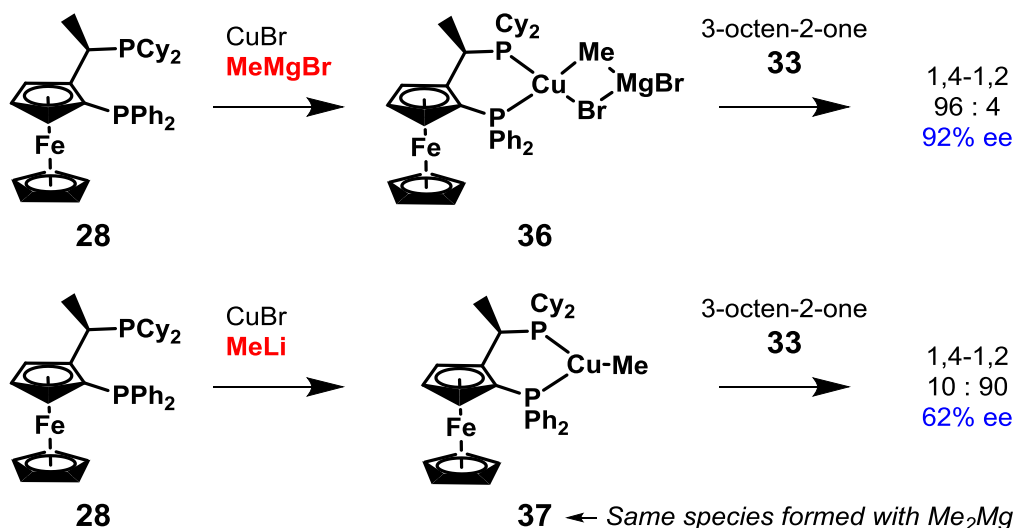
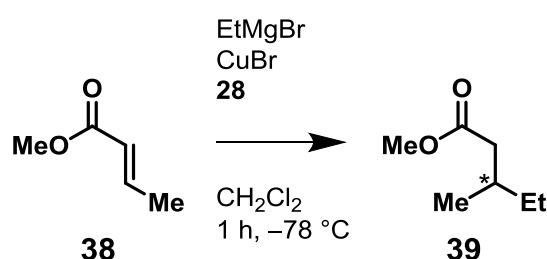


Figure 11 Copper-ligand-organometallic structures and subsequent conjugate addition reaction profiles

With this in mind, dimethylmagnesium was subjected to the same conditions. Unsurprisingly, species **37** was formed. A further experiment where 3 equivalents of additive 1,4-dioxane was incorporated to a sample containing species **36** led to formation of species **37**. This allowed the assumption to be made that the

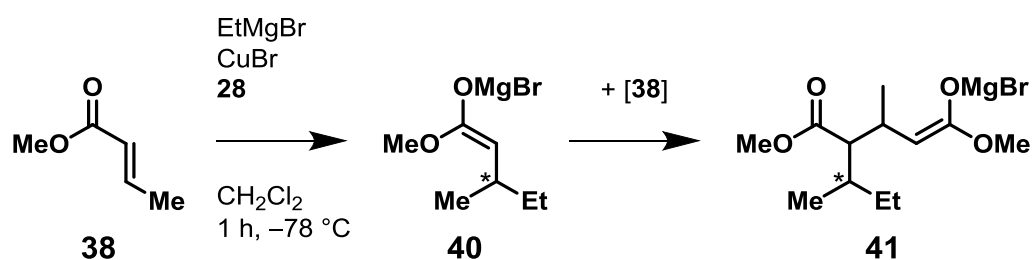
dialkylcuprate is not formed (or is sufficiently short-lived) during the pre-catalyst formation and does not play a significant role in the conjugate addition reaction of organomagnesium reagents.

Kinetic analysis was performed on the addition of ethylmagnesium bromide to methyl crotonate **38** in CH₂Cl₂ at -87 °C to form compound **39** (Scheme 6); enoates were shown to undergo conjugate addition with greater enantioselectivity compared to enones, while ethylmagnesium bromide is known to perform poorly in conjugate addition reactions with enoates.³³ Varying concentrations of substrate, organometallic and copper-ligand complex were used in the reactions to analyse their effect on the reaction rate.



Scheme 6 Conjugate addition reaction used for kinetic evaluation

While side products formed during the reaction impeded accurate kinetic analysis of varying substrate concentrations (formation of compound **41**, Scheme 7), an increase in reaction rate was observed at higher concentrations of compound **38**. This trend was also demonstrated by higher organometallic concentrations implying both play a role in the rate-limiting step for the transformation.



Scheme 7 By-product **41** formed at high concentrations of enone **38**

In the work of Feringa's group, it is stated that the order with respect to the copper-ligand complex is entirely dependent on the active species during the rate-limiting step. While a large volume of research attests to the dinuclear species **32** being the most populous in the model solvent, it does not necessarily play the key role in the transformation. The molecularity of the transition state would have a direct effect on the order of the reaction with respect to the copper-ligand complex; the dinuclear

species should exhibit an order between one and two, while the order with respect to the mononuclear species would be closer to one. Experimental results gave a value of 1.17 implying the mononuclear species **31** plays an active part in the rate-limiting step. This was clarified when the characterised heterocomplex **42** comprising the dimer of complexes with ligands **28** and **29** – prior to the organometallic induced dissociation – was used for the transformation. The copper complex **44** with ligand **29** shows greater conversion and enantioselectivity for the conjugate addition of the Grignard reagent (69% yield, 98% ee) compared to copper-ligand complex **43** with ligand **28** (4% yield, 72% ee) over the same timescale, so it stands to reason that if the mononuclear species is the key component, dissociation of the dinuclear complex induced by the organometallic reagent should occur and the product generated from the more active mononuclear species ligand should be the major component of the resulting mixture.³⁶ This was the perceived result of the reaction study giving further support to the mononuclear species forming part of the active transition state.

The catalytic cycle proposed by Feringa incorporated all these observations (Figure 12). While it appears that **43** is the opposite enantiomer to **44**, they actually differ in chirality in terms of orientation of the methyl substituent and axially, so can be considered to be configurational isomers.

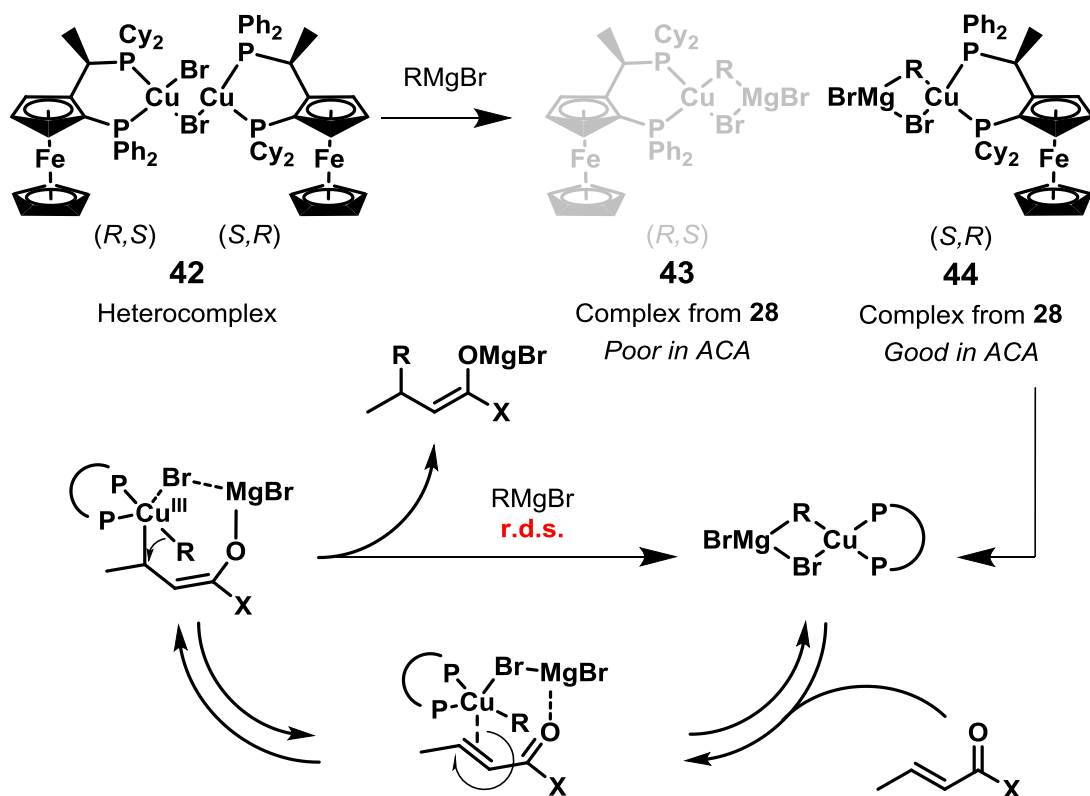
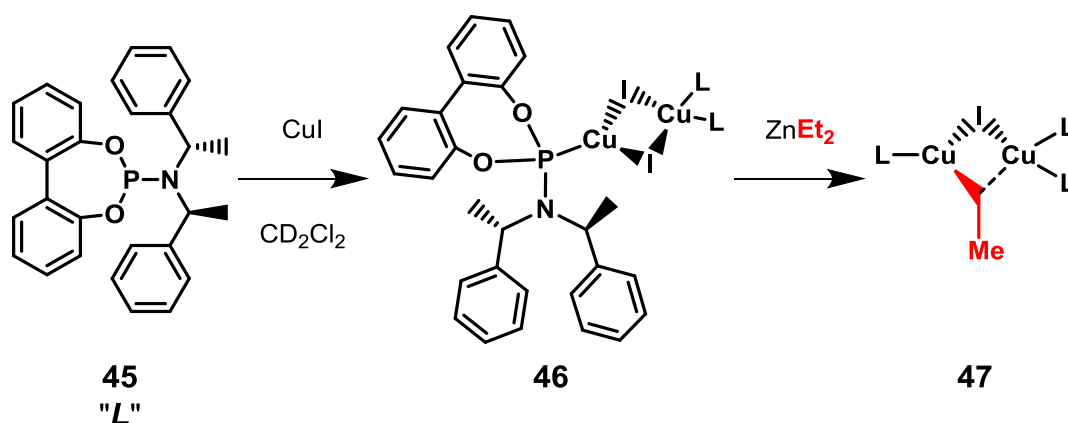


Figure 12 Formation of mononuclear complex and its role in proposed catalytic cycle

Dissociation of the stable dinuclear species **42** induced by the Grignard reagent forms the active mononuclear species **44** which binds to the substrate in the same manner as proposed by Schrader; the inactive species **43** is also formed but its inferior performance precludes its incorporation in the catalytic cycle. The importance of the magnesium bromide for reaction progression is due to its binding to the carbonyl oxygen in the substrate which is also bound *via* a bridging halide to the copper centre; without this, the active species for the enantioselective addition cannot be formed and the background non-enantioselective addition dominates. Again, as Schrader also inferred, oxidative addition of the copper at the β -position occurs forming the Cu-(III) species which subsequently reductively eliminates to reform the mononuclear species **44** and expels the conjugate addition product; **44** then re-enters the cycle and the process repeats until complete consumption of the substrate has occurred.

The depth of research undertaken for this reaction meant further developments on Schrader's work could illuminate new features of the conjugate addition reaction of alkylzinc reagents. Research to this effect was undertaken by Gschwind and co-workers using NMR spectroscopic analysis of the reaction to elucidate new phenomena; these included further evidence of the mono- and dinuclear species within the reaction mixture, the geometry of the copper centres within the active complexes and the deleterious effects of using co-ordinating solvents for alkylzinc reagents similar to the conclusion reached by Feringa in his studies on organomagnesiums.³⁷⁻⁴¹

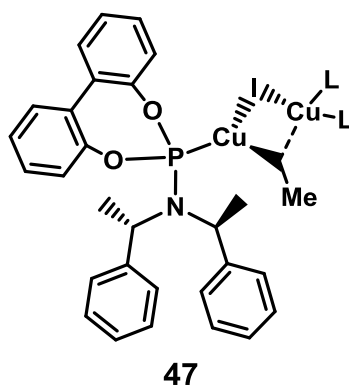
NMR spectroscopic studies also managed, for the first time, to directly detect an intermediate displaying direct transmetalation of the organic functionality from the organometallic reagent to the catalyst and subsequently provide rationalisation for a pre-catalyst complex **46** using chiral ligand **45** exhibiting $[\text{Cu}_2\text{X}_2\text{L}_3]$ stoichiometry to form active intermediate **47** (Scheme 8).⁴²



Scheme 8 Gschwind *et al.* formation of transmetalated "CuR" species analysed by NMR spectroscopy

Upon addition of diethylzinc to pre-catalyst **46**, ^1H , ^{31}P HMBC experiments were able to detect coupling between the ligand phosphorus atoms and the ethyl moiety *via* the copper atom within the active transition state. While this long range coupling has previously been visualised by Knochel and co-workers across palladium centres, the high quadrupole moment of both ^{63}Cu and ^{65}Cu isotopes permits access to a relaxation pathway for magnetisation.⁴³ Consequently, short relaxation times are exhibited which lead to broad signals in the generated spectra. Despite this, the conducted experiments allowed visualisation of magnetic interaction across the copper centre accompanied by determination of the structure of the reactive intermediates.

Pulsed NMR signals were used to eradicate relaxation interference effects from the perceived signals and leave only scalar coupling interactions in attempts to confirm the identity of species **47** (Figure 13).



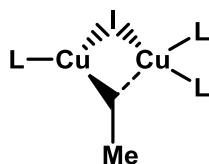
*Responsible for species
2-5 in 1D ¹H, ³¹P HMBC*

Figure 13 Comparison between ¹H NMR and 1D ¹H, ³¹P HMBC spectra containing the depicted reaction mixture

Chemical shift changes in signals between 0.8-0.3 ppm (representative of species **47**) were distinguishable from unchanged, high intensity signals assigned to non-specific diethylzinc species; the low intensity signals represent the CuR species formed after addition of the organometallic reagent to the copper-ligand complex. An unidentified species seen in the ¹H NMR spectrum was not detectable in 2D ¹H, ³¹P HMBC spectra and thus disregarded.

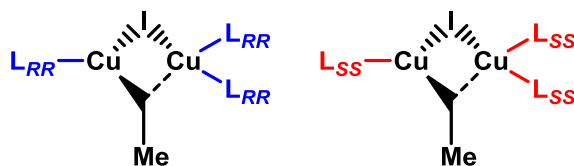
In the 2D spectrum, the ³¹P signals associated with species **47** were shifted upfield with respect to the free copper-ligand complex in agreement with the analogous observation made by Feringa for Grignard reagents.³³ This was believed to be the first description of detected transmetalation intermediates corroborating the existing literature results of Schrader and Noyori.^{29,30}

To elucidate the structure of the transmetalated species, a 1:1 enantiomeric mixture of chiral ligand **45** was used in the reaction mixture. The idea behind this was an active complex with only one ligand attached would provide an enantiomeric mixture of complexes; the respective enantiomeric complexes would be indistinguishable in the generated HMBC spectra. However, an active complex containing two or more ligands would result in a clearly recognisable mixture of diastereomeric complexes. The resultant spectra showed three new species which can be rationalised as the binding of three ligands to the dinuclear copper system; different combinations of the enantiomers give rise to four species and their respective enantiomers (Figure 14).

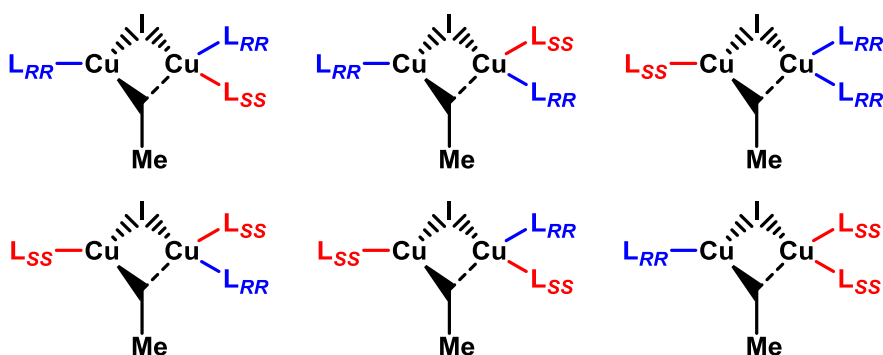


47

with 1:1 mixture of $L_{RR}:L_{SS}$



Single stereoisomers as seen in original spectrum



Regioisomers forming "2:1 diastereoisomers" of $L_{RR}:L_{SS}$ complexes (enantiomers in columns) giving rise to 3 new 1D 1H , ^{31}P HMBC signals

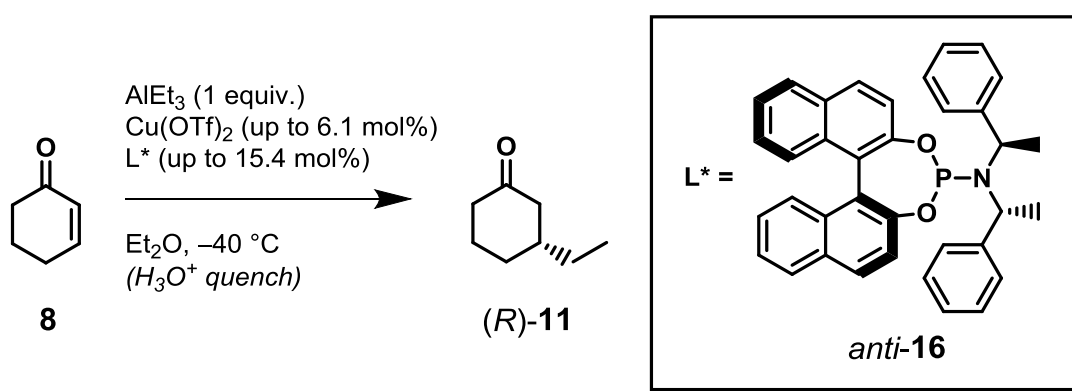
Figure 14 Rationalisation for new signals in 1D 1H , ^{31}P HMBC signals for the addition of a 1:1 mixture of ligand stereoisomers

This research provides unmistakable evidence of a new transmetalation species detected *via* utilisation of 1H , ^{31}P HMBC spectroscopy, which is notable in its circumvention of issues arising from the quadrupolar copper centre within the system.

The establishment of profound understanding for the conjugate addition mechanism using organozinc and organomagnesium reagents endorses exploration into yet untried organoaluminium reagents; research with these reagents can seek to unify the theories across the range of organometallic reagents in conjugate addition reactions whilst also providing opportunities to unveil novel hypotheses on the reaction mechanism.

1.2 Project Aims

A novel approach with unexplored organoaluminium reagents has significant potential for the complete unravelling of the mysteries surrounding conjugate addition reactions with organometallic reagents. Described in this chapter are efforts to this effect using triethylaluminium and a copper (II) acetate-phosphoramidite pre-catalyst complex based on a ligand developed by Feringa and co-workers.⁴⁴ Similar to previous studies, the substrate of choice was 2-cyclohexenone **8** due to the cyclic structure preventing undesirable *E-Z* isomerisation of the alkene bond which binds to the copper centre in the pre-catalyst prior to the conjugate addition reaction occurring (Scheme 9).



Scheme 9 Copper-catalysed conjugate addition under kinetic evaluation

To achieve a complete understanding of the mechanistic pathway which the reaction follows, repetition of the same conjugate addition reaction with varying reagent concentrations would allow establishment of the reaction order with respect to those reagents. The data collected could then be analysed – in parallel with computational studies – to postulate transition state structures that rationalise the observed rate stoichiometry. Finally, a catalytic cycle encompassing all of these features can be devised attesting to what we believe to be the most accurate representation of the reaction co-ordinate for the copper-catalysed conjugate addition of organoaluminium reagents to 2-cyclohexenone **8**.

1.3 Results and Discussion

1.3.1 Methodology Development

Initial investigation into the kinetic behaviour of the reaction had been performed within the group using a cryogenic sampling method devised by Krause and co-workers.³² While this method was prudent for some of the fundamental understanding of the reaction profile, the limited number of data points that could be collected from this form of analysis prevented reliable calculation of reaction order. The utilisation of a Mettler-Toledo ReactIR™ 15 machine allowed *in situ* reaction analysis without the need for extraction of aliquots for sampling (Figure 15). The IR signals were then interpreted over a range of 1900-1500 cm^{-1} between which it was expected the ν_{CO} signals relating to the starting material, product and co-ordinated intermediates would reside.

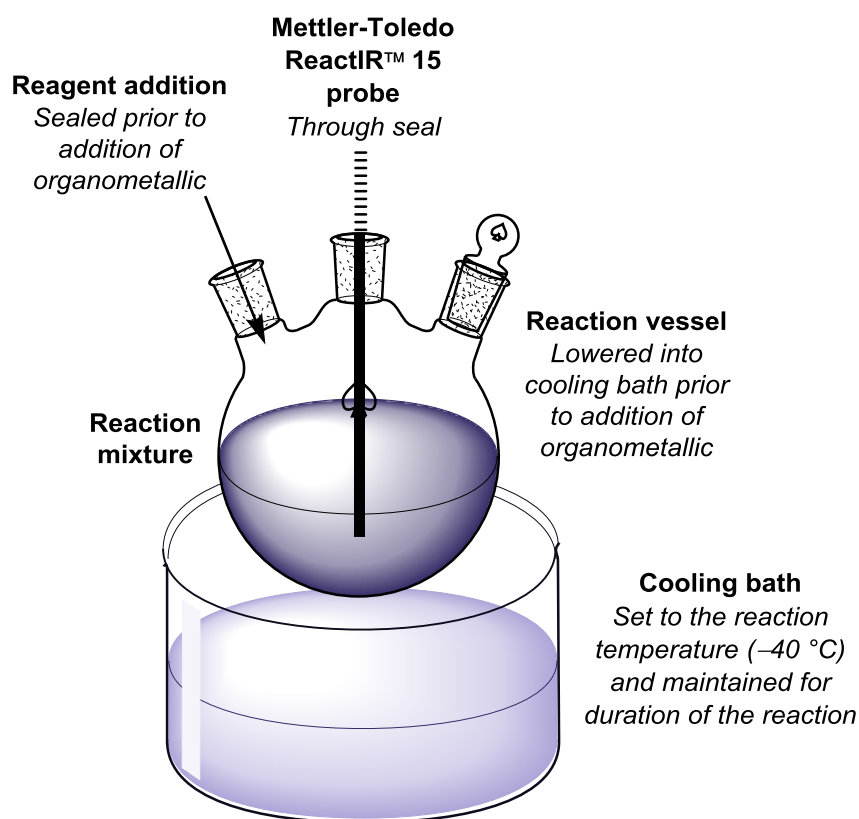


Figure 15 Reaction setup for kinetic studies

With the reaction set-up established, analysis of the interaction between the substrate and the organometallic reagent could be performed. The thought process behind this experiment was to see whether a background reaction in which uncatalysed addition of the organometallic to the substrate would occur. The absence of this reaction would

imply that the copper species is vital for the transformation to commence. As such, a titration experiment involving the sequential step-wise addition of portions of triethylaluminium to the substrate was performed. The instantaneous evolution of an increasing second peak at a lower frequency (1630 cm^{-1}) occurs proportionally to the devolution of the original absorption peak for the starting material (1676 cm^{-1}) (Figure 16).

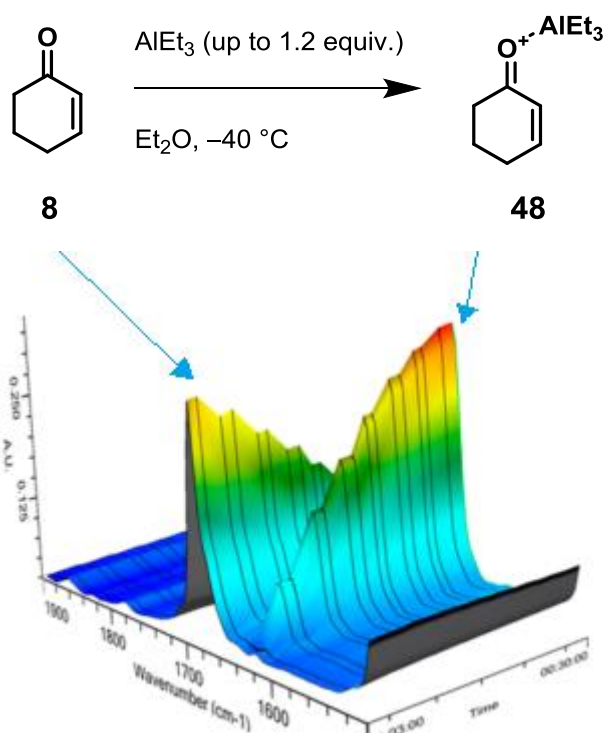


Figure 16 IR spectra generated during titration experiment for formation of Lewis acid-base complex **48** from enone **8** and triethylaluminium

Upon quenching the reaction mixture after completion of the organometallic addition, quantitative isolation of 2-cyclohexenone **8** was successfully performed. This implies that the formation of a Lewis acid-base complex comprising the α,β -unsaturated enone moiety and the organometallic reagent predominates. This species was shown to be stable for approximately 30 minutes under an argon atmosphere at $-40\text{ }^\circ\text{C}$ while background reactions (including uncatalysed conversion to the conjugate addition product **11**) were not observed. Varying the stoichiometry of the two reagents led to the conclusion that a 1:1 complex **48** between the substrate and organometallic reagent is formed.

An association equilibrium constant K for the formation of complex **48** could be derived from the titration experiment based on the following equilibrium equation:

$$K = [\mathbf{48}] \div [\mathbf{8}][\text{AlEt}_3]$$

The presumption based on the formation of the 1:1 complex and the assumed equivalent absorbance of radiation for both species **8** and **48** is that the terms **[8]** and **[AlEt₃]** can both be described by **[48]** based on the following:

$$[\mathbf{8}] = [\mathbf{8}]_{\text{TOT}} - [\mathbf{48}]$$

$$[\text{AlEt}_3] = [\text{AlEt}_3]_{\text{TOT}} - [\mathbf{48}]$$

where both **[8]_{TOT}** and **[AlEt₃]_{TOT}** are initial concentrations of the respective reagents. Expressing *K* based on these formulae gives the following equation:

$$K = [\mathbf{48}] \div ([\mathbf{8}]_{\text{TOT}} - [\mathbf{48}])([\text{AlEt}_3]_{\text{TOT}} - [\mathbf{48}])$$

Rearrangement of this formula can be performed to form a soluble quadratic with **[48]** as the undescribed term:

$$K[\mathbf{48}]^2 + (-K[\mathbf{8}]_{\text{TOT}} - K[\text{AlEt}_3]_{\text{TOT}} - 1)[\mathbf{48}] + K[\mathbf{8}]_{\text{TOT}}[\text{AlEt}_3]_{\text{TOT}} = 0$$

The values in this formula can be used in the quadratic formula as shown:

$$x = (-b \pm \{b^2 - 4ac\}^{1/2}) \div 2a$$

where $x = [\mathbf{48}]$, $a = K$, $b = (-K[\mathbf{8}]_{\text{TOT}} - K[\text{AlEt}_3]_{\text{TOT}} - 1)$ and $c = K[\mathbf{8}]_{\text{TOT}}[\text{AlEt}_3]_{\text{TOT}}$.

Since all terms must be positive, the solution to this formula based on the experimental data gave an association constant $K = 12.0(8) \text{ mol dm}^{-3}$, which corresponds to a binding energy ΔG_{react} at $-40 \text{ }^\circ\text{C}$ of $-4.8 \pm 0.4 \text{ kJ mol}^{-1}$ ($-1.1 \pm 0.1 \text{ kcal mol}^{-1}$).

This data was further reinforced by complementary computational analysis of the complex formation; CAM-B3LYP/6-31G(d,p) level DFT modelling was used to calculate the free energy of reaction for the formation of the complex (Figure 17).

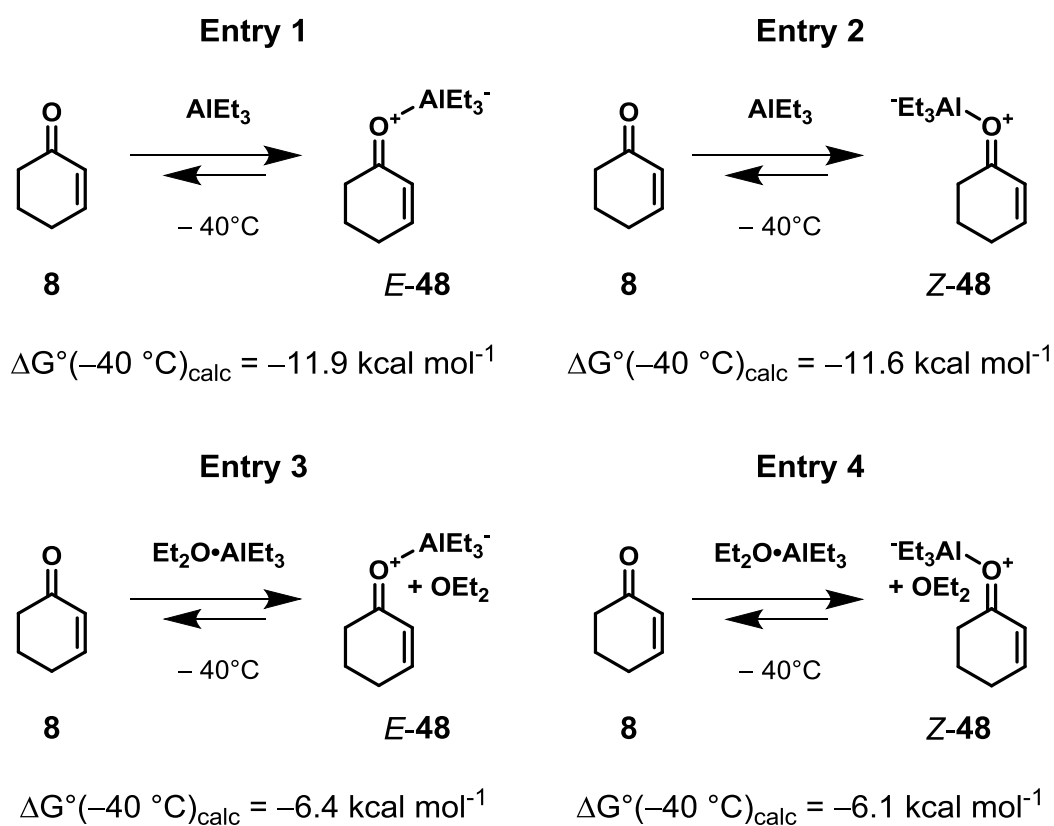
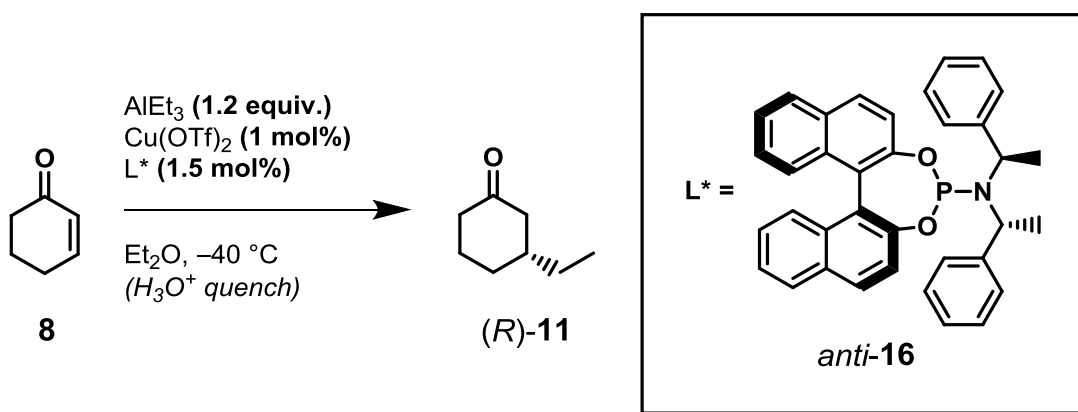


Figure 17 CAM-B3LYP/6-31G(d,p) calculated values for formation of Lewis acid-base complex **48** from enone **8** and triethylaluminium

Whilst these values are noticeably different from those obtained from the experimental analysis, the effects of solvation are ignored in these simplistic gas-phase representations of the reaction. The significant increase in the calculated ΔG_{react} upon incorporation of 1 equivalent of Et_2O (see Entries 3 and 4, Figure 17) suggest the effects of a solvent cage not replicable *via* the implemented level of computational analysis would corroborate the experimental values.

A control experiment with pre-determined concentrations of all the reagents (deemed suitable based on literature precedence) was performed; this initial experiment could then be altered accordingly to achieve the prescribed aims (Scheme 10, Figure 18).



Scheme 10 First reaction scrutinised for kinetic analysis

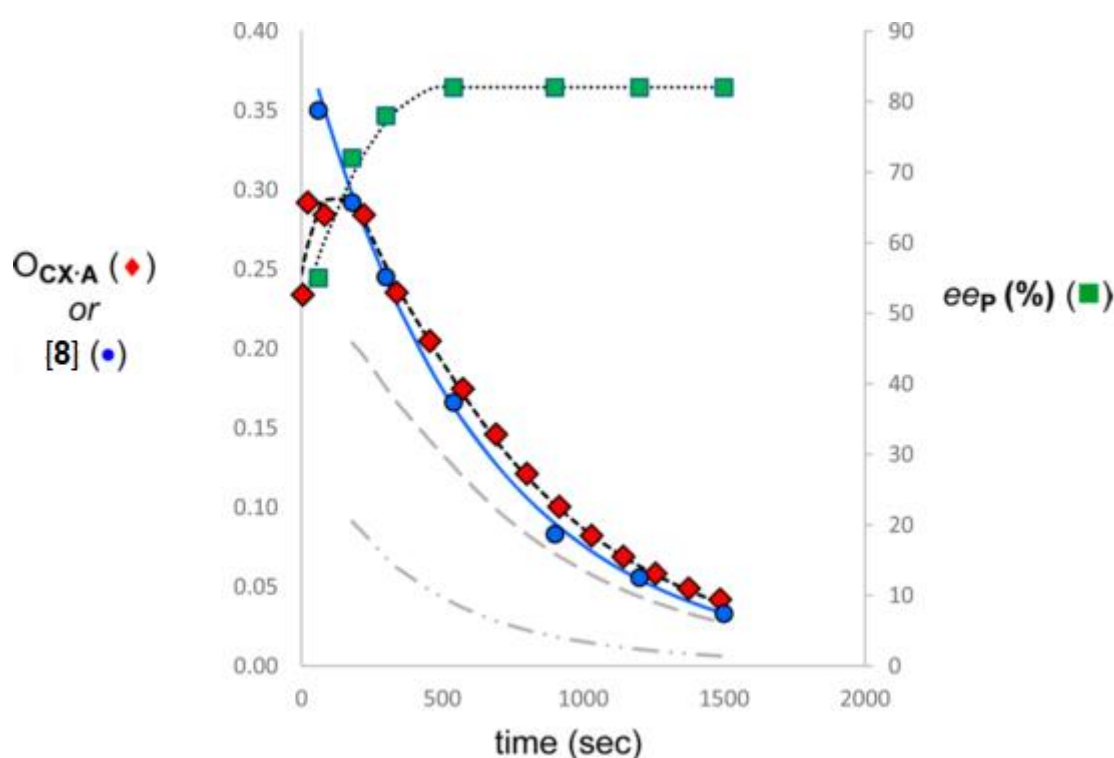


Figure 18 Data collected from kinetic analysis where O_{CX-A} measures GC absorbance of **48**; the grey lines represent calculated concentrations of **48** (---) and free concentration of **8** (- · · -)

The key observation that was made during this first experiment was the addition of 2-cyclohexenone **8** to the solution of readily formed **48** in Et₂O at -40 °C resulted in the evolution of the peak representing the Lewis acid-base complex **48** (1676 cm⁻¹) followed by another higher frequency peak relating to the conjugate addition product **11** rather than that of the non-complexed substrate; this is concordant with the computational analysis regarding the complexation. Another noticeable trend was the induction period upon addition of 2-cyclohexenone **8** prior to the steady first-order

decay after approximately 300 seconds during which an increase in the absorbance peak intensity of **48** was observed; as the reaction set-up involved pre-reduction of the Cu-(II) salt used in the reaction to the active Cu-(I) species *via* addition of the organometallic reagent and a nominal latency period prior to addition of the substrate, the induction period cannot be attributed to this reduction process. This phenomenon had been previously described in the work of Noyori and co-workers and forms a crucial part of the mechanistic pathway and the rationalisation of certain features within the perceived transition state.²⁹

Further consideration of the original cryogenic sampling method and the results gleaned from it illuminate an important feature of the reaction profile. This method allowed the conversion of the starting material to the conjugate addition product to be calculated as well as determination of the reaction enantioselectivity *via* gas chromatography. The intensity of the absorbance peak related to the Lewis acid-base complex **48** (See red line on the graph in Figure 18) can be plotted against the substrate **8** concentration (See blue line in Figure 18) calculated in the cryogenic sampling method; the complex **8** could not be isolated or characterised with the latter method due to its instability outside the reaction conditions. Both lines show similar first order decay with respect to substrate concentration, justifying the use of the absorbance intensity for the kinetic evaluation of the reaction after calibration of the ReactIR™ machine. While the kinetic data from the cryogenic sampling method contained too few data points to allow reliable reaction order calculations in comparison to the ReactIR™ analysis, it was successful in illuminating the induction period also seen in the ReactIR™ results. The enantiomeric excess of the conjugate addition products within the reaction mixture increases with time in the initial stages of the reaction until a plateau is approached at a similar time to the maximum observed absorbance in the ReactIR™ analysis (approximately 300 seconds); this plateau is reached soon afterwards at 82% ee. This implies the existence of a non-enantioselective background reaction which initially generates the racemic conjugate addition product **11** which then acts as an initiator for the enantioselective transformation and must play a part in the reaction progression.

Further information obtained from the cryogenic sampling method demonstrates a non-linear effect with respect to the phosphoramidite ligand *anti*-**16** used in the studies (Table 3, Figure 19). Non-linear effects describe the disproportional change in enantioselectivity of an asymmetric process with respect to altering the enantiomeric

ratios of a chiral additive; a positive non-linear effect can be seen in the conjugate addition reaction we were investigating.⁴⁵

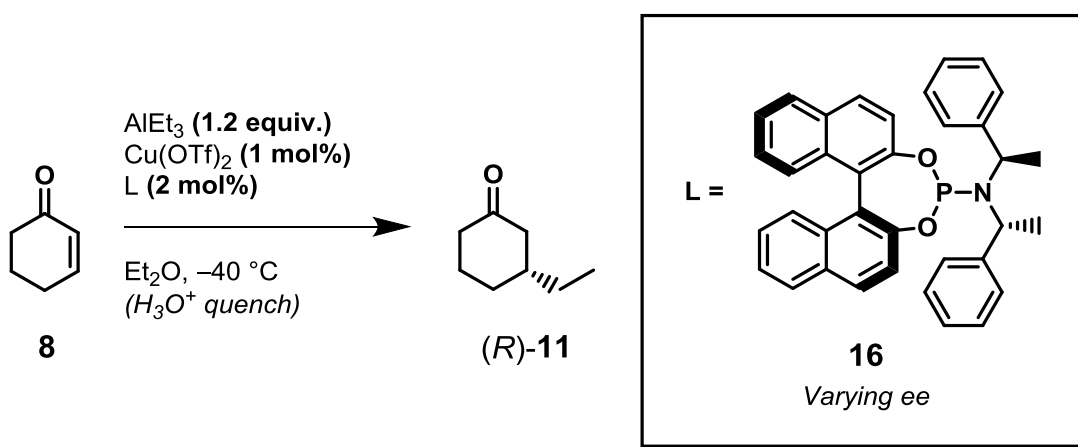


Table 3 Analysis of enantiomeric excess of **11** formed during conjugate addition reaction compared to ligand enantiopurity used exhibiting slight positive non-linear effect

| Entry | Ligand ee (%) | ee of product 11 (%) |
|-------|---------------|-----------------------------|
| 1 | 0 | 0 |
| 2 | 25 | 26 |
| 3 | 50 | 48 |
| 4 | 75 | 62 |
| 5 | 100 | 82 |

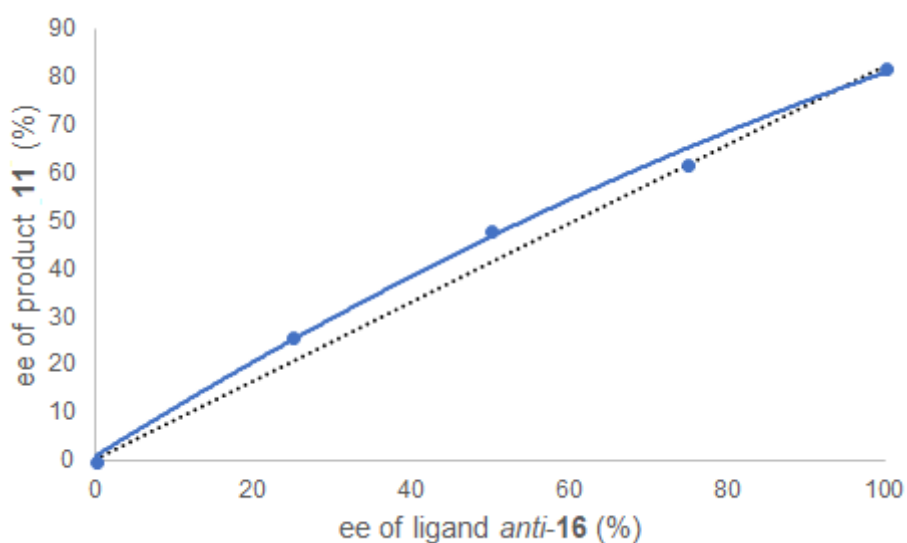


Figure 19 Graphical representation of data from Table 3

This suggests that a polynuclear complex containing multiple ligands forms part of the transition state in the active species for the transformation. This accompanies the induction period as another necessary component of the active transition state as well as a form of guidance for the interpretation of subsequent results regarding reaction order with respect to the ligand.

1.3.2 Establishing the Rate Equation

By changing the concentrations of the reagents in the conjugate addition reaction in turn whilst maintaining the concentrations of the other reagents, the reaction order with respect to the independent variable could be determined (Table 4).

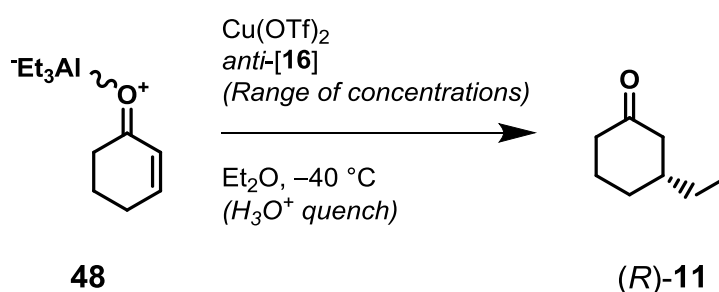
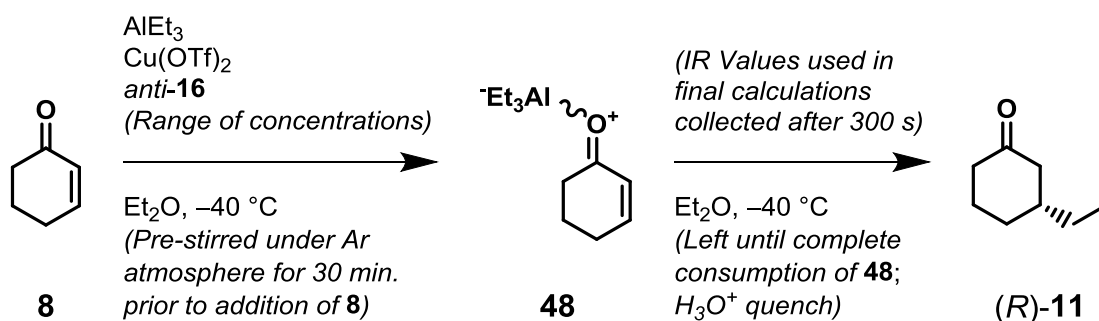


Table 4 Reagent concentration values and calculated first-order reaction rate constants, k_1 , for respective entries

| Entry | [48] (mM) ^[a] | [Cu] (mM) | [L] (mM) | k_1 (10^{-3} s^{-1}) |
|-------|--------------------------|-----------|----------|------------------------------------|
| 1 | 300 | 3.46 | 4.99 | 1.558(8) |
| 2 | 232 | 3.18 | 4.88 | 1.94(3) |
| 3 | 124 | 3.55 | 5.22 | 0.566(7) |
| 4 | 40.4 | 3.13 | 4.76 | 0.240(4) |
| 5 | 226 | 1.07 | 1.59 | 0.323(4) |
| 6 | 217 | 1.96 | 3.06 | 0.490(5) |
| 7 | 213 | 3.79 | 5.49 | 1.517(9) |
| 8 | 218 | 6.10 | 8.82 | 4.33(9) |
| 9 | 232 | 3.62 | 1.66 | 0.674(4) |
| 10 | 254 | 3.55 | 3.54 | 1.066(5) |
| 11 | 227 | 3.19 | 6.54 | 1.94(2) |
| 12 | 227 | 3.36 | 11.7 | 2.76(3) ^[b] |
| 13 | 248 | 3.35 | 13.6 | 2.60(6) ^[b] |
| 14 | 220 | 3.42 | 15.4 | 1.63(6) ^[b] |

^[a] Based on application of the equilibrium constant K for the formation of **48** from **8** and triethylaluminium; initial concentrations of individual reagents differ from this value. ^[b] Higher [L]:[Cu] concentrations exhibited zero-order reaction kinetic behaviour; values within the table represent a first-order fit of the collected results for direct comparison with the other entries

The preliminary studies using the cryogenic sampling method permitted determination of the reaction order with respect to the Lewis acid-base complex **48**, which in itself can be calculated for any given concentration of compound **8** and AlEt₃ as the equilibrium constant for its formation has already been determined. The rapid formation of this complex within the ReactIR™ analysis led to its implementation in the postulated rate formula in place of independent substrate and organometallic variables as well permitting the eradication of calibration processes to accommodate the observed induction period (Scheme 11). To this effect, results for these experiments begin after the prescribed induction period of 300 seconds.



Scheme 11 Reaction scheme with description of data collection methodology

A range of 40-300 mmol concentrations of the complex were incorporated alongside constant copper and ligand concentrations (See Entries 1-4, Table 4) (Figure 20). Fitting the intensity of the absorbance of the Lewis acid-base complex **48** to its concentration by using $[\mathbf{48}]_0 e^{-k_1 t}$, $\ln [\mathbf{48}]_0$ can be plotted against $\ln k_1$. The data demonstrates first-order behaviour for the consumption of **48** over the course of the reaction which means that the conjugate addition reaction is best described as first order with respect to **[48]**.

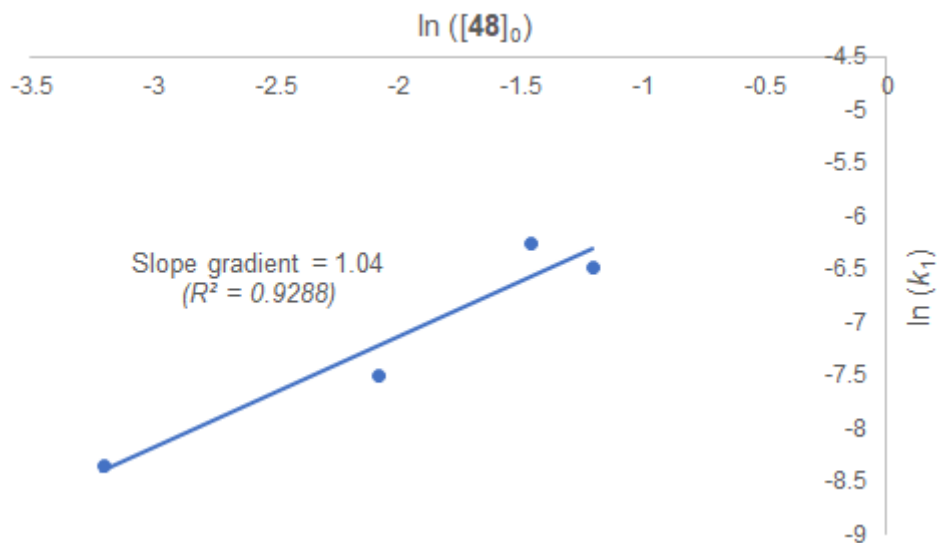


Figure 20 Derivation of reaction order with respect to **[48]**

To determine the order of the reaction with respect to the copper catalyst, the pre-reduction of the copper (II) acetate to a Cu(I) species in the presence of the organometallic reagent and the ligand needed to be considered; as such, post-induction decay data could be collected based on the intensity of the absorbance peak for the Lewis acid-base complex **48** using a consistent Cu:L molar ratio of 1:1.5 with varying [Cu] between 1-6 mmol and a constant **[48]** of 220 mmol (± 7 mmol) (See Entries 5-8, Table 4) (Figure 21).

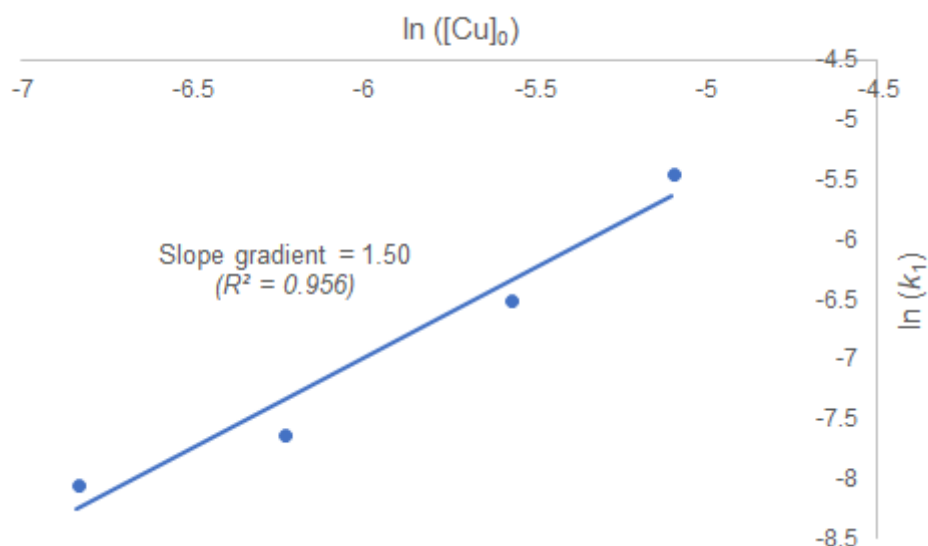


Figure 21 Derivation of reaction order with respect to [Cu]

Fitting the data in the same way as used for calculating the reaction order with respect to [48], the slope of the line of best fit for the data points was 1.50 suggesting the conjugate addition reaction after induction is complete is best described with a $[\text{Cu}]^{1.5}$ term.

The same method was used for ligand order calculations by varying [L], with fixed [Cu] and [48] (See Entries 9-14, Table 4) (Figure 22).

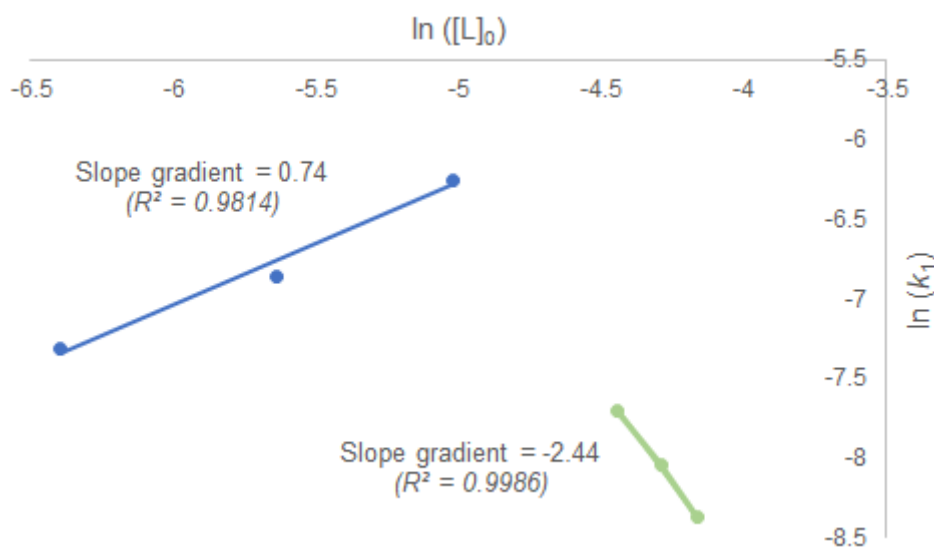


Figure 22 Derivation of reaction order with respect to [L]; separate trendlines for low ligand concentration (blue) and high ligand concentration (green) used to distinguish between expected reaction rate behaviour and reaction rates affected by observed inhibition respectively

The immediately noticeable aspect of the data collected was the presence of two seemingly distinct sections; the two lines of best fit could both be fitted in the same way as previous attempts. The slope of the line of best fit for the lower ratios of [L]:[Cu] ($0.5 \leq [L] \leq 3.5$) gave an average value of 0.67 across ReactIR™ and cryogenic sampling methods (cryogenic methods returned a value of 0.60), suggesting the conjugate addition reaction after induction is complete is best described with a $[\text{L}]^{0.67}$ term. However, a retardation process is observed at higher ratios of [L]:[Cu] ($[\text{L}]:[\text{Cu}] > 3.5$) with the reaction now exhibiting zero order kinetics. The slope of the line of best fit for the inhibition process was -2.44 . This retardation of the reaction suggests an inactive transition state within the reaction mixture which precludes the enantioselective transformation; this observation is vitally important to fully rationalise the proposed mechanistic pathway.

1.3.3 Proposal of the Mechanistic Pathway

Once the experimental data was collected by myself and two co-workers, Prof. Simon Woodward manipulated the data to propose a mechanistic pathway taking the following observations into consideration:

- The rate equation for the enantioselective conjugate addition reaction is $\text{rate} \propto [\mathbf{48}][\text{Cu}]^{1.5}[\text{L}]^{0.67}$;
- The induction period prior to the first order consumption of the Lewis acid-base **48** involves the formation of the transition state and not the pre-reduction of the Cu-(II) catalyst to Cu-(I);
- The transition state must comprise a molecule of the conjugate addition product **11** – *via* non-enantioselective addition – due to the rise in enantioselectivity during the induction period. This is corroborated by the consumption of 2-cyclohexenone **8** shown in the cryogenic sampling studies during the induction period despite maximum absorbance not having been reached for the Lewis-acid base complex **48** in the ReactIR™ data. Furthermore, redosing of the reaction mixture with compound **11** also leads to removal of the induction period and higher enantioselectivity implying its involvement in the active catalyst;
- The positive non-linear effect of the ligand enantiopurity implies a polynuclear complex for the transition state containing more than one ligand molecule;
- A non-active inhibitory species causes retardation of the reaction at high [L].

The rate equation allowed us to postulate a transition state **49** for the rate determining step with stoichiometry equal to double the observed values: $\text{Cu}_3\text{L}_{1.33}(\mathbf{8})_2(\text{AlEt}_3)_2$ (Figure 23).

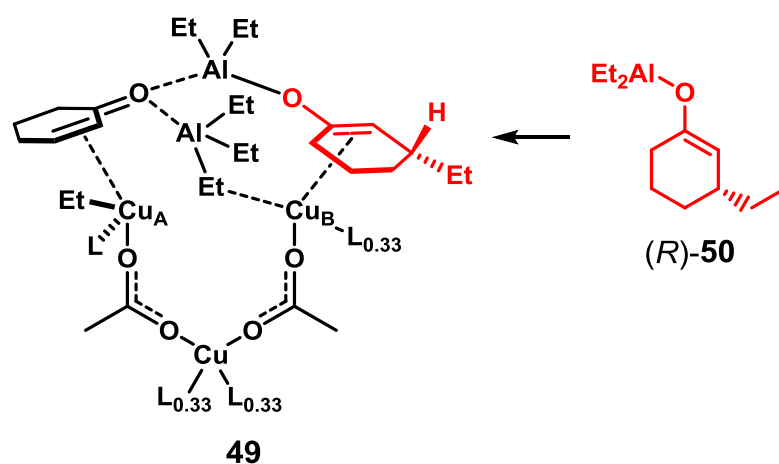


Figure 23 Proposed transition state for the conjugate addition reaction incorporating the enolate product **50** ($\equiv \mathbf{8} + \text{AlEt}_3$)

The key elements of transition state **49** account for many of the phenomena detected during the experimental analysis. The incorporation of one molecule of the conjugate addition product enolate with molecularity $\mathbf{50} = \mathbf{8} + \text{AlEt}_3$ ($\equiv \mathbf{48}$) (See structure in red, Figure 23) provides an explanation for the observed induction period; the formation of transition state **49** relies on the presence of the enolate species for the enantioselective process to commence. In the initial stages of the reaction, the concentration of transition state **49** is very low and slow non-enantioselective conjugate addition occurs forming a small amount of the enolate species **50**; since the function of this species is purely structural and its stereochemistry is inconsequential to the enantioselective process, a low concentration of this species can accumulate in the reaction mixture allowing transition state **49** to form and begin to catalyse the significantly faster enantioselective process without significant deleterious effects to the enantiomeric excess of the isolated product. The enolate product of that reaction can in turn catalyse another enantioselective transformation by forming a subsequent transition state. The enantioselective process subsequently predominates as the concentration of transition state **50** increases with each successful addition leading to a rise in the enantiomeric excess of the isolated product until a plateau is reached, as seen in the cryogenic sampling studies.

The $\text{Cu}_3\text{L}_{1.33}$ molecularity of the transition state can be rationalised by a shuttling mechanism (Figure 24).

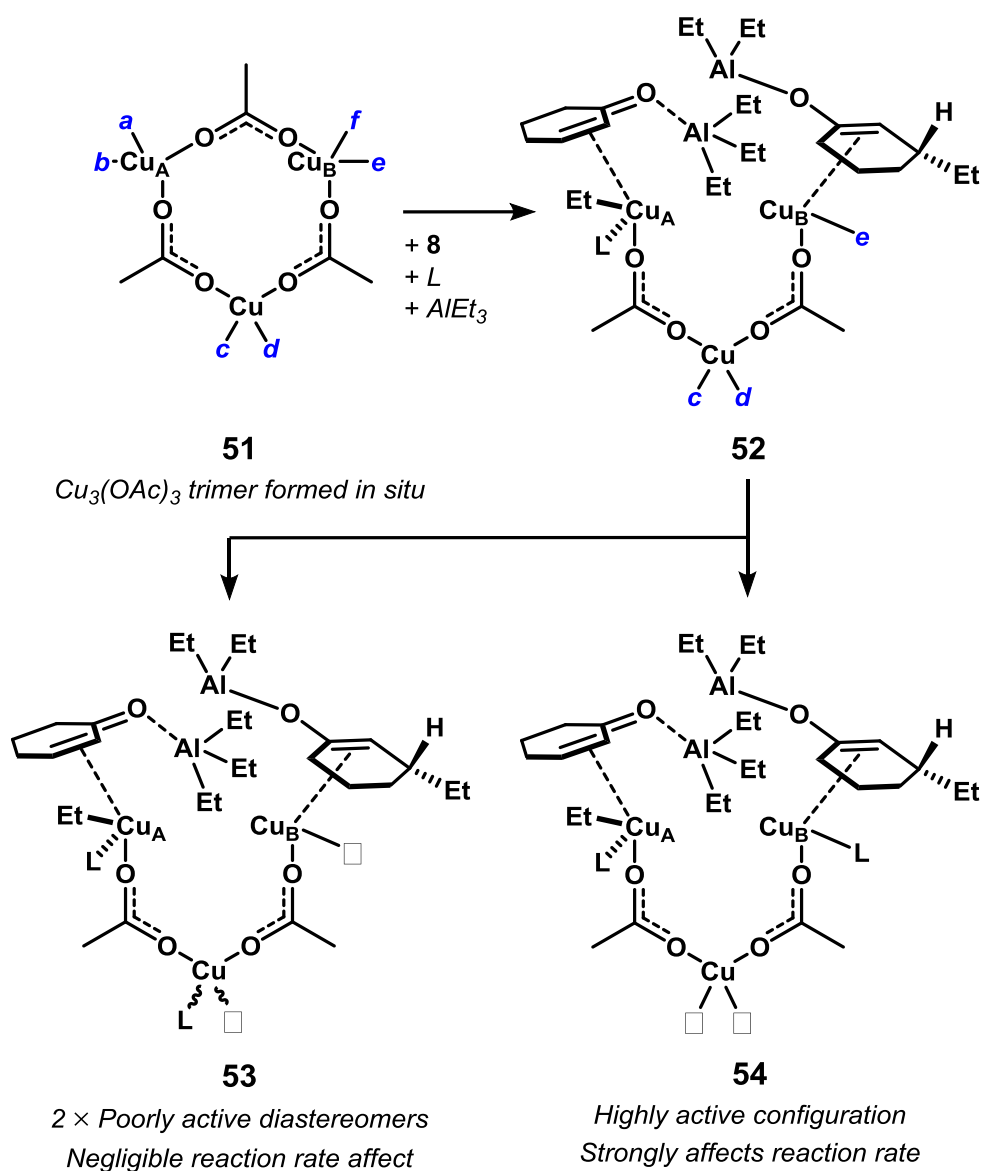


Figure 24 Ligand shuttling mechanism to rationalise rate equation stoichiometry; □ indicated vacant binding site

The multiple binding sites for the ligand in the proposed transition state are non-competitive and do not differ hugely energetically. They are, however, inequivalent in their effect on rate acceleration of the enantioselective process; only when the ligand sits in the co-ordination site proximal to the catalytic site (See structure **54**, Figure 24) does rate acceleration occur. In the structures where the ligand binding is not proximal (both diastereomers of species **53**), the ligand itself only performs a structural role and does not accelerate the reaction. Due to rapid ligand exchange, the described stoichiometry where one ligand is shared across the three sites equally can be rationalised along with the positive non-linear effect observed in the cryogenic sampling studies caused by ligand binding at the non-proximal sites.

The ratios of the respective molecules within the transition states do not align with the proposals made in the aforementioned works with organomagnesium (stoichiometry of $\text{CuL}(\mathbf{8})(\text{EtMgBr})$ in Feringa's studies)³³ and organozinc reagents (stoichiometries of $\text{CuL}(\mathbf{8})(\text{ZnEt}_2)_2$ in Schrader's experimental studies and $\text{Cu}_2\text{L}_3(\mathbf{8})(\text{ZnEt}_2)$ in Gschwind's NMR spectroscopy proposal respectively).^{30,42} Gschwind's results do attest to a trimer **55** more similar in structure to the unbound pre-catalyst **51** postulated in this analysis of organoaluminium additions, though this was disregarded by the authors in favour of Cu_2L_3 stoichiometry in their conclusions; this is due to Cu:L ratios of 1:1.5 maximising the enantioselectivity for enantioselective conjugate addition reaction with organozinc reagents (Figure 25).³⁷

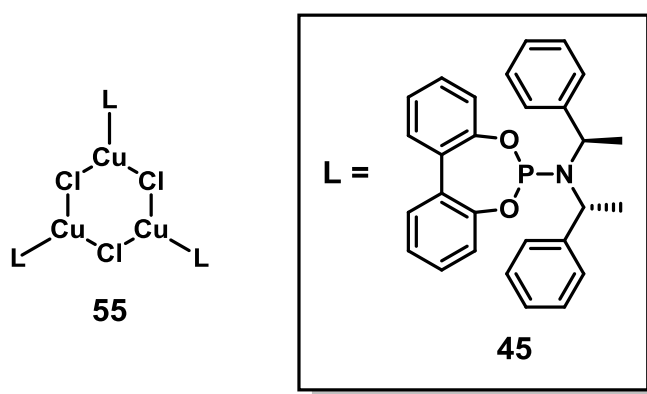


Figure 25 Gschwind *et al.* Postulated trimeric pre-catalyst structure

Conversely, the consistent high enantiomeric excess of the analogous organoaluminium reaction at 82% ee at Cu:L ratios down to approximately 1:0.45 is concordant with the $\text{Cu}_3\text{L}_{1.33}$ composition we proposed for the transition state in the rate limiting step as well as other structures formed in events leading to its formation.

The proposed mechanism for this transformation is described below (Scheme 12). It includes two C_2 -symmetric pre-catalytic structures **56a** and **56b** whose structures were confirmed computationally using the $\omega\text{B97X-D}$ functional and Stuttgart–Bonn pseudopotential and basis set for Cu with the 6-311G(d) basis set for all other atoms and; these calculated structures further attest to the accumulation of racemic enolate **50** during the induction period.^{46,47}

However, the experimental data is not consistent with this structure as the induction period exhibits an initial increase in enantiomeric excess for the isolated product; this would not occur if the achiral α,β -unsaturated enone was bound in place of the enolate species **50** as all transformations would exhibit the same enantioselectivity and a constant enantiomeric excess at all times in the reaction would be seen instead of displaying an initial increase. As such, this structure was disregarded as a potential resting state in the mechanistic pathway.

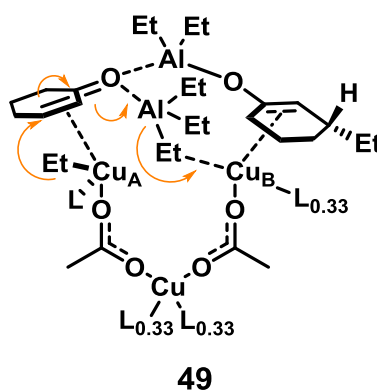
The inhibitory effects of high ligand concentration can be explained by the accumulation of inactive species **57**; the molecularity of the structure is also in accordance with the observed $[L]^{-2.5}$ order seen at high ligand concentrations in the kinetic studies as five ligand molecules are competing with two molecules of **48** on the copper trimer to prevent the formation of the active transition state **49**. The bridging ethyl unit in the structure is similar to a $\text{Cu}(\mu\text{-Me})\text{Cu}$ species detected by X-ray crystallography as described by Steffen and co-workers.⁴⁸

1.4 Conclusions

Kinetic analysis of the copper catalysed enantioselective conjugate addition reaction between triethylaluminium and 2-cyclohexenone **8** in conjunction with a phosphoramidite ligand *anti*-**16** using both ReactIR™ analysis and cryogenic sampling methods has successfully elucidated the order of reaction with respect to each respective reagent:

$$\text{Rate} \propto [\text{Cu}]^{1.5}[\text{L}]^{0.67}[\mathbf{48}]$$

The analysis also supported Gschwind's hypothesis that one predominating copper-ligand species was responsible for the rate limiting step in the enantioselective transformation; the differing stoichiometry in the results acquired for the organoaluminium reaction imply that this singular species is transition state **49** within the reaction mechanistic pathway (Figure 27).



49
Singular transition state responsible for conjugate addition reaction progression

Figure 27 Active transition state; formation of this structure is the rate-limiting step in the catalytic cycle

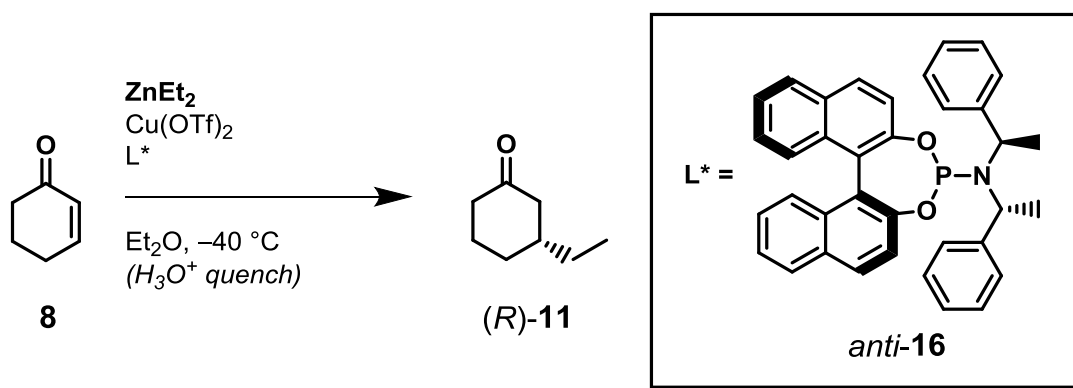
The computationally confirmed pre-catalyst structures **56a** and **56b** exist in equilibrium; the multiple binding sites in the trimeric structure account for both the order of the reaction with respect to the ligand as well as the observed non-linear effects of the ligand's enantiomeric purity. The observed zero-order retardation occurs due to the accumulation of species **57** at high ligand concentrations preventing the formation of the active transition state.

The presence of the enolate structure **50** within the active transition state **49** accounts for the induction period and initial low enantioselectivity of the isolated product. This

also aids in the rationalisation of a previously inexplicable phenomenon regarding copper catalysed enantioselective conjugate addition reactions of organoaluminium reagents. Historically, the most active and selective catalyst contain Cu(I) sources that are very labile, such as tetrakis(acetonitrile)copper (I) tetrafluoroborate; the high lability of these catalyst lends itself to enolate incorporation more readily than comparatively less labile species. While this observation has been made repeatedly for this class of reaction, these results are likely the first to provide an explicable reason for this occurrence.

1.5 Future Work

The results obtained for the analysis of the organoaluminium conjugate addition reaction, contradictory to literature precedent as they appear, encourage like-for-like investigation into the extensively studied analogous reaction with organozinc reagents (Scheme 13).



Scheme 13 Analogous research opportunity with organozinc reagents

The alternative approach adopted in this investigation using different analytical techniques may illuminate previously undetected similar trends and features to the organoaluminium addition. Initial attempts within the group have encountered problems due to the poor solubility of the copper-ligand complex incorporating the organozinc reagent in the model system for the organoaluminium addition, though this does not preclude alterations such that these issues are avoided.

The ground-breaking nature of this discovery means further exploration of the reaction may unveil more mysteries. With previous success having been achieved with NMR spectroscopic analysis by Gschwind, Noyori and Feringa, experiments to this effect may be able to confirm the structures generated by the computational analysis in these studies.^{29,33,42} The structural features of the pre-catalyst structures **56a** and **56b** within the mechanistic pathway could be potentially reinforced using both ³¹P NMR or the ¹H,³¹P HMBC spectroscopy use by Gschwind (Figure 28).⁴²

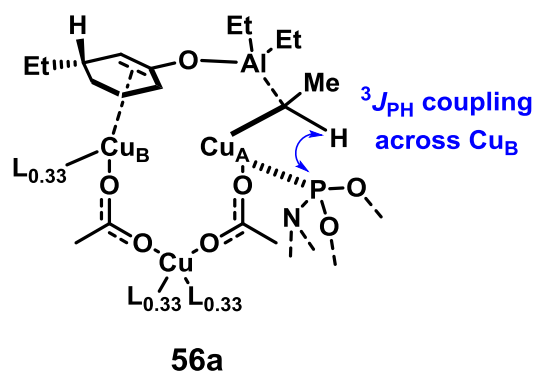


Figure 28 Potential ^1H , ^{31}P HMBC opportunity for coupling between ligand phosphorus atom and hydrogen atom on ethyl component in active intermediate

Additionally, ^{31}P NMR spectroscopy can also be used to detect the inactive species **57** responsible for the retardation at high $[\text{L}]$ (Figure 29). This would also support the discounted trimeric copper structure in Gschwind's studies.⁴²

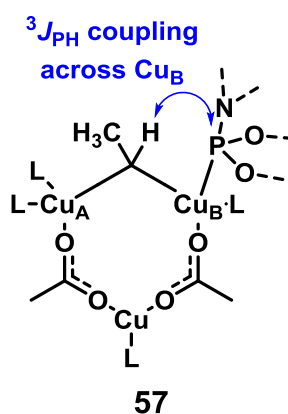


Figure 29 Potential ^1H , ^{31}P HMBC opportunity for coupling between ligand phosphorus atom and hydrogen atom on ethyl component in inactive species

SECTION 2

TOWARDS ENANTIOSELECTIVE
SYNTHESIS OF QUINOLONE
DERIVATIVES *VIA* COPPER-CATALYSED
CONJUGATE ADDITION OF
ORGANOALUMINIUM REAGENTS

2.1 Introduction

2.1.1 Introduction to Quinolones

Quinolones are a group of broad-spectrum antibacterial drugs based on a bicyclic core structure derived from 4(1*H*)-quinolone **58**. The development of this class of compounds as therapeutic agents for the treatment of bacterial infections was triggered by the serendipitous discovery of Nalidixic acid **59** by Lesher and colleagues in 1962 (Figure 30). Although it is not technically a quinolone due to the presence of a nitrogen atom in the fused ring (making it a 1,8-naphthyridone), it and other molecules with heteroatoms within their structures exhibit quinolone-like properties (i.e. bactericidal activity); Nalidixic acid itself has since been used in the treatment of urinary tract infections.⁴⁹ In the years that have followed, research has been carried out to elucidate the mechanism of action for quinolones accompanied by multiple reviews discussing their implementation.^{50–52} This has enabled access to the treatment of other diseases such as respiratory, gastrointestinal, gynaecological, skin and soft tissue diseases as well as antitumor medication and even topical pneumonia treatment.^{53–58}

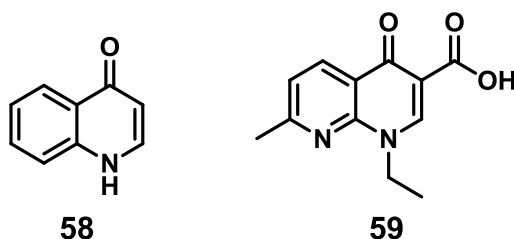


Figure 30 4(1*H*)-Quinolone **58** bicyclic core on which quinolone drug molecules are based and Nalidixic acid **59**

Development of quinolone drugs has occurred in stages since the discovery of Nalidixic acid; each generation of quinolone molecules contributes an additional desirable property over previous compounds based on structural modifications and the observed biological effects these changes induce. These include increased activity against *Staphylococcus aureus* for third generation quinolones or the dual action of fourth generation quinolones with DNA gyrase and topoisomerase IV which slows down the development of resistance.^{53,59} As such, certain structural features of the derived compounds are shown to have specific, variable effects on the activity of the quinolone (Figure 31).⁶⁰ Indeed, the ubiquity of the incorporation of a fluorine atom in the 6-position has led to an entire separate class of quinolone drugs – the

fluoroquinolones – which make up the majority of quinolone drug molecules currently in circulation.^{50,61}

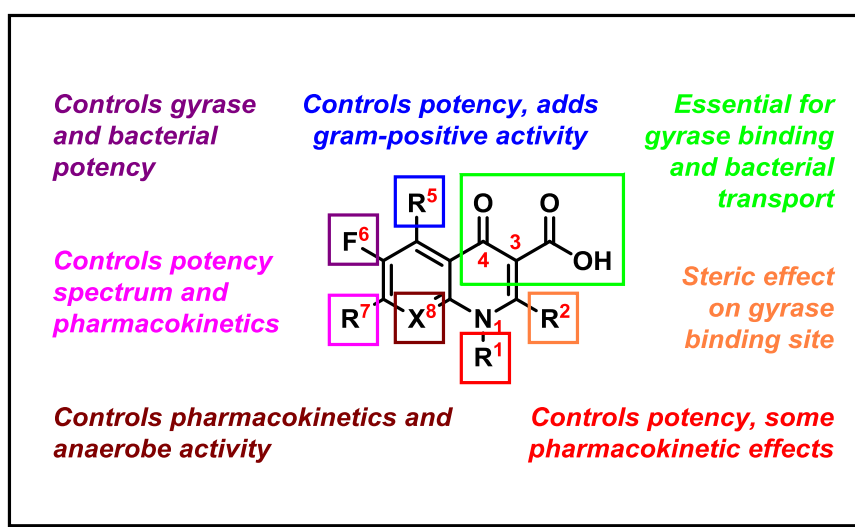


Figure 31 Effects on quinolone drug activity from alterations to core quinolone structure

The expanding range of treatments in which quinolone drugs can now be implemented as well as the documented effects structural diversification have on the biological activity of the molecules make the synthesis of quinolone derivatives an attractive prospect for early stage drug discovery. The desirable structural features of the quinolone core (low molecular weight, facile functional group incorporation and modification etc.) mean fragment-based drug design around this core structure can potentially uncover many opportunities for synthesising biologically active molecules.

2.1.2 The Synthesis of Quinolones and Their Derivatives

Numerous methods for the synthesis of the quinolone core structure have been devised over many decades. Many chemists have transformations attributed to them which afford quinolone products from derivatives of aniline **61** (Figures 32 & 33).^{62–67}

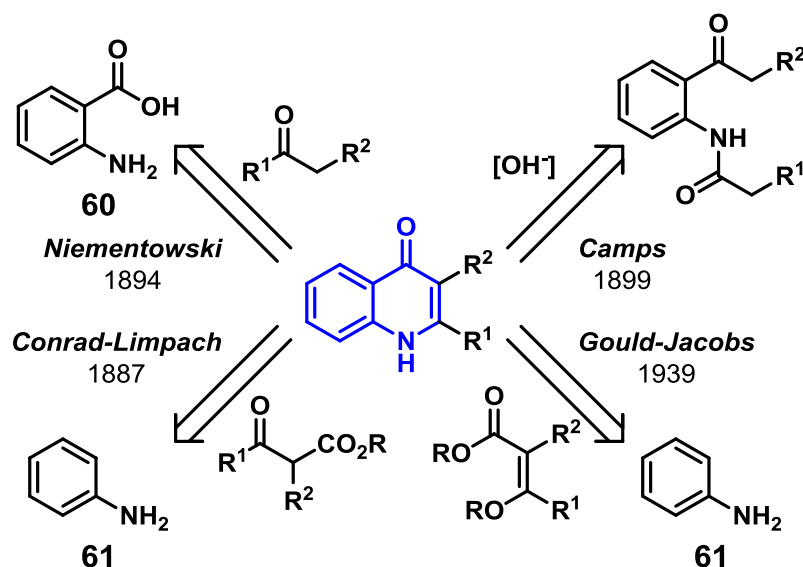


Figure 32 Selected fundamental routes to quinolones from aniline derivatives

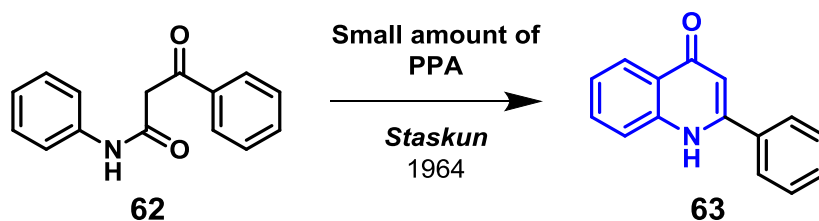
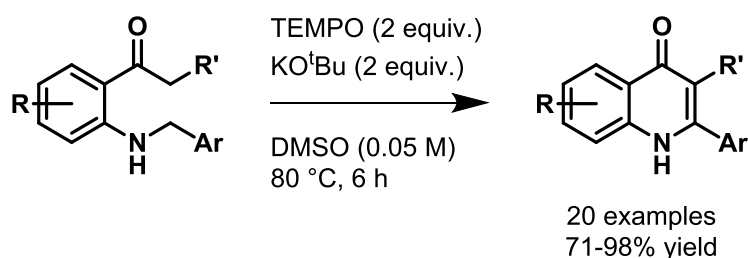


Figure 33 Staskun *et al.* adaptation of Knorr quinolone synthesis

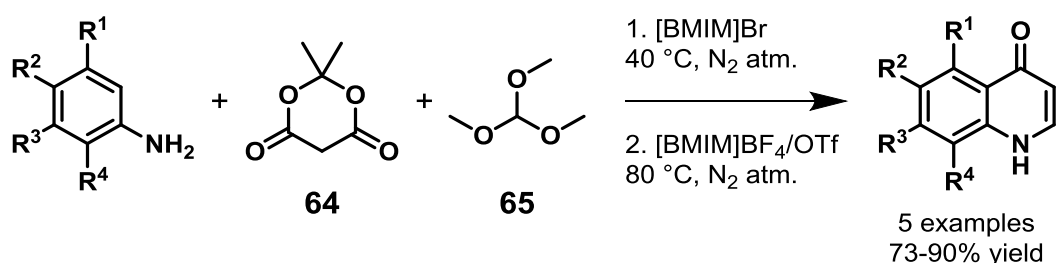
Early routes to quinolones, such as those depicted in Figures 32 & 33, normally require harsh conditions; this is due to the frequent need to disrupt the aromaticity of the phenylene linker from the aniline-based reagent to undergo cyclisation, or to augment reactivity of a functional group such as a carboxylic acid. As such, methodology has been developed over the subsequent years to eradicate the need for such harsh conditions; like early methods, aniline derivatives have also been used as starting materials. Long and co-workers devised a transition metal free intramolecular oxidative C(sp³)-H/C(sp³)-H coupling to form 2-aryl-4(1*H*)-quinolones (Scheme 14).⁶⁸



Scheme 14 Long *et al.* synthetic route to 2-aryl-4(1*H*)-quinolones via an oxidative Mannich reaction

Oxidation of the amine to the imine by TEMPO occurs followed by nucleophilic addition of the enolate formed at the ketone on the adjacent carbon atom on the arylidene linker; subsequent *in situ* oxidation of the formed tetrahydroquinoline intermediate formed the products in good to excellent yields. This route not only offered a structurally diverse library of products, but also offers an alternative greener approach to their synthesis utilising chemistry which manages to circumvent the need for toxic reagents and potentially dangerous reaction conditions.

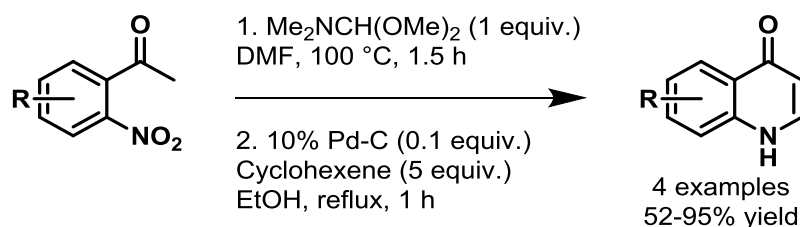
Yadav and his co-workers utilised ionic liquids as solvents in their milder method for quinolone synthesis from aniline derivatives, Meldrum's acid **64** and trimethyl orthoformate **65** (Scheme 15).⁶⁹



Scheme 15 Yadav *et al.* synthetic route to 2,3-unsubstituted-4(1*H*)-quinolones in RTILs

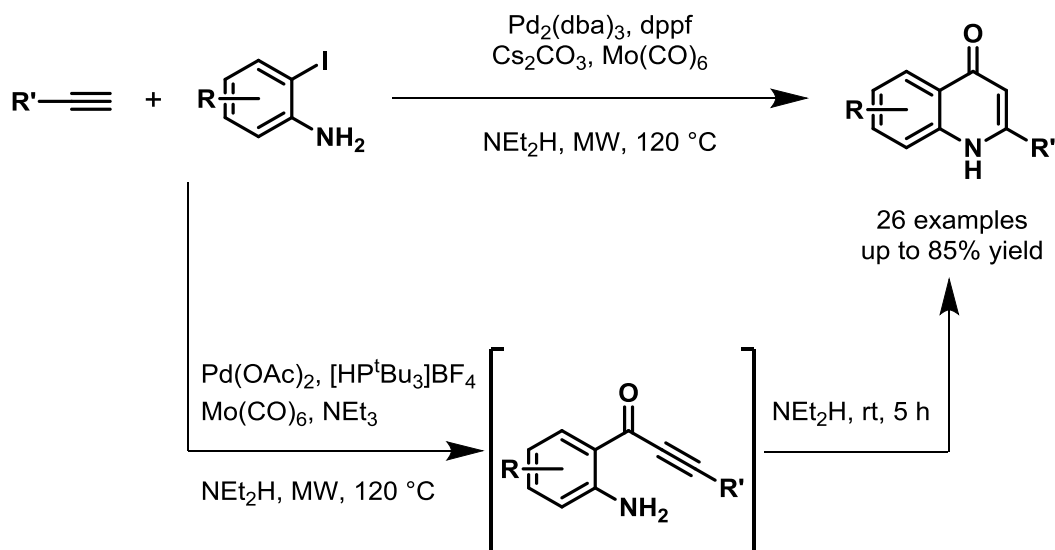
This route, like that of Long and co-workers, offers a more environmentally friendly alternative to the existing conditions. Reaction of Meldrum's Acid **64** and trimethyl orthoformate **65** forms a methoxymethylene intermediate to which aniline adds via Michael addition; subsequent ring closure and decarboxylation forms the products in good to excellent yields. Interestingly, the counteranion in the ionic liquid solvent has a drastic effect on the reaction; the ring closure does not occur when bromide is present, while total conversion to the desired product is observed when tetrafluoroborate or trifluoromethanesulfonate are used.

As well as aniline derivatives, the synthesis of quinolones from 2'-nitroacetophenone derivatives developed by Koskinen and co-workers affords the quinolone product *via* sequential installation of the unsaturated enone moiety followed by hydrogenation of the nitro-substituent to the amine which undergoes an intramolecular Michael addition to form the quinolone product (Scheme 16).⁷⁰



Scheme 16 Koskinen *et al.* synthetic route to 4(1*H*)-quinolones from 2'-nitroacetophenones

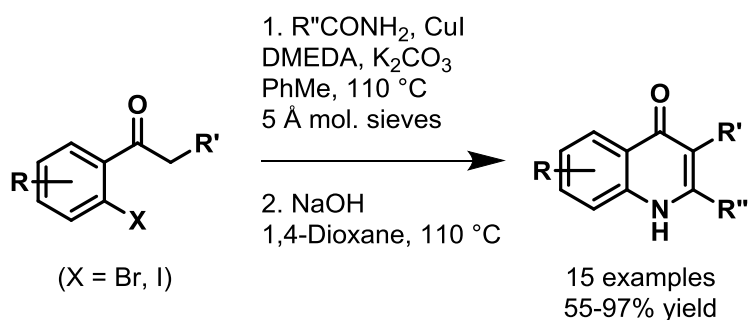
Other methods for affording quinolones have utilised transition metal catalysis and cross-coupling reactions; more than one option exists regarding which bond can be formed within the quinolone core mediated by the metal during the transformation, be this the bond between the nitrogen atom and the arylidene linker, the carbon-carbon double bond in the α,β -unsaturated enone moiety or the carbon-carbon bond between the arylidene linker and the carbonyl moiety. Larhed and co-workers implemented a one-pot carbonylative Sonogashira cross-coupling affording an extensive range of 2-substituted quinolone compounds (Scheme 17).⁷¹



Scheme 17 Larhed *et al.* synthetic route to 2-substituted-4(1*H*)-quinolones *via* ynone intermediates

The formation of two carbon-carbon bonds - firstly between the aryl ring and the carbon atom from the carbon monoxide and subsequently between the newly formed carbonyl moiety and the terminal carbon atom from the alkyne - affords an ynone intermediate; this then undergoes a sequential intermolecular-intramolecular dual aza-Michael addition cascade to form the quinolone product.

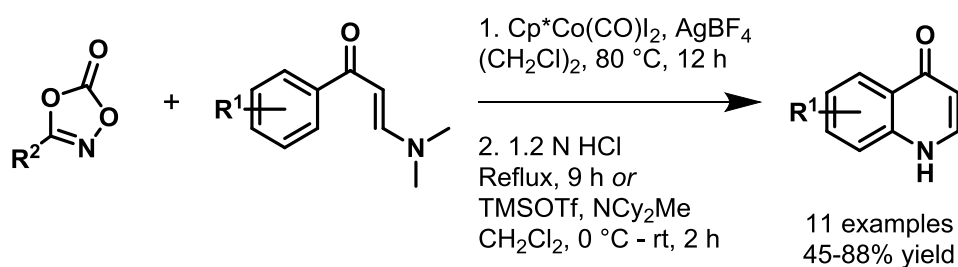
Buchwald and co-workers opted to form the phenylene carbon-nitrogen bond *via* a copper catalysed cross-coupling reaction to form an acetanilide intermediate which was then cyclised in a similar fashion to the Camps synthesis (Scheme 18, Figure 32).^{64,72}



Scheme 18 Buchwald *et al.* synthetic route to 2-aryl-4(1*H*)-quinolones from *o*-halophenones

The first step of this two-step process affords the amide. The second step proceeds *via* enolate formation and intramolecular nucleophilic condensation of the amide forming the heterocyclic portion of the molecule.

As well as these methods, a cobalt(III)-mediated C-H amidation has been devised by Zhu and co-workers to form acetanilide derivatives which can then be cyclised under acidic conditions to the desired quinolone products (Scheme 19, Figure 34).⁷³ The first step involves the formation of the acetanilide intermediate which then undergoes cyclisation *via* the familiar intramolecular Michael addition as seen in the work of Koskinen and Larhed.^{70,71}



Scheme 19 Zhu *et al.* synthetic route to 2,3-unsubstituted-4(1H)-quinolones *via* cobalt-catalysed C-H amidation

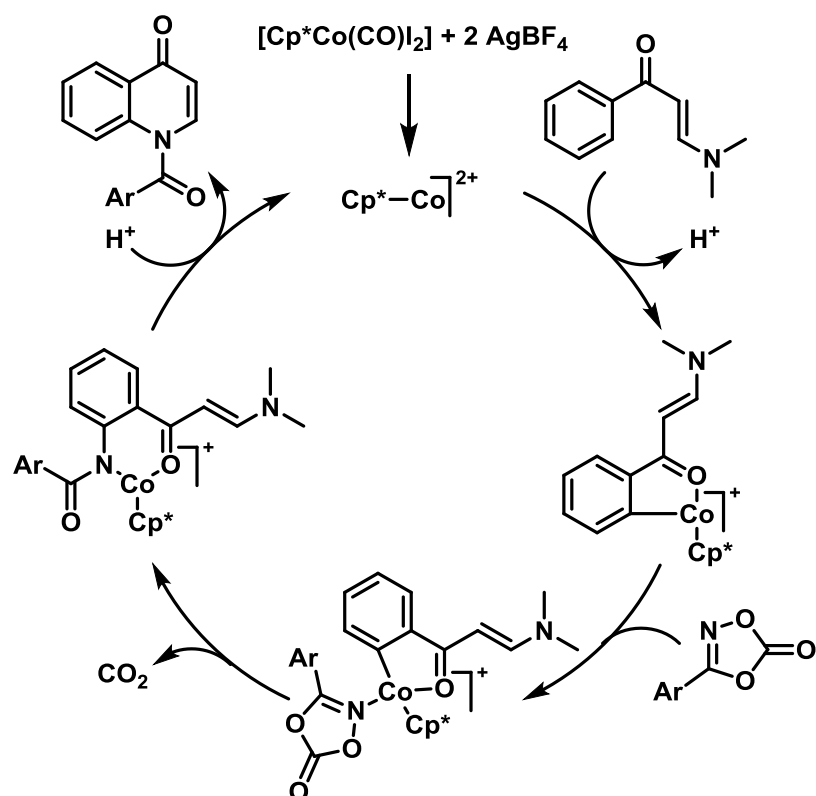


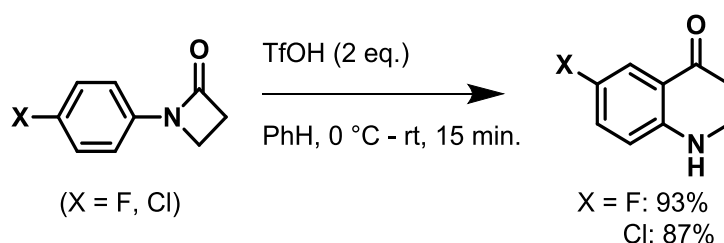
Figure 34 Proposed catalytic cycle for Co(III)-mediated C-H amidation

These examples are only a few from a voluminous repertoire of synthetic routes to quinolone structures lending further credence to their desirability as small molecule fragments. However, modifications to the aromatic core would give rise to a new set of structurally diverse molecules; with such a wide array of research existing for fully sp^2 -hybridised compounds, facile synthesis of sp^3 -hybridised derivatives represent a challenge that could enable interaction with previously inaccessible biological targets and their associated diseases. As such, research into the synthesis of these compounds may elicit valuable outcomes for the furtherment of small molecule-based drug discovery.

2.1.3 General Synthetic Routes to Racemic and Enantioenriched sp^3 -Hybridised Quinolone Derivatives

One of the primary focuses of early stage drug discovery in recent years has been the synthesis of structurally diverse novel molecules. Numerous methods exist to achieve this goal such as combinatorial database generation, cheminformatics and high-throughput screening; multiple reviews accompany these efforts attesting to their importance in the development of compounds for therapeutic applications.^{74–78} Academic interest has stretched as far as MacMillan and co-workers enacting *accelerated serendipity* for the sole purpose of discovering molecular transformations that could not otherwise have been designed; this has already yielded interesting results and enabled access to novel compounds *via* an unconventional route.⁷⁹

As previously mentioned, sp^3 -hybridised molecules are conspicuous in their scarcity due to the popularity of two-dimensional molecules in previous decades. Incorporating sp^3 -hybridisation into the quinolone structure would therefore provide a route to attractive, structurally diverse molecules based on scaffolds derived from molecules shown to have biological activity. Efforts, though success has been achieved, are not well documented. Tepe and co-workers successfully synthesised two 2,3-dihydro-4(1*H*)-quinolone compounds from *N*-aryl- β -lactams *via* an intramolecular Friedel-Crafts acylation in a simple one-step procedure (Scheme 20).⁸⁰



Scheme 20 Tepe *et al.* synthetic route to dihydroquinolones from *N*-aryl- β -lactams

The original aim of the work within this manuscript was intramolecular Friedel-Crafts acylations to form 3-amino-1-phenyl-1-propanone derivatives from unsubstituted 2-azetidinone. Nevertheless, the two *N*-aryl- β -lactam starting materials implemented in the reaction did undergo intramolecular cyclisation forming two 2,3-dihydro-4(1*H*)-quinolone derivatives.

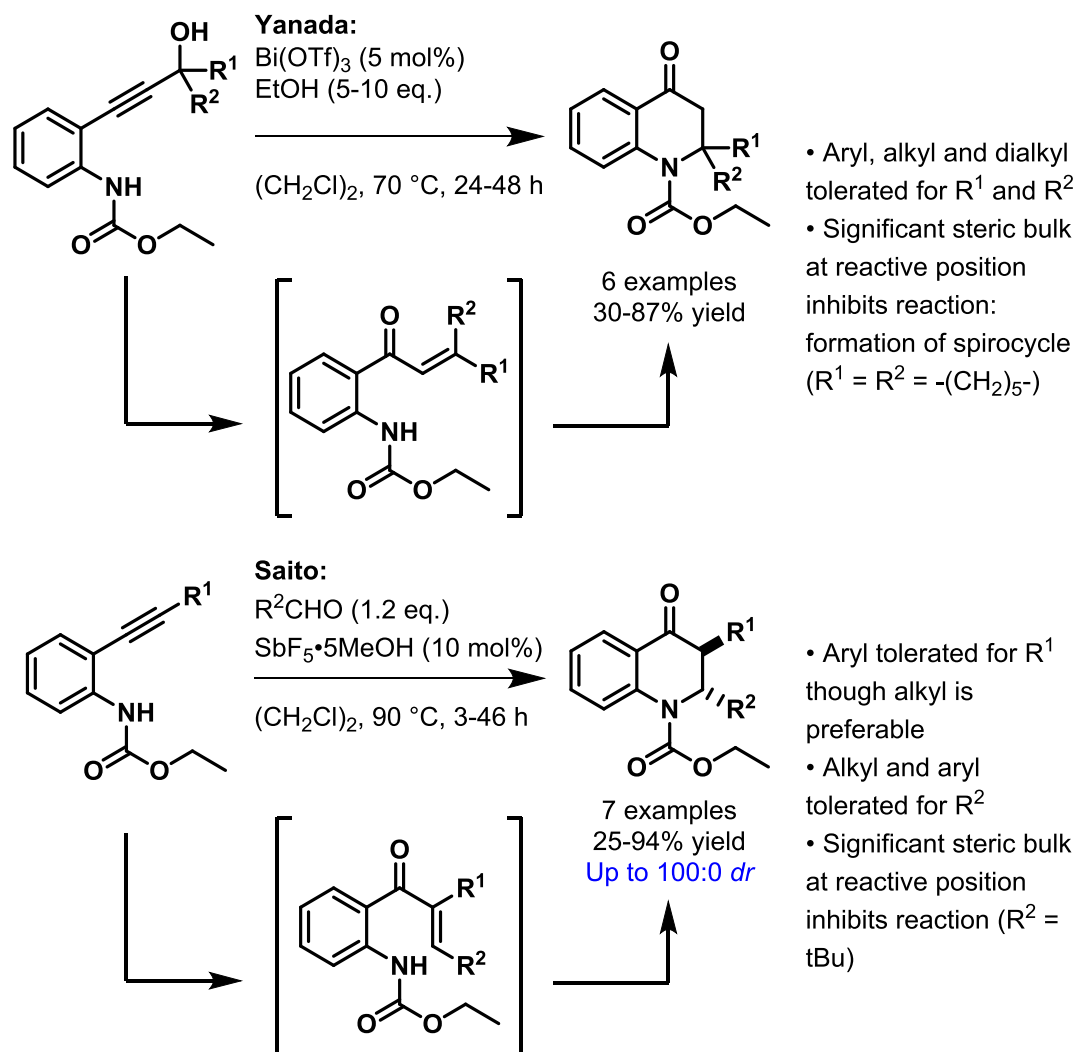
Another route to the dihydroquinolone is an intramolecular aza-Michael addition, a method used by both Su and Belfaitah (Scheme 21).^{81,82}



Scheme 21 Su and Belfaitah's intramolecular aza-Michael additions to form dihydroquinolones

The method employed by Su involved activation of the enone *via* grinding of the starting material and ytterbium (III) trifluoromethanesulfonate charged silica gel followed by elution over silica gel with no work-up required affording the products in excellent yields of 75-98% across 15 examples and a broad range of functional group tolerances. The results obtained by Belfaitah displayed similarly good yields of 70-95% across 8 examples and a comparable range of functional group tolerances, whilst also affording the desired products in a shorter timeframe.

Furthermore, *in situ* generation of the α,β -unsaturated enone followed by the subsequent aza-Michael addition has successfully been performed by Yanada and Saito enabling access to a wider variety of products (Scheme 22).⁸³⁻⁸⁵

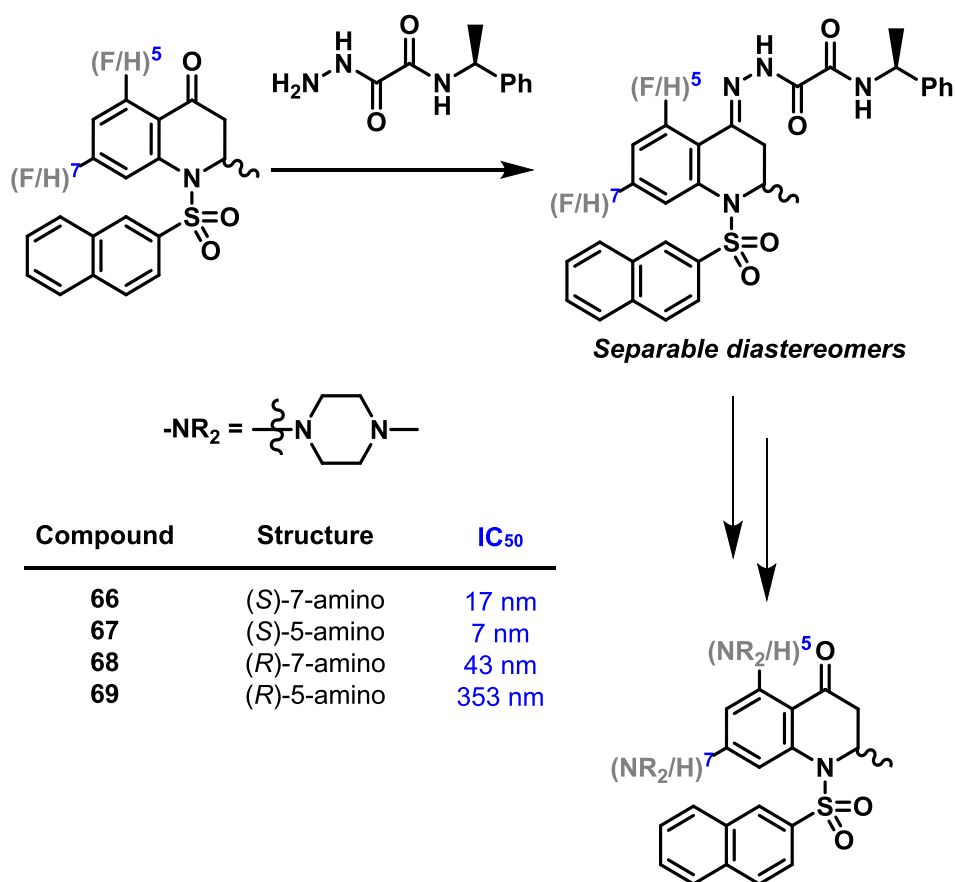


Scheme 22 Saito and Yanada's synthetic routes to dihydroquinolones *via in situ* generation of the α,β -unsaturated enone intermediate

The methodology developed by Yanada *et al.* uses substrates that can be easily accessed in two steps from readily available starting materials which undergo a novel intramolecular Meyer-Schuster reaction to form the α,β -unsaturated enone intermediate which goes on to afford the desired 2,3-dihydro-4(1*H*)-quinolone products in moderate to excellent yields. The formation of the spirocyclic derivative proved challenging with this chemistry, although the synthesis of this product had not previously been reported. Saito *et al.* developed a one-pot metal-catalysed [2+2] cycloaddition and cycloreversion to form differently substituted α,β -unsaturated enone intermediates which undergo the analogous intramolecular Michael addition reaction. The substitution pattern of these products gives rise to two stereocentres; although the stereoselective variation of this reaction was not performed, diastereoselectivity was observed for the majority of these transformations. Additionally, isolation of the enone

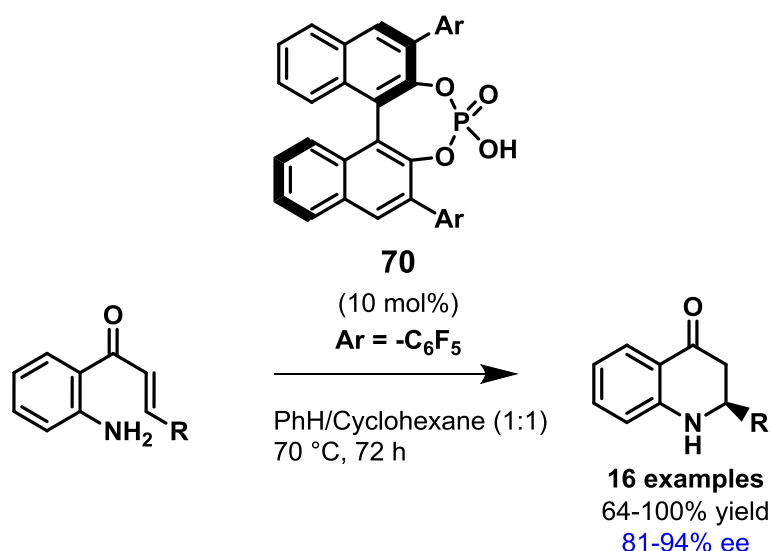
intermediate followed by cyclisation of the purified product afforded the desired products exhibiting similarly excellent yields and diastereoselectivity.

Park and co-workers were able to separate enantiomers *via* a diastereomeric semioxamazide derivative (Scheme 23).⁸⁶ The compound in question was shown to be an effective ligand for 5-HT₆ serotonin receptors. Furthermore, the (*S*)-enantiomer derivatives **66** and **67** showed lower IC₅₀ values than those pertaining to the (*R*)-enantiomer derivatives **68** and **69**, particularly in the case of **67** further suggesting enantioselective 2,3-dihydro-4(1*H*)-quinolone derivatives would be good candidates for drug discovery fragments.



Scheme 23 Park *et al.* isolation of variably biologically active individual enantiomers *via* diastereomeric separation

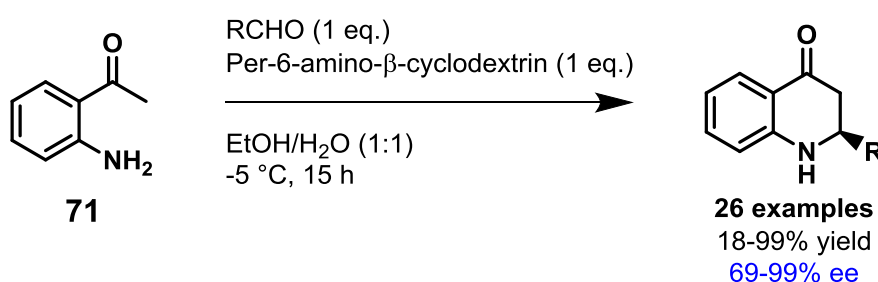
Whilst chiral resolutions are an effective way of acquiring enantiopure molecules, the major drawback is the loss of 50% of the synthesised material; enantioselective routes have also been devised. Akiyama used an intramolecular conjugate addition in which enantioselectivity was obtained by using chiral phosphoric acid **70** derived from BINOL as a Brønsted acid organocatalyst (Scheme 24).⁸⁷ This reaction was based on previous research into organocatalysed route to dihydroquinolone derivatives by Yu, Rueping and Lu.^{88–90}



Scheme 24 Akiyama *et al.* Brønsted acid catalysed cyclisation of 2'-aminochalcones

The incorporated substituents at the chiral centre of the product (labelled **R**) were substituted phenyl or heterocyclic in nature; the one exception was the *tert*-butyl substituted derivative was successfully synthesised, albeit in a lower yield of 64% with 88% ee. The low enantioselectivity of the reaction with less sterically encumbered alkyl substituents may explain the lack of these examples within those described in the paper.

Pitchumani and co-workers were able to synthesise highly enantioenriched dihydroquinolone derivatives in one-pot from 2'-aminoacetophenone **71** and selected substituted benzaldehydes by using a solid-supported base catalyst based on β -cyclodextrin (Scheme 25).⁹¹

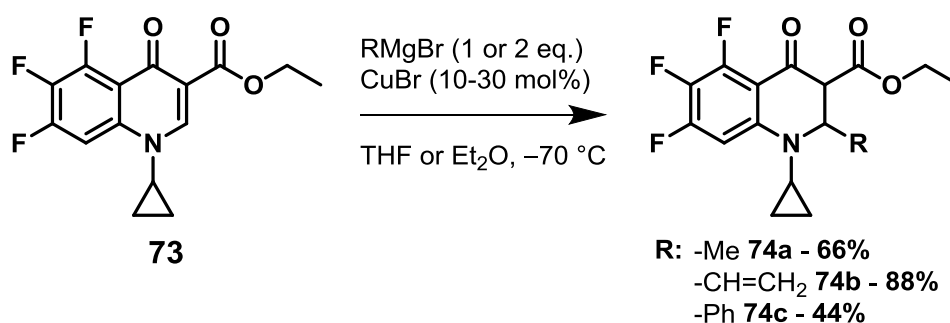


Scheme 25 Pitchumani *et al.* pseudo-Mannich cyclisation

The wide range of methodologies to these cores highlights their relevance in a research capacity. However, the primary limitation is that many of the existing syntheses, including those previously described, require incorporation of desired functionality at an early stage. Late stage functionalisation of biologically relevant molecules is preferable as a greater number of derivatives can be synthesised from a

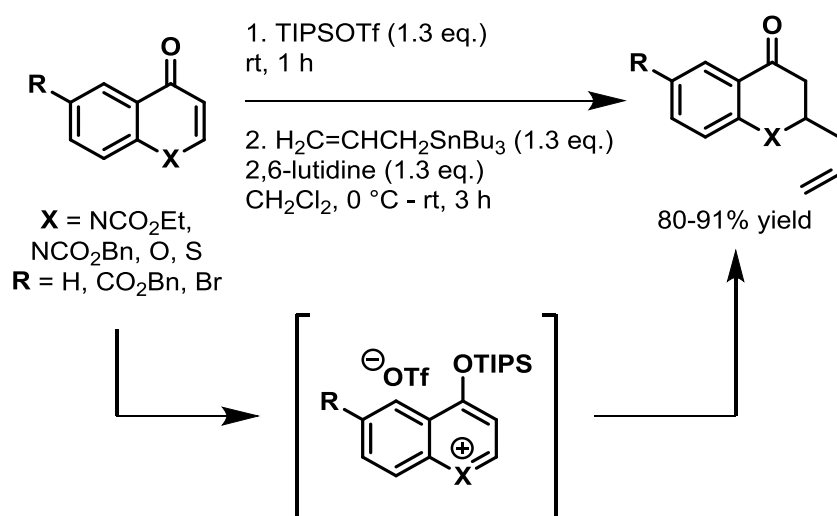
common intermediate. As such, methodology where derivatives are synthesised directly from the extensively researched 4(1*H*)-quinolone core would be highly desirable from a drug discovery standpoint.

performed by Kiley and co-workers to form substituted derivatives **74a-c**, a method also used by Clémencin-Le Guillou and co-workers in their synthesis of similar cores (Scheme 27).^{93,94}



Scheme 27 Kiely *et al.* conjugate addition of Grignard reagents to quinolone core **73**

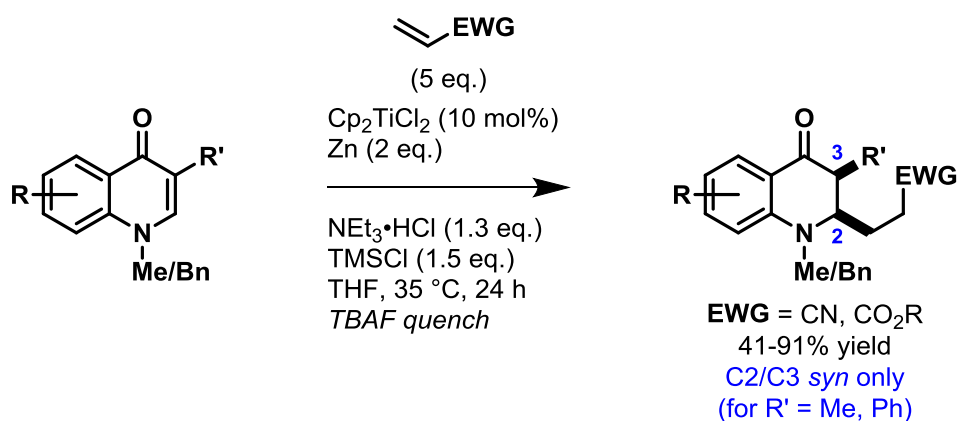
An interesting variation of the conjugate addition of organometallic reagents to these quinolone cores was performed by Beifuss and co-workers in 2001 based on earlier research conducted in their group (Scheme 28). The formation of a quinolinium intermediate followed by addition of organotin reagents led to formation of similar derivatives, though in a 1,2-addition rather than a 1,4-addition.^{95,96} The reaction was also successful on benzopyrylium and benzothiopyrylium derivatives.



Scheme 28 Beifuss *et al.* 1,2-addition of allyltributyltin to quinolinium intermediate

Although not strictly a conjugate addition reaction, this example elucidates an alternative for the elaboration of quinolone cores. The addition of an allyl substituent to this core is also unprecedented, implying alternatives to conventional organometallic reagents may be more suitable for more challenging variants of this transformation.

Another conjugate addition to quinolone cores was performed by Streuff and co-workers using a reductive umpolung strategy with activated alkenes (Scheme 29).⁹⁷



Scheme 29 Streuff *et al.* umpolung reductive coupling between activated alkenes and quinolone cores

The mechanism of this transformation has been postulated (Figure 36).

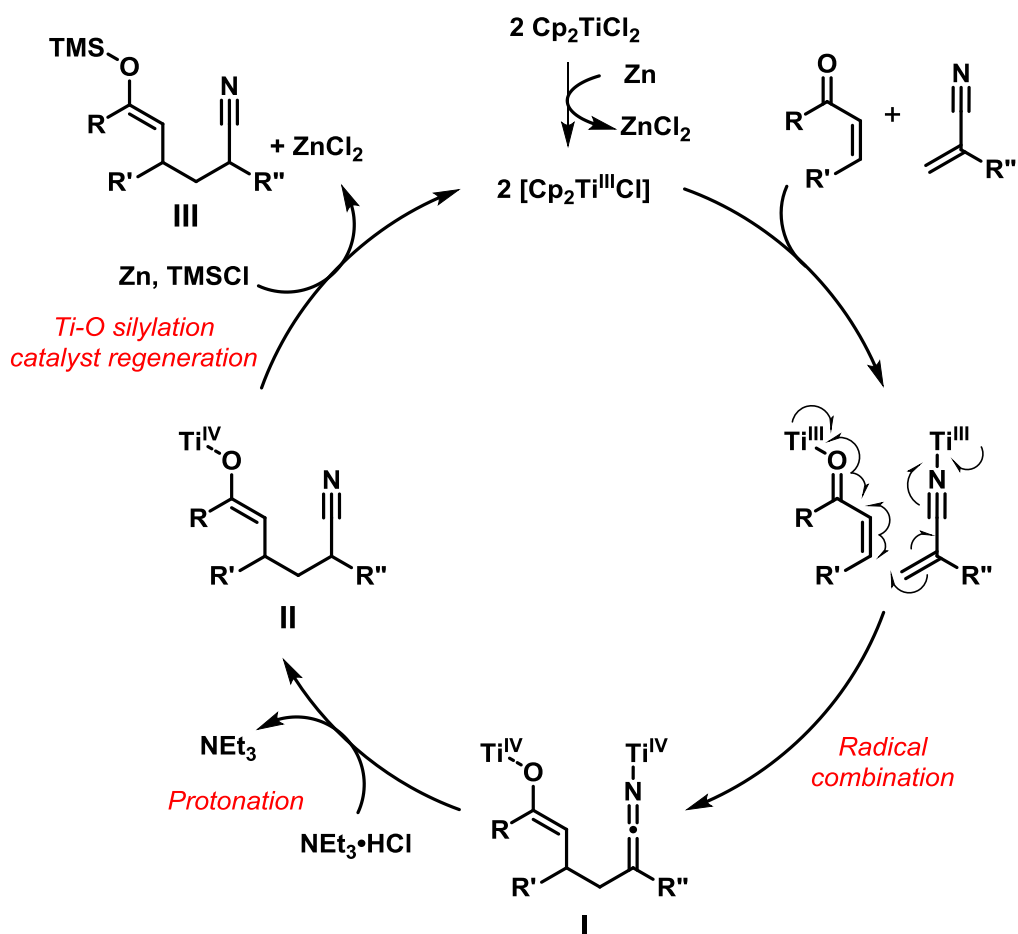


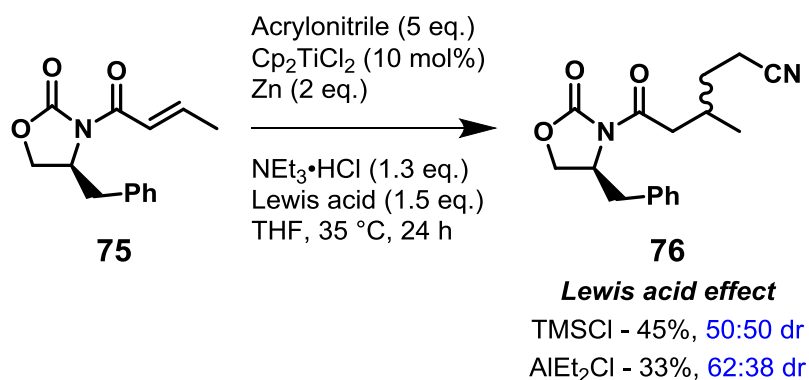
Figure 36 Mechanism for Streuff *et al.* reductive coupling

The formation of a titanium-(III) species *via* reduction of titanocene dichloride with elemental zinc is followed by co-ordination of the nucleophile to the titanium-(III) species. Radical combination of this complex with the quinolone starting material leads

to formation of the carbon-carbon bond, as seen in species **I**. Subsequent reductive elimination of the titanium enolate **II** with zinc and trimethylsilyl chloride reformed the active catalyst and afforded the silyl enolate product **III**.

The choice to quench the reaction with tetrabutylammonium fluoride at low temperatures facilitates kinetic control of the reaction and led to isolation of the desired ketone product alone; further side reactions were observed when an alternative quench with hydrochloric acid was used affording different products. Development of methodology to this effect was continued in other examples of work by Bichovski.⁹⁸

Attempts at achieving diastereoselectivity for the addition to substituted quinolone cores were successful, though the methodology could not be used effectively with simpler substrates in conjunction with a chiral auxiliary (as shown in the conversion from compound **75** to compound **76**) to afford highly diastereoenriched products (Scheme 30).⁹⁷ Nominal diastereoselectivity was observed when pre-co-ordination of the substrate with diethylaluminium chloride was performed, though the result was deemed insufficient for further development.



Scheme 30 Streuff *et al.* attempts to perform reaction diastereoselectively

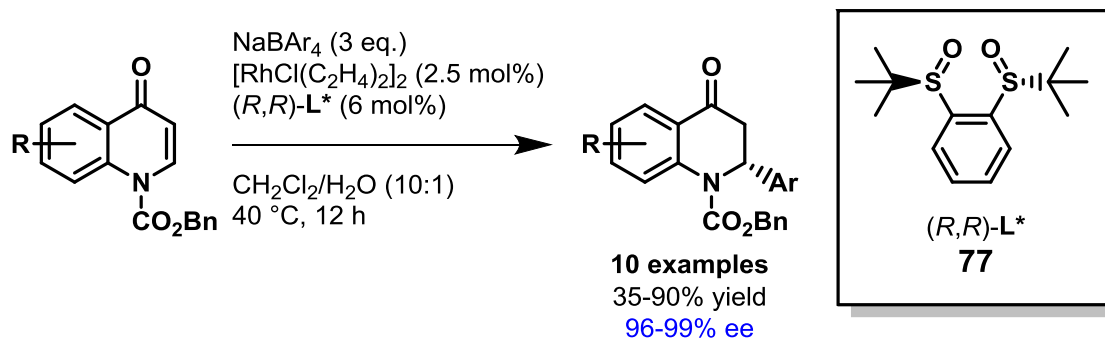
Despite the precedents for racemic conjugate addition to quinolone cores, the literature contains only a small number of successful enantioselective variants of this nature. The first successful asymmetric conjugate addition to quinolones was performed by Hayashi and co-workers in 2005 using arylzinc chlorides and a rhodium(I) catalyst (Scheme 31).⁹⁹



Scheme 31 Hayashi *et al.* conjugate addition of arylzinc chloride reagents to quinolone cores

Excellent enantioselectivity was observed across the range of entries in this study, though 2-methylphenyl chloride did exhibit slightly poorer enantioselectivity at 86% ee implying a steric effect may exist. 4-Methoxyphenylzinc chloride was similarly less enantioselective in comparison to nucleophiles bearing electron neutral or donating substituents at 88% ee further suggesting an electronic effect from the nucleophile on the transformation. Further examples would be needed to illuminate a more definitive trend in this regard; a greater number of substrates trialled in the reaction would also help to elucidate its effect on the reaction process. Nevertheless, these results provided a suitable platform from which to develop similar methodology accessing 2,3-dihydro-4(1*H*)-quinolone structures.

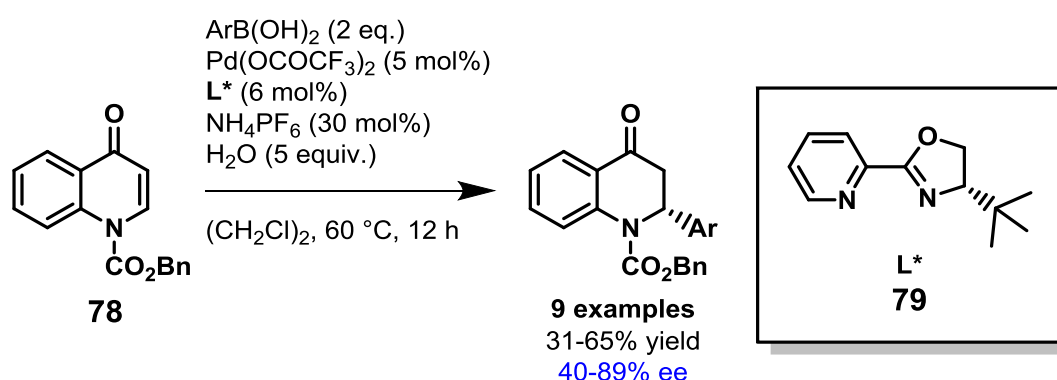
Subsequent attempts at asymmetric conjugate addition to quinolone cores have appeared, though there are only very few published examples. Liao and co-workers successfully performed another rhodium (I) catalysed conjugate addition to quinolones with chiral ligand **77** in 2011, this time using tetraarylborate salts (Scheme 32).¹⁰⁰ This addition was also applicable to chromones affording enantioenriched flavanone derivatives.



Scheme 32 Liao *et al.* conjugate addition of sodium tetraarylborate salts to quinolone cores

Whilst an improvement in the enantioselectivity over the analogous addition of arylzinc reagents by Hayashi is observed, the narrow range of tetraarylborate salts that are commercially available mean substrate scope has not been extensively explored by Liao *et al.*; excellent enantioselectivity is seen for all nucleophiles, though sodium tetra(4-fluorophenyl)borate did only afford the product in 35% yield. No significant trend based on substrate scope is observed as relatively few were trialled.

This was followed by research by Stoltz and co-workers in 2013, in which they performed palladium(II) catalysed conjugate addition of arylboronic acids to quinolone core **78** with chirality induced *via* addition of ligand **79** (Scheme 33).¹⁰¹ Similarly to Liao, this methodology could also be applied to chromones.

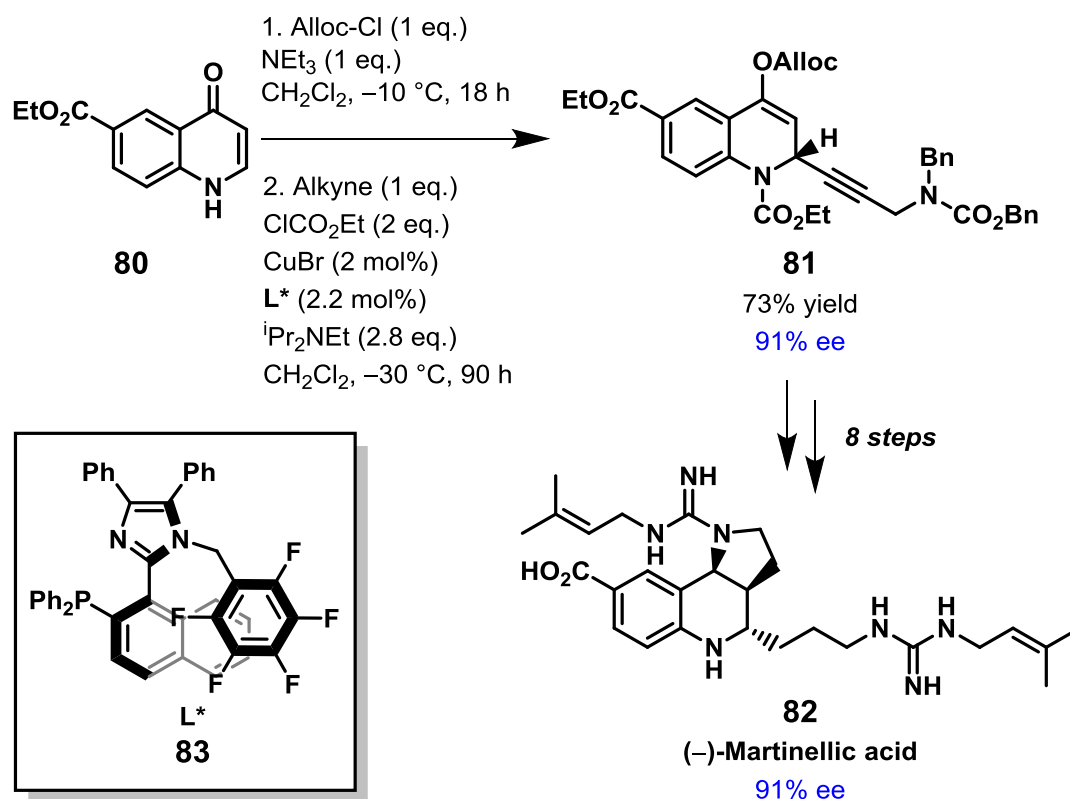


Scheme 33 Stoltz *et al.* conjugate addition of arylboronic acids to quinolone core **78**

Because of their broad commercial availability, the use of boronic acids in this methodology permits access to a range of different products. While only quinolone substrate **78** was used in the reaction, a range of substituted phenylboronic acids were used and tolerated within the reaction, with electron-rich substituents in *meta*-positions affording more enantioenriched products (80-85% ee). A significant decrease in enantioselectivity was observed when the same substituents were placed in the *para*-position on the phenylboronic acid implying a strong electronic effect from the nucleophile in the transformation. Additionally, a drastic reduction in enantioselectivity was observed when the larger dibenzo[*b,d*]furan-4-ylboronic acid was used, implying a steric disruption in the transition state can affect the reaction. Alternative boron nucleophile species such as boronate esters or potassium trifluoroborates were not trialled in the reaction.

One prevailing limitation of these transformations is the scope of the addition reagent: the methodology has only been used to yield aryl-substituted derivatives. Another is the use of catalyst based upon a rare, precious transition metal. One example of an attempted asymmetric conjugate addition of a non-aryl substituent to a quinolone core

80 utilising a cheaper copper(I) catalyst was developed by Aponick and co-workers in 2015 towards the synthesis of (-)-martinellic acid **82** (Scheme 34).¹⁰²



Scheme 34 Aponick *et al.* total synthesis of (-)-Martinellic acid **82** via conjugate addition to quinolone core

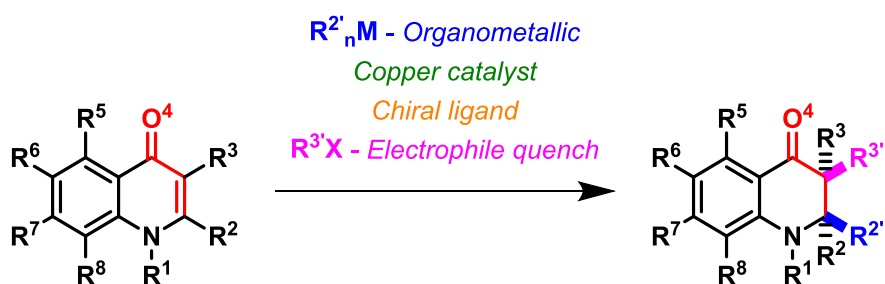
Mechanistic studies showed the reaction pathway actually proceeded from the quinoline-4-carbonate in a 1,2-addition pathway similar to the work by Beifuss *et al.* as opposed to a 1,4-addition to the quinolone.⁹⁵ Thus, the isolated quinoline-4-carbonate was used in the addition to form **81** with high enantioselectivity, which is retained in the final product.

While some success has been obtained with copper catalysed addition of sp³-hybridised alkyl substituents to chromone and coumarin cores, there is a complete absence of analogous additions to quinolone cores.^{103–106} Herein lies a description of methodology towards the copper-catalysed enantioselective synthesis of dihydroquinolone derivatives *via* conjugate addition of alkyl organometallic reagents.

2.2 Project Aims

Existing methodology for organometallic asymmetric conjugate addition reactions with quinolone cores use expensive metal catalysts and is limited in its scope, thus only affording arylated derivatives.^{99–101} Development into an alkylation and alkenylation of quinolone substrates *via* a similar route would yield novel compounds which could be used in fragment-based drug design in the pharmaceutical sector based on their desirable properties. The utilisation of a copper catalyst for this transformation is not only desirable from an economic standpoint, but also from the vast array of existing research attesting to its efficacy in asymmetric conjugate addition reactions. As well as this, further functionalisation can be performed on the products; a second chiral centre in the molecule on the adjacent carbon atom enables further access to unexplored areas of chemical space.

In summary, described in this report is the development of methodology towards the enantioselective late-stage functionalisation of desirable quinolone cores *via* copper catalysed asymmetric conjugate addition affording novel derivatives with potential biological applications (Scheme 35).



Scheme 35 General scheme for proposed asymmetric conjugate addition to quinolone cores

2.3 Results and Discussion

2.3.1 Synthesis of Unsubstituted Quinolone Substrate Cores and Organometallic Addition

Within our group, copper-catalysed asymmetric conjugate addition has been studied extensively over recent years.^{13,107–112} The group has even applied this chemistry to benzo-fused heterocyclic cores, successfully affording enantioenriched coumarin derivatives.¹⁰⁴ Routes to the quinolone substrates were present in the literature from the aforementioned successful rhodium and palladium catalysed arylations.^{99–101} Accessing molecules which have been successfully used in these types of reactions could therefore proceed immediately.

For simplicity, the original starting point was the quinolone core **78** used by Stoltz *et al.* in their asymmetric conjugate additions; this was also used by Hayashi and Liao amongst others.^{99–101} This core was chosen for the following reasons:

- Successful asymmetric conjugate additions to **78** already exist
- Ease of access due to existing chemistry affording **78**
- Lack of substitution prohibits steric or electronic effects from any functionalities other than that present in all quinolone molecules

The choice of organometallic reagent for the transformation was the first point of consideration (Table 5). Initial attempts at non-enantioselective conjugate addition were performed using ZnEt₂. Unfortunately, no conversion to the desired product **84** was observed. AlEt₃ did add to **78**, though conversion to **84** was poor and the isolated yield was low.

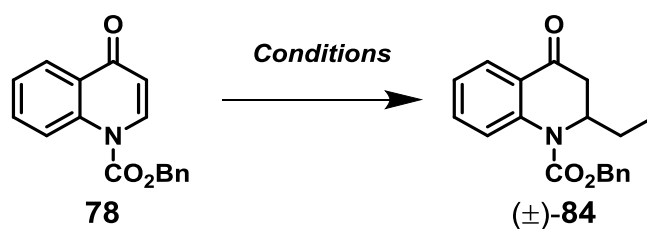


Table 5 Screened conditions for the conjugate addition reaction

| Entry | R _n M | Cu | Ligand | Solvent | T (°C) | Time (h) | Yield (%) |
|-------|-------------------------------|--|--|--------------------------------|------------|-------------|-------------------|
| 1 | ZnEt ₂ (2.5) | Cu(OAc) ₂ (0.04) | P(OPh ₃) (0.08) | Et ₂ O | -10 | 20 | - |
| 2 | ZnEt ₂ (2.5) | Cu(OAc) ₂ (0.04) | P(OPh ₃) (0.08) | PhMe | -10 | 12 | - |
| 3 | ZnEt ₂ (2.5) | Cu(OAc) ₂ (0.04) | P(OPh ₃) (0.08) | THF | -10 | 12 | - |
| 4 | AlEt ₃ (2.5) | Cu(OAc) ₂ (0.04) | P(OPh ₃) (0.08) | THF | -10 | 18 | 36 |
| 5 | AlEt ₃ (2.5) | Cu(OTf) ₂ (0.04) | P(OPh ₃) (0.08) | THF | -10 | 18 | 24 |
| 6 | EtMgBr (2.2) | CuBr.SMe ₂ (1.1) | - | Et ₂ O/THF (1:1) | -78 – 20 | 1 | 31 ^[a] |
| 7 | EtMgBr (2.2) | CuBr.SMe ₂ (1.1) | - | THF | -60 – -20 | 0.5 | 65 |
| 8 | EtMgBr (2.5) | CuBr.SMe ₂ (0.05) | - | THF | -50 – -10 | 1.5 | 34 |
| 9 | EtMgBr (2.5) | CuBr.SMe ₂ (0.05) | - | (2-Me) THF | -78 | 0.08 | 75 |
| 10 | EtMgBr (2.5) | CuBr.SMe₂ (0.05) | PPh₃ (0.1) | (2-Me) THF | -78 | 0.08 | >99 |

^[a] Substrate was insoluble in Et₂O; THF added as co-solvent in order to solubilise the material

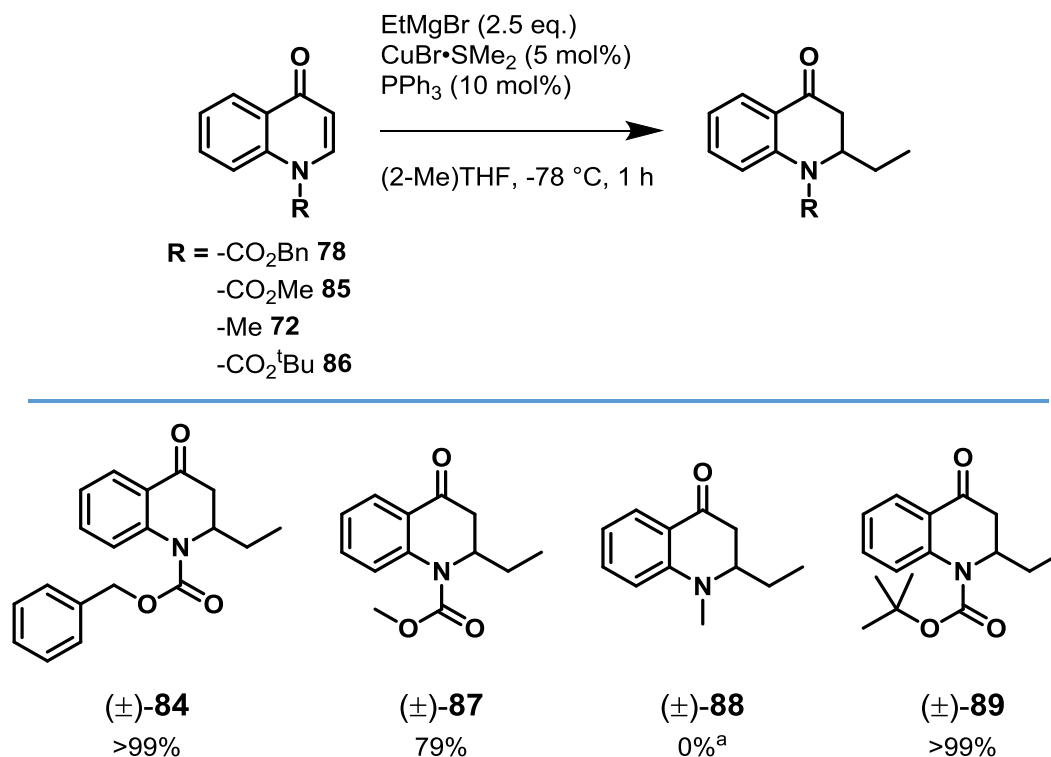
The failures of copper-catalysed addition of ZnEt₂ and AlEt₃ (Entries 1-5) led to the implementation of stoichiometric cuprates derived from Grignard reagents; these reagents are regarded as a relative certainty when considering conjugate addition reactions as the active alkyl-copper species is guaranteed to exist *in situ* which cannot be said for substoichiometric quantities of copper. This successfully afforded **84** and

allowed us to start contemplating a catalytic copper-organomagnesium system for the conjugate addition reaction. With the successful addition of the Grignard reagent seen with a catalytic copper additive in THF (Entry 8), further studies revealed effective conditions affording **84** in excellent yields when the reaction was performed in 2-methyltetrahydrofuran (Entry 9), a solvent previously used by Schmalz and co-workers for asymmetric conjugate addition using Grignard reagents.¹¹³ The further addition of a ligand to the mixture (Entry 10) led to quantitative formation of the product.

Alternative nitrogen protecting groups were also used on the quinolone core to uncover any additional effects this may have on conversion. With numerous different options at our disposal, certain structural features needed to be taken into consideration:

- The carbamate protecting group used in compound **78** will withdraw electron density from the nitrogen atom
- The size of the protecting group may also exhibit a steric effect on reaction progression

Considering these points, compounds **72**, **85** and **86** were trialed in the optimised conditions to see whether any steric or electronic effects were observed (Scheme 36).

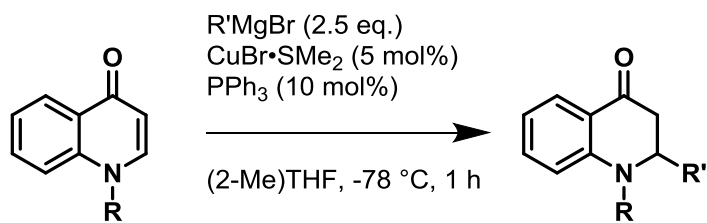


^a Starting material was insoluble in specified reaction conditions

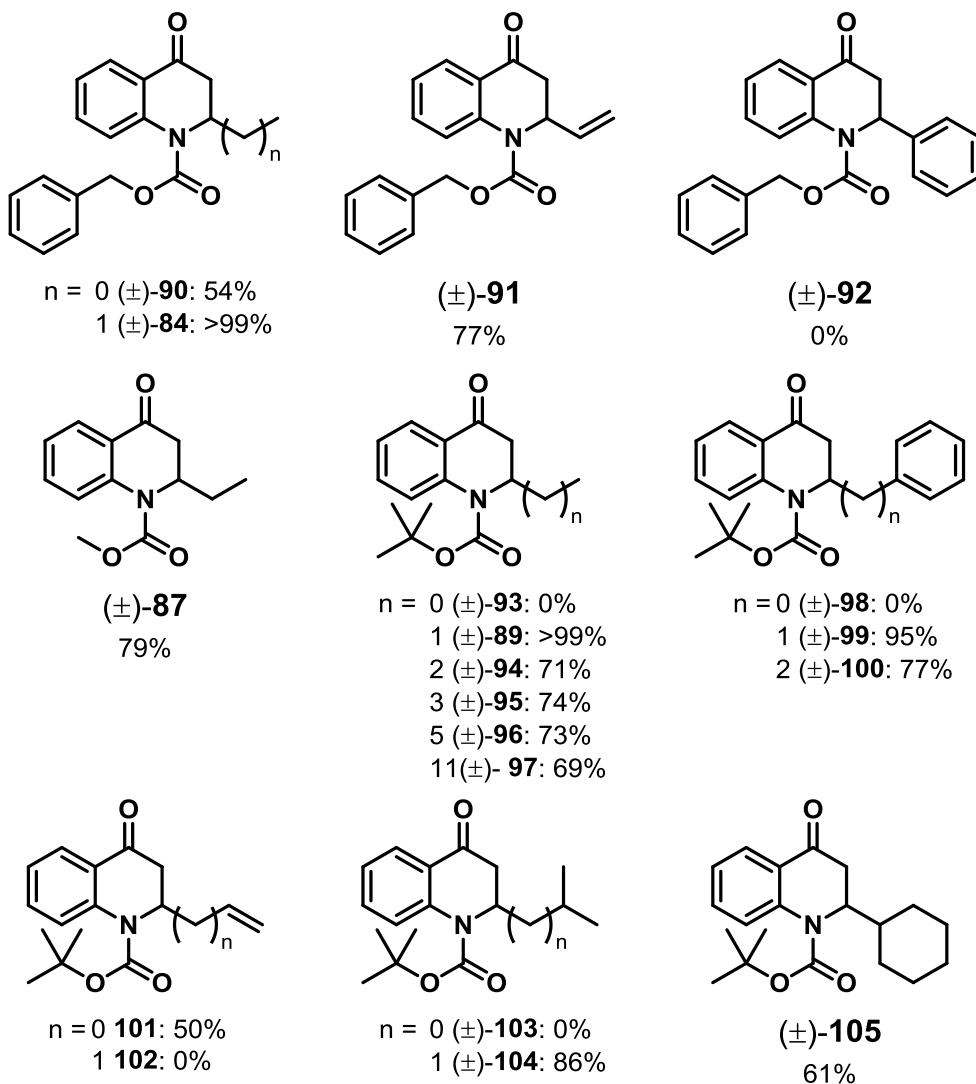
Scheme 36 Protecting group effect on conjugate addition to quinolone cores

Compounds **78** and **86** were successfully reacted under the optimised conditions affording compounds **84** and **89** respectively in almost quantitative yields. A slight decrease in yield of compound **87** for the reaction of compound **85** was observed, invalidating it as an alternative to compound **78**. Despite its success in the methodology devised by Hong *et al.*, no conversion of compound **72** to compound **88** observed.⁹² Its complete lack of solubility in the reaction solvent implies the electron withdrawing effect of the carbamate protecting group present in compounds **78**, **85** and **86** helps to reduce the polarity of the molecule; this in itself is desirable as solubility of quinolone molecules is poor. As such, development of methodology with electron poor nitrogen quinolone cores was selected as the foundation for further exploration.

The focus for reaction scope analysis was on alkyl and alkenyl Grignard additions adhering to the original project aim; additional reactions were trialled with aryl Grignard reagents to see the extent to which the methodology could be broadened (Scheme 37).



R = -CO₂Bn **78**
-CO₂Me **85**
-CO₂^tBu **86**



Scheme 37 Scope of conjugate addition reaction conditions with various Grignard reagents to prepare racemic products

Successful alkylation of both compounds **78** and **86** was observed for a wide range of alkylmagnesium bromide additions, as well as successful ethyl addition to compound **85**. Additionally, successful conversion to the vinylation product was observed in moderate yield. One observation that can be made is the failure of the addition allyl-

and isopropylmagnesium bromide to convert to compounds **102** and **103**; we cannot currently explain the poor performance of the latter. This becomes all the more interesting when both isobutyl- and cyclohexylmagnesium bromide successfully afforded compounds **104** and **105** respectively, suggesting branching of alkyl groups is not detrimental to the reaction. Another observation was the failure of the addition to both compounds **78** and **86** of the phenylmagnesium bromide to form compounds **92** and **98**, meaning this methodology could not be extended to afford these products.

With a wide range of racemic alkylated quinolone derivatives successfully synthesised, our focus shifted towards asymmetric addition of Grignard reagents (Table 6). While this has been successfully performed with other benzo-fused heterocyclic cores, no previous attempts at analogous additions to quinolones are documented at the time of writing.^{105,106}

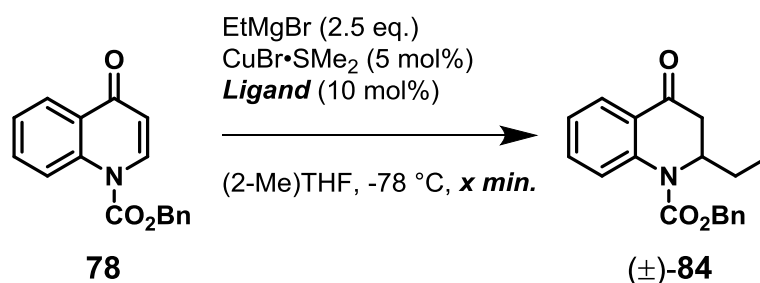


Table 6 Analysis of ligand acceleration of the conjugate addition reaction

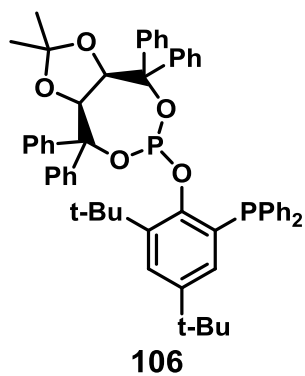
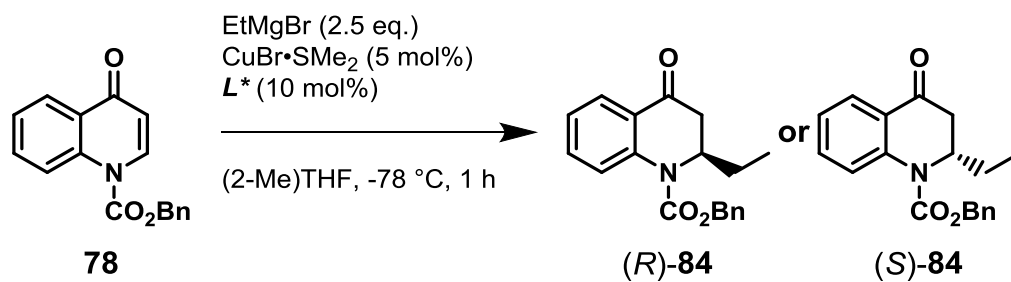
| Entry | Ligand | Time (min) | Conversion (%) ^[a] |
|-------|---------------------|------------|-------------------------------|
| 1 | None | 2.5 | 35 |
| 2 | PPh ₃ | 2.5 | 73 |
| 3 | PCy ₃ | 2.5 | 92 |
| 4 | P(OPh) ₃ | 2.5 | 88 |
| 5 | None | 5 | 61 |
| 6 | PPh ₃ | 5 | 96 |
| 7 | PCy ₃ | 5 | 98 |
| 8 | P(OPh) ₃ | 5 | 88 |

^[a] Starting material was insoluble in specified reaction conditions

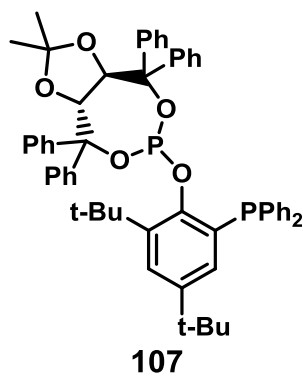
From the initial condition screening (Table 5), entry 13 shows an increase in the yield of compound **84** to almost quantitative yield from 80% for entry 12 when catalytic triphenylphosphine was added. As previously mentioned, mechanistic studies by

Schrader and co-workers in 2004 suggested phosphorus ligands aid in the reductive elimination of intermediate Cu(III) species to Cu(I) *via* lowering the activation barrier for this reduction during the conjugate addition process with alkylzinc reagents; rudimentary studies of our established conditions implied that ligand accelerated catalysis of the organomagnesium conjugate addition reaction could be achieved.³⁰ Further studies showed a nominal increase in the conversion to the desired conjugate addition product with different phosphorus-based ligands chosen due to their ubiquity for ligand accelerated catalysis (Table 6).

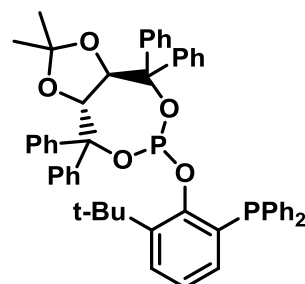
The electron density of the phosphorus atom within these ligands did not seem to have a marked effect on the reaction rate, only that it increased it compared to the conjugate addition in the absence of a ligand. A screen of chiral ligands in the established reaction conditions was performed in an attempt to achieve enantioselective conjugate addition (Scheme 38).



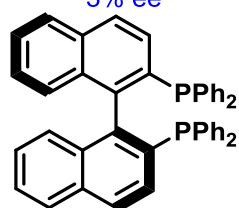
68% yield
3% ee



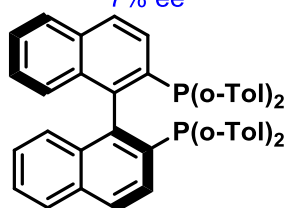
21% yield
7% ee



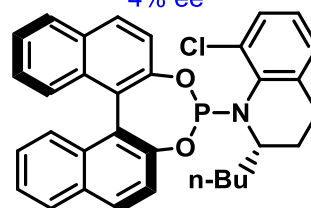
76% yield
4% ee



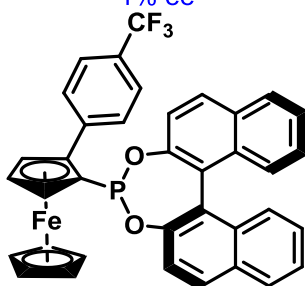
34% yield
1% ee



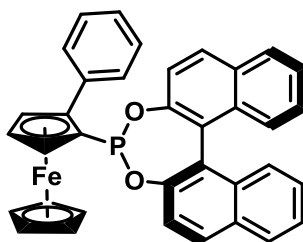
43% yield
9% ee



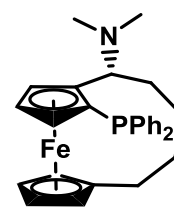
17% yield
0% ee



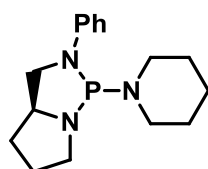
32% yield
11% ee



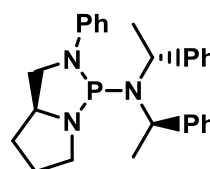
63% yield
0% ee



28% yield
5% ee



23% yield
4% ee



31% yield
6% ee

Scheme 38 Reaction scheme for chiral ligand screening

Unfortunately, no significant enantioselectivity was observed with any of the ligands used in the screen. One of the better performing ligands was compound **110**, though the yield suffered severely and enantioselectivity was still negligible at this point. Various reactions with this ligand were conducted to see whether other aspects such as solvent, equivalency, addition order or temperature could be playing a detrimental role in the poor enantioselectivity observed (Table 7).

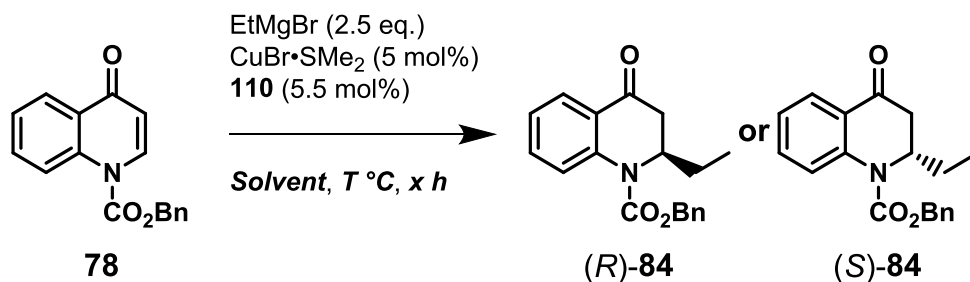


Table 7 Alterations to the conjugate addition reaction conditions

| Entry | Conditions | Yield (%)/ee (%) |
|-------|---|------------------|
| 1 | Et_2O , $-20 \text{ }^\circ\text{C}$, 20 h; slow addition of EtMgBr over initial 4 h | 44/8 |
| 2 | See Entry 1; 10 mol% 110 | 58/11 |
| 3 | See Entry 1; $-40 \text{ }^\circ\text{C}$ | 30/7 |
| 4 | Et_2O , $-78 \text{ }^\circ\text{C}$, 1 h; slow addition of 78 over initial 10 min. | 18/1 |
| 5 | See Entry 4; $-40 \text{ }^\circ\text{C}$ | 31/0 |
| 6 | See Entry 4; $-20 \text{ }^\circ\text{C}$ | -/- |
| 7 | $t\text{BuOMe}$, $-78 \text{ }^\circ\text{C}$, 1 h; slow addition of 78 over initial 10 min. | 23/8 |
| 8 | See Entry 7; $-50 \text{ }^\circ\text{C}$ | 28/7 |
| 9 | See Entry 7; $-30 \text{ }^\circ\text{C}$ | 30/6 |
| 10 | See Entry 7; $-50 \text{ }^\circ\text{C}$ for 20 min. prior to addition of 78 | 41/12 |

While interesting results were obtained for entries 2 and 10, the conclusion was that these conditions were not going to be able to yield enantioenriched products. As such, research into substrate alternatives was carried out to see if any modifications to the quinolone cores could be made to better undergo enantioselective conversion.

2.3.2 Synthesis of Quinolone Carboxylate Substrate and Organometallic Addition

A common feature of existing quinolone molecules is the carboxylic acid group at position 3 which is vital for gyrase binding.⁶⁰ Favourable binding with metal ions in biological systems suggest this functionality and others similar to it could potentially act as a “pocket” in which metal ions in the conjugate addition transition state could be stabilised. Additionally, these functional groups could increase the reactivity of the α,β -unsaturated enone by withdrawing electron density away from the reactive centre (Figure 37). Compounds **117** and **118** are both known compounds, while compounds **119** and **120** were also potential options for development. The Boc-protecting group in compound **117** was proposed due to the facile nature of its incorporation and removal compared to the Cbz-protecting group in the other postulated targets.

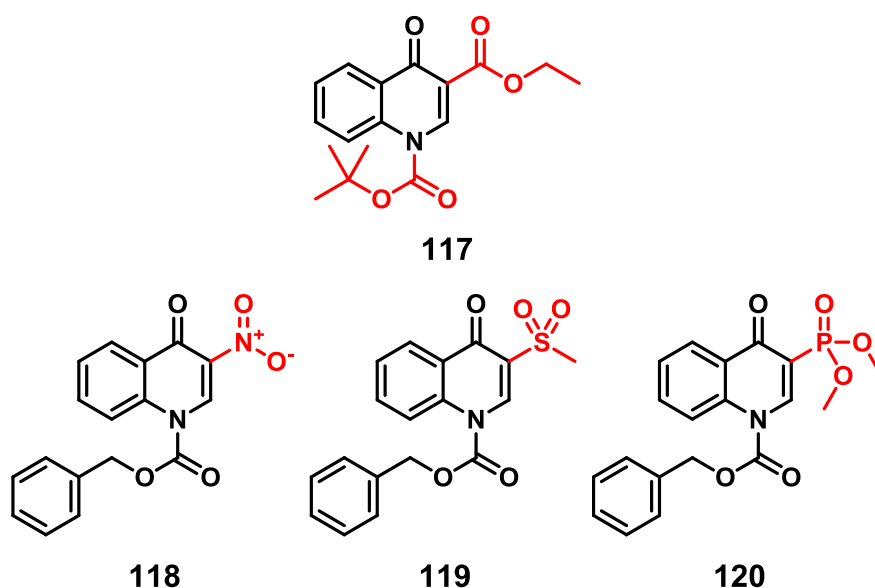


Figure 37 Options for new substrates modified from the original substrate **78**

The unsuitability of the nitro-group in compound **118** for use in organometallic chemistry due to its propensity for reduction, while the synthetic challenges faced with the synthesis of **119** and **120** made them undesirable as target substrates. Compound **117** was selected as the substrate of choice due to its well-documented synthesis with the Boc-protecting group and easily modifiable ester functionality, offering opportunity for facile substrate diversification.^{114,115} Reactions with previously unsuccessful organometallic reagents ZnEt_2 and AlEt_3 were trialled to see whether compound **117** would be more reactive than **78** (Table 8). The ligand used in these reactions – compound **122** – is a phosphoramidite; compound **122** has itself been successfully implemented in asymmetric conjugate addition reaction on numerous occasions, whilst

phosphoramidite ligands as a whole have been used extensively in this class of reactions.⁴⁴

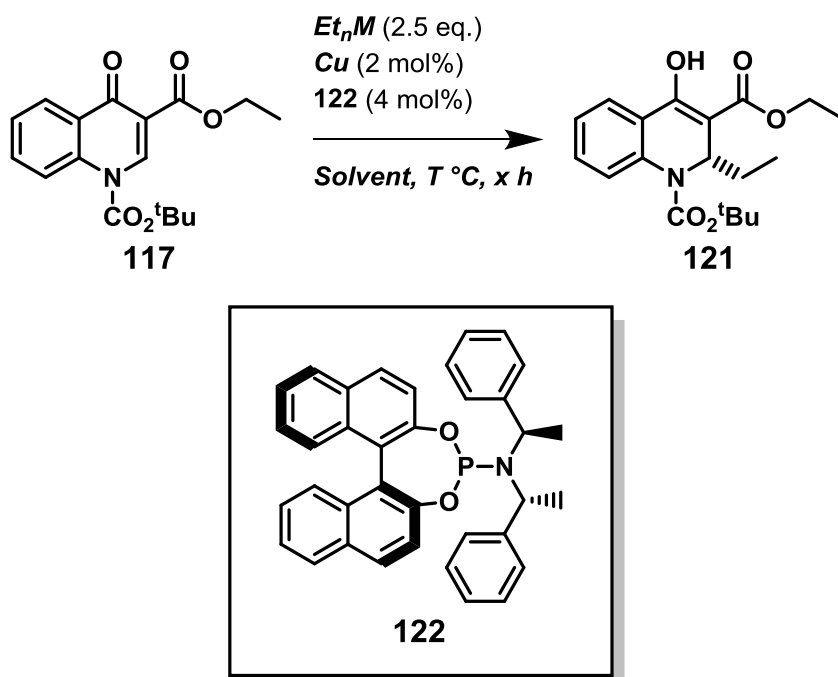


Table 8 Screened conditions for the conjugate addition reaction

| Entry | R _n M | Cu | Solvent | T (°C) | Time (min) | Conversion (%) | ee (%) |
|-------------------|-------------------|---------------------------------------|--|-----------|---------------|----------------------------|-----------|
| 1 | AlEt ₃ | Cu(OTf) ₂ | CH ₂ Cl ₂ | -10 | 5 | >99 | 0 |
| 2 | AlEt ₃ | Cu(OTf) ₂ | Et ₂ O/CH ₂ Cl ₂ (1:1) | -10 | 180 | 57 | 33 |
| 3 | AlEt ₃ | Cu(OTf) ₂ | Et ₂ O | -10 | 60 | >99 | 40 |
| 4 | AlEt ₃ | Cu(OTf) ₂ | THF | -10 | 30 | >99 | -18 |
| 5 | AlEt ₃ | Cu(OTf) ₂ | Et ₂ O | -25 | 45 | >99 | 60 |
| 6 | AlEt ₃ | Cu(OTf) ₂ | ^t BuOMe | -25 | 5 | >99 | 34 |
| 7 | ZnEt ₂ | Cu(OTf) ₂ | Et ₂ O | -25 | 5 | >99 | 15 |
| 8 | ZnEt ₂ | Cu(OTf) ₂ | ^t BuOMe | -25 | 5 | >99 | 6 |
| 9 | AlEt ₃ | Cu(OAc) ₂ | Et ₂ O | -25 | 180 | 96 | 52 |
| 10 | AlEt ₃ | Cu(NCMe) ₄ BF ₄ | Et ₂ O | -25 | 90 | 98 | 45 |
| 11 | AlEt ₃ | Cu(OTf) ₂ | Et ₂ O | -40 | 360 | >99 (68) ^[b] | 65 |
| 12 | AlEt ₃ | Cu(OTf) ₂ | Et ₂ O | -50 | 1440 | 0 ^[c] | - |
| 13 ^[d] | AlEt ₃ | none | Et ₂ O | -40 | 1440 | 74 | - |
| 14 ^[d] | AlEt ₃ | Cu(OTf) ₂ | Et ₂ O | -40 | 1440 | 91 | - |

^[a] Determined by chiral HPLC on a chiral stationary phase. ^[b] Isolate yield. ^[c] No solubilisation of the substrate was observed for the entire duration of the reaction. ^[d] Reaction performed in the absence of phosphoramidite ligand **122**

The solubility of the substrate in the solvents trialled at -10 °C was generally good, with complete solubilisation and consumption of **117** observed in CH₂Cl₂, Et₂O and a (1:1) mixture of the two solvents (Entries 1-3). Moderate enantioselectivity was observed in neat Et₂O (40% ee, Entry 3) and 1:1 Et₂O/CH₂Cl₂ (33% ee, Entry 2),

though only the racemate was afforded in CH₂Cl₂ (Entry 1). The rapid consumption of **117** implied a low-energy non-enantioselective background reaction which dominated the enantioselective variant; incorporation of or replacement with Et₂O retarded this non-enantioselective transformation and allowed the enantioselective process to occur. Poor solubility of the substrate in THF (Entry 4) was believed to contribute to the poor conversion to the desired product, though the perceived mild stereochemical inversion of the transformation is, as of yet, inexplicable.

The solubility of **117** in the selected solvent system of neat Et₂O was reduced at lower temperatures, though the same issues with poor conversion seen with THF were not observed. The addition order of the reagents involved the injection of the organometallic reagent to a stirring cold suspension of the substrate, ligand and copper catalyst. Complete solubilisation of **117** was observed over the course of the reaction at -25 °C (Entry 5) which itself became homogeneous prior to and on arrival at its conclusion, showing complete consumption of the starting material and furnishing the conjugate addition product **121** in 60% ee. As a result of this, lowering the temperature of the reaction was deemed feasible and a worthwhile effort in eliminating the non-enantioselective background process and potentially increasing enantioselectivity. Attempts with a similar solvent in t-BuOMe at -25 °C also afforded the product in moderate enantioselectivity (34% ee, Entry 6) though a similar short reaction timeframe compared with CH₂Cl₂ was observed implying the solvent did not sufficiently suppress the non-enantioselective background reaction; t-BuOMe was thus disregarded as a solvent option.

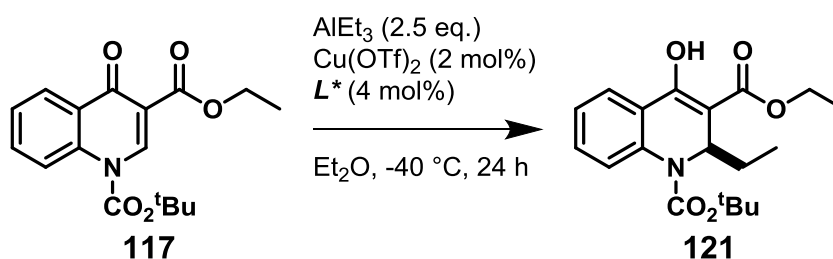
Prior to lowering the temperature of the reaction, diethylzinc was trialled to see whether it could be used as the organometallic reagent (Entries 7-8); poor enantioselectivity was observed and consequently reaction optimisation with diethylzinc was abandoned. Alternative, commercially available copper catalysts were also trialled in the reaction (Entries 9-10), though slower conversion and slightly poorer enantioselectivity was observed meaning continued use of Cu(OTf)₂ was employed.

The enantioselectivity of the reaction increased as the temperature was lowered. This did, however, reach a point at which the solubilisation of **117** never occurred at -50 °C (Entry 12). As a result, -40 °C was deemed to be the optimum temperature for the process (Entry 11). The optimised reaction conditions now afforded conjugate addition product **121** in a good isolated yield of 68% and moderate enantioselectivity of 65% ee; this allowed us to perform another screen of chiral ligands to see if other classes can promote enantioselective addition to compound **117**. The non-enantioselective background reaction still occurred at the lower reaction temperature (Entries 13 and

14), though the incomplete conversion to the conjugate addition product **121** over a considerably longer timeframe led us to believe this process was sufficiently suppressed at the lower temperature.

2.3.3 Ligand optimisation and Scope Analysis

A selection of ligands available already within the group were used in the screen, with the aim of synthesising a library of derivatives of any successful ligands to optimise the reaction (Scheme 39).



Scheme 39 Reaction scheme for chiral ligand screening

Moderate success was observed with the phosphoramidite ligands for the optimisation of the reaction conditions; as such, similar ligands containing functionalised phosphorus centres attached to chiral or axially chiral structural motifs were implemented in the screening of ligands (Figure 38).

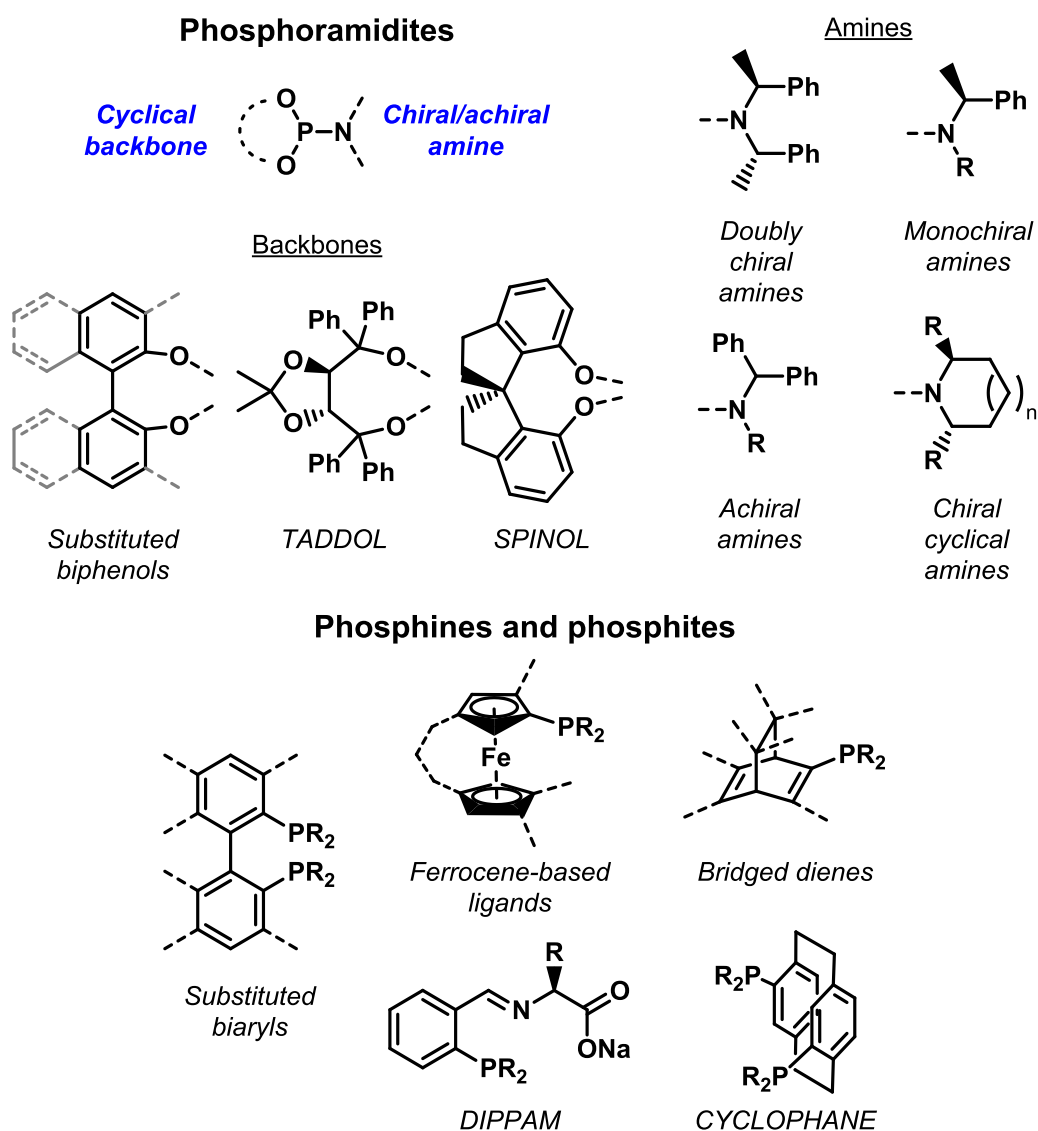


Figure 38 Classes of ligand used in the optimised conjugate addition reaction

Results indicated that the phosphoramidite class of ligands with 1,1'-bi-2-naphthol (BINOL) backbones seemed to be the most effective at promoting enantioselectivity furnishing product with up to 72% ee; all other ligands trialled in the optimised conditions showed no consumption of the starting material or negligible conversion to the racemic conjugate addition product. The facile synthesis of these phosphoramidite ligands also lends itself to the rapid generation of a library of structurally diverse ligands in this class. Other similar BINOL-phosphoramidite ligands have been utilised in previous work conducted by Schmalz and Fletcher; ligands **128** and **129** were used in their respective methodologies to perform asymmetric conjugate addition reactions (Figure 39).^{116–119} Synthesis of these ligands led to an improvement in the enantioselectivity of the reaction using compound **129** - originally used by Fletcher – affording compound **121** in 62% yield and 72% ee. Derivatives of this ligand were then

synthesised and used in the reaction (Scheme 40) leading to the discovery of ligand **133** which was able to promote enantioselective addition to compound **117** in 68% yield and 77% ee. Doubling of the ligand-catalyst loading also improved the reaction performance by halving the reaction time (limiting energy expenditure for cooling equipment) and improved isolated yield (from 58% to 68%); initial optimisation was trialled on the original 2:4 mol% Cu:L catalyst-ligand loading prior to in-depth structural modification of the ligand (Scheme 40) Further derivative synthesis was deemed unrewarding and compound **133** was selected as the ligand for the optimised conditions. Compound **133** and many similar derivatives were recently described in a patent filed by Fletcher *et al.*¹²⁰

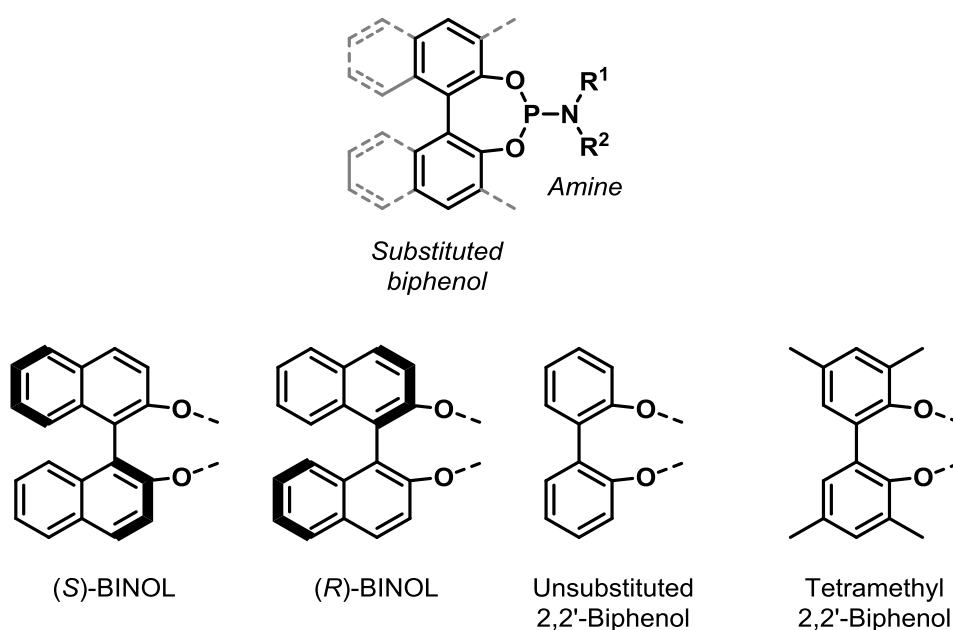
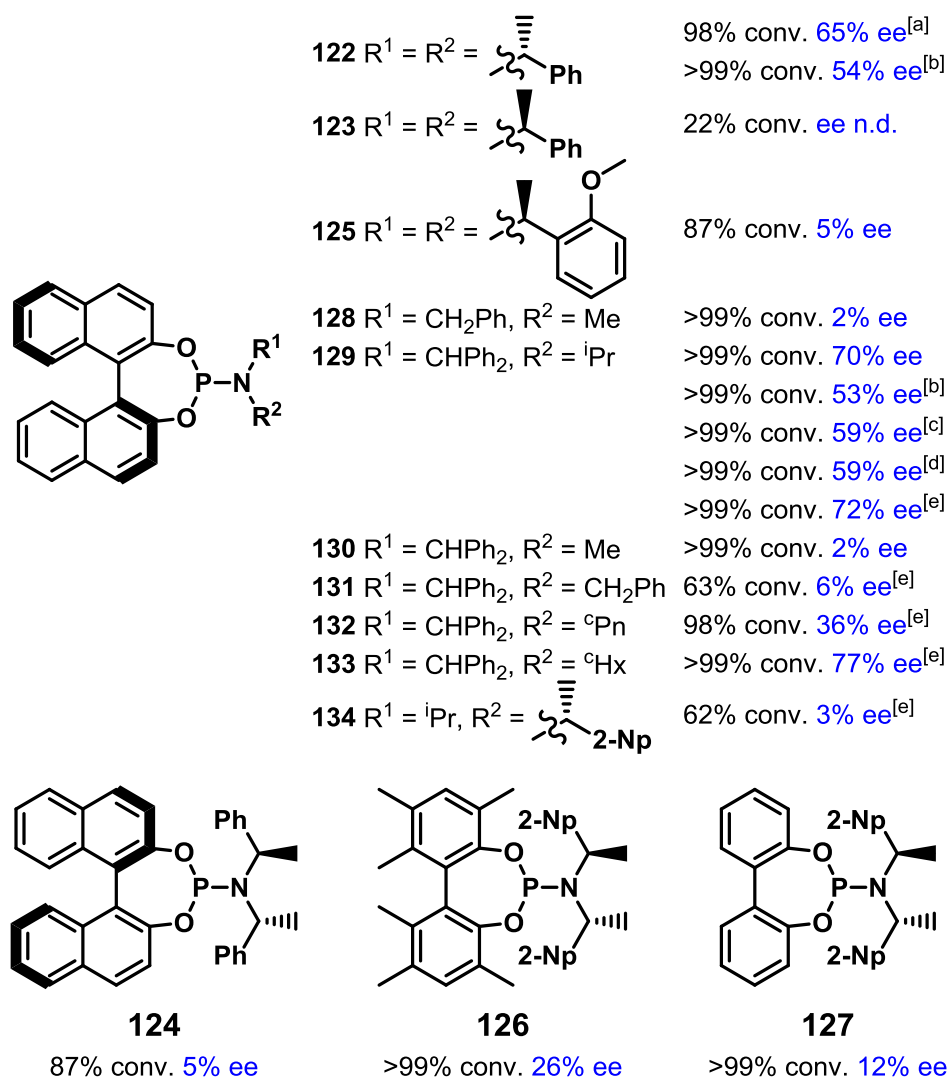
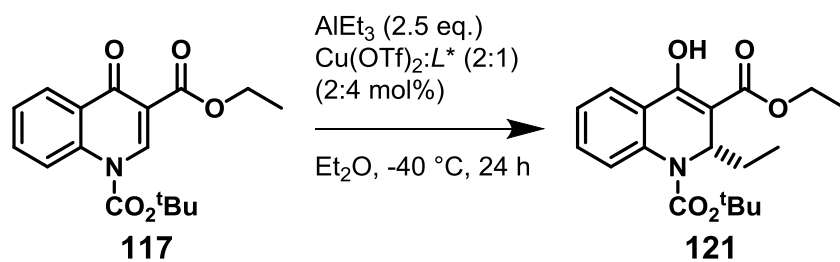


Figure 39 BINOL-Phosphoramidite structure with biphenol moieties used in ligands

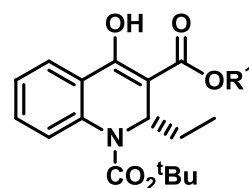
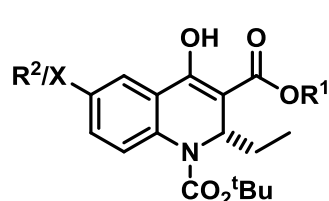
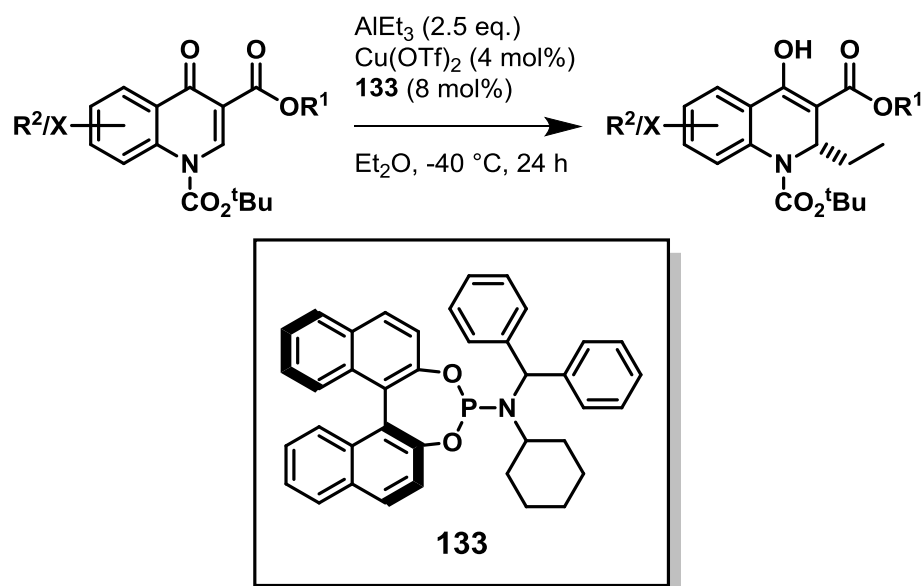


Scheme 40 Screened conditions for the conjugate addition reaction

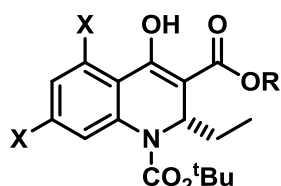
^[a] Determined by chiral HPLC on a chiral stationary phase. ^[b] Cu(OAc)₂ used in place of Cu(OTf)₂. ^[c] Substrate added in 3 portions at the start, after 1 h and after 2 h; reaction left until completion. ^[d] AlEt₃ added slowly over 3 h; reaction left until completion. ^[e] 4:8 mol% Cu:L ratio used. n.d. = not determined.

The established conditions were used to analyse substrate scope; the substitution patterns on compounds **135-149** are the result of using symmetrical aniline starting

materials and allowed us to elucidate electronic effects of the substituents on the conjugate addition reaction (Scheme 41).



| | | | |
|--|----------------------------|--|-------------|
| 137 → 151 X = F | 77%, 86% ee ^[a] | 117 → 122 R ¹ = Et | 68%, 77% ee |
| 138 → 152 X = Cl | 91%, 83% ee | 135 → 149 R ¹ = Me | 67%, 62% ee |
| 139 → 153 X = Br | 64%, 77% ee | 136 → 150 R ¹ = CHPh ₂ | 0% |
| 140 → 154 X = I | 71%, 79% ee | | |
| 141 → 155 R ² = Me | 77%, 83% ee | | |
| 142 → 156 R ² = Et | 91%, 60% ee | | |
| 143 → 157 R ² = ⁱ Pr | 64%, 45% ee | | |
| 144 → 158 R ² = ^t Bu | 71%, 30% ee | | |
| 145 → 159 R ² = CF ₃ | 64%, 17% ee | | |
| 146 → 160 R ² = OMe | 71%, 80% ee | | |



| | |
|--------------------------------|--------------|
| 147 → 161 X = F | 77%, 13% ee |
| 148 → 162 X = Cl | 74%, -10% ee |

Scheme 41 Substrate scope for established conditions

^[a] Determined by chiral HPLC on a chiral stationary phase.

The stereochemistry of the 1,4-ethyl addition was unknown at this point but is depicted as 2*S*-configuration in as this is in accord with subsequent X-ray crystal structure on a derivative of the parent product **121**, supported by circular dichroism studies. Related derivatives **149** and **151-161** are assumed to have the same sense of absolute stereochemistry based on comparison of their HPLC elution order and sign of optical rotation (see experimental section). The absolute stereochemistry of **162** is assumed

to be 2*R*-configuration by equivalent logic, although the absolute asymmetric induction is low. A clear electronic effect can be deduced from the results in Scheme 41; electron withdrawing substituents such as halogens and trihaloalkyl substituents – as in the conjugate addition reaction with compounds **137-140** and **145** to form compounds **151-154** and **159** – afford products with high enantioselectivity and greater yields (Entries 4-7 & 12, Scheme 41), while electron donating substituents – particularly the methoxy-substitution in the conjugate addition reaction with compound **146** to form compound **160** (Entry 13, Scheme 41) – were detrimental to both of these features in the afforded dihydroquinolone derivatives.

Steric effects for the conjugate addition were only evaluated with respect to the substitution on the ester moiety; no clear trend was observed for the effect of substituent size on the reaction, though the solubility profile changed greatly between the different esters. The benzhydryl ester meant compound **136** exhibited extremely poor solubility and consequently no conversion to the conjugate addition product **150** was observed (Entry 3, Scheme 41). Substituent steric effects on the phenylidene linker were not studied extensively due to the difficulty in the synthesis of the starting materials; substitution at the 8-position on the aniline starting material precluded carbamate protection meaning the substrate could not be used. Equally, substitution at the 2-position at the reactive centre in the molecule for the conjugate addition reaction proved detrimental in the same way. Steric clash with the carbamate protection group may prohibit the compound from forming in the reaction. Furthermore, quinolone derivatives with a greater number of substituents - such as **163** and **164** - tend to exhibit poor solubility profiles meaning protection of these compounds required harsh conditions detrimental to conversion to the desired product. Steric and electronic effects can be analysed if the synthesis of molecules containing these functionalities can be achieved. Examples of molecules that could not be synthesised with our methodology are shown below (Figure 40).

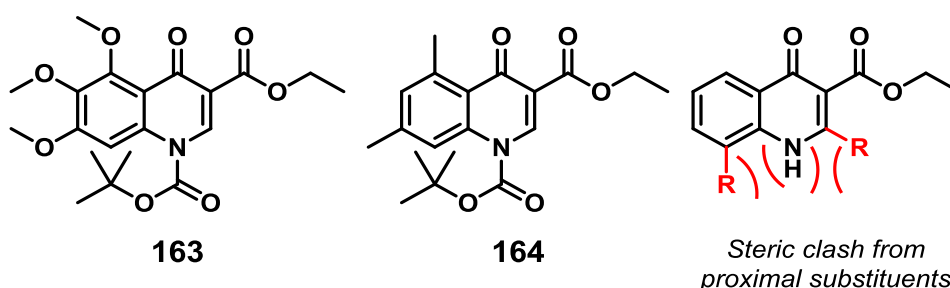
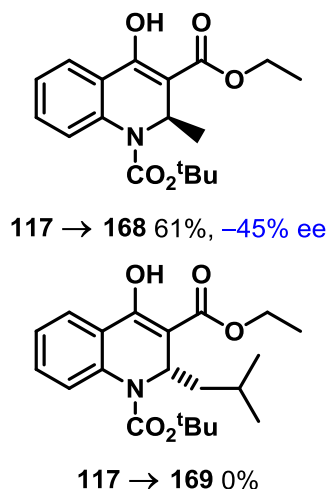
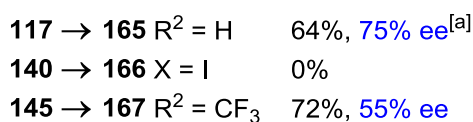
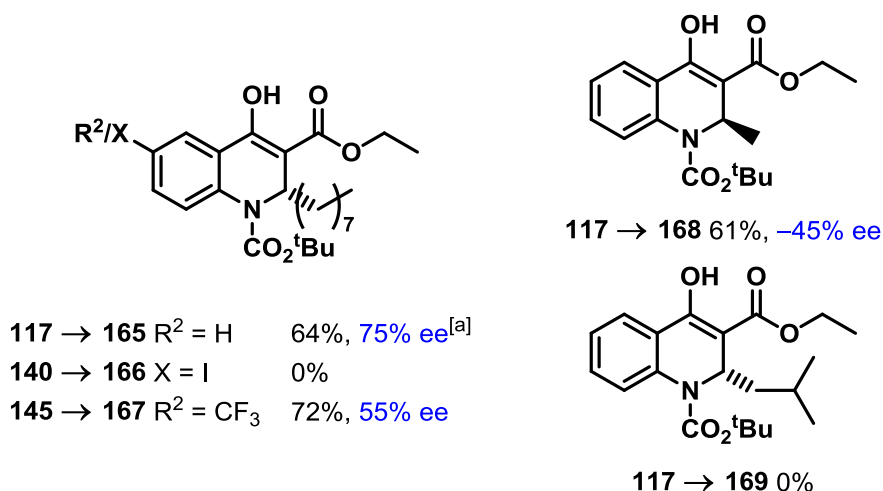
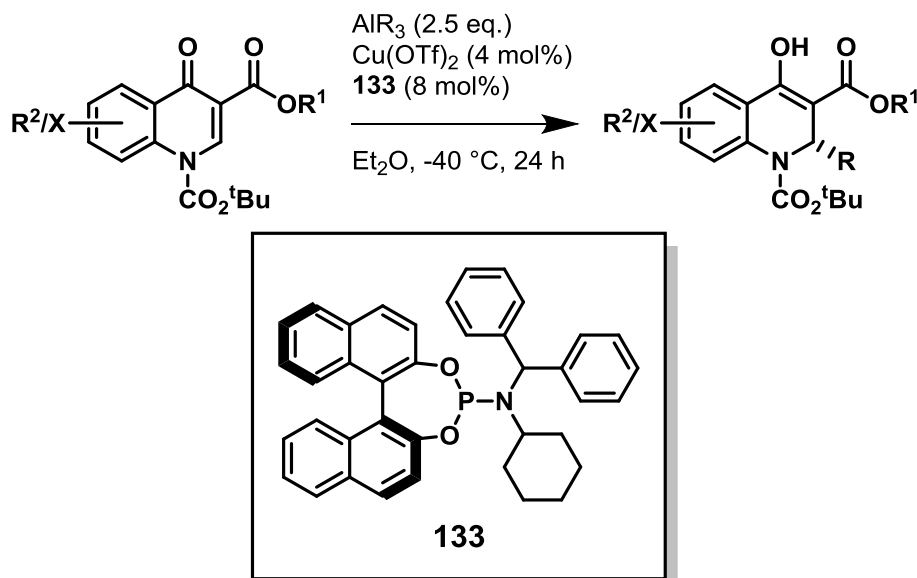


Figure 40 Unavailable substrates for conjugate addition reaction

The scope of the organometallic was assessed using commercially available alkylaluminium reagents aside from triethylaluminium (Scheme 42). These included trimethyl-, trioctyl- and triisobutylaluminium. Unfortunately, the scarcity of these reagents limited the number of different derivatives that could be explored.



Scheme 42 Organometallic scope for the conjugate addition reaction

^[a] Determined by chiral HPLC on a chiral stationary phase.

Compound **165** was successfully formed in 64% yield and 75% ee, values comparable to the synthesis of ethyl substituted conjugate addition product **121**, indicating longer, linear alkyl addition to quinolones can be achieved enantioselectively and in sufficiently good yields. However, the electronic effect exhibited with the addition of triethylaluminium where electron-withdrawing substituents improved the enantioselectivity of the transformation was not observed for the addition of trioctylaluminium; addition to trifluoromethyl-substituted substrate **145** to form

compound **167** afforded the product in a comparable yield of 72%, but with poorer enantioselectivity of 55% ee. The iodo-substituted conjugate addition product **166** was present in the crude mixture after the reaction was worked up, though isolation of clean material for characterisation was unsuccessful. Methylation of compound **117** proceeded with poor enantioselectivity of -45% ee; this could be due to the deficiencies in the use of trimethylaluminium in conjugate addition reactions that have been reported.¹³ Additionally, triisobutylaluminium failed to form the product in any appreciable yield; an unidentified by-product was formed during this reaction, though analysis into its structure was not performed due to trace amounts of material formed. One postulated structure is the optically inactive compound **170**, in which β -hydride elimination of the alkyl aluminium has occurred and reduced the α,β -unsaturated enone to the ketone (Figure 41). Should this structure be correct, it provides an opportunity for hydrogenation of the β,β -disubstituted- α,β -unsaturated enone as a different route 2-alkyl-substituted dihydroquinolones (Scheme 43).

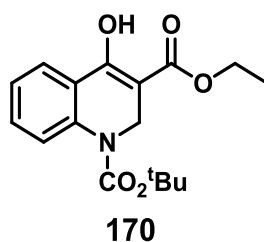
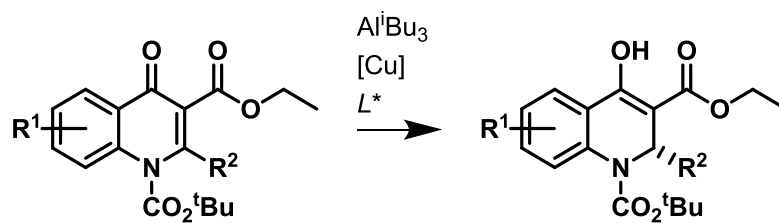


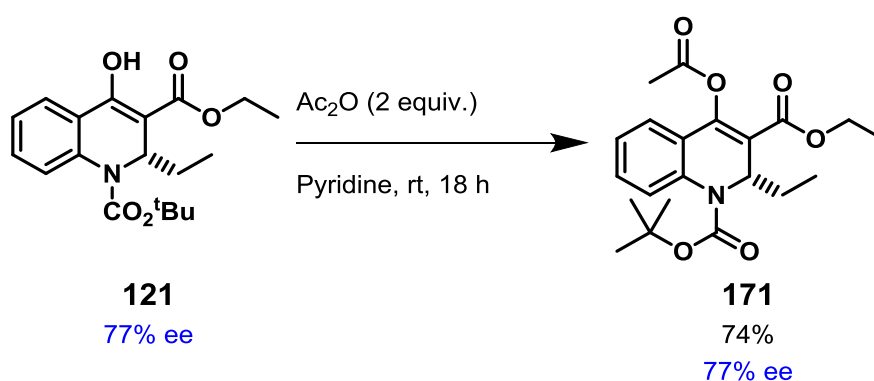
Figure 41 Postulated structure of by-product from triisobutylaluminium conjugate addition reaction



Scheme 43 Potential scheme for hydride conjugate addition to quinolone substrates

2.3.4 Diversification of Enantioenriched Products

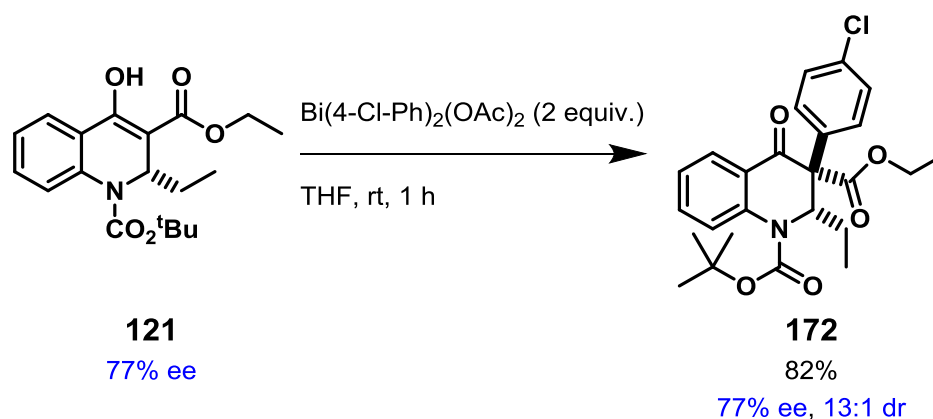
As these compounds were synthesised with early stage drug discovery in mind, further diversification of these molecules was necessary. As such, reactions were performed on compound **121** to analyse its utility as a fragment (Scheme 44-47). One of the issues that was encountered when attempts were made to elucidate the enantiomeric ratio of the afforded compounds was the equilibrium between enol- and keto-ester tautomers; broadening or poor but noticeable separation of the absorption peaks in the HPLC chromatograms was observed in many of the synthesised examples. With this in mind, acetylation of compound **121** was performed to “lock” the conformation in the enol tautomer (Scheme 44).



Scheme 44 Elaboration of the conjugate addition products

Conservation of enantioselectivity was observed as well as resolution of the HPLC chromatogram for acetylated compound **171**. Acetylation of all the conjugate addition products was subsequently performed allowing irrefutable analysis of enantioselectivity. As all of the conjugate addition products were amorphous upon isolation, it was hoped that the acetylated product would be a solid which could be recrystallised in efforts to determine the absolute stereochemistry of the products. However, the isolated product was also amorphous as were the full collection of acetylated derivatives. It was therefore deemed unsuitable for this purpose.

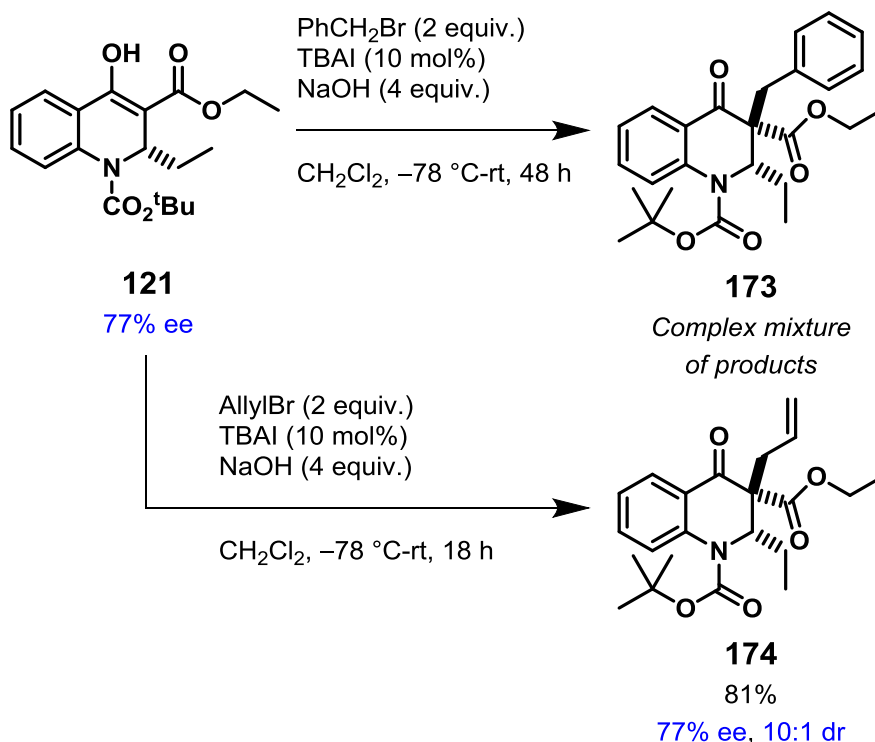
A benefit of the enol/keto-ester functionality in the afforded products is its nucleophilic nature. Within the laboratory, ongoing projects involving the synthesis of bismuth-(V) compounds presented the opportunity of their implementation in arylation of the 1,3-dicarbonyl moiety within the conjugate addition products (Scheme 45). This reaction was originally developed by Barton *et al.* in 1980.¹²¹



Scheme 45 Elaboration of the conjugate addition products

The diastereoselectivity of the formation of arylated product **172** was high at 13:1 dr; rationale for this observation is the steric clash of the aryl group with the adjacent alkyl group will be far greater than that of the hydrogen atom, leading to the lower energy *trans*-arylation isomer being formed as the major product. The compound was solubilised in pentane at 0 °C at concentrations greater than 50 mg/mL; this precluded the isolation of crystals to determine absolute stereochemistry.

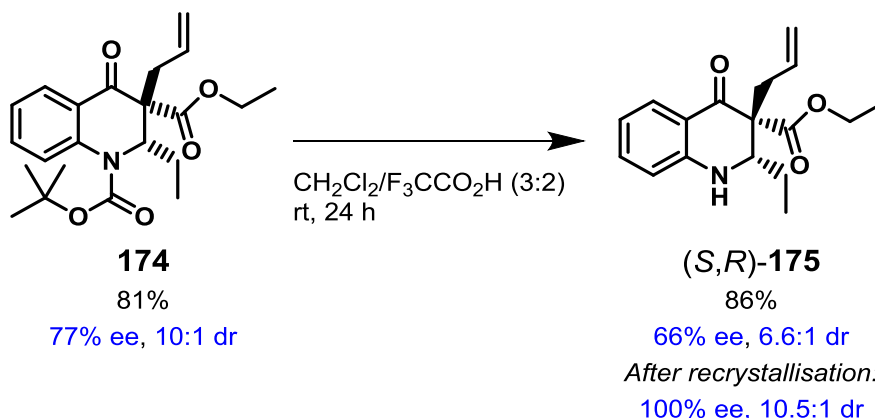
Alkylation of the 1,3-dicarbonyl moiety was also performed affording further examples of diversification of the molecular scaffold (Scheme 46).



Scheme 46 Elaboration of the conjugate addition products

The steric demand of the alkyl substituents incorporated in the molecules led to differing diastereomeric compositions of the alkylated products **173** and **174**. Benzylation of compound **121** led to formation compound **173**, though this could only be confirmed by mass spectrometry; incomplete conversion was observed due to the presence of starting material **121** in the reaction mixture amongst numerous other mass peaks and TLC spots. Attempted isolation of **173** was unsuccessful as the numerous unidentified by-products were present in the crude material and inseparable from the desired product after numerous attempts at purification. Allylation of compound **121** did occur cleanly affording compound **174** in a yield of 81% and with good diastereoselectivity of 10:1 dr, whilst also conserving the enantiomeric composition of the product at 77% ee. Unfortunately, this compound was amorphous in state and unsuitable for attempts at recrystallisation. The successful synthesis of allylated compound **174** and difficulty with the synthesis and isolation of benzylated compound **173** indicates that alkylation at the 3-position in the quinolone conjugate addition product can therefore be considered as incredibly sensitive to steric hindrance.

With copious quantities of allylated compound **174** in hand, deprotection of the Boc-amine was performed (Scheme 47). Removal of the highly lipophilic *tert*-butyl group was considered to be beneficial in the efforts reduce the amorphous nature of the afforded products and form a crystalline derivative.



Scheme 47 Elaboration of the conjugate addition products

Removal of the protecting group under acidic conditions followed by a basic work-up afforded the free-base compound **175** with a loss of both enantiomeric and diastereomeric excesses, though the afforded compound was a solid. Recrystallisation of the compound in Et₂O and pentane led to the formation of a highly crystalline solid as a single enantiomer which also enriched the diastereomeric composition of compound **175** to 10.5:1, as confirmed by HPLC. This allowed X-ray crystallography

to be performed on the isolated crystals and the determination of the absolute stereochemistry of **175** shown to be the (*S,R*)-product (Figure 42).

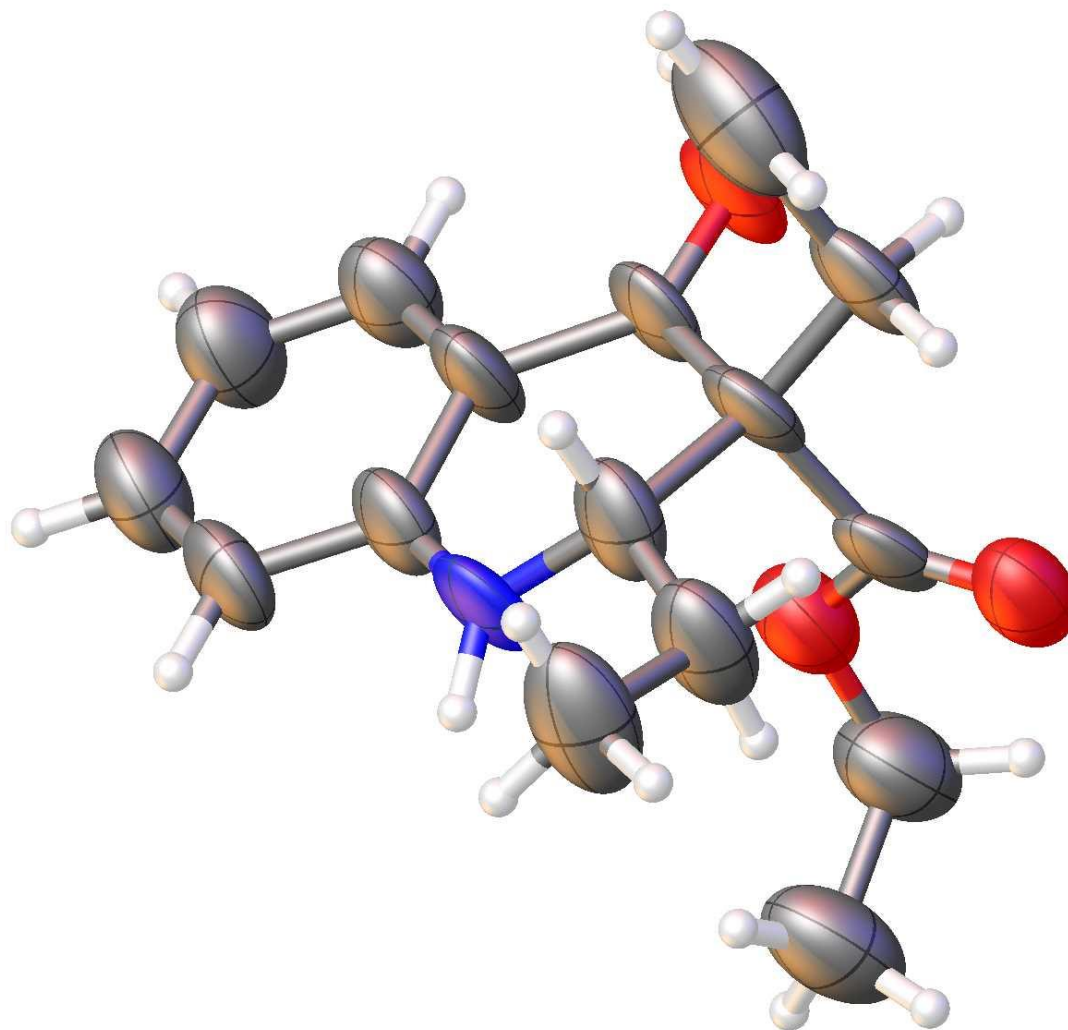
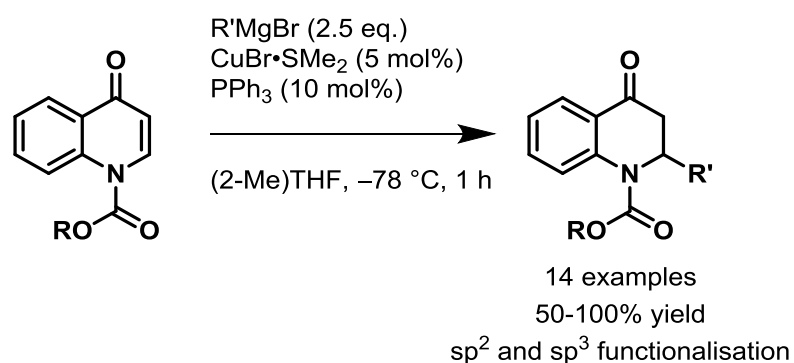


Figure 42 Structure of compound **175** as determined by X-ray crystallography

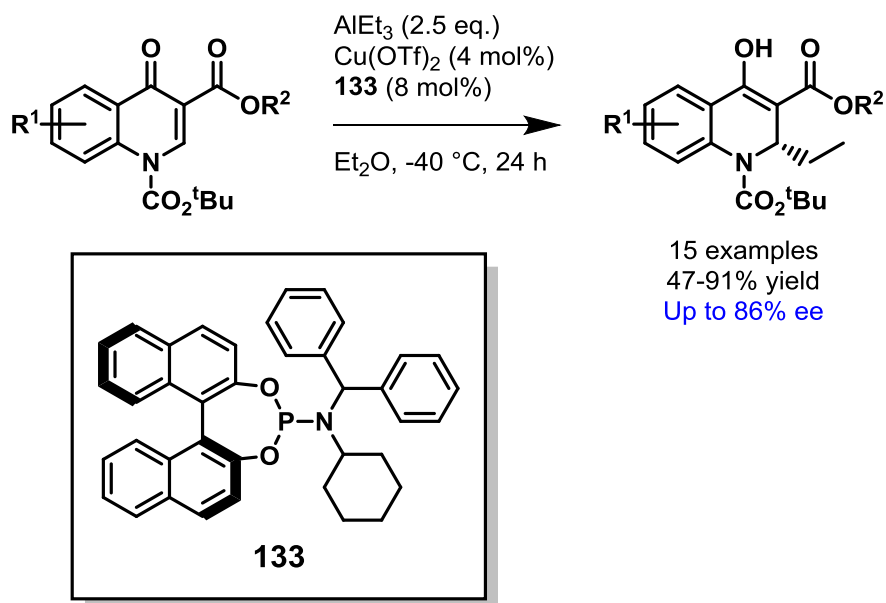
2.4 Conclusions

Initial methodology towards enantioselective synthesis of dihydroquinolones using an economical copper catalyst and alkyl- and alkenylmagnesium reagents afforded a broad range of derivatives bearing linear alkyl, branched alkyl and vinyl substituents (Scheme 48). The synthesised products were novel and further research may uncover reactions in which they can be used in a pharmaceutical setting for early stage drug discovery. Attempts at achieving enantioselectivity for these conditions were unsuccessful on addition of a chiral ligand, though further investigation may unearth a way of combatting this issue.



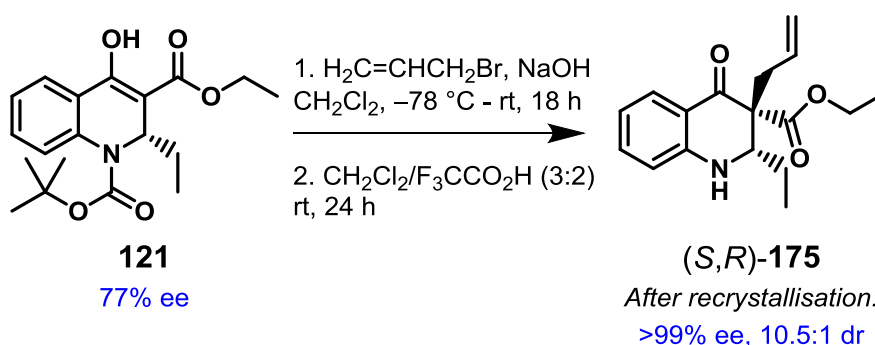
Scheme 48 Racemic conjugate addition of Grignard reagents to unsubstituted quinolones

The enantioselective conjugate addition of alkylaluminium reagent to quinolone substrates including a carboxylate substituent has been achieved; in many cases, enantioselectivity is excellent as well as affording good to excellent yields of the dihydroquinolone derivatives (Scheme 49). The methodology incorporates a phosphoramidite ligand optimised for the reaction conditions. Different linear alkyl groups have been successfully added to this effect, though methylation and branched alkyl substitution is currently not viable *via* this methodology.



Scheme 49 Enantioselective conjugate addition of alkylaluminum reagents to quinolone carboxylates

Substrate scope elucidated an apparent trend in the electronic effect exhibited by the substituent(s) on the phenylene linker; electron-rich phenylene moieties were detrimental to both conversion and enantioselectivity of the conjugate addition. Further investigation into this phenomenon may uncover ways to counteract this effect. Simple transformations have been conducted on the afforded products providing us access to crystalline derivatives **175** which were isolated in >99% ee; this allowed us to deduce the absolute stereochemistry of the conjugate addition products (Scheme 50).



Scheme 50 Synthesis of crystalline allylated derivative **175** from conjugate addition product **121**

2.5 Future Work

The substrates in this reaction were used due to the facile nature of their synthesis from symmetrical anilines; accessing different substitution patterns would not only enable the synthesis of more novel derivatives, but also uncover more information regarding the electronic effect of the substituents themselves. Other substrate alternatives include naphthyridones, furopyridones, thienopyridones, 4(1*H*)-pyrrolo[1,2-*a*]pyrimidones and pyrrolopyridones with heterocyclic linkers to potentially allow access to compounds **176-180** (Figure 43). These compounds would also be deemed suitable for pharmaceutical research.

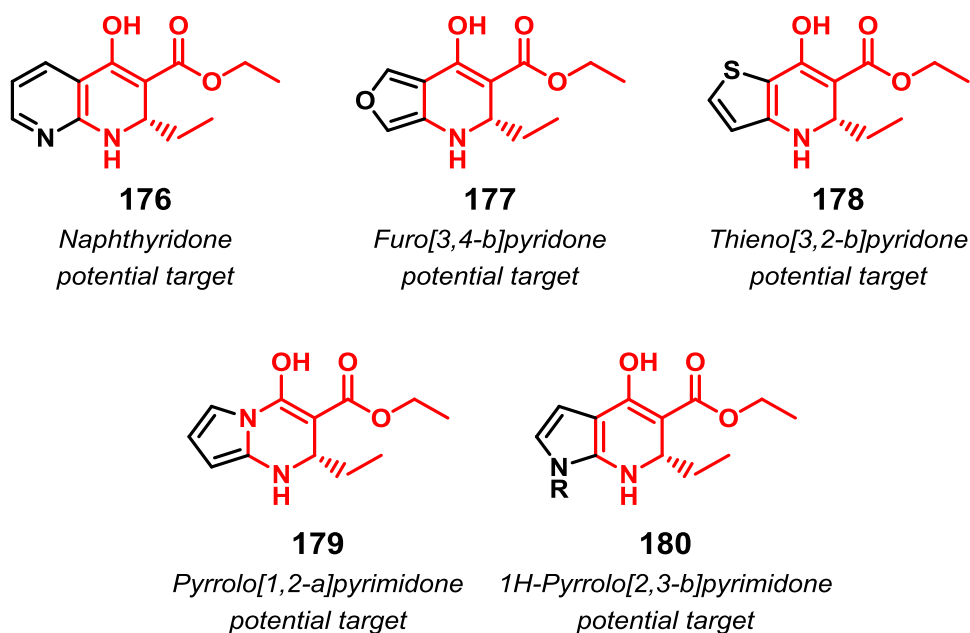


Figure 43 Quinolone-like substrates with heterocyclic linkers

Another substrate option that could be of interest is the β,β -disubstituted- α,β -unsaturated enone **181** towards conjugate addition product **182** containing a quaternary centre (Figure 44). Literature precedents show considerable success in achieving excellent enantioselectivity for the conjugate addition of organometallics to form quaternary centres.^{13,16,122} Not only might this improve the enantioselectivity of the reaction, but the products that would be afforded would also be novel and diverse; both are these features are attractive from a drug discovery perspective.

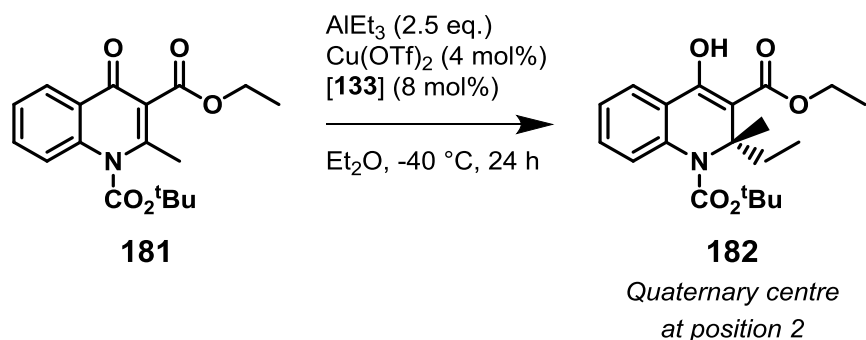
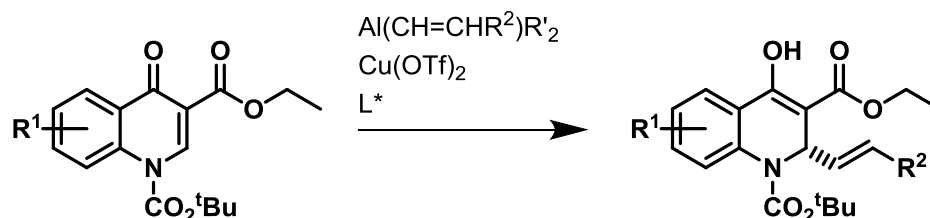


Figure 44 Quinolone substrates containing the β,β -disubstituted- α,β -unsaturated enone moiety

Though the successful synthesis of enantioenriched dihydroquinolones has been achieved, the current methodology only allows for a small range of alkylations of quinolone cores based on the availability of the necessary alkylaluminium reagents. Alongside efforts towards novel alkylaluminium species to be used in the conjugate addition reaction, investigation into the alkenylation of these cores would, if enantioselectivity could be achieved, allow access to a significantly broader range of novel compounds. The synthesis of alkenylaluminium reagents has been well documented and reviewed, meaning they can be formed and used in the reaction with little need for optimisation (Scheme 51).¹²³



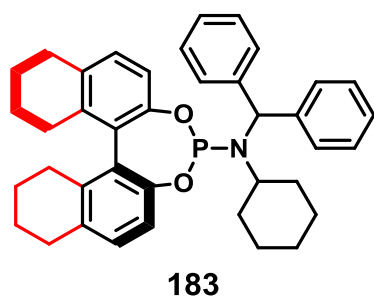
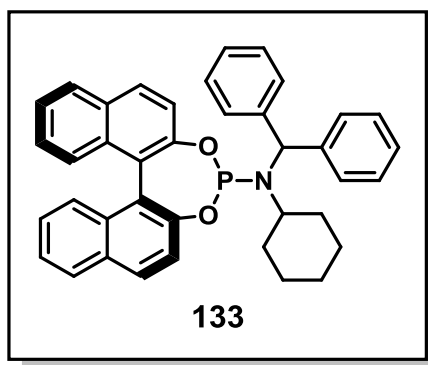
Scheme 51 Alkenylaluminium conjugate addition reaction

In terms of methodology development, consideration should be given to the challenges that exist regarding the substrates; their poor solubility means that certain conditions such as low temperatures of apolar solvents are not prudent for utilisation in this reaction. With that being said, the reaction does begin as a heterogeneous suspension in which the quinolone is slowly solubilised over the course of the reaction. The mixture becomes a solution in which no precipitate is present meaning that although poor solubility has prevented reaction progression under certain extreme conditions (Entry 12, Table 8), conversion could still be seen with only minor alterations.

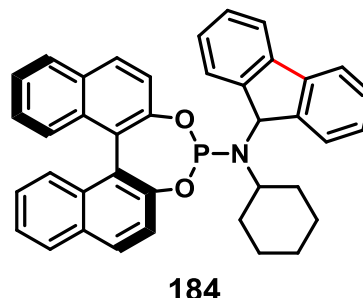
Similar enantioselectivity of the afforded product was observed in a 1:1 $\text{CH}_2\text{Cl}_2/\text{Et}_2\text{O}$ solvent mixture compared to neat Et_2O used in the final conditions (Entries 2-3, Table 8); the increased solubility of the substrate in this solvent mixture may allow the

reaction to be performed at a lower temperature which improves the enantioselectivity of the conjugate addition reaction, as demonstrated during the optimisation process. Additionally, formation of the active catalyst-ligand complex between the phosphoramidite could potentially occur at significantly lower temperatures. Pre-formation of this catalyst at the lowest possible temperature in Et₂O followed by slow addition of the solubilised substrate in the minimum volume of CH₂Cl₂ to this solution may afford the desired conjugate addition product with greater ee.

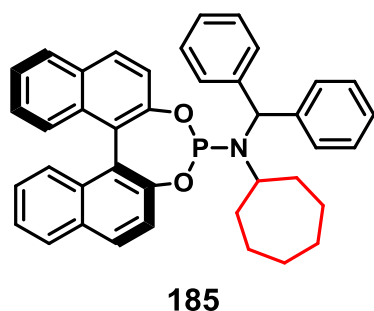
Additionally, the ligand that was being used – compound **133** – was optimised until a point was reached from which we deemed suitable to start: 77% ee for compound **121**. That is not to say that the ligand cannot be further optimised to enhance the enantioselectivity of the reaction. As previously mentioned, Fletcher *et al.* describe a number of structurally similar ligands used for conjugate addition in their patent filed in 2014.¹²⁰ Knowing that these compounds are not only synthetically tractable, but desirable for their implementation in this area of chemistry provides a compelling argument for further ligand synthesis and screening. Proposals for modifications to ligand **133** can be seen below (Figure 45).



BINOL hydrogenation



Benzhydryl linkage/alteration



Ring expansion on amine or incorporation of sterically encumbering functionality

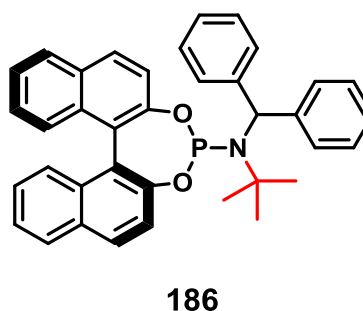


Figure 45 Proposed modified structures based on ligand **133**

With the amount of opportunities to develop this work and the numerous ways in which this could be done, further investigation into the formation of dihydroquinolones using the described methodology, modified versions of it or similar conjugate addition reactions have enormous potential for success.

3.1 Supplementary Information

3.1.1 General Information and Specifications for Kinetic Studies

Diethyl ether was distilled from sodium-benzophenone under argon; hexanes were dried over freshly cut clean sodium for >16 h and deoxygenated with argon. Feringa's (*R,S,S*)-phosphoramidite ligand **16** was prepared from fresh PCl_3 , (*R*)-BINOL and (*S*)-*N*-((*S*)-1'-phenylethanyl)-1-phenylethan-1-amine by a literature method.¹²⁴ Triethylaluminum (98% pure) was either commercial 2.0 M, 25% w/w, solutions in hexanes (originally Aldrich, now available from Alfa Aesar: Cat. No. 89054), corresponding to a molality of 2.19 mmol g^{-1} . Alternatively, solutions were prepared from neat triethylaluminum (>98%, CARE! pyrophoric) and hexane under argon to concentrations of 2.09-2.26 M (molalities of 2.47-2.67 mmol g^{-1}). The molarity/molalities of organometallics was determined via gas evolution on quench into wet THF using a gas monometer; identical results were attained by Gilman-titration methods.¹²⁵ Triethylaluminum solutions were stored in flame-dried glass Schlenk storage flasks, equipped with Teflon 'Young's taps'; their concentrations/purities were stable for the two week period batches were used over. Septa/'Sure-seal' closures were avoided as they were found to favour solvent loss and alkoxide formation. Maintaining pure AlEt_3 is critical to attaining high kinetic reproducibility. Anhydrous $\text{Cu}(\text{OAc})_2$ (Cu, Aldrich 326755) was certified as analytically pure (>98%). Ligand **16** was purified from a CH_2Cl_2 solution by layering with pentane (under argon) to yield large, clear, colourless, pentagonal crystals that assayed by multinuclear NMR spectroscopy as >99% pure. Cyclohex-2-en-1-one **8** (Aldrich 92509) was distilled/dried (4Å molecular sieves) and assayed >98% pure by ^1H NMR spectroscopy or GC techniques. Accurate quantification of AlEt_3 solutions was attained by pre- and post-weighing of the addition syringes used (to ± 0.1 mg). Similar dual weighing of all other component delivery vials/syringes (Cu, compounds **8** and **16** and Et_2O solvent) was used (± 0.1 mg). Bath temperatures were controlled by a Huber TC50E cryostat and were accurate to ± 0.5 °C at -40 °C. Aliquots from GC kinetic samples were analysed using a Bruker GC-430 using internal standards. ReactIR™ data were collected using a Mettler-Toledo ReactIR™ 15. The derived rate constants were found to be reproducible to within 3-5% on duplicate runs.

3.1.2 Reagent Order Determination in Kinetic Studies

Experimental Procedure: Run 4 (Representative of general procedure) - To a flame-dried three necked flask under argon, (*R,S,S*)-phosphoramidite ligand **16** (79.8 mg, 148 μmol) and $\text{Cu}(\text{OAc})_2$ (17.6 mg, 97 μmol) were added to anhydrous anaerobic Et_2O (16.507 g, 23.15 mL) and the mixture stirred at room temperature for 30 minutes. The solution was cooled to $-40\text{ }^\circ\text{C}$ for 10 minutes, after which time AlEt_3 (2.09 M in hexane, 2.47 mmol g^{-1} , 4.928 g, 6.12 mL of solution, 12.17 mmol) was added to the mixture and stirred at this temperature for an additional 10 minutes at $-40\text{ }^\circ\text{C}$. Experiments confirmed reproducible reduction to a homogeneous stable Cu^{I} precatalyst was attained by this procedure. At this timepoint, t_0 , compound **8** (1.002 g, 1.01 mL, 10.44 mmol) was added and data collection using the ReactIR™ started. Calculated initial values: $[\mathbf{8}]_0 = 345\text{ mM}$, $[\text{AlEt}_3]_0 = 402\text{ mM}$, $[\text{Cu}]_0 = 3.18\text{ mM}$, $[\text{L}]_0 = 4.88\text{ mM}$; $[\text{L}]/[\text{Cu}] = 1.54$; total volume = 30.28 mL. Data (O_{48} in A_{obs} absorbance units) for the 1630 cm^{-1} carbonyl band of adduct **48** were collected until complete consumption of this IR band was observed, recording 1 scan every 10 seconds. Following completion, the reaction was quenched with 1M aq. HCl solution (10 mL), extracted with Et_2O , washed with water, dried over MgSO_4 and solvent removed *in vacuo* to provide (*R*)-**11** with identical properties to genuine independent samples [chiral GC range (Lipodex-A) of final product $82 \pm 2\%$ ee].¹³ The volumes used were estimated from standard densities for **8** (0.993 g mL^{-1}) and Et_2O (0.713 g mL^{-1}), while that of 2.09 M AlEt_3 solutions in Et_2O was determined experimentally to be 0.83 g mL^{-1} in the kinetic runs. Reaction component volumes were assumed to be additive (i.e. partial molar volume/phase change effects were assumed minimal). Similarly, the volumes of dissolved Cu and L were assumed contribute negligibly ($<0.5\%$) to the total volume of the system.

Data analysis for reaction order calculation with respect to 48: Due to the higher data density of the ReactIR™ technique genesis of the catalyst could clearly be detected in the behaviour of the absorbance of **48** at 1630 cm^{-1} up to ca. 300 sec. Thus, at fixed $[\text{Cu}]$ (3.5 mM) and $[\text{L}]$ (5 mM) the absorbance data for **48** at 1630 cm^{-1} (O_{48}) were used from 305 or 395 sec (the latter for slightly slower catalyst genesis at lower values of $[\mathbf{8}]$) until the signal for species **48** was no longer apparent. A range of $[\mathbf{48}]_0$ (300-40 mM) concentrations were investigated. Values of $[\mathbf{48}]_t$ were attained *via* the relationship $[\mathbf{48}] = \epsilon_{48} \times O_{48}$. Values of $[\mathbf{48}]_t$ were fitted to $[\mathbf{48}]_t = [\mathbf{48}]_0 e^{-k_1 t}$ by non-linear least squares procedures. This approach has been described in detail by Billo.¹²⁶ In brief, for each data point the squared error is calculated: $\delta = \{[\mathbf{48}]_t(\text{obs}) - [\mathbf{48}]_t(\text{calc})\}^2$ and the total squared error over all data points summed = $\Sigma(\delta)$. Minimisation of $\Sigma(\delta)$ is

attained by use of the solver function in Excel providing $[48]_0(\text{calc})$ and k_1 directly. Based on the solver stat analysis approach of Billo the fit of the data by this approach is superior to traditional linearisation of the $[48]_t$ data via $\ln([48]_t)/\ln([48]_0)$ plots. For the rate order plots in **48** values of $[48]_0$ were based on the added (accurately weighed) $[48]_0$ and $[\text{AlEt}_3]_0$ in each run via the illustrated quadratic equation (Section 1.3.1). The fitted $[48]_0$ concentrations derived from the kinetic best fits were found to be rather sensitive to background A_{obs} offsets effects in the ReactIR™ set up and were thus not used. Fortunately, the value of $[48]_0$ does not affect k_1 determination/accuracy as this is independent of $(A_{\text{obs}})_0$. The main error sources on the order **48** data are, partly the experimental difficulty in systematically varying $[48]$ while keeping both the both the ratios $[\text{AlEt}_3]/[\mathbf{8}]$ and $[\text{L}]/[\text{Cu}]$ constant in this sensitive system. Duplicated/reanalysed $[48]^c$ order runs gave values of $c = 0.9\text{-}1.1$, in line with statistical error. Based on this (and the vastly superior fit to first order of the primary data to all other trialled rate laws), first order behaviour in $[48]$ is clearly the dominant behaviour (Figure 20).

Data analysis for reaction order calculation with respect to [Cu]: Identical reaction procedures to Run 4 as previously described. Under conditions providing $[48]_0 = 220 \pm 7$ mM and $[\text{L}]/[\text{Cu}] = 1.5 \pm 0.05$ the concentration of copper $[\text{Cu}]$ was varied 1-6 mM. The catalytic reaction was initiated and the data collected as described for that concerning reaction order calculation with respect to $[48]$. Identical procedures were applied providing an order of the catalytic reaction in the copper concentration of 1.5 (Figure 21).

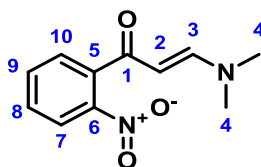
Data analysis for reaction order calculation with respect to [L]: Identical reaction procedures to Run 4 as previously described. Under conditions providing nominal $[48]_0 = 230$ mM and $[\text{Cu}]_0 = 3.5$ mM the concentration of L was varied 1.7 to 15.4 mM. The catalytic reaction was initiated and the data collected as described for that concerning reaction order calculation with respect to $[48]$. Identical procedures were applied to determine the order of the catalytic reaction in the ligand concentration. Above ratios of $\text{L}:\text{Cu} \geq 3$ consumption of **48** was observed to transition from first order dependence in the adduct to zero order behaviour showing that a switch of mechanism from ligand accelerated to ligand inhibited catalysis was observed (Figure 22). The two regimes were clearly apparent in order plots of k_1 and k_0 respectively vs. $[\text{L}]_0$. Identical procedures were applied providing an order of the catalytic reaction in the ligand concentration of 0.67 at $\text{L}:\text{Cu} < 3$ with the introduction of a zero-order reaction rate degradation observed at $\text{L}:\text{Cu} \geq 3$; this corresponds with an inhibitory reaction order with respect to the ligand of -2.5 (Figure 22).

3.1.3 General Information and Specifications for Quinolone Conjugate Addition Reactions

All air-sensitive reactions were carried out under an argon atmosphere using oven-dried apparatus with further purging using a Schlenk line. All ethereal solvents used for air sensitive reactions were distilled from sodium wire and benzophenone. Dichloromethane was distilled over calcium hydride. All other solvents and commercially available compounds were purchased from commercial sources and used as received unless stated otherwise. All organometallic reagents were either used as received or synthesised as described in the experimental information; all organometallic reagents (including those acquired from commercial sources) were titrated using the Gilman double titration prior to use. Thin layer chromatography was performed on aluminium sheets coated with silica gel 60 Å F254, 0.2 mm thickness. Compounds were visualised *via* exposure to light emissions at 254 nm and 365 nm and developed with potassium permanganate with gentle heating. Flash chromatography was performed with silica gel (Fisher Scientific 60 Å particle size 35-70 micron). Infra-red spectra were recorded on a Nicolet Avatar 360 FT instrument *via* ATR FTIR analysis. NMR spectra were acquired on Bruker DPX-400 (400.2 MHz), Bruker DPX-300 (300.1 MHz), Bruker AV(III)400 (400.1 MHz), Bruker AV400 (400.1 MHz), Bruker Ascend™ 400 (400.1 MHz) or Bruker Ascend™ 500 (500.1 MHz) spectrometers. Chemical shifts are quoted in parts per million (ppm) and were referenced to residual solvent peaks using values provided by the MestReNova processing software in the cases of ¹H and ¹³C NMR spectra. Abbreviations used in the description of resonances are: s (singlet), d (doublet), t (triplet), q (quartet), p (pentet), h (hextet), hept (heptet), app (apparent), br (broad) and m (multiplet). Coupling constants (*J*) are quoted to the nearest 0.1 Hz. High-resolution mass spectra were recorded using electrospray ionisation (ESI) techniques. Theoretical HRMS molecular weights were taken from the spectrometer output file; HRMS analyses deviations from expected values (σ) are given in ppm. The specific rotation $[\alpha]_D^{25}$ was measured using an Anton-Paar MC P100. Melting points were measured on a Gallenkampf melting point apparatus. High performance liquid chromatography spectra were recorded on a Thermo Scientific UltiMate3000 with a UV detector at 254 nm.

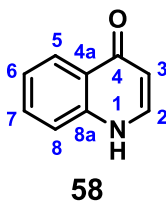
3.1.4 Experimental Data

3-(Dimethylamino)-1-(2-nitrophenyl)prop-2-en-1-one



2'-Nitroacetophenone (12.9 mL, 96.1 mmol) and DMF-DMA (12.9 mL, 97.1 mmol) were heated to 100 °C and stirred under an inert atmosphere for 3 hours. The mixture was allowed to cool to r.t. after which Et₂O was added to induce precipitation of the desired product which was collected *via* filtration and further washed with Et₂O to afford 3-(dimethylamino)-1-(2-nitrophenyl)prop-2-en-1-one as bright orange crystals (16.2 g, 73.7 mmol, 77%); **m.p.** 125-127 °C (lit. 124-127 °C); **¹H NMR** (CDCl₃, 400 MHz): δ_H 7.97 (d, *J* = 7.8 Hz, 1H, C³H), 7.63-7.10 (m, 4H, C⁷H, C⁸H, C⁹H, C¹⁰H), 5.29 (d, *J* = 12.6 Hz, 1H, C²H), 3.11 (s, 3H, N[C^{4a}H₃][C^{4b}H₃]), 2.88 (s, 3H, N[C^{4a}H₃][C^{4b}H₃]); **¹³C {¹H} NMR** (CDCl₃, 101 MHz): δ_C 191.9 (C), 147.3 (CH), 133.1 (C, CH), 129.6 (CH), 128.9 (C, CH), 124.2 (CH), 77.3 (CH), 45.2 (CH₃), 37.3 (CH₃); **IR** (ATR) 3010, 2810, 1649 (C=O), 1531, 1435, 1421, 1355, 1315, 1281, 1240, 1110, 1056; **HRMS** *m/z* calc. for C₁₁H₁₂N₂NaO₃ [M+Na]: 243.0740; found: 243.0726 (σ = 4.30 ppm). These values are concordant with literature precedents.¹²⁷

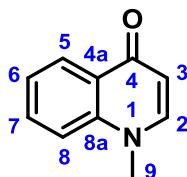
4(1H)-Quinolone 58



To a solution of 3-(dimethylamino)-1-(2-nitrophenyl)prop-2-en-1-one (16.2 g, 73.7 mmol) and cyclohexene (37.3 mL, 368 mmol) in EtOH (220 mL) was added palladium on charcoal (10%) (7.8 g, 7.36 mmol) after which the suspension was stirred at 80 °C for 3 hours. The suspension was cooled to r.t., filtered through celite[®] and concentrated *in vacuo*. The crude material was stirred in EtOAc at reflux for 1 hour and hot filtered to afford compound **58** as a yellow solid (9.56 g, 65.9 mmol, 90%); **m.p.** 199-200 °C (lit. 200-202 °C); **¹H NMR** (400 MHz, DMSO-*d*₆) δ_H 8.14 – 8.06 (m, 1H, C²H), 7.90 (d, *J* = 7.0 Hz, 1H, C⁵H), 7.64 (dd, *J* = 8.4, 7.0 Hz, 1H, C⁶H), 7.54 (dd, *J* = 8.4, 1.2 Hz, 1H, C⁷H), 7.33-7.29 (m, 1H, C⁸H), 6.04 (d, *J* = 7.4 Hz, 1H, C³H), exchangeable NH proton

not seen in spectrum; ^{13}C $\{^1\text{H}\}$ NMR (101 MHz, DMSO- d_6) δ_{C} 177.3 (C), 140.6 (CH), 139.9 (C), 132.1 (CH), 126.3 (CH), 125.4 (C), 123.5 (CH), 118.7 (CH), 109.1 (CH); IR (CHCl₃): ν_{max} 3690, 3608, 3436, 3011, 2999, 1633 (C=O), 1618, 1601, 1540, 1476, 1193; HRMS m/z calc. for C₉H₈NO [M+H]: 146.0600; found: 146.0611 (σ = 6.70 ppm). These values are concordant with literature precedents.¹²⁸

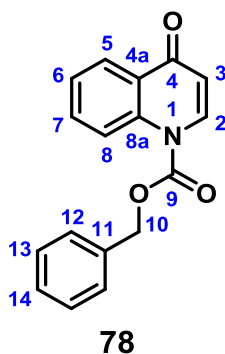
1-Methyl-4(1H)-quinolone 72



72

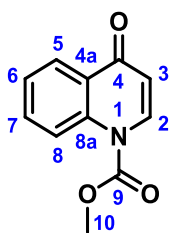
To a stirred suspension of compound **58** (480 mg, 3.31 mmol) and KOH (275 mg, 4.90 mmol) in MeOH (1.5 mL) was added iodomethane (2.0 mL, 32.1 mmol) dropwise at rt. The reaction mixture was stirred at rt for 2 hours. The reaction mixture was filtered *via* suction to remove the precipitate and the mother liquors were concentrated *in vacuo*. The crude material was purified by column chromatography (silica, 4:1 MeOH/EtOAc) to afford compound **72** as a grey solid (302 mg, 1.90 mmol, 57%); **m.p.** 153-155 °C; ^1H NMR (400 MHz, CD₃OD) δ_{H} 8.36 (dd, J = 8.2, 1.5 Hz, 1H, C⁵H), 8.05 (d, J = 7.5 Hz, 1H, C²H), 7.85 (ddd, J = 8.6, 6.9, 1.5 Hz, 1H, C⁷H), 7.78 (d, J = 8.6 Hz, 1H, C⁸H), 7.55 – 7.48 (m, 1H), 6.33 (d, J = 7.5 Hz, 1H, C³H), 3.97 (s, 3H, C⁹H₃); ^{13}C $\{^1\text{H}\}$ NMR (101 MHz, CD₃OD) δ_{C} 176.8 (C), 145.5 (CH), 141.1 (C), 132.5 (CH), 127.0 (C), 126.0 (CH), 123.8 (CH), 117.2 (CH), 109.1 (CH), additional peak obscured by solvent at ~49.0 (CH₃); HRMS m/z calc. for C₁₀H₁₀NO [M+H]: 160.0757; found: 160.0762 (σ = 3.10 ppm). These values are concordant with literature precedents.¹²⁹

Benzyl 4(1*H*)-quinolone-1-carboxylate **78**



To a stirred suspension of compound **58** (184 mg, 1.27 mmol) and NaH (60% wt.) (152 mg, 3.80 mmol) in THF (8.5 mL) was added benzyl chloroformate (0.27 mL, 1.90 mmol) under argon at 55 °C. The reaction mixture was allowed to cool to room temperature and stirred for 24 hours under argon. H₂O (1 mL) was added to the reaction mixture dropwise which was stirred until a homogeneous solution had formed. The reaction mixture was partitioned between Et₂O (5 mL) and H₂O (3 mL) and the phases were separated; the aqueous layer was extracted with Et₂O (3 × 3 mL). The combined organic phases were washed with H₂O (8 mL), dried (MgSO₄), concentrated *in vacuo* and purified by column chromatography (silica, 2:1 Et₂O-Pentane) to afford compound **78** as a cream solid (264 mg, 0.945 mmol, 75%); **m.p.** 66-68 °C; **¹H NMR** (400 MHz, CDCl₃) δ_H 8.69 (d, *J* = 8.8 Hz, 1H, C²H), 8.42 – 8.35 (m, 2H, C⁵H, C⁷H), 7.68 (ddd, *J* = 8.8, 7.2, 1.7 Hz, 1H, C⁷H), 7.53 – 7.41 (m, 6H, C⁶H, 2 × C¹²H, 2 × C¹³H, C¹⁴H), 6.27 (d, *J* = 8.6 Hz, 1H, C³H), 5.49 (s, 2H, C¹⁰H₂); **¹³C {¹H} NMR** (101 MHz, CDCl₃) δ_C 178.9 (C), 151.3 (C), 138.5 (C), 138.2 (CH), 134.0 (C), 132.9 (CH), 129.3 (CH), 129.0 (CH), 128.9 (CH), 126.6 (C, CH), 125.5 (CH), 120.0 (CH), 112.5 (CH), 70.5 (CH₂); **IR** (CHCl₃): ν_{max} 3009, 1756, 1644 (C=O), 1602, 1565, 1471, 1379, 1358, 1193, 1016; **HRMS** *m/z* calc. for C₁₇H₁₄NO₃ [M+H]: 280.0968; found: 280.0966 (σ = 0.70 ppm). These values are concordant with literature precedents.⁹⁹

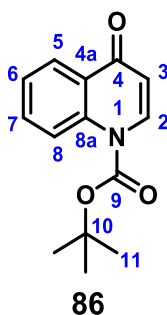
Methyl 4(1*H*)-quinolone-1-carboxylate **85**



85

To a stirred suspension of compound **58** (479 mg, 3.30 mmol) and NaH (60% wt.) (400 mg, 10.0 mmol) in THF (22 mL) was added methyl chloroformate (0.39 mL, 5.05 mmol) under argon at 55 °C. The reaction mixture was allowed to cool to room temperature and stirred for 24 hours under argon. H₂O (2.5 mL) was added to the reaction mixture dropwise which was stirred until a homogeneous solution had formed. The reaction mixture was partitioned between Et₂O (10 mL) and H₂O (5 mL) and the phases were separated; the aqueous layer was extracted with Et₂O (3 × 8 mL). The combined organic phases were washed with H₂O (20 mL), dried (MgSO₄), concentrated *in vacuo* and purified by column chromatography (silica, 2:1 Et₂O-Pentane) to afford compound **85** was formed as a cream solid (470 mg, 2.31 mmol, 71%); **m.p.** 72-74 °C; **¹H NMR** (400 MHz, MeOD) δ_H 8.36 (dd, *J* = 8.2, 1.5 Hz, 1H, C⁵H), 8.05 (d, *J* = 7.5 Hz, 1H, C²H), 7.85 (ddd, *J* = 8.6, 6.9, 1.5 Hz, 1H, C⁷H), 7.78 (d, *J* = 8.6 Hz, 1H, C⁸H), 7.60 – 7.41 (m, 1H, C⁶H), 6.33 (d, *J* = 7.5 Hz, 1H, C³H), 3.97 (s, 3H, C¹⁰H₃); **¹³C {¹H} NMR** (101 MHz, CDCl₃) δ_C 179.0 (C), 152.0 (C), 138.5 (C), 138.3 (CH), 133.0 (CH), 126.6 (C, CH), 125.5 (CH), 120.0 (CH), 112.5 (CH), 55.3 (CH₃); **IR** (CHCl₃): ν_{max} 3010, 2961, 1760, 1644 (C=O), 1602, 1470, 1440, 1360, 1277, 1240, 1164, 1030, 831; **HRMS** *m/z* calc. for C₁₁H₁₀NO₃ [M+H]: 204.0657; found: 204.0655 (σ = 0.80 ppm).

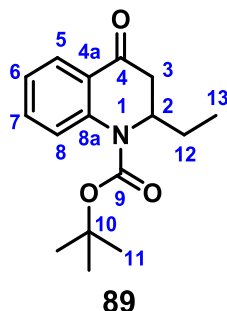
tert-Butyl 4(1*H*)-quinolone-1-carboxylate **86**



To a suspension of **58** (3 g, 20.7 mmol), DMAP (1.26 g, 10.3 mmol) and NEt₃ (2.88 mL, 20.7 mmol) in CH₂Cl₂ (120 mL) was added Boc₂O (9 g, 41.2 mmol); the suspension became homogeneous and was allowed to stir at r.t. for 24 hours. The solution was poured into H₂O (60 mL) and the phases were separated; the aqueous phase was extracted with CH₂Cl₂ (60 mL). The combined organic phases were washed with H₂O (80 mL), dried (MgSO₄), concentrated *in vacuo* and purified by column chromatography (silica, Et₂O) to afford compound **86** as a colourless solid (3.78 g, 15.4 mmol, 75%); **m.p.** 92-94 °C; **¹H NMR** (400 MHz, CDCl₃) δ_H 8.61 (1H, d, *J* = 8.8 Hz, C⁸H), 8.40 (1H, dd, *J* = 8.0, 1.8 Hz, C⁵H), 8.34 (1H, d, *J* = 8.5 Hz, C²H), 7.69 (1H, ddd, *J* = 8.8, 7.1, 1.8 Hz, C⁶H), 7.45 (1H, app. t, *J* = 7.1 Hz, C⁷H), 6.29 (1H, d, *J* = 8.5 Hz, C³H), 1.70 (9H, s, 3 × C¹¹H₃); **¹³C {¹H} NMR** (101 MHz, CDCl₃) δ_C 179.1 (C), 149.9 (C), 138.7 (C), 132.6 (CH), 126.6 (C), 126.5 (CH), 125.2 (2 × CH), 120.0 (CH), 111.9 (CH), 86.6 (C), 28.0 (CH₃); **IR** (CHCl₃): ν_{max} 3011, 2987, 2930, 2856, 1753, 1643 (C=O), 1602, 1562, 1471, 1420, 1397, 1373, 1356, 1277, 1240, 1147, 1076, 1011; **HRMS** *m/z* calc. for C₁₄H₁₅NNaO₃ [M+Na]: 268.0944; found: 268.0943 (σ = 0.40 ppm).

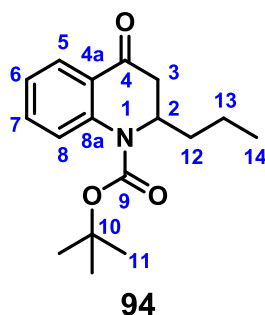
General procedure A for the conjugate addition reactions using Grignard reagents: To a solution of the quinolone substrate (1 equiv.), copper bromide dimethyl sulfide complex (0.05 equiv.) and triphenylphosphine (0.1 equiv.) in 2-methyl tetrahydrofuran (0.2 M solution) stirring at -78 °C under an argon atmosphere was added a solution of the Grignard reagent (2.5 equiv.). The reaction mixture was stirred at -78 °C under an argon atmosphere for 1 hour. H₂O (0.1 mL per mmol of quinolone) was added to the reaction mixture which was allowed to warm to r.t. whilst stirring over 10 minutes. The reaction mixture was partitioned between Et₂O and H₂O; the phases were separated. The aqueous phase was extracted with Et₂O (3 × 10 mL). The combined organic phases were washed with H₂O (15 mL), dried (MgSO₄), concentrated *in vacuo* and purified by column chromatography (silica, 9:1 Pentane-Et₂O) to afford the products as described.

tert-Butyl 2-ethyl-4(1*H*)-quinolone-1-carboxylate 89



General procedure A was followed with compound **86** (245 mg, 1.00 mmol) and ethylmagnesium bromide (3.0 M solution in THF) (0.85 mL, 2.55 mmol) to afford compound **89** as a colourless solid (273 mg, 0.991 mmol, 99%); **m.p.** 65-66 °C; **¹H NMR** (400 MHz, CDCl₃) δ_H 7.98 (dd, *J* = 7.8, 1.6 Hz, 1H, C⁵H), 7.79 (app. d, *J* = 8.6 Hz, 1H, C⁸H), 7.52 (ddd, *J* = 8.6, 7.3, 1.6 Hz, 1H, C⁷H), 7.15 (dd, *J* = 7.8, 7.3 Hz, 1H, C⁶H), 4.85 (app. dtd, *J* = 7.3, 5.8, 1.6 Hz, 1H, C²H), 3.06 (dd, *J* = 17.5, 5.8 Hz, 1H, C³H_AH_B), 2.65 (dd, *J* = 17.5, 1.7 Hz, 1H, C³H_AH_B), 1.79 – 1.37 (m, 11H, 3 × C¹¹H₃, C¹²H₂), 0.91 (t, *J* = 7.3 Hz, 3H, C¹³H₃); **¹³C {¹H} NMR** (101 MHz, CDCl₃) δ_C 193.8 (C), 153.3 (C), 141.5 (C), 134.1 (C, CH), 126.7 (CH), 124.8 (CH), 123.6 (CH), 82.0 (C), 55.0 (CH), 43.2 (CH₂), 28.3 (CH₃), 24.7 (CH₂), 10.7 (CH₃); **IR** (CHCl₃): ν_{max} 3078, 3011, 2976, 2934, 2879, 1683 (C=O), 1601, 1576, 1480, 1461, 1370, 1348, 1304, 1284, 1256, 1163, 1127, 1066, 1047, 1025, 1003; **HRMS** *m/z* calc. for C₁₆H₂₁NNaO₃ [M+Na]: 298.1404; found: 298.1407 (σ = 1.40 ppm).

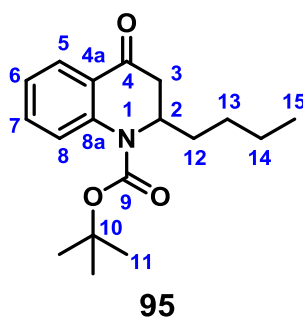
tert-Butyl 2-propyl-4(1*H*)-quinolone-1-carboxylate 94



General procedure A was followed with compound **86** (245 mg, 1.00 mmol) and propylmagnesium bromide (1.85 M in THF) (1.35 mL, 2.50 mmol) to afford compound **94** as a colourless oil (205 mg, 0.708 mmol, 71%); **¹H NMR** (300 MHz, CDCl₃) δ_H 7.97 (dd, *J* = 7.9, 1.5 Hz, 1H, C⁵H), 7.75 (app. d, *J* = 8.2 Hz, 1H, C⁸H), 7.50 (ddd, *J* = 8.2,

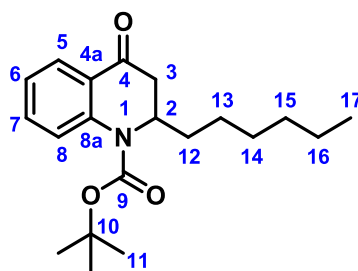
7.2, 1.5 Hz, 1H, C⁷H), 7.14 (dd, $J = 7.9, 7.2$ Hz, 1H, C⁶H), 4.94 (app. dtd, $J = 11.3, 5.7, 1.8$ Hz, 1H, C²H), 3.04 (dd, $J = 17.5, 5.7$ Hz, 1H, C³H_AH_B), 2.61 (dd, $J = 17.5, 1.8$ Hz, 1H, C³H_AH_B), 1.66 – 1.52 (m, 10H, 3 × C¹¹H₃, C¹²H_AH_B), 1.44 – 1.25 (m, 3H, C¹²H_AH_B, C¹³H₂), 0.87 (t, $J = 7.1$ Hz, 3H, C¹⁴H₃); ¹³C {¹H} NMR (75 MHz, CDCl₃) δ_C 193.8 (C), 153.1 (C), 141.6 (C), 134.1 (C), 126.7 (CH), 124.9 (CH), 124.8 (CH), 123.6 (CH), 81.9 (C), 53.3 (CH), 43.3 (CH₂), 33.6 (CH₂), 28.3 (CH₃), 19.4 (CH₂), 13.6 (CH₃); IR (CHCl₃): ν_{max} 3012, 2957, 2926, 2854, 1689 (C=O), 1601, 1479, 1461, 1382, 1369, 1338, 1303, 1292, 1163, 1128; HRMS ^{m/z} calc. for C₁₇H₂₄NO₃ [M+H]: 290.1751; found: 290.1753 (σ = 0.70 ppm).

tert*-Butyl 2-butyl-4(1*H*)-quinolone-1-carboxylate **95*



General procedure was followed with compound **86** (245 mg, 1.00 mmol) and butylmagnesium chloride (2.0 M in THF) (1.25 mL, 2.50 mmol) to afford compound **95** as a colourless oil (224 mg, 0.738 mmol, 74%); ¹H NMR (400 MHz, CDCl₃) δ_H 7.98 (dd, $J = 8.0, 1.7$ Hz, 1H, C⁵H), 7.75 (app. d, $J = 8.5$ Hz, 1H, C⁸H), 7.51 (ddd, $J = 8.5, 7.3, 1.7$ Hz, 1H, C⁷H), 7.14 (dd, $J = 8.0, 7.3$ Hz, 1H, C⁶H), 4.92 (app. dtd, $J = 9.7, 5.8, 1.8$ Hz, 1H, C²H), 3.04 (dd, $J = 17.5, 5.8$ Hz, 1H, C³H_AH_B), 2.64 (dd, $J = 17.5, 1.8$ Hz, 1H, C³H_AH_B), 1.57 (s, 9H, 3 × C¹¹H₃), 1.51 – 1.15 (m, 6H, C¹²H₂, C¹³H₂, C¹⁴H₂), 0.84 (t, $J = 6.9$ Hz, 3H, C¹⁵H₃); ¹³C {¹H} NMR (101 MHz, CDCl₃) δ_C 193.8 (C), 153.1 (C), 141.6 (C), 134.1 (C), 126.7 (CH), 124.9 (CH), 124.8 (CH), 123.6 (CH), 81.9 (C), 53.5 (CH), 43.3 (CH₂), 31.2 (CH₂), 28.4 (CH₃), 28.3 (CH₂), 22.1 (CH₂), 13.9 (CH₃); IR (CHCl₃): ν_{max} 3010, 2961, 2931, 2859, 1683 (C=O), 1602, 1480, 1460, 1384, 1370, 1347, 1305, 1257, 1162; HRMS ^{m/z} calc. for C₁₈H₂₆NO₃ [M+H]: 304.1907; found: 304.1910 (σ = 1.30 ppm).

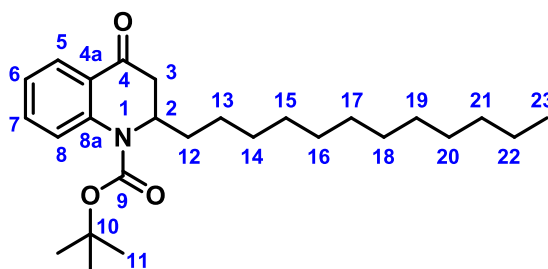
tert-Butyl 2-hexyl-4(1*H*)-quinolone-1-carboxylate 96



96

General procedure A was followed with compound **86** (245 mg, 1.00 mmol) and hexylmagnesium bromide (1.36 M in THF) (1.85 mL, 2.52 mmol) to afford compound **96** as a colourless oil (242 mg, 0.730 mmol, 73%); $^1\text{H NMR}$ (400 MHz, CDCl_3) δ_{H} 7.98 (dd, $J = 7.9, 1.8$ Hz, 1H, C^5H), 7.72 (app. d, $J = 8.4$ Hz, 1H, C^8H), 7.50 (ddd, $J = 8.4, 7.2, 1.8$ Hz, 1H, C^7H), 7.15 (dd, $J = 7.9, 7.2$ Hz, 1H, C^6H), 4.92 (app. dtd, $J = 9.8, 5.8, 1.8$ Hz, 1H, C^2H), 3.04 (dd, $J = 17.5, 5.8$ Hz, 1H, $\text{C}^3\text{H}_\text{A}\text{H}_\text{B}$), 2.55 (dd, $J = 17.5, 1.8$ Hz, 1H, $\text{C}^3\text{H}_\text{A}\text{H}_\text{B}$), 1.66 – 1.51 (m, 10H, $3 \times \text{C}^{11}\text{H}_3$, $\text{C}^{12}\text{H}_\text{A}\text{H}_\text{B}$), 1.49 – 1.37 (m, 1H, $\text{C}^3\text{H}_\text{A}\text{H}_\text{B}$), 1.37 – 1.12 (m, 8H, C^{13}H_2 , C^{14}H_2 , C^{15}H_2 , C^{16}H_2), 0.84 (t, $J = 7.0$ Hz, 3H, C^{17}H_3); ^{13}C $\{^1\text{H}\}$ NMR (101 MHz, CDCl_3) δ_{C} 193.8 (C), 153.1 (C), 141.6 (C), 134.1 (C), 126.7 (CH), 124.9 (CH), 124.8 (CH), 123.6 (CH), 81.9 (C), 53.5 (CH), 43.4 (CH_2), 31.6 (CH_2), 31.4 (CH_2), 28.7 (CH_2), 28.3 (CH_3), 26.1 (CH_2), 22.5 (CH_2), 14.0 (CH_3); IR (CHCl_3): ν_{max} 3011, 2957, 2930, 2858, 1691 (C=O), 1601, 1576, 1480, 1460, 1383, 1368, 1343, 1303, 1254, 1163, 1128, 1045, 1017; HRMS m/z calc. for $\text{C}_{20}\text{H}_{30}\text{NO}_3$ [M+H]: 332.2220; found: 332.2204 ($\sigma = 1.80$ ppm).

tert-Butyl 2-dodecyl-4(1*H*)-quinolone-1-carboxylate 97

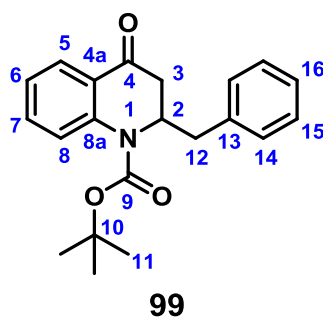


97

General procedure was followed with compound **86** (245 mg, 1.00 mmol) and dodecylmagnesium bromide (1.15 M in THF) (2.17 mL, 2.50 mmol) to afford compound **97** as a colourless solid (287 mg, 0.691 mmol, 69%); m.p. 40-42 °C; $^1\text{H NMR}$ (400 MHz, CDCl_3) δ_{H} 7.98 (dd, $J = 7.9, 1.8$ Hz, 1H, C^5H), 7.77 (d, $J = 8.5$ Hz, 1H, C^8H), 7.52

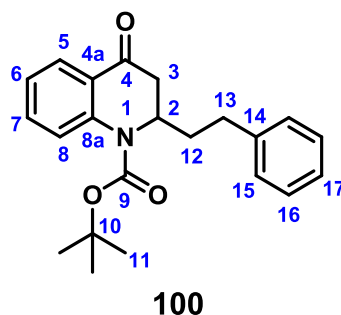
(ddd, $J = 8.5, 7.2, 1.8$ Hz, 1H, C⁷H), 7.16 (dd, $J = 7.9, 7.2$ Hz, 1H, C⁶H), 4.93 (app. dtd, $J = 9.8, 5.9, 1.8$ Hz, 1H, C²H), 3.05 (dd, $J = 17.5, 5.9$ Hz, 1H, C³H_AH_B), 2.63 (dd, $J = 17.5, 1.8$ Hz, 1H, C³H_AH_B), 1.63 (app. d, $J = 2.9$ Hz, 2H, C¹²H), 1.58 (s, 9H, 3 × C¹¹H₃), 1.34 – 1.20 (m, 20H, C¹³H₂, C¹⁴H₂, C¹⁵H₂, C¹⁶H₂, C¹⁷H₂, C¹⁸H₂, C¹⁹H₂, C²⁰H₂, C²¹H₂, C²²H₂), 0.91 (t, $J = 6.8$ Hz, 3H, C²³H₃); ¹³C {¹H} NMR (101 MHz, CDCl₃) δ_C 193.9 (C), 153.2 (C), 141.6 (C), 134.1 (C), 128.5 (CH), 126.7 (CH), 124.9 (CH), 123.7 (CH), 82.0 (C), 53.6 (CH₂), 43.4 (CH), 31.9 (CH₂), 31.4 (CH₂), 29.7 (CH₂), 29.6 (CH₂), 29.5 (CH₂), 29.4(3) (CH₂), 29.3(7) (CH₂), 29.3 (CH₂), 29.0 (CH₂), 28.3 (CH₃), 26.1 (CH₂), 22.7 (CH₂), 14.1 (CH₃); IR (CHCl₃): ν_{max} 3012, 2956, 2923, 2851, 1679 (C=O), 1603, 1523, 1477, 1426, 1383, 1370, 1346, 1334, 1293, 1193, 1097; HRMS *m/z* calc. for C₂₆H₄₂NO₃ [M+H]: 416.3159; found: 416.3147 (σ = 3.70 ppm).

tert*-Butyl 2-benzyl-4(1*H*)-quinolone-1-carboxylate **99*



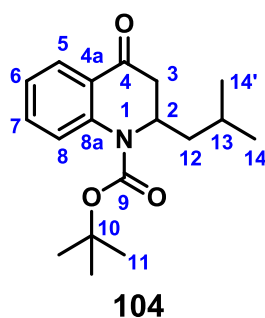
General procedure was followed with compound **86** (245 mg, 1.00 mmol) and benzylmagnesium bromide (1.62 M in THF) (1.55 mL, 2.51 mmol) to afford compound **99** as a colourless oil (322 mg, 0.954 mmol, 95%); ¹H NMR (400 MHz, CDCl₃) δ_H 8.07 (dd, $J = 7.9, 1.7$ Hz, 1H, C⁵H), 7.89 (d, $J = 8.5$ Hz, 1H, C⁸H), 7.58 (ddd, $J = 8.5, 7.2, 1.7$ Hz, 1H, C⁷H), 7.33 – 7.17 (m, 4H, 2 × C¹⁴H, 2 × C¹⁵H), 7.08 – 7.03 (m, 2H, C⁶H, C¹⁶H), 5.14 (app. dtd, $J = 9.2, 6.1, 1.7$ Hz, 1H, C²H), 3.06 (dd, $J = 17.5, 6.1$ Hz, 1H, C³H_AH_B), 2.97 – 2.67 (m, 3H, C³H_AH_B, C¹²H₂), 1.39 (s, 9H, 3 × CH₃); ¹³C {¹H} NMR (101 MHz, CDCl₃) δ_C 193.3 (C), 152.6 (C), 141.7 (C), 137.7 (C), 134.5 (C), 129.2 (CH), 128.4 (CH), 127.0 (CH), 126.0 (CH), 124.5 (2 × CH), 123.5 (CH), 81.9 (C), 55.2 (CH₂), 42.5 (CH), 37.9 (CH₂), 28.0 (CH₃); IR (CHCl₃): ν_{max} 3065, 3005, 2977, 2929, 2859, 1708, 1689 (C=O), 1601, 1575, 1479, 1459, 1383, 1368, 1346, 1303, 1274, 1254, 1162, 1136, 1084, 1044, 1019; HRMS *m/z* calc. for C₂₁H₂₄NO₃ [M+H]: 338.1751; found: 338.1754 (σ = 0.90 ppm).

tert-Butyl 2-(2-phenylethyl)-4(1H)-quinolone-1-carboxylate 100



General procedure was followed with compound **86** (245 mg, 1.00 mmol) and 2-phenylethylmagnesium bromide (1.36 M in THF) (1.85 mL, 2.52 mmol) to afford compound **100** as a colourless oil (270 mg, 0.768 mmol, 77%); $^1\text{H NMR}$ (400 MHz, CDCl_3) δ_{H} 7.99 (1H, dd, $J = 8.0, 1.7$ Hz, C^5H), 7.67 (1H, d, $J = 8.5$ Hz, C^8H), 7.52 (1H, ddd, $J = 8.5, 7.3, 1.7$ Hz, C^7H), 7.28 – 7.14 (4H, m, $2 \times \text{C}^{15}\text{H}$, $2 \times \text{C}^{16}\text{H}$), 7.12 – 7.06 (2H, m, C^6H , C^{17}H), 5.00 (1H, app. dtd, $J = 10.0, 5.8, 1.8$ Hz, C^2H), 3.08 (1H, dd, $J = 17.6, 5.8$ Hz, $\text{C}^3\text{H}_\text{A}\text{H}_\text{B}$), 2.77 – 2.56 (3H, m, $\text{C}^3\text{H}_\text{A}\text{H}_\text{B}$, C^{13}H_2), 1.95 (1H, app. dtd, $J = 14.1, 9.6, 6.1$ Hz, C, $\text{C}^{12}\text{H}_\text{A}\text{H}_\text{B}$), 1.81 (1H, ddt, $J = 14.1, 9.4, 6.0$ Hz, $\text{C}^{12}\text{H}_\text{A}\text{H}_\text{B}$), 1.56 (9H, s, $3 \times \text{C}^{11}\text{H}_3$); ^{13}C $\{^1\text{H}\}$ NMR (101 MHz, CDCl_3) δ_{C} 193.6 (C), 153.1 (C), 141.4 (C), 140.9 (C), 134.2 (C), 128.4 (CH), 128.2 (CH), 126.7 (CH), 126.0 (CH), 125.1 (CH), 124.9 (CH), 123.9 (CH), 82.1 (C), 53.4 (CH), 43.4 (CH_2), 33.1 (CH_2), 32.6 (CH_2), 28.3 (CH_3); IR (CHCl_3): ν_{max} 3063, 3004, 2977, 2930, 2859, 1688 (C=O), 1601, 1576, 1479, 1458, 1368, 1337, 1303, 1253, 1160, 1133, 1046; HRMS m/z calc. for $\text{C}_{22}\text{H}_{25}\text{NNaO}_3$ [$\text{M}+\text{Na}$]: 374.1727; found: 374.1729 ($\sigma = 0.60$ ppm).

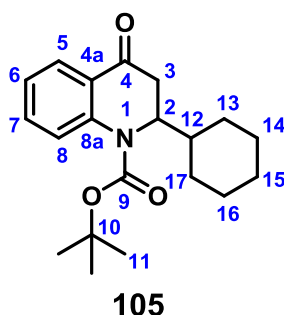
tert-Butyl 2-isobutyl-4(1H)-quinolone-1-carboxylate 104



General procedure was followed with compound **86** (245 mg, 1.00 mmol) and isobutylmagnesium bromide (1.9 M in THF) (1.32 mL, 2.51 mmol) to afford compound **104** as a colourless oil (261 mg, 0.860 mmol, 86%); $^1\text{H NMR}$ (400 MHz, CDCl_3) δ_{H} 7.98 (dd, $J = 8.0, 1.7$ Hz, 1H, C^5H), 7.74 (app. d, $J = 8.5$ Hz, 1H, C^8H), 7.51 (ddd, $J = 8.5,$

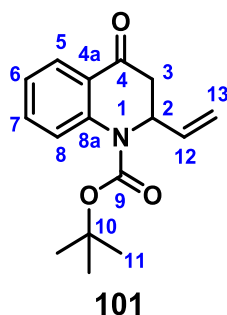
7.2, 1.7 Hz, 1H, C⁷H), 7.15 (dd, $J = 8.0, 7.2$ Hz, 1H, C⁶H), 4.97 (app. dtd, $J = 9.5, 5.7, 1.8$ Hz, 1H, C²H), 3.05 (dd, $J = 17.4, 5.7$ Hz, 1H, C³H_AH_B), 2.59 (dd, $J = 17.4, 1.8$ Hz, 1H, C³H_AH_B), 1.64 – 1.17 (m, 12H, 3 × C¹¹H₃, C¹²H₂, C¹³H), 0.96 (d, $J = 6.4$ Hz, 3H, C¹⁴H₃), 0.82 (d, $J = 6.4$ Hz, 3H, C¹⁴H₃); ¹³C {¹H} NMR (101 MHz, CDCl₃) δ_C 193.8 (C), 153.0 (C), 141.6 (C), 134.1 (C), 126.6 (CH), 125.1 (CH), 125.0 (CH), 123.8 (CH), 82.0 (C), 52.0 (CH), 43.5 (CH), 40.5 (CH₂), 28.3 (CH₃), 25.2 (CH), 22.7 (CH₃), 22.2 (CH₃); IR (CHCl₃): ν_{max} 3012, 2956, 2924, 2853, 1684 (C=O), 1602, 1479, 1460, 1385, 1370, 1350, 1335, 1304, 1294, 1163, 1131; HRMS ^{m/z} calc. for C₁₈H₂₆NO₃ [M+H]: 304.1907; found: 304.1905 (σ = 0.60 ppm).

***tert*-Butyl 2-cyclohexyl-4(1*H*)-quinolone-1-carboxylate 105**



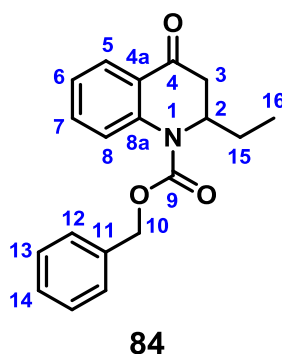
General procedure was followed with compound **86** (245 mg, 1.00 mmol) and cyclohexylmagnesium bromide (1.74 M in THF) (1.44 mL, 2.51 mmol) to afford compound **105** as a colourless oil (200 mg, 0.607 mmol, 61%); ¹H NMR (400 MHz, CDCl₃) δ_H 7.97 (dd, $J = 8.0, 1.6$ Hz, 1H, C⁵H), 7.73 (app. d, $J = 8.5$ Hz, 1H, C⁸H), 7.51 (ddd, $J = 8.5, 7.2, 1.6$ Hz, 1H, C⁷H), 7.14 (dd, $J = 8.0, 7.2$ Hz, 1H, C⁶H), 4.56 (ddd, $J = 10.6, 5.1, 2.4$ Hz, 1H, C²H), 2.96 (dd, $J = 17.5, 5.1$ Hz, 1H, C³H_AH_B), 2.87 (dd, $J = 17.5, 2.4$ Hz, 1H, C³H_AH_B), 1.79 – 1.60 (m, 6H, 6 × [cyclohexyl-C]H), 1.56 (s, 9H, 3 × C¹¹H₃), 1.23 – 0.83 (m, 5H, 5 × [cyclohexyl-C]H); ¹³C {¹H} NMR (101 MHz, CDCl₃) δ_C 193.9 (C), 153.3 (C), 142.0 (C), 134.0 (C), 126.6 (CH), 125.2 (CH), 124.9 (CH), 123.6 (CH), 81.9 (C), 58.8 (CH), 40.9 (CH₂), 37.5 (CH), 29.8 (CH₂), 29.7 (CH₂), 28.3 (CH₂), 26.0 (CH₂), 25.6(1) (CH₂), 25.5(8) (CH₂); IR (CHCl₃): ν_{max} 3012, 2927, 2855, 1681 (C=O), 1601, 1519, 1461, 1422, 1371, 1342, 1307, 1288, 1163, 1130; HRMS ^{m/z} calc. for C₂₀H₂₈NO₃ [M+H]: 330.2064; found: 330.2063 (σ = 0.20 ppm).

tert-Butyl 2-vinyl-4(1*H*)-quinolone-1-carboxylate **101**



General Procedure A was followed with compound **86** (245 mg, 1.00 mL) and vinylmagnesium bromide (1.0 M in THF) (2.50 mL, 2.50 mmol) to afford compound **101** as a colourless oil (136 mg, 0.498 mmol, 50%); **¹H NMR** (400 MHz, CDCl₃) δ_H 7.97 (dd, *J* = 7.7, 1.8 Hz, 1H, C⁵H), 7.82 (dd, *J* = 8.5, 1.0 Hz, 1H, C⁸H), 7.51 (ddd, *J* = 8.5, 7.2, 1.8 Hz, 1H, C⁷H), 7.14 (td, *J* = 7.7, 7.2, 1.0 Hz, 1H, C⁶H), 5.80 (ddd, *J* = 17.2, 10.9, 4.3 Hz, 1H, C¹²H), 5.53 (app. ddq, *J* = 6.1, 4.3, 2.0 Hz, 1H, C¹³H_AH_B), 5.15 (app. d, *J* = 2.0 Hz, 1H, C¹³H_AH_B), 5.14 – 5.10 (m, 1H, C²H), 3.11 (dd, *J* = 17.4, 6.1 Hz, 1H, C³H_AH_B), 2.87 (dd, *J* = 17.4, 2.0 Hz, 1H, C³H_AH_B), 1.59 (s, 9H, 3 × C¹¹H₃); **¹³C {¹H} NMR** (101 MHz, CDCl₃) δ_C 193.1 (C), 152.9 (C), 142.0 (C), 135.2 (C), 134.2 (CH), 126.9 (CH), 124.6 (CH), 124.2 (CH), 123.6 (CH), 117.8 (CH₂), 82.4 (C), 55.0 (CH), 42.1 (CH₂), 28.3 (CH₃); **IR** (CHCl₃): ν_{max} 3012, 2956, 2926, 2854, 1739, 1691 (C=O), 1602, 1520, 1479, 1462, 1426, 1370, 1334, 1302, 1193, 1162, 1129; **HRMS** *m/z* calc. for C₁₆H₂₀NO₃ [M+H]: 274.1438; found: 274.1442 (σ = 1.20 ppm).

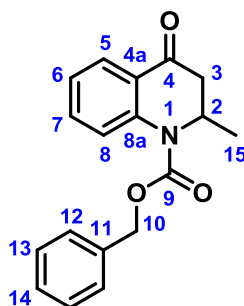
Benzyl 2-ethyl-4(1*H*)-quinolone-1-carboxylate **84**



General Procedure A was followed with compound **78** (903 mg, 3.23 mmol) and ethylmagnesium bromide (3.0 M in THF) (2.70 mL, 8.10 mmol) to afford compound **84** as a colourless solid (798 mg, 2.58 mmol, 80%); **m.p.** 74-76 °C; **¹H NMR** (400 MHz, CDCl₃) δ_H 8.00 (dd, *J* = 7.8, 1.7 Hz, 1H, C⁵H), 7.81 (d, *J* = 8.2 Hz, 1H, C⁸H), 7.54 (ddd,

$J = 8.2, 7.8, 1.7$ Hz, 1H), 7.46 – 7.33 (m, 5H, 2 × C¹²H, 2 × C¹³H, C¹⁴H), 7.19 (dd, $J = 7.8$ Hz, 7.8 Hz, 1H, C⁶H), 5.32 (s, 2H, C¹⁰H₂), 4.94 (dtd, $J = 9.9, 5.8, 1.7$ Hz, 1H, C²H), 3.07 (dd, $J = 17.6, 5.8$ Hz, 1H, C³H_AH_B), 2.67 (dd, $J = 17.6, 1.8$ Hz, 1H, C³H_AH_B), 1.73 – 1.38 (m, 2H, C¹⁵H₂), 0.90 (t, $J = 7.4$ Hz, 3H, C¹⁶H₃); ¹³C {¹H} NMR (101 MHz, CDCl₃) δ_C 193.4 (C), 154.2 (C), 140.9 (C), 135.8 (C), 134.4 (C), 128.7 (CH), 128.4 (CH), 128.1 (CH), 126.8 (CH), 125.0 (CH), 124.7 (CH), 124.2 (CH), 68.2 (CH₂), 55.4 (CH), 43.2 (CH₂), 24.6 (CH₂), 10.7 (CH₃); IR (CHCl₃): ν_{max} 3051, 2968, 1685 (C=O), 1602, 1481, 1461, 1395, 1341, 1323, 1304, 1272, 1240, 1127, 909; HRMS ^{m/z} calc. for C₁₉H₂₀NO₃ [M+H]: 310.1438; found: 310.1451 (σ = 3.70 ppm).

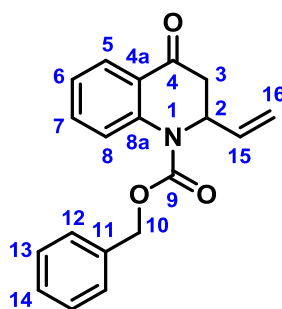
Benzyl 2-methyl-4(1*H*)-quinolone-1-carboxylate **90**



90

General Procedure A was followed with compound **78** (112 mg, 0.401 mmol) and methylmagnesium bromide (2.0 M in THF) (0.500 mL, 1.00 mmol) to afford compound **90** as a colourless oil (64 mg, 0.217 mmol, 54%); ¹H NMR (400 MHz, CDCl₃) δ_H 8.03 (dd, $J = 7.8, 1.7$ Hz, 1H, C⁵H), 7.87 (d, $J = 8.4$ Hz, 1H, C⁸H), 7.58 – 7.50 (m, 1H, C⁷H), 7.47 – 7.35 (m, 5H, 2 × C¹²H, 2 × C¹³H, C¹⁴H), 7.23 – 7.16 (m, 1H, C⁶H), 5.33 (s, 2H, C¹⁰H₂), 5.23 (qdd, $J = 7.0, 5.8, 1.8$ Hz, 1H, C²H), 3.08 (dd, $J = 17.3, 5.8$ Hz, 1H, C³H_AH_B), 2.60 (dd, $J = 17.3, 1.8$ Hz, 1H, C³H_AH_B), 1.28 (d, $J = 7.0$ Hz, 3H, C¹⁵H₃); ¹³C {¹H} NMR (101 MHz, CDCl₃) δ_C 193.3 (C), 153.7 (C), 141.0 (C), 135.8 (C), 134.6 (C), 128.7 (CH), 128.5 (CH), 128.2 (CH), 126.9 (CH), 124.4 (CH), 124.3 (CH), 124.0 (CH), 68.2 (CH₂), 50.0 (CH), 44.4 (CH₂), 17.9 (CH₃); IR (CHCl₃): ν_{max} 3011, 2972, 2900, 1685 (C=O), 1602, 1577, 1481, 1461, 1394, 1350, 1326, 1305, 1275, 1246, 1163, 1128, 1107, 1061, 1047, 1011; HRMS ^{m/z} calc. for C₁₈H₁₇NNaO₃ [M+Na]: 318.1101; found: 318.1108 (σ = 2.20 ppm).

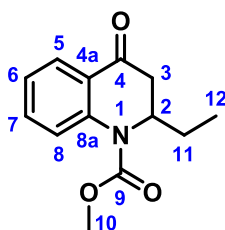
Benzyl 2-vinyl-4(1*H*)-quinolone-1-carboxylate **91**



91

General procedure was followed with compound **78** (909 mg, 3.25 mmol) and vinylmagnesium bromide (1.0 M in THF) (8.1 mL, 8.1 mmol) to afford compound **91** as a colourless oil (767 mg, 2.50 mmol, 77%); **¹H NMR** (400 MHz, CDCl₃) δ_H 7.99 (dd, *J* = 7.8, 1.7 Hz, 1H, C⁵H), 7.87 (d, *J* = 8.5 Hz, 1H, C⁸H), 7.53 (ddd, *J* = 8.5, 7.3, 1.7 Hz, 1H, C⁷H), 7.45 – 7.35 (m, 5H, 2 × C¹²H, 2 × C¹³H, C¹⁴H), 7.18 (dd, *J* = 7.8, 7.3 Hz, 1H, C⁶H), 5.80 (ddd, *J* = 17.3, 10.7, 4.3 Hz, 1H, C¹⁵H), 5.34 (s, 2H, C¹⁰H₂), 5.19 – 5.11 (m, 2H, C¹⁶H₂), 4.87 – 4.80 (m, 1H, C²H), 3.12 (dd, *J* = 17.4, 5.9 Hz, 1H, C³H_AH_B), 2.89 (dd, *J* = 17.4, 2.0 Hz, 1H, C³H_AH_B); **¹³C {¹H} NMR** (101 MHz, CDCl₃) δ_C 192.7 (C), 154.0 (C), 141.0 (C), 135.6 (C), 134.8 (C), 134.5 (CH), 128.7 (CH), 128.5 (CH), 128.2 (CH), 127.0 (2 × CH), 124.1 (2 × CH), 118.2 (CH₂), 68.4 (CH₂), 55.4 (CH), 42.1 (CH₂); **IR** (CHCl₃): ν_{max} 3012, 2956, 2926, 2854, 1739, 1691 (C=O), 1602, 1520, 1479, 1462, 1426, 1370, 1334, 1302, 1193, 1162, 1129; **HRMS** *m/z* calc. for C₁₉H₁₇NNaO₃ [M+Na]: 330.1101; found: 330.1102 (σ = 0.30 ppm).

Methyl 2-ethyl-4(1*H*)-quinolone-1-carboxylate **87**

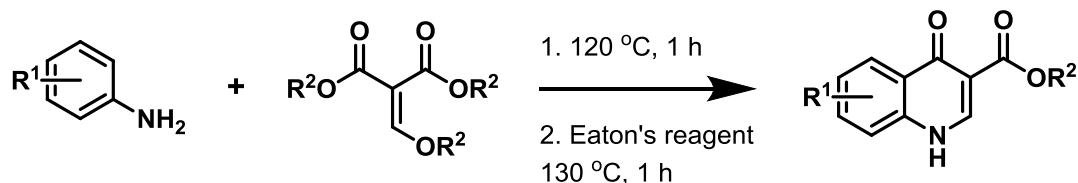


87

General Procedure A was followed with compound **85** (88 mg, 0.429 mmol) and ethylmagnesium bromide (3.0 M in THF) (0.36 mL, 1.08 mmol) to afford compound **87** as a colourless oil (79 mg, 0.339 mmol, 79%); **m.p.** 74-76 °C; **¹H NMR** (400 MHz, CDCl₃) δ_H 7.99 (dd, *J* = 7.8, 1.2 Hz, 1H), 7.76 (d, *J* = 8.3 Hz, 1H), 7.58 – 7.51 (m, 1H), 7.19 (t, *J* = 7.5 Hz, 1H), 4.94 – 4.86 (m, 1H, C²H), 3.87 (s, 3H, C¹⁰H₃), 3.06 (dd, *J* = 17.6, 5.8 Hz, 1H, C³H_AH_B), 2.66 (dd, *J* = 17.6, 1.0 Hz, 1H, C³H_AH_B), 1.68 – 1.43 (m,

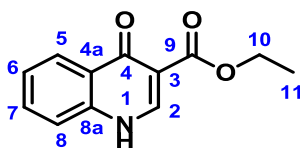
1H, C¹¹H_AH_B), 1.22 (app. t, *J* = 7.2 Hz, 1H, C¹¹H_AH_B), 0.90 (app. t, *J* = 7.2 Hz, 3H); ¹³C {¹H} NMR (101 MHz, CDCl₃) δ_C 193.5 (C), 154.9 (C), 140.9 (C), 134.4 (C), 126.8 (CH), 125.0 (CH), 124.7 (CH), 124.2 (CH), 55.4 (CH), 53.3 (CH₃), 43.1 (CH₂), 24.6 (CH₂), 10.7 (CH₃); IR (CHCl₃): ν_{max} 3011, 2972, 1684, 1603, 1481, 1461, 1442, 1389, 1348, 1304, 1282, 1193; HRMS ^{m/z} calc. for C₁₃H₁₆NO₃ [M+H]: 234.1125; found: 234.1120 (σ = 2.20 ppm).

General procedure B for the synthesis of substituted quinolones



A modification of the literature procedure reported by Christopoulos, Scammells and co-workers was used to synthesise the quinolone derivatives.¹³⁰ A mixture of neat dialkyl alkoxymethylenemalonate (1.05 equiv.) and substituted aniline (1 equiv.) was stirred at 120 °C for 1 hour. The mixture was allowed to cool to r.t. after which Eaton's reagent (0.8 mL per mmol of aniline) was added.¹³¹ The mixture was stirred at 130 °C for 1 hour then cooled to r.t. The reaction mixture was added dropwise to a saturated aqueous solution of NaHCO₃ (15 × volume of Eaton's reagent). The precipitate that formed was collected *via* vacuum filtration and washed sequentially with large amounts of water, EtOAc and Et₂O to afford the quinolone derivatives as described.

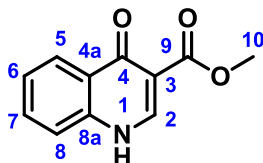
Ethyl 4(1*H*)-quinolone-3-carboxylate



General procedure B was followed using compound **61** (9.1 mL, 99.8 mmol) and diethyl ethoxymethylenemalonate (20.0 mL, 99.9 mmol) to afford ethyl 4(1*H*)-quinolone-3-carboxylate as a tan solid (17.4 g, 80.1 mmol, 80%); **m.p.** >250 °C; ¹H NMR (400 MHz, DMSO-*d*₆): δ_H 12.33 (s, 1H, NH), 8.56 (s, 1H, C²H), 8.17 (dd, *J* = 8.1, 1.6 Hz, 1H, C⁵H), 7.71 (ddd, *J* = 8.4, 6.9, 1.6 Hz, 1H, C⁷H), 7.62 (dd, *J* = 8.4, 1.2 Hz, 1H, C⁸H), 7.42 (ddd, *J* = 8.1, 6.9, 1.2 Hz, 1H, C⁶H), 4.22 (q, *J* = 7.1 Hz, 2H, C¹⁰H₂), 1.29 (t, *J* = 7.1 Hz, 3H, C¹¹H₃); ¹³C {¹H} NMR (101 MHz, DMSO-*d*₆): δ_C 173.9 (C), 165.3 (C), 145.4 (CH), 139.4 (C), 132.9 (CH), 127.7 (C), 126.1 (CH), 125.2 (CH), 119.3 (CH), 110.2 (C), 60.0 (CH₂),

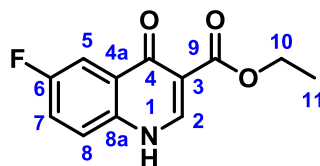
14.8 (CH₃); **IR** (ATR): ν_{\max} 3162, 3127, 3066, 2973, 2900, 1696 (C=O), 1620, 1592, 1553, 1527, 1474, 1441, 1379, 1357, 1339, 1286, 1263, 1214, 1195, 1137, 1109, 1093, 1035, 1022, 962, 938, 849, 800, 761, 741, 684, 627, 612, 563, 492, 422; **HRMS** m/z calc. for C₁₂H₁₂NO₃ [M+H]: 218.0812; found: 218.0809 (σ = 1.10 ppm). These values are concordant with literature precedents.¹¹⁴

Methyl 4(1*H*)-quinolone-3-carboxylate



General procedure B was followed using aniline (0.46 mL, 5.05 mmol) and dimethyl methoxymethylenemalonate (880 mg, 5.05 mmol) to afford methyl 4(1*H*)-quinolone-3-carboxylate as a brown solid (760 mg, 3.74 mmol, 74%); **m.p.** 227-229 °C; **¹H NMR** (400 MHz, DMSO-*d*₆): δ_{H} 12.36 (s, 1H, NH), 8.58 (s, 1H, C²H), 8.17 (dd, J = 8.1, 1.5 Hz, 1H, C⁵H), 7.71 (ddd, J = 8.3, 7.0, 1.5 Hz, 1H, C⁷H), 7.63 (dd, J = 8.3, 1.2 Hz, 1H, C⁸H), 7.42 (ddd, J = 8.1, 7.0, 1.2 Hz, 1H, C⁶H), 3.75 (s, 3H, C¹⁰H₃); **¹³C {¹H} NMR** (101 MHz, DMSO-*d*₆): δ_{C} 173.9 (C), 165.9 (C), 145.6 (CH), 139.4 (C), 132.9 (CH), 127.7 (C), 126.1 (CH), 125.2 (CH), 119.3 (CH), 110.0 (C), 51.6 (CH₃); **IR** (ATR): ν_{\max} 3250, 3163, 3121, 3086, 3048, 3016, 2983, 2952, 2902, 2872, 2819, 1708 (C=O), 1615, 1588, 1533, 1477, 1443, 1373, 1295, 1218, 1205, 1136, 1092, 1042, 1030, 997, 953, 902, 863, 805, 760, 740, 681, 630, 606, 563, 542, 498, 475, 414; **HRMS** m/z calc. for C₁₁H₁₀NO₃ [M+H]: 204.0655; found: 204.0659 (σ = 1.70 ppm).

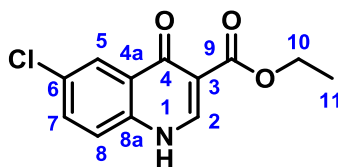
Ethyl 6-fluoro-4(1*H*)-quinolone-3-carboxylate



General procedure B was followed using 4-fluoroaniline (0.28 mL, 2.96 mmol) and diethyl ethoxymethylenemalonate (0.63 mL, 3.15 mmol) to afford ethyl 6-fluoro-4(1*H*)-quinolone-3-carboxylate as a tan solid (495 mg, 2.10 mmol, 71%); **m.p.** >250 °C; **¹H NMR** (500 MHz, DMSO-*d*₆): δ_{H} 12.45 (s, 1H, NH), 8.59 (s, 1H, C²H), 7.81 (dd, J = 9.3, 3.0 Hz, 1H, C⁵H), 7.72 (dd, J = 9.0, 4.7 Hz, 1H, C⁸H), 7.63 (ddd, J = 9.0, 8.6, 3.0 Hz, 1H, C⁷H), 4.23 (q, J = 7.1 Hz, 2H, C¹⁰H₂), 1.29 (t, J = 7.1 Hz, 3H, C¹¹H₃); **¹³C {¹H} NMR**

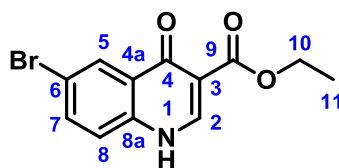
(126 MHz, DMSO- d_6): δ_c 173.0 (C), 165.2 (C), 159.7 (d, $J = 243.4$ Hz, C), 145.4 (CH), 136.2 (C), 129.2 (d, $J = 6.6$ Hz, C), 122.1 (d, $J = 8.3$ Hz, CH), 121.5 (d, $J = 25.3$ Hz, CH), 110.5 (d, $J = 23.0$ Hz, CH), 109.5 (C), 60.1 (CH₂), 14.8 (CH₃); **^{19}F NMR** (471 MHz, DMSO- d_6): δ_F -116.1 (1F); **IR** (ATR): ν_{max} 3132, 3102, 3046, 2983, 1692 (C=O), 1618, 1593, 1561, 1534, 1483, 1457, 1397, 1381, 1360, 1297, 1280, 1224, 1195, 1168, 1134, 1077, 1031, 956, 910, 893, 858, 826, 798, 756, 747, 724, 631, 608, 566, 539, 520, 462, 432, 407; **HRMS** m/z calc. for C₁₂H₁₁FNO₃ [M+H]: 236.0717; found: 236.0717 ($\sigma = 0.20$ ppm). These values are concordant with literature precedents.¹³² ^{19}F NMR and HRMS data have not previously been obtained for the compound.

Ethyl 6-chloro-4(1*H*)-quinolone-3-carboxylate



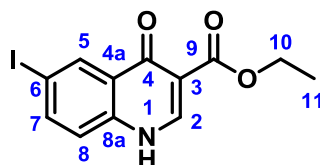
General procedure B was followed using 4-chloroaniline (383 mg, 3.00 mmol) and diethyl ethoxymethylenemalonate (0.63 mL, 3.15 mmol) to afford ethyl 6-chloro-4(1*H*)-quinolone-3-carboxylate as a tan solid (513 mg, 2.04 mmol, 68%); **m.p.** >250 °C; **^1H NMR** (500 MHz, DMSO- d_6): δ_H 12.47 (s, 1H, NH), 8.59 (s, 1H, C²H), 8.08 (d, $J = 2.5$ Hz, 1H, C⁵H), 7.76 (dd, $J = 8.8, 2.5$ Hz, 1H, C⁷H), 7.68 (d, $J = 8.8$ Hz, 1H, C⁸H), 4.23 (q, $J = 7.1$ Hz, 2H, C¹⁰H₂), 1.29 (t, $J = 7.1$ Hz, 3H, C¹¹H₃); **^{13}C { $^1\text{H}}$ NMR** (126 MHz, DMSO- d_6): δ_c 172.7 (C), 165.1 (C), 145.7 (CH), 138.2 (C), 133.0 (CH), 129.9 (C), 128.9 (C), 125.1 (CH), 121.8 (CH), 110.5 (C), 60.2 (CH₂), 14.8 (CH₃); **IR** (ATR): ν_{max} 3152, 3091, 2985, 2906, 1694 (C=O), 1620, 1553, 1525, 1470, 1398, 1378, 1360, 1340, 1294, 1253, 1202, 1187, 1152, 1116, 1104, 1032, 959, 902, 862, 823, 799, 756, 742, 644, 629, 603, 559, 524, 505, 442, 424; **HRMS** m/z calc. for C₁₂H₁₀³⁵ClNNO₃ [M+Na]: 274.0241; found: 274.0235 ($\sigma = 2.30$ ppm). These values are concordant with literature precedents.¹³³ ^{13}C { $^1\text{H}}$ NMR and HRMS data have not previously been obtained for the compound.

Ethyl 6-bromo-4(1*H*)-quinolone-3-carboxylate



General procedure B was followed using 4-bromoaniline (516 mg, 3.00 mmol) and diethyl ethoxymethylenemalonate (0.63 mL, 3.15 mmol) to afford ethyl 6-bromo-4(1*H*)-quinolone-3-carboxylate as a tan solid (571 mg, 1.93 mmol, 64%); **m.p.** >250 °C; **¹H NMR** (500 MHz, DMSO-*d*₆): δ_H 12.46 (br s, 1H, NH), 8.60 (d, *J* = 5.2 Hz, 1H, C²H), 8.23 (d, *J* = 2.4 Hz, 1H, C⁵H), 7.87 (dd, *J* = 8.7, 2.4 Hz, 1H, C⁷H), 7.61 (d, *J* = 8.7 Hz, 1H, C⁸H), 4.23 (q, *J* = 7.1 Hz, 2H, C¹⁰H₂), 1.29 (t, *J* = 7.1 Hz, 3H, C¹¹H₃); **¹³C {¹H} NMR** (126 MHz, DMSO-*d*₆): δ_C 172.6 (C), 165.0 (C), 145.7 (CH), 138.5 (C), 135.6 (CH), 129.2 (C), 128.3 (CH), 121.9 (CH), 117.9 (C), 110.6 (C), 60.2 (CH₂), 14.8 (CH₃); **IR** (ATR): ν_{max} 3152, 3090, 2983, 1693 (C=O), 1617, 1552, 1524, 1468, 1397, 1378, 1359, 1339, 1294, 1252, 1202, 1187, 1153, 1113, 1100, 1032, 960, 902, 861, 823, 799, 756, 742, 644, 630, 618, 598, 557, 519, 500, 438, 422; **HRMS** *m/z* calc. for C₁₂H₁₀⁷⁹BrNNaO₃ [M+Na]: 317.9736; found: 317.9733 (σ = 1.00 ppm). These values are concordant with literature precedents.^{114,134}

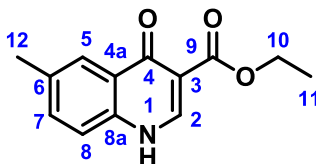
Ethyl 6-iodo-4(1*H*)-quinolone-3-carboxylate



General procedure B was followed using 4-iodoaniline (657 mg, 3.00 mmol) and diethyl ethoxymethylenemalonate (0.63 mL, 3.15 mmol) to afford ethyl 6-iodo-4(1*H*)-quinolone-3-carboxylate as a tan solid (748 mg, 2.18 mmol, 73%); **m.p.** >250 °C; **¹H NMR** (500 MHz, DMSO-*d*₆): δ_H 12.41 (s, 1H, NH), 8.58 (br s, 1H, C²H), 8.43 (d, *J* = 2.0 Hz, 1H, C⁵H), 8.00 (dd, *J* = 8.6, 2.0 Hz, 1H, C⁷H), 7.45 (d, *J* = 8.6 Hz, 1H, C⁸H), 4.22 (q, *J* = 7.1 Hz, 2H, C¹⁰H₂), 1.28 (t, *J* = 7.1 Hz, 3H, C¹¹H₃); **¹³C {¹H} NMR** (126 MHz, DMSO-*d*₆): δ_C 172.4 (C), 165.0 (C), 145.7 (CH), 141.0 (CH), 138.8 (C), 134.6 (CH), 129.4 (C), 121.7 (CH), 110.8 (C), 90.1 (C), 60.2 (CH₂), 14.8 (CH₃); **IR** (ATR): ν_{max} 3148, 3126, 3087, 3022, 2978, 2937, 2903, 1691 (C=O), 1614, 1549, 1520, 1464, 1395, 1376, 1358, 1335, 1291, 1253, 1203, 1184, 1156, 1108, 1096, 1064, 1029, 961, 948m 903, 886, 858, 821, 799, 756, 742, 629, 612, 586, 556, 514, 494, 441, 418; **HRMS** *m/z*

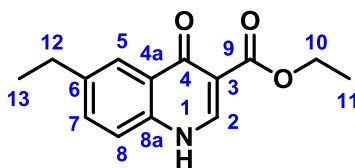
calc. for $C_{12}H_{11}INO_3$ [M+H]: 343.9778; found: 343.9775 ($\sigma = 0.80$ ppm). These values are concordant with literature precedents.^{135,136}

Ethyl 6-methyl-4(1*H*)-quinolone-3-carboxylate



General procedure B was followed using *p*-toulidine (0.33 mL, 3.00 mmol) and diethyl ethoxymethylenemalonate (0.63 mL, 3.15 mmol) to afford ethyl 6-methyl-4(1*H*)-quinolone-3-carboxylate as a tan solid (539 mg, 2.33 mmol, 78%); **m.p.** >250 °C; **¹H NMR** (500 MHz, DMSO- d_6): δ_H 12.24 (s, 1H, NH), 8.50 (s, 1H, C²H), 7.95 (s, 1H, C⁵H), 7.64 – 7.43 (m, 2H, C⁷H, C⁸H), 4.21 (q, $J = 7.1$ Hz, 2H, C¹⁰H₂), 2.43 (s, 3H, C¹²H₃), 1.28 (t, $J = 7.1$ Hz, 3H, C¹¹H₃); **¹³C {¹H} NMR** (126 MHz, DMSO- d_6): δ_C 173.7 (C), 165.3 (C), 144.9 (CH), 137.4 (C), 134.6 (C), 134.1 (CH), 127.7 (C), 125.4 (CH), 119.2 (CH), 110.0 (C), 60.0 (CH₂), 21.3 (CH₃), 14.8 (CH₃); **IR** (ATR): ν_{max} 3150, 3098, 2983, 2916, 1692 (C=O), 1612, 1589, 1559, 1527, 1488, 1449, 1397, 1377, 1357, 1295, 1205, 1169, 1154, 1115, 1092, 1037, 960, 902, 856, 819, 802, 759, 743, 719, 634, 606, 562, 532, 503, 459, 424; **HRMS** m/z calc. for $C_{13}H_{14}NO_3$ [M+H]: 232.0968; found: 232.0968 ($\sigma = 0.10$ ppm). These values are concordant with literature precedents.¹³⁷ HRMS data has not previously been obtained for the compound.

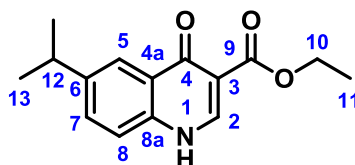
Ethyl 6-ethyl-4(1*H*)-quinolone-3-carboxylate



General procedure B was followed using 4-ethylaniline (0.37 mL, 2.98 mmol) and diethyl ethoxymethylenemalonate (0.63 mL, 3.15 mmol) to afford ethyl 6-ethyl-4(1*H*)-quinolone-3-carboxylate as a tan solid (559 mg, 2.28 mmol, 77%); **m.p.** >250 °C; **¹H NMR** (400 MHz, DMSO- d_6): δ_H 12.26 (d, $J = 6.7$ Hz, 1H, NH), 8.51 (d, $J = 6.7$ Hz, 1H, C²H), 7.97 (d, $J = 1.9$ Hz, 1H, C⁵H), 7.58 (dd, $J = 8.4, 1.9$ Hz, 1H, C⁷H), 7.55 (d, $J = 8.4$ Hz, 1H, C⁸H), 4.21 (q, $J = 7.1$ Hz, 2H, C¹⁰H₂), 2.73 (q, $J = 7.6$ Hz, 2H, C¹²H₂), 1.28 (t, $J = 7.1$ Hz, 3H, C¹¹H₃), 1.23 (t, $J = 7.6$ Hz, 3H, C¹³H₃); **¹³C {¹H} NMR** (101 MHz, DMSO- d_6): δ_C 173.8 (C), 165.3 (C), 144.9 (CH), 140.9 (C), 137.6 (C), 133.1 (CH), 127.7

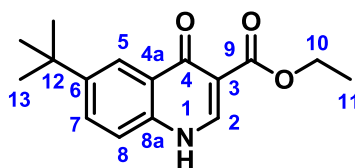
(C), 124.1 (CH), 119.3 (CH), 109.9 (C), 60.0 (CH₂), 28.3 (CH₂), 16.0 (CH₃), 14.8 (CH₃); **IR** (ATR): ν_{\max} 3159, 3099, 2962, 2928, 1696 (C=O), 1612, 1588, 1558, 1527, 1486, 1456, 1411, 1395, 1377, 1358, 1287, 1203, 1166, 1093, 1063, 1034, 981, 963, 949, 910, 898, 852, 830, 803, 760, 744, 716, 634, 609, 587, 526, 464, 424; **HRMS** m/z calc. for C₁₄H₁₆NO₃ [M+H]: 246.1125; found: 246.1125 (σ = 0.10 ppm). These values are concordant with literature precedents.¹³⁴ IR data has not previously been obtained for the compound.

Ethyl 6-isopropyl-4(1*H*)-quinolone-3-carboxylate



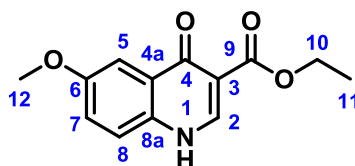
General procedure B was followed using 4-isopropylaniline (0.41 mL, 3.00 mmol) and diethyl ethoxymethylenemalonate (0.63 mL, 3.15 mmol) to afford ethyl 6-isopropyl-4(1*H*)-quinolone-3-carboxylate as an off-white solid (537 mg, 0.690 mmol, 69%); **m.p.** >250 °C; **¹H NMR** (400 MHz, DMSO-*d*₆): δ_{H} 12.28 (s, 1H, NH), 8.51 (s, 1H C²H), 8.00 (d, J = 2.1 Hz, 1H, C⁵H), 7.63 (dd, J = 8.5, 2.1 Hz, 1H, C⁷H), 7.56 (d, J = 8.5 Hz, 1H, C⁸H), 4.21 (q, J = 7.1 Hz, 2H, C¹⁰H₂), 3.03 (hept, J = 6.9 Hz, 1H, C¹²H), 1.28 (t, J = 7.1 Hz, 3H, C¹¹H₃), 1.25 (d, J = 6.9 Hz, 6H, 2 × C¹³H₃); **¹³C {¹H} NMR** (101 MHz, DMSO-*d*₆): δ_{C} 173.9 (C), 165.3 (C), 145.4 (C), 144.9 (CH), 137.7 (C), 131.8 (CH), 127.7 (C), 122.6 (CH), 119.3 (CH), 109.9 (C), 60.0 (CH₂), 33.6 (CH), 24.3 (CH₃), 14.8 (CH₃); **IR** (ATR): ν_{\max} 3228, 3181, 3055, 2950, 2906, 2869, 1707 (C=O), 1634, 1588, 1557, 1535, 1488, 1412, 1394, 1376, 1358, 1332, 1308, 1288, 1208, 1182, 1148, 1092, 1034, 965, 908, 830, 806, 758, 744, 689, 632, 609, 593, 555, 535, 486, 456, 429; **HRMS** m/z calc. for C₁₅H₁₈NO₃ [M+H]: 260.1281; found: 260.1282 (σ = 0.30 ppm). These values are concordant with literature precedents.¹³⁴ IR data has not previously been obtained for the compound.

Ethyl 6-*tert*-butyl-4(1*H*)-quinolone-3-carboxylate



General procedure B was followed using 4-*tert*-butylaniline (0.48 mL, 3.01 mmol) and diethyl ethoxymethylenemalonate (0.63 mL, 3.15 mmol) to afford ethyl 6-*tert*-butyl-4(1*H*)-quinolone-3-carboxylate as a white solid (613 mg, 2.24 mmol, 75%); **m.p.** >250 °C; **¹H NMR** (400 MHz, DMSO-*d*₆): δ_H 12.27 (s, 1H, NH), 8.52 (s, 1H, C²H), 8.14 (d, *J* = 2.3 Hz, 1H, C⁵H), 7.81 (dd, *J* = 8.7, 2.3 Hz, 1H, C⁷H), 7.57 (d, *J* = 8.7 Hz, 1H, C⁸H), 4.21 (q, *J* = 7.1 Hz, 2H, C¹⁰H₂), 1.34 (s, 9H, 3 × C¹³H₃), 1.28 (t, *J* = 7.1 Hz, 3H); **¹³C {¹H} NMR** (101 MHz, DMSO-*d*₆): δ_C 174.0 (C), 165.4 (C), 147.7 (C), 144.9 (CH), 137.4 (C), 130.9 (CH), 127.2 (C), 121.3 (CH), 119.1 (CH), 110.0 (C), 60.0 (CH₂), 35.0 (C), 31.5 (CH₃), 14.8 (CH₃); **IR** (ATR): ν_{max} 3160, 3096, 2962, 1699 (C=O), 1614, 1583, 1558, 1528, 1490, 1394, 1377, 1359, 1288, 1254, 1204, 1187, 1153, 1115, 1092, 1033, 963, 950, 910, 831, 805, 744, 633, 605, 542, 504, 466, 424; **HRMS** *m/z* calc. for C₁₆H₂₀NO₃ [M+H]: 274.1438; found: 274.1430 (σ = 2.70 ppm).

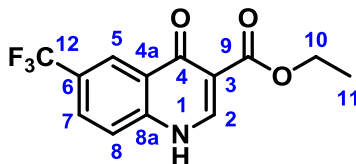
Ethyl 6-methoxy-4(1*H*)-quinolone-3-carboxylate



General procedure B was followed using *p*-anisidine (369 mg, 3.00 mmol) and diethyl ethoxymethylenemalonate (0.63 mL, 3.15 mmol) to afford ethyl 6-methoxy-4(1*H*)-quinolone-3-carboxylate as a brown solid (351 mg, 1.42 mmol, 47%); **m.p.** >250 °C; **¹H NMR** (400 MHz, DMSO-*d*₆): δ_H 12.30 (d, *J* = 6.4 Hz, 1H, NH), 8.49 (d, *J* = 6.4 Hz, 1H, C²H), 7.59 (d, *J* = 8.9 Hz, 1H, C⁸H), 7.58 (d, *J* = 3.0 Hz, C⁵H), 7.34 (dd, *J* = 8.9, 3.0 Hz, 1H, C⁷H), 4.22 (q, *J* = 7.1 Hz, 2H, C¹⁰H₂), 3.85 (s, 3H, C¹²H₃), 1.28 (t, *J* = 7.1 Hz, 3H, C¹¹H₃); **¹³C {¹H} NMR** (101 MHz, DMSO-*d*₆): δ_C 173.3 (C), 165.4 (C), 157.0 (C), 144.1 (CH), 133.8 (C), 129.0 (C), 122.6 (CH), 121.0 (CH), 109.1 (C), 106.0 (CH), 59.9 (CH₂), 55.9 (CH₃), 14.8 (CH₃); **IR** (ATR): ν_{max} 3153, 3098, 2904, 1699 (C=O), 1615, 1582, 1558, 1526, 1487, 1468, 1441, 1379, 1293, 1266, 1231, 1197, 1170, 1139, 1085, 1032, 973, 903, 874, 824, 798, 745, 716, 631, 605, 576, 558, 527, 491, 450, 430; **HRMS** *m/z* calc. for C₁₃H₁₄NO₄ [M+H]: 248.0917; found: 248.0916 (σ = 0.40 ppm).

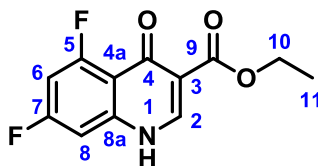
Only melting point and ^1H NMR (δ_{H} to 1 d.p., no J couplings) previously been collected on the compound.¹³⁸

Ethyl 6-trifluoromethyl-4(1*H*)-quinolone-3-carboxylate



General procedure B was followed using 4-(trifluoromethyl)aniline (0.38 mL, 3.03 mmol) and diethyl ethoxymethylenemalonate (0.63 mL, 3.15 mmol) to afford ethyl 6-trifluoromethyl-4(1*H*)-quinolone-3-carboxylate as a tan solid (568 mg, 1.99 mmol, 66%); **m.p.** >250 °C; ^1H NMR (500 MHz, DMSO- d_6): δ_{H} 12.62 (s, 1H, NH), 8.66 (s, 1H, C²H), 8.41 (d, J = 2.2 Hz, 1H, C⁵H), 8.04 (dd, J = 8.7, 2.2 Hz, 1H, C⁷H), 7.84 (d, J = 8.7 Hz, 1H, C⁸H), 4.24 (q, J = 7.1 Hz, 2H, C¹⁰H₂), 1.30 (t, J = 7.1 Hz, 3H, C¹¹H₃); ^{13}C { ^1H } NMR (126 MHz, DMSO- d_6): δ_{C} 173.2 (C), 164.9 (C), 146.5 (CH), 141.9 (C), 129.0 (q, J = 3.0 Hz, CH), 127.2 (C), 125.27 (q, J = 32.2 Hz), 124.3 (q, J = 272.5 Hz, C), 123.57 (q, J = 4.4 Hz, CH), 121.1 (CH), 111.5 (C), 60.3 (CH₂), 14.8 (CH₃); ^{19}F NMR (376 MHz, DMSO- d_6): δ_{F} -60.7 (1F); **IR** (ATR): ν_{max} 3146, 3090, 2989, 1693 (C=O), 1636, 1613, 1595, 1561, 1529, 1496, 1454, 1409, 1380, 1361, 1322, 1294, 1253, 1208, 1195, 1172, 1145, 1100, 1066, 1028, 972, 924, 895, 862, 837, 803, 762, 743, 714, 633, 618, 595, 517, 419; **HRMS** m/z calc. for C₁₃H₁₀F₃NNaO₃ [M+Na]: 308.0505; found: 308.0506 (σ = 0.20 ppm). These values are concordant with literature precedents.¹³² ^{19}F NMR and HRMS data have not previously been obtained for the compound.

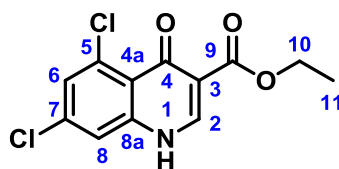
Ethyl 5,7-difluoro-4(1*H*)-quinolone-3-carboxylate



General procedure B was followed using 3,5-difluoroaniline (387 mg, 3.00 mmol) and diethyl ethoxymethylenemalonate (0.63 mL, 3.15 mmol) to afford ethyl 5,7-difluoro-4(1*H*)-quinolone-3-carboxylate as a tan solid (471 mg, 1.86 mmol, 62%); **m.p.** >250 °C (lit. 313 °C); ^1H NMR (500 MHz, DMSO- d_6): δ_{H} 12.32 (s, 1H, NH), 8.50 (s, 1H, C²H), 7.26 – 7.14 (m, 2H, C⁶H, C⁸H), 4.21 (q, J = 7.1 Hz, 2H, C¹⁰H₂), 1.28 (t, J = 7.1 Hz, 3H, C¹¹H₃); ^{13}C { ^1H } NMR (126 MHz, DMSO- d_6): δ_{C} 172.1 (C), 164.8 (C), 163.6 (dd, J =

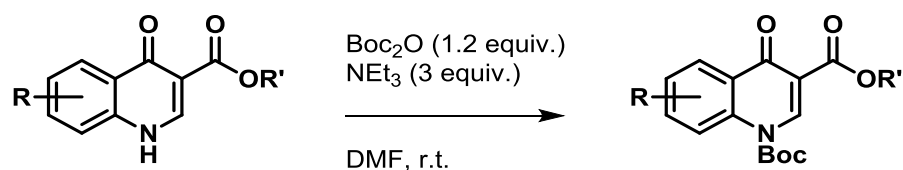
249.7, 14.6 Hz, C), 162.7 (dd, $J = 263.9, 15.0$ Hz, C), 145.2 (CH), 142.8 (dd, $J = 13.6, 5.1$ Hz, C), 114.6 (dd, $J = 8.6, 2.5$ Hz, C), 112.4 (C), 101.3 (app. t, $J = 26.1$ Hz, CH), 101.1 (dd, $J = 25.2, 4.6$ Hz, CH), 60.2 (CH₂), 14.7 (CH₃); **¹⁹F NMR** (471 MHz, DMSO-*d*₆): δ_F -103.8 (1F), -107.5 (1F); **IR** (ATR): ν_{max} 3093, 2984, 2934, 1701 (C=O), 1618, 1597, 1568, 1537, 1454, 1424, 1372, 1361, 1294, 1251, 1212, 1180, 1112, 1071, 1029, 1000, 925, 873, 828, 807, 761, 749, 677, 645, 623, 600, 559, 543, 511, 469, 408; **HRMS** m/z calc. for C₁₂H₉F₂NNaO₃ [M+Na]: 276.0443; found: 276.0442 ($\sigma = 0.40$ ppm). These values are concordant with literature precedents.¹³⁹ NMR, HRMS and IR data have not previously been obtained for the compound.

Ethyl 5,7-dichloro-4(1*H*)-quinolone-3-carboxylate



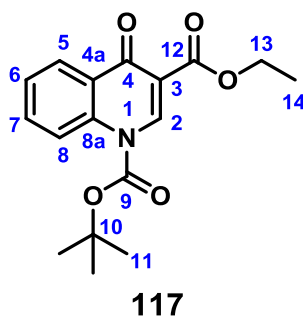
General procedure B was followed using 3,5-dichloroaniline (486 mg, 3.00 mmol) and diethyl ethoxymethylenemalonate (0.63 mL, 3.15 mmol) to afford ethyl 5,7-dichloro-4(1*H*)-quinolone-3-carboxylate as a tan solid (561 mg, 1.96 mmol, 65%); **m.p.** >250 °C (lit. 306 °C); **¹H NMR** (500 MHz, DMSO-*d*₆): δ_H 12.28 (s, 1H, NH), 8.50 (s, 1H, C²H), 7.61 (d, $J = 2.1$ Hz, 1H, C⁸H), 7.49 (d, $J = 2.1$ Hz, 1H, C⁶H), 4.22 (q, $J = 7.1$ Hz, 2H, C¹⁰H₂), 1.28 (t, $J = 7.1$ Hz, 3H, C¹¹H₃); **¹³C {¹H} NMR** (126 MHz, DMSO-*d*₆): δ_C 164.9 (C), 144.7 (CH), 140.2 (C), 136.3 (C), 134.7 (C), 127.2 (CH), 122.4 (C), 118.0 (CH), 112.8 (C), 60.3 (CH₂), 14.8 (CH₃), missing peak for C⁴ due to low signal intensity; **IR** (ATR): ν_{max} 3138, 3083, 2985, 2938, 1699, 1606, 1585, 1552, 1516, 1475, 1426, 1374, 1359, 1331, 1290, 1260, 1225, 1178, 1134, 1107, 1082, 1032, 972, 921, 881, 853, 843, 798, 756, 715, 673, 628, 603, 574, 521, 475, 460, 426, 409; **HRMS** m/z calc. for C₁₂H₉³⁵Cl₂NNaO₃ [M+Na]: 307.9852; found: 307.9852 ($\sigma = 0.00$ ppm). These values are concordant with literature precedents.¹³⁹ HRMS and IR data has not previously been obtained for the compound. NMR data only previously collected in TFA-*d*.¹⁴⁰

General procedure C for the synthesis of protected compounds 118 and 135-148



To a stirring suspension of the substituted quinolone (1 equiv.) and NEt_3 (3 equiv.) in DMF (0.17 M solution) at r.t. was added Boc_2O (1.2 equiv.). The suspension was stirred until it became homogeneous after which the solution was diluted with EtOAc and washed thoroughly with a 5% w/w aqueous solution of LiCl (at least 5 times until DMF was completely removed). The organic phase was dried (MgSO_4), concentrated *in vacuo* and eluted through a plug of silica (Et_2O) to afford the crude product. The solid material was stirred in a small volume of Et_2O at $-78\text{ }^\circ\text{C}$ for 10 minutes and filtered cold. The collected solid was washed with a small volume of Et_2O (cooled to $-78\text{ }^\circ\text{C}$) and dried under vacuum for 15 minutes to afford the protected quinolone derivatives as described.

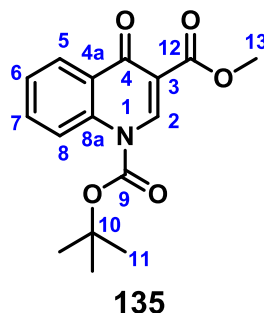
1-*tert*-Butyl 3-ethyl 4(1*H*)-quinolone-1,3-dicarboxylate 117



General procedure C was followed using ethyl 4(1*H*)-quinolone-3-carboxylate (6.85 g, 31.5 mmol) and di-*tert*-butyl dicarbonate (11.0 mL, 47.9 mmol) to afford compound **117** as an off-white solid (7.37 g, 23.2 mmol, 74%); **m.p.** $>250\text{ }^\circ\text{C}$; **$^1\text{H NMR}$** (400 MHz, CDCl_3): δ_{H} 9.17 (s, 1H, C²H), 8.52 (app d, $J = 8.8\text{ Hz}$, 1H, C⁸H), 8.48 (dd, $J = 8.0, 1.8\text{ Hz}$, 1H, C⁵H), 7.70 (ddd, $J = 8.8, 7.1, 1.8\text{ Hz}$, 1H, C⁶H), 7.49 (ddd, $J = 8.0, 7.1, 1.0\text{ Hz}$, 1H, C⁷H), 4.44 (q, $J = 7.1\text{ Hz}$, 2H, C¹³H₂), 1.73 (s, 9H, 3 \times C¹¹H₃), 1.44 (t, $J = 7.1\text{ Hz}$, 3H, C¹⁴H₃); **$^{13}\text{C}\{^1\text{H}\}\text{NMR}$** (101 MHz, CDCl_3): δ_{C} 174.9 (C), 164.8 (C), 149.2 (C), 145.0 (CH), 137.5 (C), 132.9 (CH), 128.0 (C), 127.4 (CH), 126.1 (CH), 119.8 (CH), 113.4 (C), 87.9 (C), 61.3 (CH₂), 27.9 (CH₃), 14.3 (CH₃); **IR** (ATR): ν_{max} 2990, 2938, 2910, 1764,

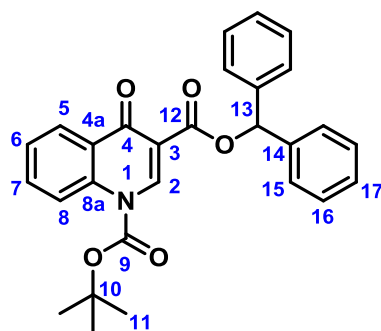
1734 (C=O), 1639 (C=O), 1612, 1599, 1561, 1469, 1415, 1400, 1367, 1321, 1299, 1275, 1230, 1200, 1163, 1148, 1129, 1087, 1053, 1013, 953, 933, 877, 853, 833, 780, 750, 727, 707, 683, 638, 590, 555, 499, 449, 412; **HRMS** m/z calc. for $C_{17}H_{20}NO_5$ [M+H]: 318.1336; found: 318.1331 ($\sigma = 1.40$ ppm). These values are concordant with literature precedents.¹¹⁴

1-*tert*-Butyl 3-methyl 4(1*H*)-quinolone-1,3-dicarboxylate **135**



General procedure C was followed using the methyl 4(1*H*)-quinolone-3-carboxylate (203 mg, 1.00 mmol) and di-*tert*-butyl dicarbonate (0.35 mL, 1.52 mmol) to afford compound **135** as an off-white solid (184 mg, 0.607 mmol, 61%); **m.p.** 199-201 °C (decomposition); **¹H NMR** (400 MHz, DMSO- d_6): δ_H 9.18 (s, 1H, C²H), 8.54 – 8.46 (m, 2H, C⁵H, C⁸H), 7.70 (ddd, $J = 8.9, 7.1, 1.8$ Hz, 1H, C⁶H), 7.49 (ddd, $J = 8.0, 7.1, 1.0$ Hz, 1H, C⁷H), 3.97 (s, 3H, C¹³H₃), 1.73 (s, 9H, 3 × C¹¹H₃); **¹³C {¹H} NMR** (101 MHz, DMSO- d_6): δ_C 174.9 (C), 165.5 (C), 149.2 (C), 146.8 (C), 145.3 (CH), 137.5 (C), 132.9 (CH), 127.4 (CH), 126.1 (CH), 119.8 (CH), 113.0 (C), 88.0 (CH₂), 52.5 (CH₃), 27.9 (CH₃); **IR** (ATR): ν_{max} 3150, 3116, 2986, 2953, 1809, 1737 (C=O), 1636 (C=O), 1600, 1563, 1466, 1439, 1401, 1372, 1248, 1324, 1304, 1263, 1245, 1223, 1187, 1117, 1100, 1067, 1053, 1012, 995, 964, 932, 887, 832, 814, 798, 759, 678, 665, 600, 551, 519, 497, 458, 406; **HRMS** m/z calc. for $C_{16}H_{18}NO_5$ [M+H]: 304.1179; found: 304.1178 ($\sigma = 0.60$ ppm).

3-Benzhydryl 1-*tert*-butyl 4(1*H*)-quinolone-1,3-dicarboxylate **136**

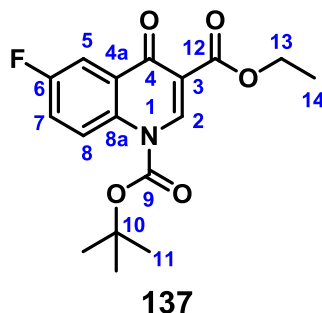


136

Ethyl 4(1*H*)-quinolone-3-carboxylate (430 mg, 2.00 mmol) was suspended in 2 N aqueous NaOH (5 mL) and heated to reflux for 1 hour. The reaction mixture was then cooled to rt and acidified to pH 2 with 2 N aqueous HCl. The precipitate was filtered *via* suction and washed with copious water. The collected solid (189 mg) was suspended in DMF (1 mL) and was stirred under argon and heated until it was homogeneous after which the solution was allowed to cool to r.t. To the solution was added oxalyl chloride (86 μ L, 1.00 mmol) dropwise; the solution was allowed to stir under argon at r.t. for 15 minutes after which a precipitate had formed. Pyridine (2 mL) was added to the suspension which again became homogeneous. To the solution was added benzhydryl (184 mg, 1.00 mmol) and the solution was left to stir under argon at r.t. for 15 minutes. The solution was quenched with H₂O (3 mL) forming a precipitate which was filtered off and washed comprehensively with H₂O; ¹H NMR and TLC analysis confirmed complete conversion to the benzhydryl ester (*ca.* 85% purity) which was carried into the next step without further purification. The crude mixture was subjected to General procedure C with di-*tert*-butyl dicarbonate (0.35 mL, 1.52 mmol) to afford compound **136** as an off-white solid (196 mg, 0.430 mmol, 43% over 3 steps) (*ca.* 90% purity, small amount of *tert*-butanol present in final sample); **m.p.** 216-218 °C (decomposition); **¹H NMR** (400 MHz, DMSO-*d*₆): δ_{H} 9.23 (s, 1H, C²H), 8.57 – 8.50 (m, 2H, C⁵H, C⁸H), 7.70 (ddd, *J* = 8.8, 7.1, 1.8 Hz, 1H, C⁶H), 7.60 – 7.55 (m, 4H, 4 \times C¹⁵H), 7.50 (ddd, *J* = 8.1, 7.1, 1.0 Hz, 1H, C⁷H), 7.42 – 7.35 (m, 4H, 4 \times C¹⁶H), 7.32 – 7.26 (m, 2H, 4 \times C¹⁷H) overlapped by solvent peak, 7.14 (s, 1H, C¹³H), 1.71 (s, 9H, 3 \times C¹¹H₃); **¹³C {¹H} NMR** (101 MHz, DMSO-*d*₆): δ_{C} 174.8 (C), 163.8 (C), 149.1 (C), 145.5 (CH), 140.5 (2 \times C), 137.5 (C), 132.9 (CH), 128.6 (CH), 128.1 (C), 127.8 (CH), 127.4 (CH), 127.1 (CH), 126.2 (CH), 119.8 (CH), 113.0 (C), 77.9 (CH), 27.9 (CH₃); **IR** (ATR): ν_{max} 3089, 3064, 3008, 2986, 2935, 2855, 1808, 1768, 1732 (C=O), 1688 (C=O), 1650 (C=O), 1606, 1561, 1496, 1471, 1459, 1393, 1372, 1346, 1317, 1303, 1277, 1236, 1213, 1192, 1165, 1151, 1127, 1101, 1070, 1016, 963, 939, 925, 873, 855, 844, 807,

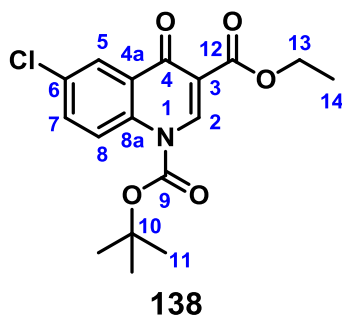
798, 773, 756, 744, 701, 655, 641, 619, 599, 588, 561, 544, 496, 454, 411; **HRMS** m/z calc. for $C_{28}H_{26}NO_5$ [M+H]: 456.1805; found: 456.1802 ($\sigma = 0.80$ ppm).

1-*tert*-Butyl 3-ethyl 6-fluoro-4(1*H*)-quinolone-1,3-dicarboxylate **137**



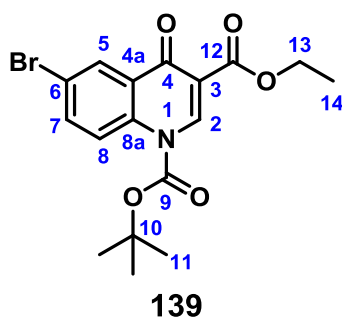
General procedure C was followed using ethyl 6-fluoro-4(1*H*)-quinolone-3-carboxylate (118 mg, 0.502 mmol) and di-*tert*-butyl dicarbonate (0.17 mL, 0.740 mmol) to afford compound **137** as a yellow solid (98 mg, 0.292 mmol, 58%); **m.p.** >250 °C; **¹H NMR** (400 MHz, $CDCl_3$): δ_H 9.18 (s, 1H, C²H), 8.61 (dd, $J = 9.5, 4.4$ Hz, 1H, C⁸H), 8.11 (dd, $J = 8.7, 3.2$ Hz, 1H, C⁵H), 7.41 (ddd, $J = 9.5, 7.3, 3.2$ Hz, 1H, C⁷H), 4.43 (q, $J = 7.2$ Hz, 2H, C¹³H₂), 1.73 (s, 9H, 3 × C¹¹H₃), 1.44 (t, $J = 7.2$ Hz, 3H, C¹⁴H₃); **¹³C {¹H} NMR** (101 MHz, $CDCl_3$): δ_C 173.9 (d, $J = 2.8$ Hz, C), 164.6 (C), 160.3 (d, $J = 248.8$ Hz, C), 149.0 (C), 145.1 (CH), 133.9 (d, $J = 2.2$ Hz, C), 130.2 (d, $J = 7.2$ Hz, C), 122.5 (d, $J = 7.8$ Hz, CH), 121.0 (d, $J = 24.1$ Hz, CH), 112.8 (C), 112.6 (d, $J = 23.3$ Hz, CH), 88.3 (C), 61.5 (CH₂), 27.9 (CH₃), 14.3 (CH₃); **¹⁹F NMR** (376 MHz, $CDCl_3$): δ_F -114.1 (1F); **IR** (ATR): ν_{max} 3160, 3078, 2932, 2872, 1771, 1733 (C=O), 1644 (C=O), 1616, 1572, 1479, 1456, 1393, 1368, 1327, 1298, 1266, 1232, 1196, 1170, 1133, 1077, 1048, 1023, 973, 947, 890, 854, 829, 803, 761, 732, 707, 636, 581, 562, 501, 456, 421; **HRMS** m/z calc. for $C_{17}H_{19}FNO_5$ [M+H]: 336.1242; found: 336.1239 ($\sigma = 0.90$ ppm).

1-*tert*-Butyl 3-ethyl 6-chloro-4(1*H*)-quinolone-1,3-dicarboxylate **138**



General procedure C was followed using ethyl 6-chloro-4(1*H*)-quinolone-3-carboxylate (252 mg, 1.00 mmol) and di-*tert*-butyl dicarbonate (0.35 mL, 1.52 mmol) to afford compound **138** as an off-white solid (225 mg, 0.640 mmol, 64%); **m.p.** >250 °C; **¹H NMR** (400 MHz, CDCl₃): δ_H 9.16 (s, 1H, C²H), 8.54 (d, *J* = 9.3 Hz, 1H, C⁸H), 8.42 (d, *J* = 2.7 Hz, 1H, C⁵H), 7.63 (dd, *J* = 9.3, 2.7 Hz, 1H, C⁷H), 4.43 (q, *J* = 7.1 Hz, 2H, C¹³H₂), 1.73 (s, 9H, 3 × C¹¹H₃), 1.44 (t, *J* = 7.1 Hz, 3H, C¹⁴H₃); **¹³C {¹H} NMR** (101 MHz, CDCl₃): δ_C 173.7 (C), 164.5 (C), 148.9 (C), 145.1 (CH), 135.9 (C), 133.0 (CH), 132.4 (C), 129.3 (C), 126.7 (CH), 121.7 (CH), 113.5 (C), 88.4 (C), 61.5 (CH₂), 27.9 (CH₃), 14.3 (CH₃); **IR** (ATR): ν_{max} 3147, 3129, 29865, 2932, 2870, 1773, 1731 (C=O), 1646 (C=O), 1613, 1596, 1552, 1470, 1394, 1369, 1298, 1255, 1226, 1142, 1107, 1023, 946, 907, 861, 829, 804, 761, 705m 658, 552; **HRMS** *m/z* calc. for C₁₇H₁₉³⁵ClNO₅ [M+H]: 352.0946; found: 352.0942 (σ = 1.40 ppm).

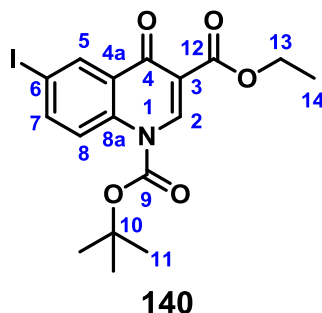
1-*tert*-Butyl 3-ethyl 6-bromo-4(1*H*)-quinolone-1,3-dicarboxylate **139**



General procedure C was followed using ethyl 6-bromo-4(1*H*)-quinolone-3-carboxylate (296 mg, 1.00 mmol) and di-*tert*-butyl dicarbonate (0.35 mL, 1.52 mmol) to afford compound **139** as a pale-orange solid (249 mg, 0.629 mmol, 63%); **m.p.** >250 °C; **¹H NMR** (400 MHz, CDCl₃): δ_H 9.16 (s, 1H, C²H), 8.58 (d, *J* = 2.5 Hz, 1H, C⁵H), 8.46 (d, *J* = 9.3 Hz, 1H, C⁸H), 7.77 (dd, *J* = 9.3, 2.5 Hz, 1H, C⁷H), 4.43 (q, *J* = 7.1 Hz, 2H, C¹³H₂), 1.73 (s, 9H, 3 × C¹¹H₃), 1.43 (t, *J* = 7.1 Hz, 3H, C¹⁴H₃); **¹³C {¹H} NMR** (101

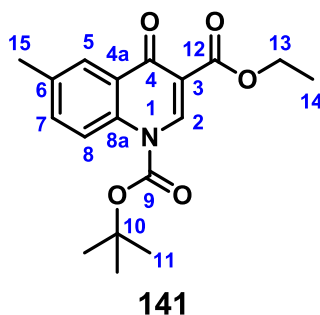
MHz, CDCl₃): δ_c 173.6 (C), 164.4 (C), 148.9 (C), 145.1 (CH), 136.4 (C), 135.8 (CH), 129.9 (CH), 129.5 (C), 121.8 (CH), 120.2 (C), 113.6 (C), 88.4 (C), 61.5 (CH₂), 27.9 (CH₃), 14.3 (CH₃); **IR** (ATR): ν_{\max} 3146, 3127, 306, 2980, 2931, 2871, 1772, 1730 (C=O), 1646 (C=O), 1612, 1590, 1549, 1467, 1454, 1438, 1392, 1369, 1352, 1297, 1255, 1226, 1207, 1141, 1100, 1046, 1020, 946, 907, 873, 857, 827, 803, 760, 725, 704, 680, 646, 616, 550, 536, 479, 451, 413; **HRMS** m/z calc. for C₁₇H₁₉⁷⁹BrNO₅ [M+H]: 396.0441; found: 396.0446 (σ = 1.20 ppm).

1-*tert*-Butyl 3-ethyl 6-iodo-4(1*H*)-quinolone-1,3-dicarboxylate **140**



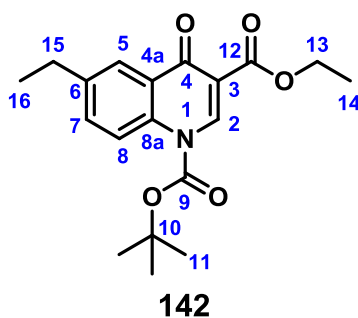
General procedure C was followed using ethyl 6-iodo-4(1*H*)-quinolone-3-carboxylate (343 mg, 1.00 mmol) and di-*tert*-butyl dicarbonate (0.35 mL, 1.52 mmol) to afford compound **140** as a pale-orange solid (300 mg, 0.677 mmol, 68%); **m.p.** >250 °C; **¹H NMR** (400 MHz, CDCl₃): δ_H 9.15 (s, 1H, C²H), 8.78 (d, J = 2.3 Hz, 1H, C⁵H), 8.31 (d, J = 9.2 Hz, 1H, C⁸H), 7.95 (dd, J = 9.2, 2.3 Hz, 1H, C⁷H), 4.43 (q, J = 7.1 Hz, 2H, C¹³H₂), 1.72 (s, 9H, 3 × C¹¹H₃), 1.43 (t, J = 7.1 Hz, 3H); **¹³C {¹H} NMR** (101 MHz, CDCl₃): δ_c 173.4 (C), 164.4 (C), 148.9 (C), 145.0 (CH), 141.4 (CH), 137.0 (C), 136.2 (CH), 129.5 (C), 121.8 (CH), 113.8 (C), 91.1 (C), 88.4 (C), 61.5 (CH₂), 27.9 (CH₃), 14.3 (CH₃); **IR** (ATR): ν_{\max} 3144, 3059, 2977, 2931, 2870, 1772, 1730 (C=O), 1646 (C=O), 1611, 1583, 1545, 1466, 1454, 1434, 1392, 1366, 1350, 1297, 1255, 1228, 1206, 1158, 1136, 1096, 1045, 1018, 943, 908, 873, 855, 826, 802, 761, 725, 704, 679, 643, 611, 549, 528, 477, 451, 411; **HRMS** m/z calc. for C₁₇H₁₉IINO₅ [M+H]: 444.0302; found: 444.0298 (σ = 1.00 ppm).

1-*tert*-Butyl 3-ethyl 6-methyl-4(1*H*)-quinolone-1,3-dicarboxylate **141**



General procedure C was followed using ethyl 6-methyl-4(1*H*)-quinolone-3-carboxylate (116 mg, 0.502 mmol) and di-*tert*-butyl dicarbonate (0.17 mL, 0.740 mmol) to afford compound **141** as an off-white solid (122 mg, 0.370 mmol, 74%); **m.p.** >250 °C; **¹H NMR** (400 MHz, CDCl₃): δ_H 9.14 (s, 1H, C²H), 8.41 (d, *J* = 8.9 Hz, 1H, C⁸H), 8.26 (d, *J* = 2.3 Hz, 1H, C⁵H), 7.50 (dd, *J* = 8.9, 2.3 Hz, 1H, C⁷H), 4.43 (q, *J* = 7.1 Hz, 2H, C¹³H₂), 2.48 (s, 3H, C¹⁵H₃), 1.72 (s, 9H, 3 × C¹¹H₃), 1.43 (t, *J* = 7.1 Hz, 3H, C¹⁴H₃); **¹³C {¹H} NMR** (101 MHz, CDCl₃): δ_C 175.0 (C), 164.9 (C), 149.3 (C), 144.7 (CH), 136.1 (C), 135.4 (C), 134.1 (CH), 127.9 (C), 126.9 (CH), 119.7 (CH), 113.2 (C), 87.7 (C), 61.3 (CH₂), 27.9 (CH₃), 20.9 (CH₃), 14.3 (CH₃); **IR** (ATR): ν_{max} 3158, 3132, 2988, 2908, 1763, 1735 (C=O), 1638, 1609, 1558, 1529, 1480, 1436, 1375, 1365, 1324, 1297, 1275, 1229, 1195, 1177, 1159, 1133, 1084, 1052, 1032, 955, 904, 879, 843, 831, 807, 768, 746, 702, 639, 607, 576, 556, 526, 496, 458, 434, 414; **HRMS** *m/z* calc. for C₁₈H₂₂NO₅ [M+H]: 332.1492; found: 332.1478 (σ = 4.50 ppm).

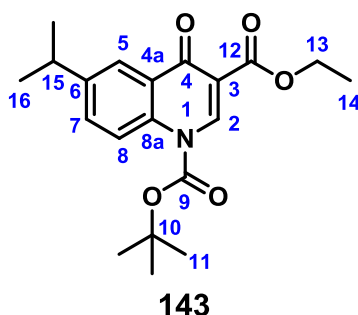
1-*tert*-Butyl 3-ethyl 6-ethyl-4(1*H*)-quinolone-1,3-dicarboxylate **142**



General procedure C was followed using ethyl 6-ethyl-4(1*H*)-quinolone-3-carboxylate (123 mg, 0.502 mmol) and di-*tert*-butyl dicarbonate (0.17 mL, 0.740 mmol) to afford compound **142** as an off-white solid (127 mg, 0.368 mmol, 74%); **m.p.** 248-250 °C; **¹H NMR** (400 MHz, CDCl₃): δ_H 9.14 (s, 1H, C²H), 8.43 (d, *J* = 8.9 Hz, 1H, C⁸H), 8.29 (d, *J* = 2.4 Hz, 1H, C⁵H), 7.53 (dd, *J* = 8.9, 2.4 Hz, 1H, C⁷H), 4.43 (q, *J* = 7.1 Hz, 2H, C¹³H₂),

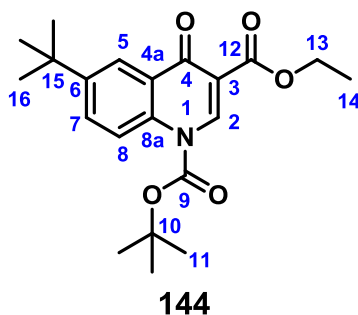
2.79 (q, $J = 7.6$ Hz, 2H, C¹⁵H₂), 1.72 (s, 9H, 3 × C¹¹H₃), 1.44 (t, $J = 7.1$ Hz, 3H, C¹⁴H₃), 1.31 (t, $J = 7.6$ Hz, 3H, C¹⁶H₃); ¹³C {¹H} NMR (101 MHz, CDCl₃): δ_C 175.1 (C), 165.0 (C), 149.3 (C), 144.7 (CH), 142.4 (C), 135.6 (C), 133.0 (CH), 128.0 (C), 125.7 (CH), 119.8 (CH), 113.2 (C), 87.7 (C), 61.3 (CH₂), 28.2 (CH₂), 27.9 (CH₃), 15.3 (CH₃), 14.3 (CH₃); IR (ATR): ν_{max} 3135, 2975, 2933, 2874, 1767, 1732 (C=O), 1642 (C=O), 1611, 1561, 1525, 1479, 1446, 1397, 1366, 1331, 1303, 1277, 1227, 1196, 1179, 1134, 1090, 1070, 1047, 1025, 947, 914, 875, 848, 835, 805, 761, 704, 691, 639, 593, 569, 491, 459, 418; HRMS ^{m/z} calc. for C₁₉H₂₄NO₅ [M+H]: 346.1649; found: 346.1641 (σ = 2.20 ppm).

1-*tert*-Butyl 3-ethyl 6-isopropyl-4(1*H*)-quinolone-1,3-dicarboxylate **143**



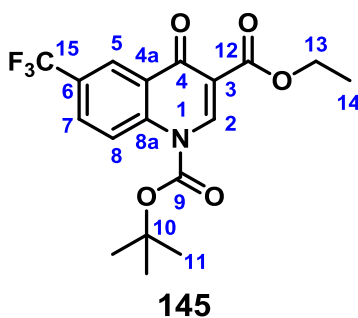
General procedure C was followed using ethyl 6-isopropyl-4(1*H*)-quinolone-3-carboxylate (129 mg, 0.498 mmol) and di-*tert*-butyl dicarbonate (0.17 mL, 0.740 mmol) to afford compound **143** as an off-white solid (123 mg, 0.343 mmol, 69%); **m.p.** >250 °C; ¹H NMR (400 MHz, CDCl₃): δ_H 9.14 (s, 1H, C²H), 8.44 (d, $J = 9.0$ Hz, 1H, C⁸H), 8.32 (d, $J = 2.4$ Hz, 1H, C⁵H), 7.57 (dd, $J = 9.0, 2.4$ Hz, 1H, C⁷H), 4.43 (q, $J = 7.1$ Hz, 2H, C¹³H₂), 3.07 (hept, $J = 6.9$ Hz, 1H, C¹⁵H), 1.72 (s, 9H, 3 × C¹¹H₃), 1.44 (t, $J = 7.1$ Hz, 3H, C¹⁴H₃), 1.32 (d, $J = 6.9$ Hz, 6H, 2 × C¹⁶H₃); ¹³C {¹H} NMR (101 MHz, CDCl₃): δ_C 175.1 (C), 165.0 (C), 149.3 (C), 146.9 (C), 144.7 (CH), 135.6 (C), 131.7 (CH), 128.0 (C), 124.3 (CH), 119.8 (CH), 113.2 (C), 87.7 (C), 61.3 (CH₂), 33.6 (CH), 27.9 (CH₃), 23.8 (CH₃), 14.3 (CH₃); IR (ATR): ν_{max} 3165, 3113, 2977, 2902, 2876, 1735 (C=O), 1642 (C=O), 1608, 1480, 1438, 1396, 1377, 1368, 1330, 1306, 1273, 1251, 1221, 1188, 1130, 1088, 1031, 958, 933, 916, 898, 837, 821, 806, 761, 715, 648, 608, 573, 457, 407; HRMS ^{m/z} calc. for C₂₀H₂₆NO₅ [M+H]: 360.1805; found: 360.1799 (σ = 1.80 ppm).

1-*tert*-Butyl 3-ethyl 6-*tert*-butyl-4(1*H*)-quinolone-1,3-dicarboxylate **144**



General procedure C was followed using ethyl 6-*tert*-butyl-4(1*H*)-quinolone-3-carboxylate (136 mg, 0.498 mmol) and di-*tert*-butyl dicarbonate (0.17 mL, 0.740 mmol) to afford compound **144** as an off-white solid (134 mg, 0.359 mmol, 72%); **m.p.** >250 °C; **¹H NMR** (400 MHz, CDCl₃): δ_H 9.14 (s, 1H, C²H), 8.48 (d, *J* = 2.5 Hz, 1H, C⁵H), 8.45 (d, *J* = 9.2 Hz, 1H, C⁸H), 7.74 (dd, *J* = 9.2, 2.5 Hz, 1H, C⁷H), 4.43 (q, *J* = 7.1 Hz, 2H, C¹³H₂), 1.72 (s, 9H, 3 × C¹¹H₃), 1.44 (t, *J* = 7.1 Hz, 3H, C¹⁴H₃), 1.40 (s, 9H, 3 × C¹⁶H₃); **¹³C {¹H} NMR** (101 MHz, CDCl₃): δ_C 175.2 (C), 165.1 (C), 149.3 (C), 149.3 (C), 144.7 (CH), 135.4 (C), 130.7 (CH), 127.7 (C), 123.3 (CH), 119.6 (CH), 113.3 (C), 87.7 (C), 61.3 (CH₂), 34.8 (C), 31.1 (CH₃), 27.9 (CH₃), 14.3 (CH₃); **IR** (ATR): ν_{max} 3154, 3101, 2971, 2908, 2872, 1758, 1699 (C=O), 1651 (C=O), 1605, 1558, 1527, 1485, 1463, 1439, 1395, 1374, 1346, 1325, 1289, 1266, 1240, 1203, 1175, 1145, 1123, 1094, 1026, 958, 927, 916, 891, 847, 817, 805, 779, 763, 709, 652, 596, 580, 527, 475, 456; **HRMS** *m/z* calc. for C₂₁H₂₈NO₅ [M+H]: 374.1962; found: 374.1960 (σ = 0.50 ppm).

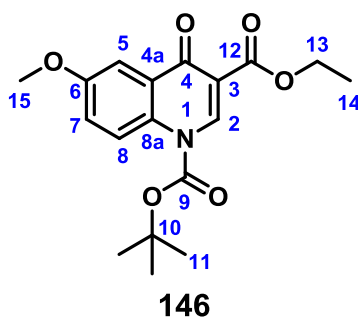
1-*tert*-Butyl 3-ethyl 6-trifluoromethyl-4(1*H*)-quinolone-1,3-dicarboxylate **145**



General procedure C was followed using ethyl 6-trifluoromethyl-4(1*H*)-quinolone-3-carboxylate (285 mg, 1.00 mmol) and di-*tert*-butyl dicarbonate (0.35 mL, 1.52 mmol) to afford compound **145** as an off-white solid (247 mg, 0.641 mmol, 64%); **m.p.** >250 °C; **¹H NMR** (400 MHz, CDCl₃): δ_H 9.19 (d, *J* = 0.5 Hz, 1H, C²H), 8.75 (br s, 1H, C⁵H), 8.70 (d, *J* = 9.1 Hz, 1H, C⁸H), 7.90 (dd, *J* = 9.1, 2.3 Hz, 1H, C⁷H), 4.44 (q, *J* = 7.1 Hz,

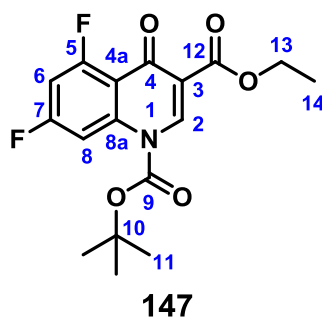
2H, C¹³H₂), 1.74 (s, 9H, 3 × C¹¹H₃), 1.44 (t, *J* = 7.1 Hz, 3H, C¹⁴H₃); ¹³C {¹H} NMR (101 MHz, CDCl₃): δ_C 173.9 (C), 164.3 (C), 148.8 (C), 145.4 (CH), 139.6 (C), 129.1 (q, *J* = 3.3 Hz, CH), 128.3 (q, *J* = 34.0 Hz, C), 128.0 (C), 125.1 (q, *J* = 4.0 Hz, CH), 123.5 (q, *J* = 272.3 Hz, C), 121.0 (CH), 114.1 (C), 88.8 (C), 61.6 (CH₂), 27.9 (CH₃), 14.3 (CH₃); ¹⁹F NMR (376 MHz, CDCl₃): δ_F -62.6 (3F); IR (ATR): ν_{max} 3141, 3082, 2987, 2936, 1775, 1733 (C=O), 1695 (C=O), 1655 (C=O), 1612, 1548, 1517, 1490, 1480, 1462, 1397, 1373, 1355, 1337, 1316, 1290, 1267, 1253, 1236, 1198, 1155, 1126, 1094, 1020, 948, 927, 903, 865, 840, 822, 806, 763, 741, 712, 697, 644, 615, 584, 556, 530, 493, 479, 453, 419; HRMS *m/z* calc. for C₁₈H₁₉F₃NO₅ [M+H]: 386.1210; found: 386.1214 (σ = 1.20 ppm).

1-*tert*-Butyl 3-ethyl 6-methoxy-4(1*H*)-quinolone-1,3-dicarboxylate **146**



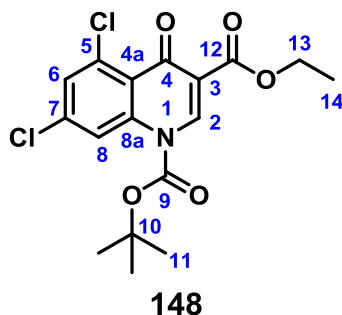
General procedure C was followed using ethyl 6-methoxy-4(1*H*)-quinolone-3-carboxylate (124 mg, 0.502 mmol) and di-*tert*-butyl dicarbonate (0.17 mL, 0.740 mmol) to afford compound **146** as an orange solid (88 mg, 0.253 mmol, 51%); **m.p.** >250 °C; ¹H NMR (400 MHz, CDCl₃): δ_H 9.14 (s, 1H, C²H), 8.47 (d, *J* = 9.5 Hz, 1H C⁸H), 7.89 (d, *J* = 3.2 Hz, 1H, C⁵H), 7.27 (dd, *J* = 9.5, 3.2 Hz, 1H, C⁷H), 4.43 (q, *J* = 7.2 Hz, 2H, C¹³H₂), 3.94 (s, 3H, C¹⁵H₃), 1.72 (s, 9H, 3 × C¹¹H₃), 1.45 (t, *J* = 7.2 Hz, 3H, C¹⁴H₃); ¹³C {¹H} NMR (101 MHz, CDCl₃): δ_C 174.6 (C), 165.0 (C), 157.5 (C), 149.2 (C), 144.3 (CH), 131.7 (C), 129.5 (C), 122.4 (CH), 121.6 (CH), 112.6 (C), 107.1 (CH), 87.8 (C), 61.3 (CH₂), 55.7 (CH₃), 27.9 (CH₃), 14.3 (CH₃); IR (ATR): ν_{max} 3102, 2973, 2908, 2873, 2849, 1760, 1700 (C=O), 1686 (C=O), 1650 (C=O), 1599, 1562, 1486, 1442, 1395, 1371, 1306, 1288, 1266, 1240, 1202, 1175, 1123, 1095, 1026, 1009, 958, 891, 863, 843, 826, 817, 804, 763, 699, 685, 654, 569, 538, 510, 499, 487, 476, 460, 450, 428, 422, 412; HRMS *m/z* calc. for C₁₈H₂₂NO₆ [M+H]: 348.1442; found: 348.1448 (σ = 1.80 ppm).

1-*tert*-Butyl 3-ethyl 5,7-difluoro-4(1*H*)-quinolone-1,3-dicarboxylate **147**



General procedure C was followed using ethyl 5,7-difluoro-4(1*H*)-quinolone-3-carboxylate (253 mg, 1.00 mmol) and di-*tert*-butyl dicarbonate (0.35 mL, 1.52 mmol) to afford compound **147** as an off-white solid (237 mg, 0.671 mmol, 67%); **m.p.** >250 °C; **¹H NMR** (400 MHz, CDCl₃): δ_H 9.01 (s, 1H, C²H), 8.15 (app. dt, *J* = 11.8, 2.3 Hz, 1H, C⁸H), 6.90 (ddd, *J* = 11.0, 8.4, 2.3 Hz, 1H, C⁶H), 4.41 (q, *J* = 7.1 Hz, 2H, C¹³H₂), 1.72 (s, 9H, 3 × C¹¹H₃), 1.42 (t, *J* = 7.1 Hz, 3H, C¹⁴H₃); **¹³C {¹H} NMR** (101 MHz, CDCl₃): δ_C 172.7 (d, *J* = 1.9 Hz, C), 164.3 (dd, *J* = 252.3, 14.8 Hz, C), 164.3 (C), 163.1 (dd, *J* = 267.8, 14.9 Hz, C), 148.8 (C), 143.9 (CH), 140.2 (dd, *J* = 14.4, 4.4 Hz, C), 115.3 (C), 115.1 (dd, *J* = 7.5, 3.4 Hz, C), 103.2 (dd, *J* = 28.7, 5.1 Hz, CH), 102.8 (d, *J* = 25.6 Hz, CH), 88.8 (C), 61.6 (CH₂), 27.8 (CH₃), 14.3 (CH₃); **¹⁹F NMR** (376 MHz, CDCl₃): δ_F -100.1 (1F), -105.6 (1F); **IR** (ATR): ν_{max} 3148, 3110, 3087, 2982, 2937, 2916, 2872, 1758, 1709 (C=O), 1667 (C=O), 1620, 1579, 179, 1464, 1443, 1398, 1373, 1286, 1269, 1251, 1212, 1182, 1139, 1121, 1022, 918, 862, 840, 822, 808, 769, 743, 692, 669, 642, 620, 607, 578, 528, 447, 434; **HRMS** *m/z* calc. for C₁₇H₁₈F₂NO₅ [M+H]: 354.1148; found: 354.1141 (σ = 1.90 ppm).

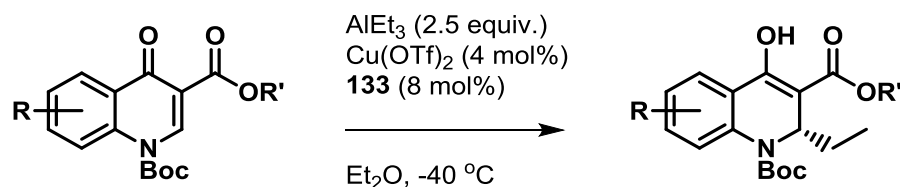
1-*tert*-Butyl 3-ethyl 5,7-dichloro-4(1*H*)-quinolone-1,3-dicarboxylate **148**



General procedure C was followed using ethyl 5,7-dichloro-4(1*H*)-quinolone-3-carboxylate (286 mg, 1.00 mmol) and di-*tert*-butyl dicarbonate (0.35 mL, 1.52 mmol) to afford compound **148** as a pale yellow solid (263 mg, 0.681 mmol, 68%); **m.p.** >250

°C; **¹H NMR** (400 MHz, CDCl₃): δ_H 8.98 (s, 1H, C²H), 8.44 (d, *J* = 2.0 Hz, 1H, C⁸H), 7.49 (d, *J* = 2.0 Hz, 1H, C⁶H), 4.42 (q, *J* = 7.1 Hz, 2H, C¹³H₂), 1.72 (s, 9H, 3 × C¹¹H₃), 1.42 (t, *J* = 7.1 Hz, 3H, C¹⁴H₃); **¹³C {¹H} NMR** (101 MHz, CDCl₃): δ_C 173.4 (C), 164.2 (C), 148.9 (C), 143.3 (CH), 140.0 (C), 137.8 (C), 135.9 (C), 129.5 (CH), 123.4 (C), 119.1 (CH), 115.6 (C), 88.8 (C), 61.6 (CH₂), 27.9 (CH₃), 14.3 (CH₃); **IR** (ATR): ν_{max} 3174, 3147, 3115, 2978, 2934, 2908, 1767, 1702 (C=O), 1667 (C=O), 1615, 1583, 1547, 1476, 1444, 1398, 1369, 1343, 1308, 1269, 1248, 1211, 1185, 1134, 1099, 1023, 958, 930, 892, 861, 840, 804, 754, 695, 671, 621, 598, 546, 499, 452, 420; **HRMS** *m/z* calc. for C₁₇H₁₈³⁵Cl₂NO₅ [M+H]: 386.0557; found: 386.0551 (σ = 1.50 ppm).

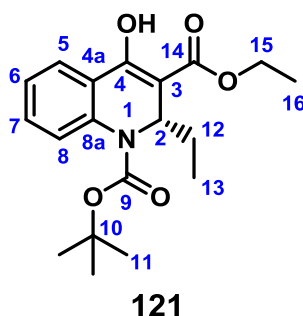
General procedures D and E for the synthesis of ethyl conjugate addition products 121, 149-162, and 165-168 and their subsequent acetylation



General procedure D: A suspension of protected quinolone derivative (1 equiv.), CuOTf₂ (4 mol%) and compound **133** (8 mol%) in freshly distilled anhydrous Et₂O (0.1 M solution) was stirred under an argon atmosphere at r.t. for 30 minutes. The suspension was then cooled to -40 °C and stirred at this temperature under an argon atmosphere for a further 15 minutes. To the suspension was added AlEt₃ (1.3 M solution in heptane) (2.5 equiv.) *via* dropwise addition allowing the organometallic solution to cool prior to contact with the suspension by running down the side of the reaction vessel. The reaction mixture was stirred under an atmosphere of argon at -40 °C until completion (see specified times). A saturated solution of potassium sodium tartrate was then added to the reaction mixture and allowed to warm to r.t. whilst stirring over 30 minutes. The reaction mixture was partitioned between CH₂Cl₂ and water and the phases were separated. The aqueous phase was extracted with CH₂Cl₂ (3 times). The combined organics were washed with water (once), dried (MgSO₄), concentrated *in vacuo* and purified either by column chromatography (silica, 97:3 Pentane/Et₂O) or preparative thin layer chromatography (silica, CH₂Cl₂) to afford the conjugate addition products as described. Enol tautomers dominate (Enol:keto between 95:5-80:20). Only signals relating to enol form are reported. Exchange of the products with minor keto tautomers can cause signal broadening; formation of the acetate avoids this.

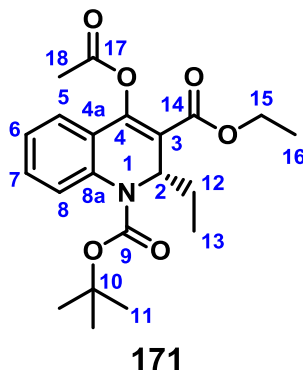
General procedure E: The conjugate addition product was dissolved in 1:1 mixture of Ac₂O/Pyridine (0.5 M solution) and stirred at r.t. for 24 h. Isolated acetate products have been fully characterized for the compound **171** (acetylated derivative of compound **121**). HPLC chromatograms were obtained on small amounts of acetylated material isolated *via* thin layer chromatography on the remainder of the products; the structures were confirmed by ¹H NMR.

1-tert-Butyl 3-ethyl (S)-2-ethyl-4-hydroxy-1,2-dihydroquinoline-1,3-dicarboxylate
121



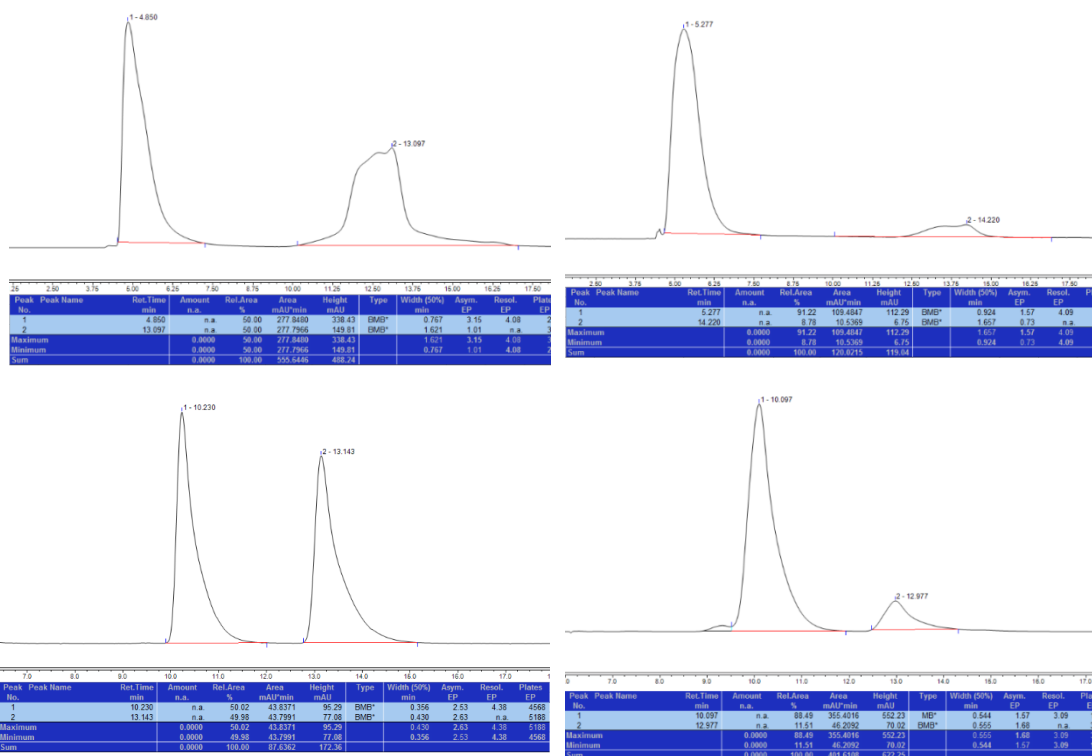
General procedure D was followed using the protected quinolone carboxylate **117** (2.54 g, 8.00 mmol) and triethylaluminium (1.3 M in heptane) (15.5 mL, 20.2 mmol) to afford compound **121** as a colourless oil (2.03 g, 5.84 mmol, 73%); ¹H NMR (400 MHz, CDCl₃): δ_H 12.12 (s, 1H, OH), 7.78 (dd, *J* = 7.7, 1.6 Hz, 1H, C⁵H), 7.63 (br s, 1H, C⁸H), 7.40 (ddd, *J* = 8.4, 7.4, 1.6 Hz, 1H, C⁷H), 7.17 (ddd, *J* = 7.7, 7.4, 1.1 Hz, 1H, C⁶H), 5.39 (dd, *J* = 9.7, 4.9 Hz, 1H, C²H), 4.42 – 4.25 (m, 2H, C¹⁵H₂), 1.55 (s, 9H, 3 × C¹¹H₃) overlapped by 1.56 – 1.45 (m, 1H, C¹²H_AH_B), 1.38 (t, *J* = 7.1 Hz, 3H, C¹⁶H₃) overlapped by 1.42 – 1.34 (m, 1H, C¹²H_AH_B), 0.87 (t, *J* = 7.4 Hz, 3H, C¹³H₃); ¹³C {¹H} NMR (101 MHz, CDCl₃): δ_C 170.5 (C), 162.3 (C), 152.9 (C), 137.9 (C), 130.7 (CH), 125.0 (CH), 124.2 (CH), 123.8 (CH), 123.1 (C), 100.7 (C), 81.4 (C), 60.8 (CH₂), 51.9 (CH), 28.3 (CH₃), 26.7 (CH₂), 14.3 (CH₃), 10.3 (CH₃); IR (ATR): ν_{max} 3488, 2977, 2933, 2875, 1702 (C=O), 1651, 1624, 1569, 1488, 1457, 1403, 1368, 1350, 1328, 1280, 1252, 1232, 1145, 1094, 1074, 1023, 904, 818, 766, 675, 521, 457; HRMS *m/z* calc. for C₁₉H₂₅NNaO₅ [M+Na]: 370.1625; found: 370.1625 (σ = 0.10 ppm); HPLC Keto-enol tautomerism led to broad signals in the chromatograms and increased error bars. Accurate ee measurement was attained on the derived acetate (See below for data). Chiralpak AD-H; mobile phase: hexane:2-propanol (99:1 v/v); flow rate: 0.8 mL min⁻¹; retention times: major enantiomer – 5.3 min (91.2%), minor enantiomer – 14.2 min (8.8%), 82% ee; [α]_D²⁰ +256.3 (*c* = 1.0 in CHCl₃, 82% ee).

1-tert-Butyl 3-ethyl (S)-4-acetoxy-2-ethyl-1,2-dihydroquinoline-1,3-dicarboxylate
171

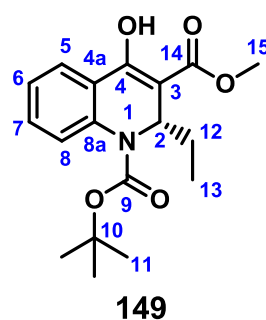


General procedure E was followed using the conjugate addition product **121** (278 mg, 0.800 mmol) to afford compound **171** as a pale yellow oil (229 mg, 0.588 mmol, 74%); **¹H NMR** (400 MHz, CDCl₃): δ_H 7.71 (br s, 1H, C⁸H), 7.42 – 7.32 (m, 2H), 7.13 (ddd, *J* = 8.2, 7.4, 1.1 Hz, 1H, C⁶H), 5.56 (dd, *J* = 10.0, 4.4 Hz, 1H, C²H), 4.33 – 4.21 (m, 2H, C¹⁵H₂), 2.39 (s, 3H, C¹⁸H₃), 1.68 – 1.59 (m, 1H, C¹²H_AH_B) overlapped by H₂O peak, 1.56 (s, 9H, 3 × C¹¹H₃), 1.47 (dtd, *J* = 14.1, 7.2, 2.7 Hz, 1H, C¹²H_AH_B), 1.35 (t, *J* = 7.1 Hz, 3H, C¹⁶H₃), 0.89 (t, *J* = 7.4 Hz, 3H, C¹³H₃); **¹³C {¹H} NMR** (101 MHz, CDCl₃): δ_C 168.0 (C), 163.4 (C), 152.7 (C), 149.2 (C), 137.2 (C), 130.5 (CH), 124.8 (CH), 123.8 (CH), 123.6 (CH), 123.4 (C), 118.1 (C), 81.7 (C), 60.8 (CH₂), 53.8 (CH), 28.3 (CH₃), 25.5 (CH₂), 20.9 (CH₃), 14.2 (CH₃), 10.0 (CH₃); **IR** (ATR): ν_{max} 2974, 2933, 2875, 1773 (C=O), 1700 (C=O), 1635, 1602, 1572, 1485, 1456, 1368, 1329, 1249, 1223, 1184, 1156, 1133, 1106, 1069, 1020, 1005, 904, 887, 870, 855, 759, 732, 646, 584, 521, 459, 433; **HRMS** *m/z* calc. for C₂₁H₂₇NNaO₆ [M+Na]: 412.1731; found: 412.1732 (σ = 0.40 ppm); **HPLC** Chiralpak AD-H; mobile phase: hexane:2-propanol (95:5 v/v); flow rate: 0.5 mL min⁻¹; retention times: major enantiomer – 10.1 min (88.5%), minor enantiomer – 13.0 min (11.5%), 77% ee; [α]_D²⁰ +295.5 (*c* = 1.0 in CHCl₃, 77% ee).

HPLC chromatograms for racemic and enantioenriched **121** (enol, top traces) and derived acetate **171** (lower traces):



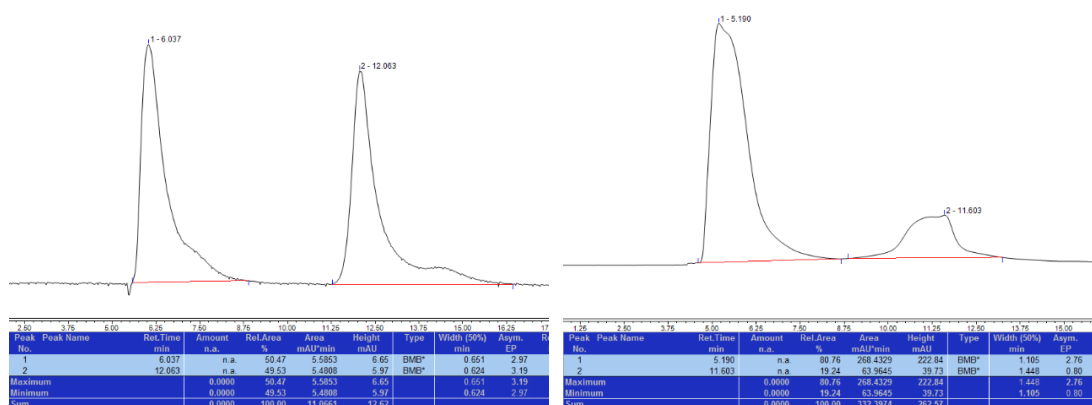
1-tert-Butyl 3-methyl (S)-2-ethyl-4-hydroxy-1,2-dihydroquinoline-1,3-dicarboxylate 149



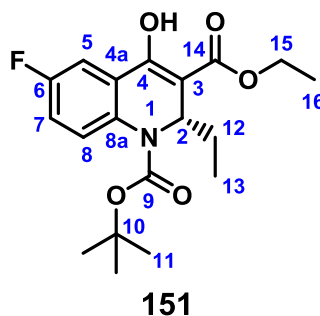
General procedure D was followed using the protected quinolone carboxylate **135** (45.8 mg, 0.150 mmol) and triethylaluminium (1.3 M in heptane) (0.29 mL, 0.377 mmol) to afford compound **149** as a colourless oil (33.4 mg, 0.100 mmol, 67%); ¹H NMR (400 MHz, CDCl₃): δ_H 12.04 (s, 1H, OH), 7.78 (dd, *J* = 7.8, 1.6 Hz, 1H, C⁵H), 7.62 (br s, 1H, C⁸H), 7.41 (td, *J* = 8.3, 7.3, 1.6 Hz, 1H, C⁷H), 7.18 (td, *J* = 7.8, 7.3, 1.1 Hz, 1H, C⁶H), 5.37 (dd, *J* = 9.7, 4.6 Hz, 1H, C²H), 3.87 (s, 3H, C¹⁵H), 1.55 (s, 9H, 3 × C¹¹H₃) overlapped by 1.51 (dq, *J* = 14.0, 7.2, 4.6 Hz, 1H, C¹²H_AH_B), 1.39 (ddq, *J* = 14.0, 9.7, 7.2 Hz, 1H, C¹²H_AH_B), 0.87 (app t, *J* = 7.3 Hz, 3H, C¹³H₃); ¹³C {¹H} NMR (101 MHz,

CDCl₃): δ_C 170.8 (C), 162.4 (C), 152.9 (C), 137.9 (C), 130.8 (CH), 125.1 (C), 124.3 (CH), 123.8 (CH), 123.0 (CH), 112.7 (CH), 100.6 (C), 81.5 (C), 51.9 (CH₃), 28.3 (CH₃), 26.6 (CH₂), 10.2 (CH₃); **IR** (ATR): ν_{max} 3490, 2933, 2875, 1705 (C=O), 1648, 1621, 1570, 1487, 1454, 1421, 1368, 1331, 1291, 1262, 1244, 1150, 1088, 1035, 904, 819, 767, 670, 518, 459; **HRMS** m/z calc. for C₁₈H₂₄NO₅ [M+H]: 334.1639; found: 334.1636 (σ = 1.40 ppm); **HPLC** Chiralpak AD-H; mobile phase: hexane:2-propanol (99:1 v/v); flow rate: 0.8 mL min⁻¹; retention times: major enantiomer – 5.2 min (80.8%), minor enantiomer – 11.6 min (19.2%), 62% ee; [α]_D²⁰ +198.0 (c = 1.0 in CHCl₃, 62% ee).

HPLC chromatograms for racemic **149** (left) and enantioenriched **149** (right):



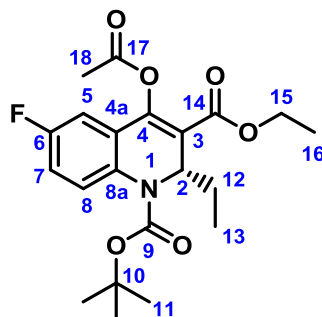
1-*tert*-Butyl 3-ethyl (S)-2-ethyl-6-fluoro-4-hydroxy-1,2-dihydroquinoline-1,3-dicarboxylate **151**



General procedure D was followed using the protected quinolone carboxylate **139** (46.4 mg, 0.138 mmol) and triethylaluminium (1.3 M in heptane) (0.27 mL, 0.351 mmol) to afford compound **151** as a colourless oil (38.9 mg, 0.106 mmol, 77%); **¹H NMR** (500 MHz, CDCl₃): δ_H 12.05 (s, 1H, OH), 7.59 (br s, 1H, C⁸H), 7.47 (dd, *J* = 8.7, 3.1 Hz, 1H, C⁵H), 7.10 (ddd, *J* = 8.6, 8.6, 3.1 Hz, 1H, C⁷H), 5.37 (dd, *J* = 9.7, 4.8 Hz, 1H, C²H), 4.40 – 4.27 (m, 2H, C¹⁵H₂), 1.54 (s, 9H, 3 × C¹¹H₃) overlapped by 1.55 – 1.46 (m, 1H, C¹²H_AH_B), 1.38 (t, *J* = 7.1 Hz, 3H, C¹⁶H₃) overlapped by 1.42 – 1.33 (m, 1H, C¹²H_AH_B),

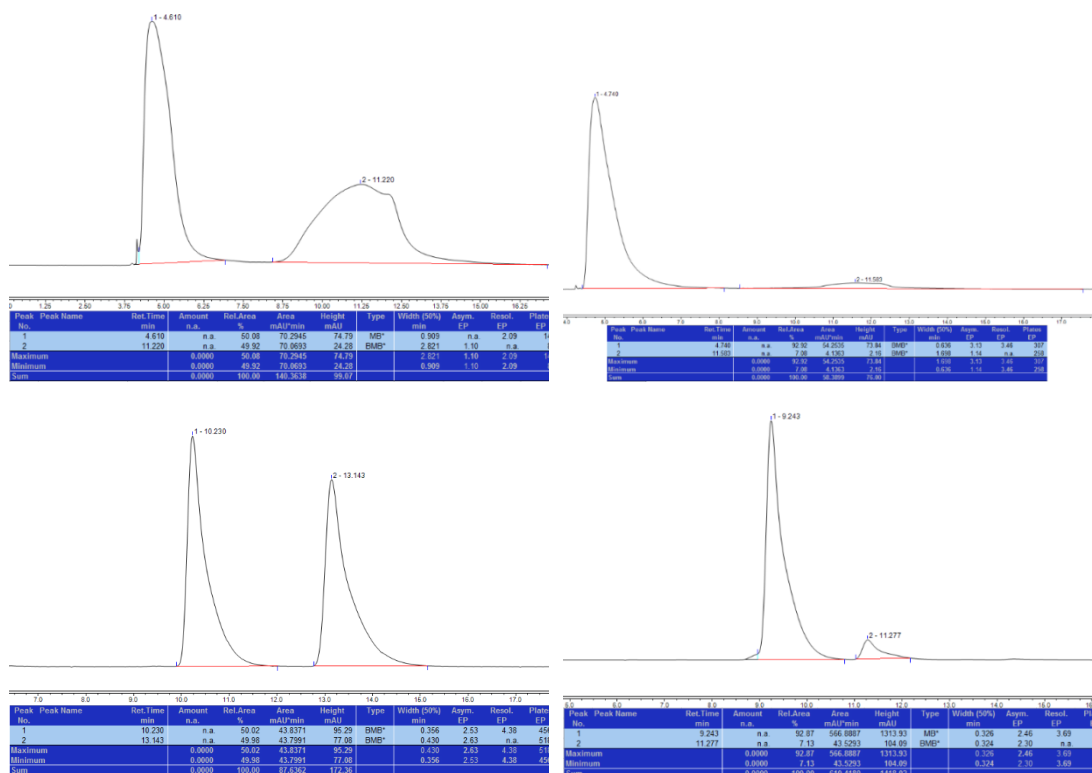
0.87 (t, $J = 7.4$ Hz, 3H, $C^{13}H_3$); ^{13}C { 1H } NMR (126 MHz, $CDCl_3$): δ_C 170.3 (C), 161.0 (C), 159.0 (d, $J = 243.6$ Hz, C), 152.9 (C), 133.8 (d, $J = 3.0$ Hz, C), 126.8 (d, $J = 7.3$ Hz, CH), 124.7 (d, $J = 8.1$ Hz, C), 117.6 (d, $J = 22.9$ Hz, CH), 110.5 (d, $J = 24.5$ Hz, CH), 101.7 (C), 81.6 (C), 61.0 (CH_2), 51.9 (CH), 28.3 (CH_3), 26.6 (CH_2), 14.2 (CH_3), 10.3 (CH_3); ^{19}F NMR (471 MHz, $CDCl_3$): δ_F -117.91 (1F); IR (ATR): ν_{max} 2973, 2932, 2875, 2859, 1706 (C=O), 1655, 1632, 1612, 1579, 1493, 1457, 1404, 1383, 1368, 1348, 1325, 1276, 1237, 1198, 1163, 1086, 1025, 882, 818, 764, 464; HRMS m/z calc. for $C_{19}H_{24}FNNaO_5$ [M+Na]: 388.1531; found: 388.1532 ($\sigma = 0.30$ ppm); HPLC Keto-enol tautomerism led to broad signals in the chromatograms and increased error bars. Accurate ee measurement was attained on the derived acetate (See below for data). Chiralpak AD-H; mobile phase: hexane:2-propanol (99:1 v/v); flow rate: 0.8 mL min^{-1} ; retention times: major enantiomer – 4.7 min (92.9%), minor enantiomer – 11.6 min (7.1%), 86% ee; $[\alpha]_D^{20} +290.8$ ($c = 1.0$ in $CHCl_3$, 86% ee).

1-tert-Butyl 3-ethyl (S)-4-acetoxy-2-ethyl-6-fluoro-1,2-dihydroquinoline-1,3-dicarboxylate

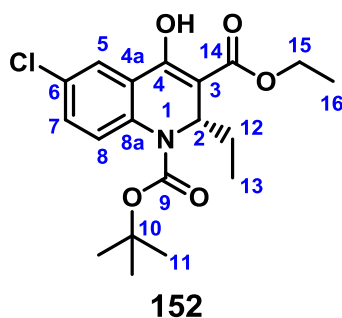


General procedure E was followed using the conjugate addition product **151** to the acetylated derivative; 1H NMR (400 MHz, $CDCl_3$): δ_H 7.67 (br s, 1H, C^8H), 7.13 – 7.01 (m, 2H, C^5H , C^7H), 5.55 (dd, $J = 10.2, 4.3$ Hz, 1H, C^2H), 4.28 (q, $J = 7.1$ Hz, 2H, $C^{15}H_2$), 2.40 (s, 3H, $C^{18}H_3$), 1.55 (s, 9H, 3 \times $C^{11}H_3$) overlapped by 1.64 – 1.51 (m, 1H, $C_{12}H_AH_B$), 1.50 – 1.40 (m, 1H, $C_{12}H_AH_B$), 1.35 (t, $J = 7.1$ Hz, 3H, $C^{16}H_3$), 0.89 (t, $J = 7.4$ Hz, 3H, $C^{13}H_3$); HPLC Chiralpak AD-H; mobile phase: hexane:2-propanol (95:5 v/v); flow rate: 0.5 mL min^{-1} ; retention times: major enantiomer – 9.2 min (92.9%), minor enantiomer – 11.3 min (7.1%), 86% ee. Only 1H NMR data was collected for the compound to confirm structure prior to HPLC analysis.

HPLC chromatograms for racemic and enantioenriched **151** (enol, top traces) and the derived acetate (lower traces):



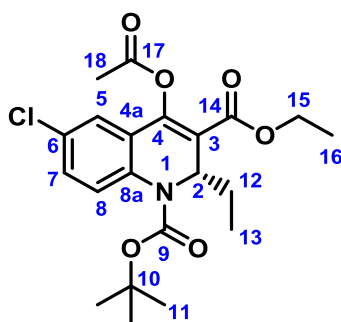
1-tert-Butyl 3-ethyl (S)-6-chloro-2-ethyl-4-hydroxy-1,2-dihydroquinoline-1,3-dicarboxylate 152



General procedure D was followed using the protected quinolone carboxylate **138** (48.6 mg, 0.138 mmol) and triethylaluminium (1.3 M in heptane) (0.27 mL, 0.351 mmol) to afford compound **152** as a colourless oil (48.0 mg, 0.126 mmol, 91%); ¹H NMR (500 MHz, CDCl₃): δ_H 12.05 (s, 1H, OH), 7.75 (d, *J* = 2.5 Hz, 1H, C⁵H), 7.58 (br s, 1H, C⁸H), 7.34 (dd, *J* = 8.8, 2.5 Hz, 1H, C⁷H), 5.37 (dd, *J* = 9.7, 4.8 Hz, 1H, C²H), 4.40 – 4.27 (m, 2H, C¹⁵H₂), 1.54 (s, 9H, 3 × C¹¹H₃) overlapped by 1.57 – 1.46 (m, 1H, C¹²H_AH_B), 1.38 (t, *J* = 7.1 Hz, 3H, C¹⁶H₃) overlapped by 1.45 – 1.32 (m, 1H, C¹²H_AH_B), 0.86 (t, *J* = 7.4 Hz, 3H, C¹³H₃); ¹³C {¹H} NMR (126 MHz, CDCl₃): δ_C 170.3 (C), 160.9 (C), 152.7 (C),

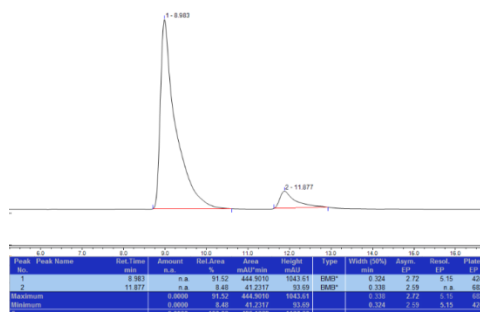
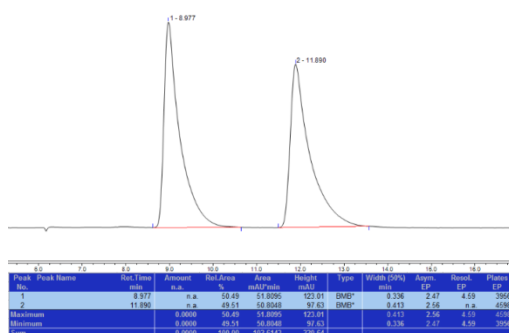
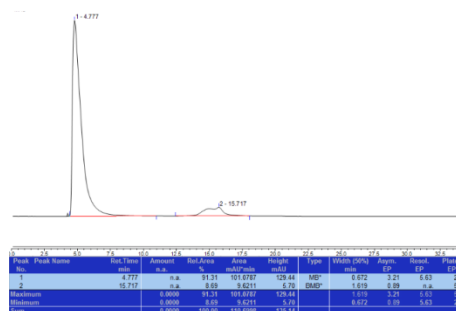
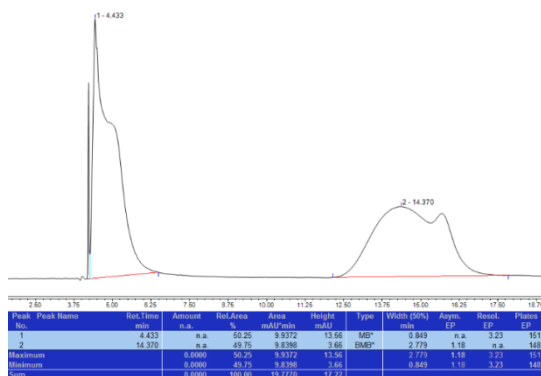
136.3 (C), 130.5 (CH), 129.3 (C), 126.3 (CH), 124.5 (C), 124.0 (CH), 101.5 (C), 81.9 (C), 61.0 (CH₂), 51.9 (CH), 28.3 (CH₃), 26.8 (CH₂), 14.2 (CH₃), 10.2 (CH₃); **IR** (ATR): ν_{max} 2968, 2930, 2874, 2855, 1708 (C=O), 1656, 1628, 1594, 1562, 1482, 1404, 1381, 1368, 1348, 1323, 1253, 1233, 1150, 1113, 1025, 858, 817, 764, 576, 465; **HRMS** m/z calc. for C₁₉H₂₄³⁵ClNNaO₅ [M+Na]: 404.1235; found: 404.1236 (σ = 0.20 ppm); **HPLC** Keto-enol tautomerism led to broad signals in the chromatograms and increased error bars. Accurate ee measurement was attained on the derived acetate (See below for data). Chiralpak AD-H; mobile phase: hexane:2-propanol (99:1 v/v); flow rate: 0.8 mL min⁻¹; retention times: major enantiomer – 4.8 min (91.3%), minor enantiomer – 15.7 min (8.7%), 83% ee; $[\alpha]_{\text{D}}^{20}$ +206.4 (c = 1.0 in CHCl₃, 83% ee).

1-tert-Butyl 3-ethyl (S)-4-acetoxy-6-chloro-2-ethyl-1,2-dihydroquinoline-1,3-dicarboxylate

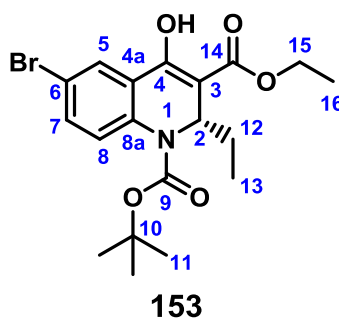


General procedure E was followed using the conjugate addition product **152** to afford the acetylated derivative; **¹H NMR** (400 MHz, CDCl₃): δ_{H} 7.67 (br s, 1H, C⁸H), 7.35 – 7.30 (m, 2H, C⁵H, C⁷H), 5.55 (dd, J = 10.0, 4.4 Hz, 1H, C²H), 4.28 (q, J = 7.1 Hz, 2H, C¹⁵H₂), 2.41 (s, 3H, C¹⁸H₂), 1.64 (ddd, J = 14.1, 7.3, 4.4 Hz, 1H, C¹²H_AH_B), 1.56 (s, 9H, 3 × C¹¹H₃), 1.45 (ddd, J = 14.1, 10.0, 7.3 Hz, 1H, C¹²H_AH_B), 1.35 (t, J = 7.1 Hz, 3H, C¹⁶H₃), 0.89 (t, J = 7.3 Hz, 3H, C¹³H₃); **HPLC** Chiralpak AD-H; mobile phase: hexane:2-propanol (95:5 v/v); flow rate: 0.5 mL min⁻¹; retention times: major enantiomer – 9.0 min (91.5%), minor enantiomer – 11.9 min (8.5%), 83% ee. Only ¹H NMR data was collected for the compound to confirm structure prior to HPLC analysis.

HPLC chromatograms for racemic and enantioenriched **152** (enol, top traces) and derived acetate (lower traces):



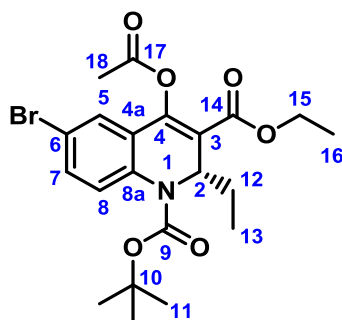
1-tert-Butyl 3-ethyl (S)-6-bromo-2-ethyl-4-hydroxy-1,2-dihydroquinoline-1,3-dicarboxylate 153



General procedure D was followed using the protected quinolone carboxylate **139** (54.8 mg, 0.138 mmol) and triethylaluminium (1.3 M in heptane) (0.27 mL, 0.351 mmol) to afford compound **153** as a colourless oil (37.7 mg, 0.088 mmol, 64%); ¹H NMR (500 MHz, CDCl₃): δ_H 12.05 (s, 1H, OH), 7.90 (br s, 1H, C⁵H), 7.58 – 7.45 (m, 2H, C⁷H, C⁸H), 5.37 (dd, *J* = 9.6, 4.8 Hz, 1H, C²H), 4.41 – 4.27 (m, 2H, C¹⁵H₂), 1.54 (s, 9H, 3 × C¹¹H₃) overlapped by 1.58 – 1.46 (m, 1H, C¹²H_AH_B), 1.38 (t, *J* = 7.1 Hz, 3H, C¹⁶H₃) overlapped by 1.43 – 1.33 (m, 1H, C¹²H_AH_B), 0.86 (t, *J* = 7.4 Hz, 3H, C¹³H₃); ¹³C {¹H}

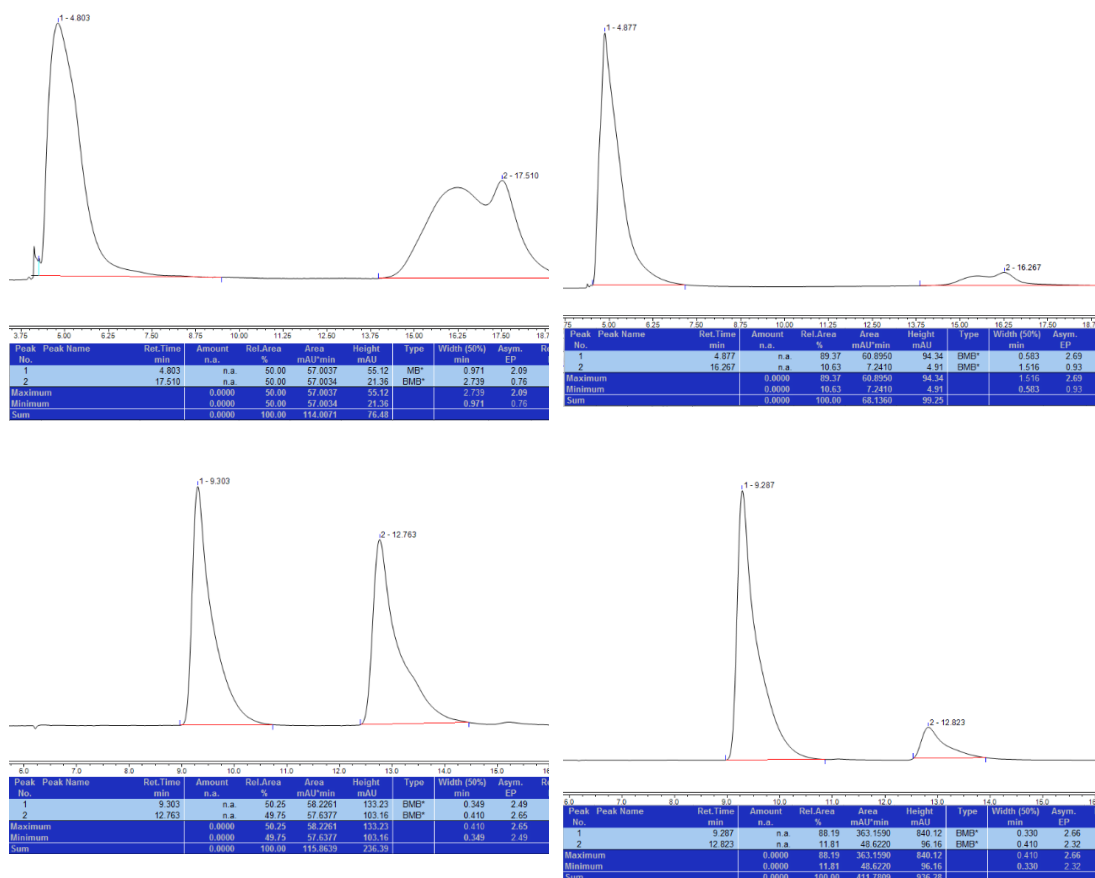
NMR (126 MHz, CDCl₃): δ_c 170.3 (C), 160.8 (C), 152.6 (C), 136.9 (C), 133.4 (CH), 127.0 (CH), 126.6 (CH), 124.8 (C), 116.9 (C), 101.4 (C), 81.9 (C), 61.0 (CH₂), 51.9 (CH), 28.3 (CH₃), 26.8 (CH₂), 14.2 (CH₃), 10.2 (CH₃); **IR** (ATR): ν_{\max} 2973, 2931, 2874, 2856, 1707 (C=O), 1655, 1627, 1590, 1559, 1477, 1403, 1381, 1369, 1322, 1252, 1151, 1101, 1076, 1024, 816, 764, 556, 464; **HRMS** m/z calc. for C₁₉H₂₄⁷⁹BrNNaO₅ [M+Na]: 448.0730; found: 448.0726 (σ = 1.00 ppm); **HPLC** Keto-enol tautomerism led to broad signals in the chromatograms and increased error bars. Accurate ee measurement was attained on the derived acetate (See below for data). Chiralpak AD-H; mobile phase: hexane:2-propanol (99:1 v/v); flow rate: 0.8 mL min⁻¹; retention times: major enantiomer – 4.9 min (89.4%), minor enantiomer – 16.4min (10.6%), 79% ee; $[\alpha]_D^{20}$ +134.0 (c = 1.0 in CHCl₃, 79% ee).

1-tert-Butyl 3-ethyl (S)-4-acetoxy-6-bromo-2-ethyl-1,2-dihydroquinoline-1,3-dicarboxylate

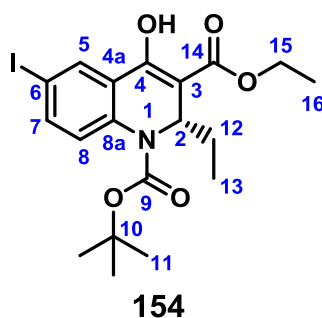


General procedure E was followed using the conjugate addition product **153** to afford the acetylated derivative; **¹H NMR** (400 MHz, CDCl₃): δ_H 7.61 (br s, 1H, C⁸H), 7.50 – 7.43 (m, 2H, C⁵H, C⁷H), 5.55 (dd, J = 10.0, 4.4 Hz, 1H, C²H), 4.28 (q, J = 7.1 Hz, 2H, C¹⁵H₂), 2.41 (s, 3H, C¹⁸H₃), 1.64 (ddd, J = 14.0, 7.3, 4.4 Hz, 1H, C¹²H_AH_B), 1.55 (s, 9H, 3 × C¹¹H₃), 1.46 (ddd, J = 14.0, 10.0, 7.3 Hz, 1H, C¹²H_AH_B), 1.35 (t, J = 7.1 Hz, 3H, C¹⁶H₃), 0.88 (t, J = 7.3 Hz, 3H, C¹³H₃); **HPLC** Chiralpak AD-H; mobile phase: hexane:2-propanol (95:5 v/v); flow rate: 0.5 mL min⁻¹; retention times: major enantiomer – 9.3 min (88.2%), minor enantiomer – 12.8 min (11.8%), 76% ee. Only ¹H NMR data was collected for the compound to confirm structure prior to HPLC analysis.

HPLC chromatograms for racemic and enantioenriched **153** (enol, top traces) and derived acetate (lower traces):



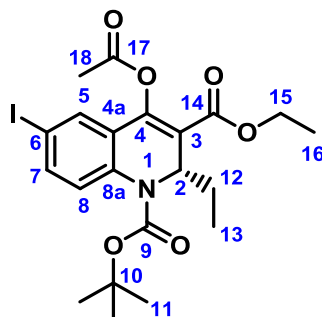
1-*tert*-Butyl 3-ethyl (S)-2-ethyl-4-hydroxy-6-iodo-1,2-dihydroquinoline-1,3-dicarboxylate 154



General procedure D was followed using the protected quinolone carboxylate **140** (61.2 mg, 0.138 mmol) and triethylaluminium (1.3 M in heptane) (0.27mL, 0.351 mmol) to afford compound **154** as a colourless oil (46.5 mg, 0.098 mmol, 71%); ¹H NMR (400 MHz, CDCl₃): δ_H 12.05 (s, 1H, OH), 8.08 (d, *J* = 2.1 Hz, 1H, C⁵H), 7.68 (dd, *J* = 8.7, 2.1 Hz, 1H, C⁷H), 7.42 (br s, 1H, C⁸H), 5.36 (dd, *J* = 9.7, 4.8 Hz, 1H, C²H), 4.40 – 4.27

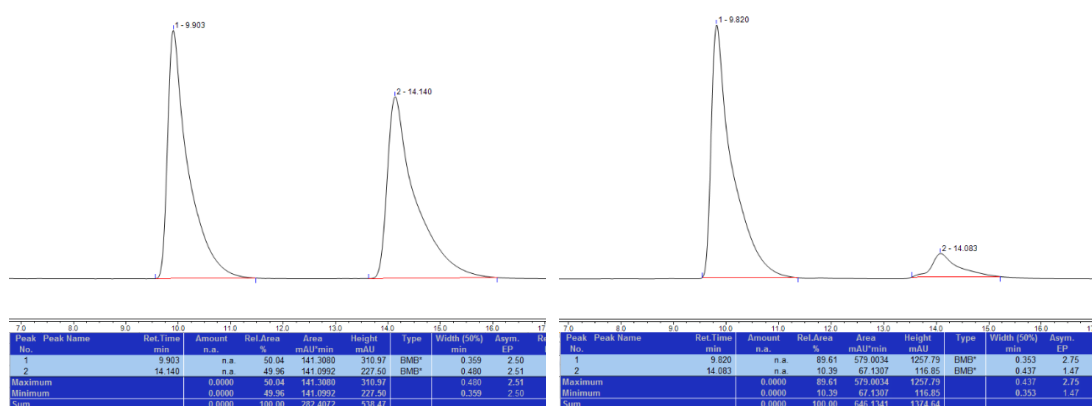
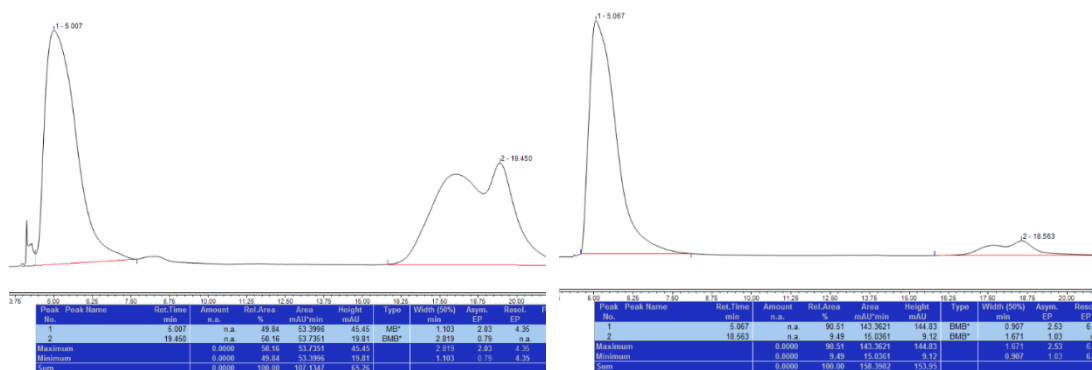
(m, 2H, C¹⁵H₂), 1.54 (s, 9H, 3 × C¹¹H₃) overlapped by 1.57 – 1.46 (m, 1H, C¹²H_AH_B), 1.38 (t, *J* = 7.1 Hz, 3H, C¹⁶H₃) overlapped by 1.43 – 1.32 (m, 1H, C¹²H_AH_B), 0.85 (t, *J* = 7.4 Hz, 3H, C¹³H₃); ¹³C {¹H} NMR (101 MHz, CDCl₃): δ_C 170.2 (C), 160.7 (C), 152.5 (C), 139.3 (CH), 137.6 (C), 132.9 (CH), 126.8 (CH), 125.0 (C), 101.3 (C), 87.2 (C), 81.9 (C), 61.0 (CH₂), 51.9 (CH), 28.3 (CH₃), 26.8 (CH₂), 14.2 (CH₃), 10.2 (CH₃); IR (ATR): ν_{max} 2973, 2931, 2874, 1707 (C=O), 1655, 1626, 1585, 1557, 1477, 1406, 1381, 1368, 1322, 1253, 1153, 1100, 1000, 1075, 1024, 895, 816, 764; HRMS *m/z* calc. for C₁₉H₂₄INNaO₅ [M+Na]: 496.0591; found: 496.0588 (σ = 0.60 ppm); HPLC Keto-enol tautomerism led to broad signals in the chromatograms and increased error bars. Accurate ee measurement was attained on the derived acetate (See below for data). Chiralpak AD-H; mobile phase: hexane:2-propanol (99:1 v/v); flow rate: 0.8 mL min⁻¹; retention times: major enantiomer – 5.1 min (90.5%), minor enantiomer – 18.6 min (9.5%), 81% ee; [α]_D²⁰ +170.3 (*c* = 1.0 in CHCl₃, 81% ee).

1-tert-Butyl 3-ethyl (S)-4-acetoxy-2-ethyl-6-iodo-1,2-dihydroquinoline-1,3-dicarboxylate

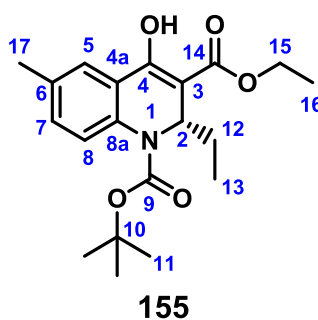


General procedure E was followed using the conjugate addition product **154** to afford the acetylated derivative; ¹H NMR (400 MHz, CDCl₃): δ_H 7.66 (dd, *J* = 8.6, 2.1 Hz, 1H, C⁷H), 7.62 (d, *J* = 2.1 Hz, 1H, C⁵H), 7.48 (br s, 1H, C⁸H), 5.54 (dd, *J* = 10.0, 4.5 Hz, 1H, C²H), 4.27 (q, *J* = 7.1 Hz, 2H, C¹⁵H₂), 2.40 (s, 3H, C¹⁸H₃), 1.64 (ddd, *J* = 14.0, 7.3, 4.5 Hz, 1H, C¹²H_AH_B), 1.55 (s, 9H, 3 × C¹¹H₃), 1.46 (ddd, *J* = 14.0, 10.0, 7.3 Hz, 1H, C¹²H_AH_B), 1.35 (t, *J* = 7.1 Hz, 3H, C¹⁶H₃), 0.88 (t, *J* = 7.3 Hz, 3H, C¹³H₃); HPLC Chiralpak AD-H; mobile phase: hexane:2-propanol (95:5 v/v); flow rate: 0.5 mL min⁻¹; retention times: major enantiomer – 9.8 min (89.6%), minor enantiomer – 14.1 min (10.4%), 79% ee. Only ¹H NMR data was collected for the compound to confirm structure prior to HPLC analysis.

HPLC chromatograms for racemic and enantioenriched **154** (enol, top traces) and derived acetate (lower traces):



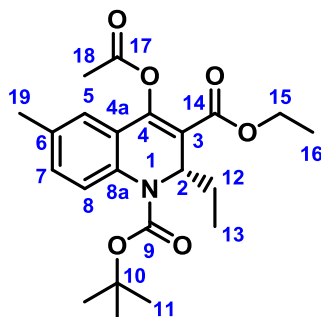
1-tert-Butyl 3-ethyl (S)-2-ethyl-4-hydroxy-6-methyl-1,2-dihydroquinoline-1,3-dicarboxylate 155



General procedure D was followed using the protected quinolone carboxylate **141** (45.8 mg, 0.138 mmol) and triethylaluminium (1.3 M in heptane) (0.27 mL, 0.351 mmol) to afford compound **155** as a colourless oil (39.0 mg, 0.108 mmol, 78%); ¹H NMR (500 MHz, CDCl₃): δ_H 12.14 (s, 1H, OH), 7.58 (d, *J* = 2.2 Hz, 1H, C⁵H), 7.49 (br s, 1H, C⁸H), 7.21 (dd, *J* = 8.4, 2.2 Hz, 1H, C⁷H), 5.37 (dd, *J* = 9.6, 4.8 Hz, 1H, C²H), 4.42 – 4.22 (m, 2H, C¹⁵H₂), 2.38 (s, 3H, C¹⁷H₃), 1.54 (s, 9H, 3 × C¹¹H₃) overlapped by 1.55 – 1.47 (m,

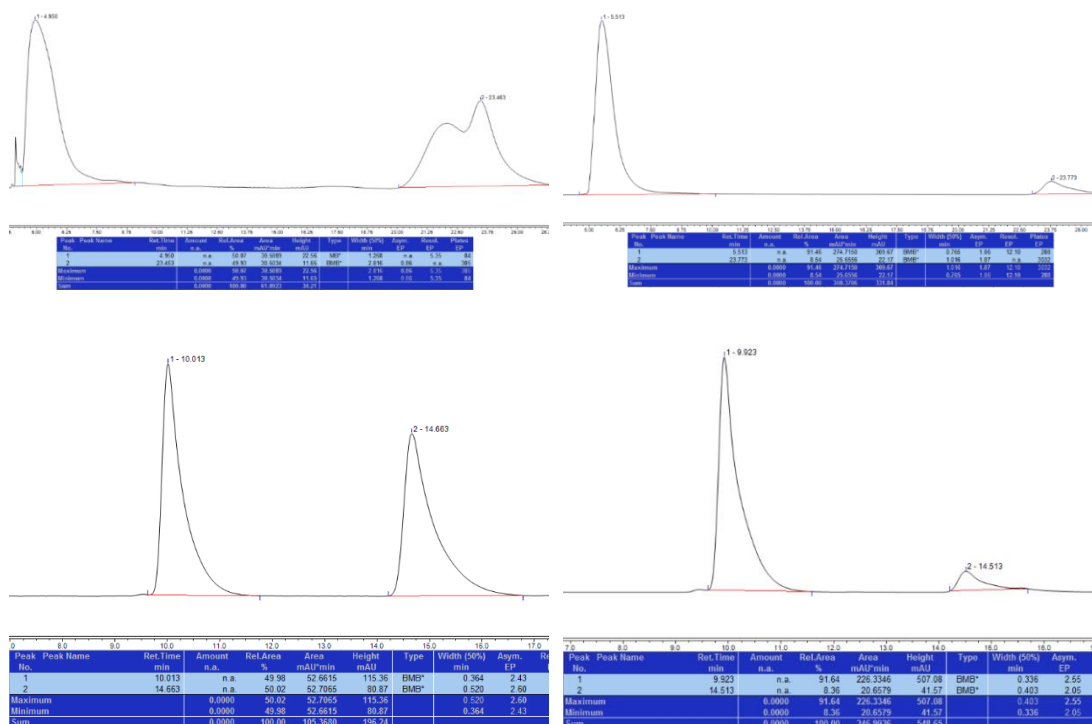
1H, C¹²H_AH_B), 1.38 (t, *J* = 7.1 Hz, 3H, C¹⁶H₃) overlapped by 1.42 – 1.34 (m, 1H, C¹²H_AH_B), 0.86 (t, *J* = 7.4 Hz, 3H, C¹³H₃); ¹³C {¹H} NMR (126 MHz, CDCl₃): δ_C 170.6 (C), 162.4 (C), 153.0 (C), 135.4 (C), 133.5 (C), 131.6 (CH), 124.9 (CH), 124.4 (CH), 122.9 (C), 100.7 (C), 81.3 (C), 60.7 (CH₂), 28.3 (CH₃), 26.6 (CH₂), 20.9 (CH₃), 14.3 (CH₃), 10.3 (CH₃); IR (ATR): ν_{max} 2971, 2928, 2874, 2857, 1703 (C=O), 1652, 1627, 1603, 1574, 1496, 1457, 1404, 1368, 1349, 1328, 1278, 1254, 1235, 1212, 1165, 1097, 1076, 1027, 818, 765, 458; HRMS ^{m/z} calc. for C₂₀H₂₇NNaO₅ [M+Na]: 384.1781; found: 384.1785 (σ = 0.60 ppm); HPLC Keto-enol tautomerism led to broad signals in the chromatograms and increased error bars. Accurate ee measurement was attained on the derived acetate (See below for data). Chiralpak AD-H; mobile phase: hexane:2-propanol (99:1 v/v); flow rate: 0.8 mL min⁻¹; retention times: major enantiomer – 5.5 min (91.5%), minor enantiomer – 23.8 min (8.5%), 83% ee; [α]_D²⁰ +192.5 (c = 1.0 in CHCl₃, 83% ee).

1-tert-Butyl 3-ethyl (S)-4-acetoxy-2-ethyl-6-methyl-1,2-dihydroquinoline-1,3-dicarboxylate

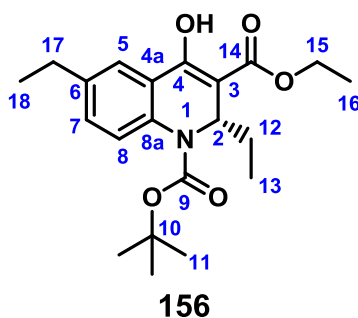


General procedure E was followed using the conjugate addition product **155** to afford acetylated derivative; ¹H NMR (400 MHz, CDCl₃): δ_H 7.59 (br s, 1H, C⁸H), 7.19 (d, *J* = 8.7 Hz, 1H, C⁷H), 7.13 (d, *J* = 2.0 Hz, 1H, C⁵H), 5.54 (dd, *J* = 10.1, 4.4 Hz, 1H, C²H), 4.27 (q, *J* = 7.1 Hz, 2H, C¹⁵H₂), 2.40 (s, 3H, C¹⁸H₃), 2.35 (s, 3H, C¹⁹H₂), 1.62 (ddd, *J* = 14.0, 7.4, 4.4 Hz, 1H, C¹²H_AH_B), 1.55 (s, 9H, 3 × C¹¹H₃), 1.46 (ddd, *J* = 14.0, 10.1, 7.4 Hz, 1H, C¹²H_AH_B), 1.35 (t, *J* = 7.1 Hz, 3H, C¹⁶H₃), 0.88 (t, *J* = 7.4 Hz, 3H, C¹³H₃); HPLC Chiralpak AD-H; mobile phase: hexane:2-propanol (95:5 v/v); flow rate: 0.5 mL min⁻¹; retention times: major enantiomer – 9.9 min (91.6%), minor enantiomer – 14.3 min (8.4%), 83% ee. Only ¹H NMR data was collected for the compound to confirm structure prior to HPLC analysis.

HPLC chromatograms for racemic and enantioenriched **155** (enol, top traces) and derived acetate (lower traces):



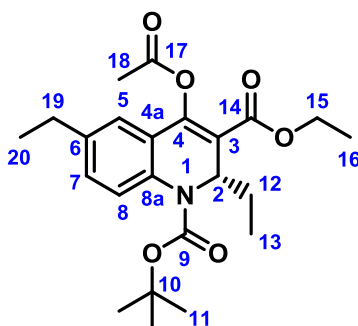
1-tert-Butyl 3-ethyl (S)-2,6-diethyl-4-hydroxy-1,2-dihydroquinoline-1,3-dicarboxylate 156



General procedure D was followed using the protected quinolone carboxylate **142** (47.7 mg, 0.138 mmol) and triethylaluminium (1.3 M in heptane) (0.27 mL, 0.351 mmol) to afford compound **156** as a colourless oil (39.4 mg, 0.105 mmol, 76%); ¹H NMR (500 MHz, CDCl₃): δ_H 12.16 (s, 1H, OH), 7.61 (d, *J* = 2.2 Hz, 1H, C⁵H), 7.53 (br s, 1H, C⁸H), 7.24 (dd, *J* = 8.4, 2.2 Hz, 1H, C⁷H), 5.37 (dd, *J* = 9.5, 4.8 Hz, 1H, C²H), 4.39 – 4.26 (m, 2H, C¹⁵H₂), 2.68 (q, *J* = 7.6 Hz, 2H, C¹⁷H₂), 1.54 (s, 9H, 3 × C¹¹H₃) overlapped by 1.56 – 1.46 (m, 1H, C¹²H_AH_B), 1.38 (t, *J* = 7.1 Hz, 3H, C¹⁶H₃) overlapped by 1.43 – 1.33 (m, 1H, C¹²H_AH_B), 1.27 (t, *J* = 7.6 Hz, 3H, C¹⁸H₃), 0.87 (t, *J* = 7.4 Hz, 3H, C¹³H₃); ¹³C {¹H}

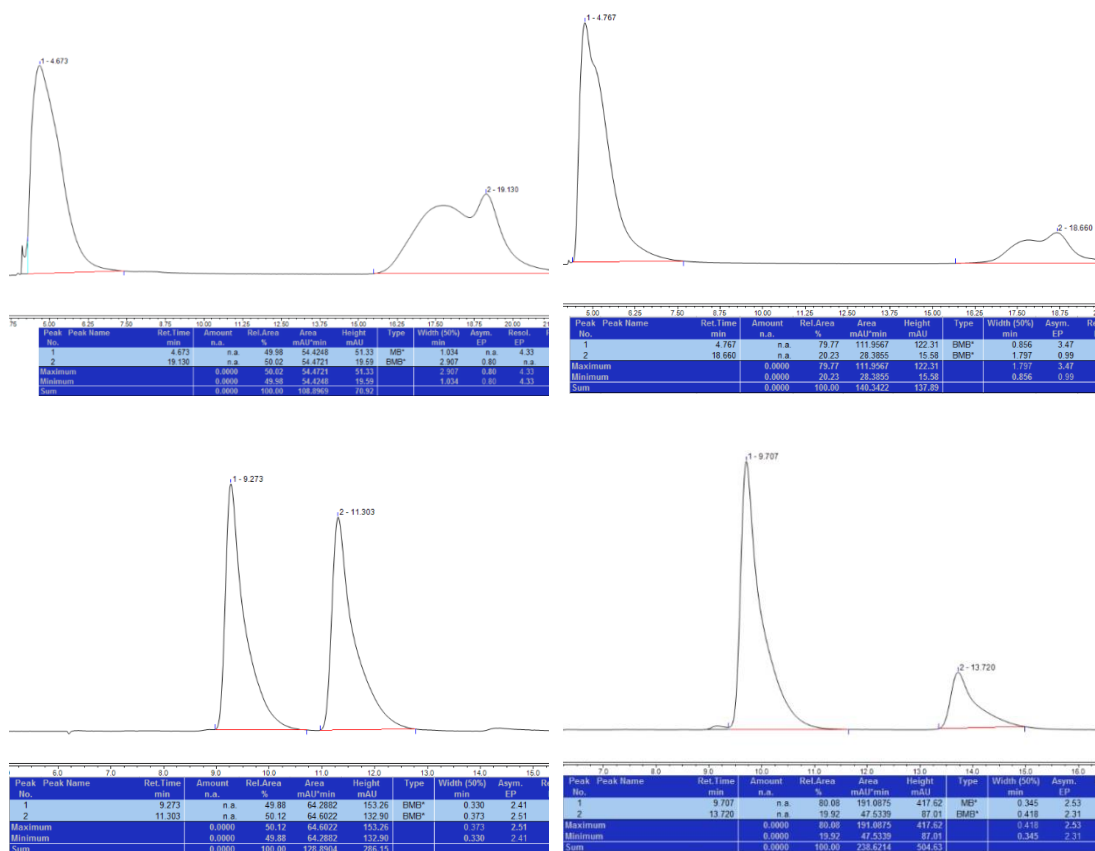
NMR (126 MHz, CDCl₃): δ_C 170.6 (C), 162.5 (C), 153.0 (C), 139.8 (C), 135.6 (C), 130.5 (CH), 124.9 (CH), 123.2 (CH), 122.9 (C), 100.6 (C), 81.3 (C), 60.7 (CH₂), 51.8 (CH), 28.3 (CH₃, CH₂), 26.6 (CH₂), 15.4 (CH₃), 14.3 (CH₃), 10.3 (CH₃), **IR** (ATR): ν_{max} 2968, 2933, 2874, 1703 (C=O), 1651, 1627, 1602, 1572, 1495, 1457, 1404, 1368, 1350, 1328, 1271, 1254, 1235, 1206, 1165, 1097, 1076, 1026, 900, 870, 820, 765; **HRMS** *m/z* calc. for C₂₁H₂₉NNaO₅ [M+Na]: 398.1938; found: 398.1944 (σ = 1.50 ppm); **HPLC** Keto-enol tautomerism led to broad signals in the chromatograms and increased error bars. Accurate ee measurement was attained on the derived acetate (See below for data). Chiralpak AD-H; mobile phase: hexane:2-propanol (99:1 v/v); flow rate: 0.8 mL min⁻¹; retention times: major enantiomer – 4.8 min (79.8%), minor enantiomer – 18.7 min (20.2%), 60% ee; [α]_D²⁰ +173.9 (c = 1.0 in CHCl₃, 60% ee).

1-tert-Butyl 3-ethyl (S)-4-acetoxy-2,6-diethyl-1,2-dihydroquinoline-1,3-dicarboxylate

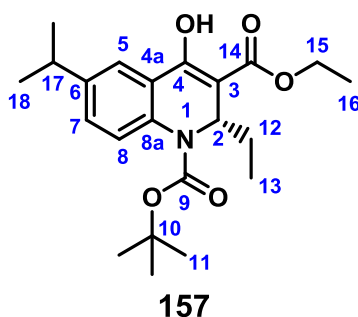


General procedure E was followed using the conjugate addition product **156** to afford the acetylated derivative; **¹H NMR** (400 MHz, CDCl₃): δ_H 7.61 (br s, 1H, C⁸H), 7.22 (dd, *J* = 8.6, 2.1 Hz, 1H, C⁷H), 7.14 (d, *J* = 2.1 Hz, 1H, C⁵H), 5.54 (dd, *J* = 10.0, 4.4 Hz, 1H, C²H), 4.27 (q, *J* = 7.1 Hz, 2H, C¹⁵H₂), 2.65 (q, *J* = 7.6 Hz, 2H, C¹⁹H₂), 2.41 (s, 3H, C¹⁸H₃), 1.62 (ddd, *J* = 14.0, 7.3, 4.4 Hz, 1H), 1.46 (ddd, *J* = 14.0, 10.0, 7.3 Hz, 1H), 1.35 (t, *J* = 7.1 Hz, 3H), 1.26 (t, *J* = 7.6 Hz, 3H), 0.88 (t, *J* = 7.3 Hz, 3H); **HPLC** Chiralpak AD-H; mobile phase: hexane:2-propanol (95:5 v/v); flow rate: 0.5 mL min⁻¹; retention times: major enantiomer – 9.7 min (80.1%), minor enantiomer – 13.7 min (19.9%), 60% ee. Only ¹H NMR data was collected for the compound to confirm structure prior to HPLC analysis.

HPLC chromatograms for racemic and enantioenriched **156** (enol, top traces) and derived acetate (lower traces):



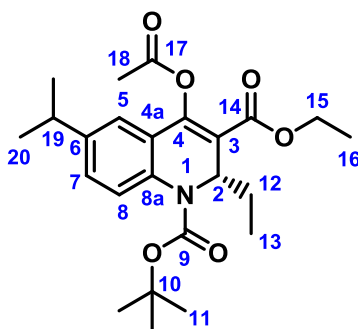
1-tert-Butyl 3-ethyl (S)-2-ethyl-4-hydroxy-6-isopropyl-1,2-dihydroquinoline-1,3-dicarboxylate 157



General procedure D was followed using the protected quinolone carboxylate **143** (49.7 mg, 0.138 mmol) and triethylaluminium (1.3 M in heptane) (0.27 mL, 0.351 mmol) to afford compound **157** as a colourless oil (32.8 mg, 0.084 mmol, 61%); ¹H NMR (500 MHz, CDCl₃): δ_H 12.17 (s, 1H, OH), 7.63 (d, *J* = 2.2 Hz, 1H, C⁵H), 7.49 (br s, 1H, C⁸H), 7.27 (dd, *J* = 8.4, 2.2 Hz, 1H, C⁷H), 5.36 (dd, *J* = 9.8, 4.9 Hz, 1H, C²H), 4.40 – 4.25 (m, 2H, C¹⁵H₂), 2.94 (hept, *J* = 6.9 Hz, 1H, C¹⁷H), 1.54 (s, 9H, 3 × C¹¹H₃) overlapped by

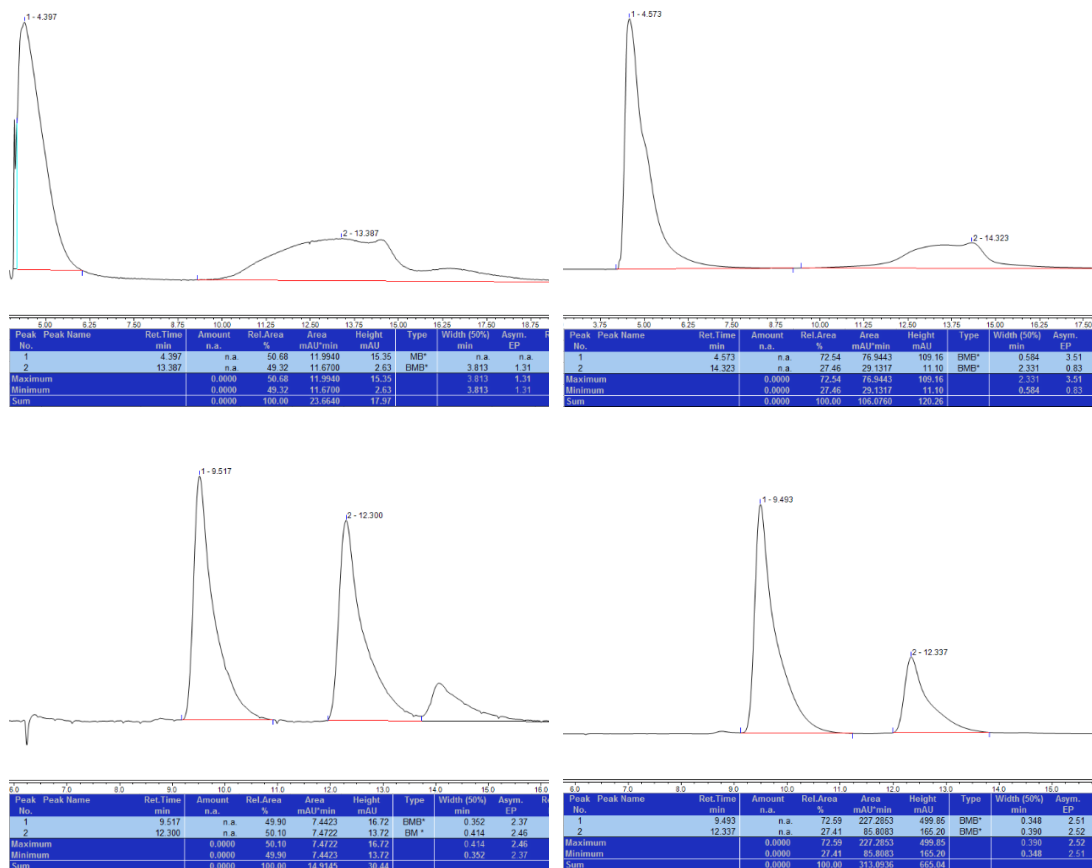
1.55 – 1.46 (m, 1H, C¹²H_AH_B), 1.38 (t, *J* = 7.1 Hz, 3H, C¹⁶H₃) overlapped by 1.44 – 1.34 (m, 1H, C¹²H_AH_B), 1.28 (d, *J* = 6.9 Hz, 6H, 2 × C¹⁸H₃), 0.87 (t, *J* = 7.3 Hz, 3H, C¹³H₃); ¹³C {¹H} NMR (126 MHz, CDCl₃): δ_C 170.6 (C), 162.6 (C), 153.0 (C), 144.4 (C), 135.6 (C), 129.1 (CH), 124.9 (CH), 122.8 (C), 121.8 (CH), 100.6 (C), 81.3 (C), 60.7 (CH₂), 51.8 (CH), 33.6 (CH), 28.3 (CH₃), 26.6 (CH₂), 23.9 (CH₃), 14.3 (CH₃), 10.3 (CH₃); IR (ATR): ν_{max} 2965, 2932, 2873, 1736 (C=O), 1704 (C=O), 1652, 1627, 1602, 1572, 1496, 1457, 1404, 1368, 1352, 1327, 1272, 1254, 1236, 1213, 1163, 1097, 1077, 1026, 900, 818, 764, 669, 463, 408; HRMS *m/z* calc. for C₂₂H₃₁NNaO₅ [M+Na]: 412.2094; found: 412.2098 (σ = 0.90 ppm); HPLC Keto-enol tautomerism led to broad signals in the chromatograms and increased error bars. Accurate ee measurement was attained on the derived acetate (See below for data). Chiralpak AD-H; mobile phase: hexane:2-propanol (99:1 v/v); flow rate: 0.8 mL min⁻¹; retention times: major enantiomer – 4.6 min (72.5%), minor enantiomer – 14.3 min (27.5%), 45% ee; [α]_D²⁰ +146.6 (c = 1.0 in CHCl₃, 45% ee).

1-*tert*-Butyl 3-ethyl (S)-4-acetoxy-2-ethyl-6-isopropyl-1,2-dihydroquinoline-1,3-dicarboxylate

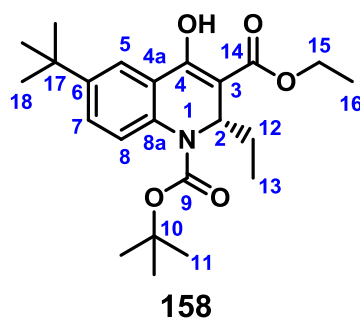


General procedure E was followed using the conjugate addition product **157** to afford the acetylated derivative; ¹H NMR (400 MHz, CDCl₃): δ_H 7.62 (br s, 1H, C⁸H), 7.27 – 7.22 (m, 1H, C⁷H, obscured by solvent peak), 7.16 (d, *J* = 2.1 Hz, 1H, C⁵H), 5.54 (dd, *J* = 10.1, 4.4 Hz, 1H, C²H), 4.27 (q, *J* = 7.1 Hz, 2H, C¹⁵H₂), 2.91 (hept, *J* = 6.9 Hz, 1H, C¹⁹H), 2.41 (s, 3H, C¹⁸H₃), 1.62 (ddd, *J* = 14.0, 7.3, 4.4 Hz, 1H, C¹²H_AH_B), 1.55 (s, 9H, 3 × C¹¹H₃), 1.47 (ddd, *J* = 14.0, 10.1, 7.3 Hz, 1H, C¹²H_AH_B), 1.35 (t, *J* = 7.1 Hz, 3H, C¹⁶H₃), 1.26 (d, *J* = 6.9 Hz, 6H, 2 × C²⁰H₃), 0.88 (d, *J* = 7.3 Hz, 3H, C¹³H₃); HPLC Chiralpak AD-H; mobile phase: hexane:2-propanol (95:5 v/v); flow rate: 0.5 mL min⁻¹; retention times: major enantiomer – 9.5 min (72.6%), minor enantiomer – 12.3 min (27.4%), 45% ee. Only ¹H NMR data was collected for the compound to confirm structure prior to HPLC analysis.

HPLC chromatograms for racemic and enantioenriched **157** (enol, top traces) and derived acetate (lower traces):



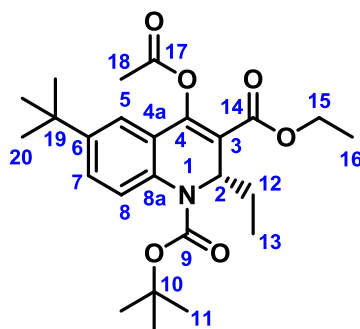
1-tert-Butyl 3-ethyl (S)-6-tert-butyl-2-ethyl-4-hydroxy-1,2-dihydroquinoline-1,3-dicarboxylate **158**



General procedure D was followed using the protected quinolone carboxylate **144** (51.6 mg, 0.138 mmol) and triethylaluminium (1.3 M in heptane) (0.27 mL, 0.351 mmol) to afford compound **158** as a colourless oil (36.3 mg, 0.090 mmol, 65%); $^1\text{H NMR}$ (500 MHz, CDCl_3): δ_{H} 12.20 (s, 1H, OH), 7.78 (d, $J = 2.4$ Hz, 1H, C^5H), 7.56 (br s, 1H, C^8H), 7.43 (dd, $J = 8.7, 2.4$ Hz, 1H, C^7H), 5.36 (dd, $J = 9.7, 4.9$ Hz, 1H, C^2H), 4.39 – 4.25 (m,

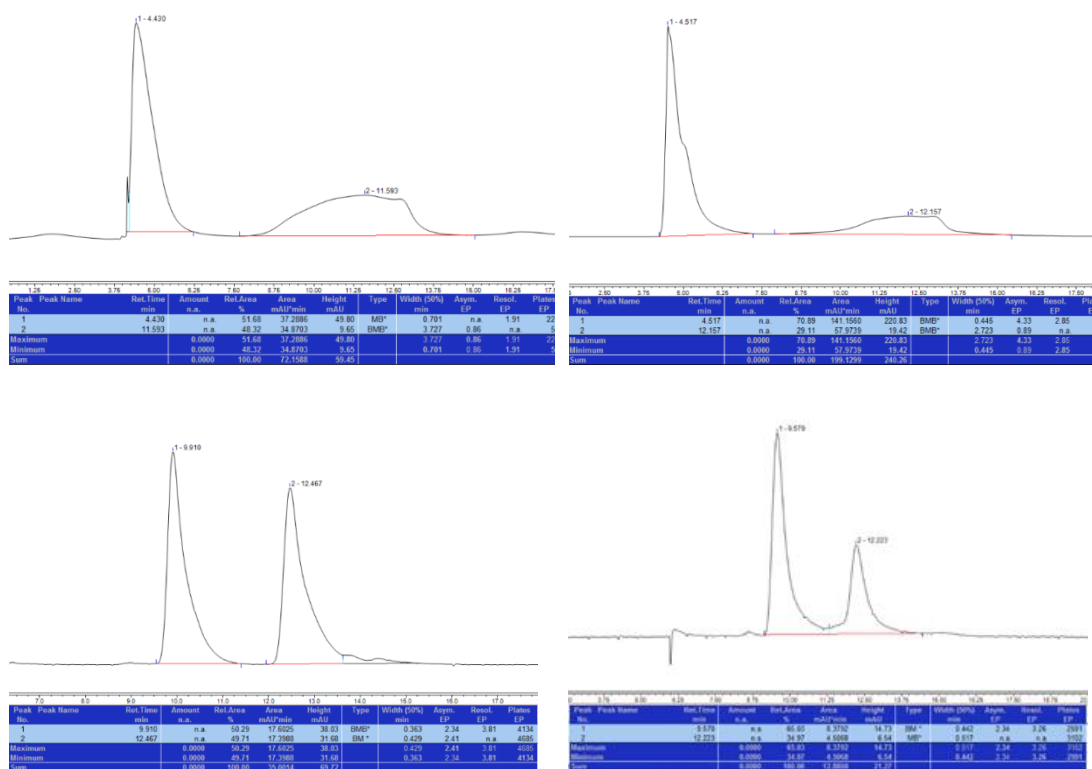
2H, C¹⁵H₂), 1.55 (s, 9H, 3 × C¹¹H₃) overlapped by 1.56 – 1.47 (m, 1H, C¹²H_AH_B), 1.37 (s, 9H, 3 × C¹⁸H₃) overlapped by 1.38 (t, *J* = 7.1 Hz, 3H, C¹⁶H₃) and 1.40 – 1.32 (m, 1H, C¹²H_AH_B), 0.87 (t, *J* = 7.4 Hz, 3H, C¹³H₃); ¹³C {¹H} NMR (101 MHz, CDCl₃): δ_C 170.6 (C), 162.8 (C), 153.0 (C), 146.7 (C), 135.4 (C), 128.1 (CH), 124.5 (CH), 122.5 (C), 120.8 (CH), 100.5 (C), 81.3 (C), 60.7 (CH₂), 51.9 (CH), 34.5 (C), 31.3 (CH₃), 28.3 (CH₃), 26.7 (CH₂), 14.3 (CH₃), 10.3 (CH₃); IR (ATR): ν_{max} 2964, 2931, 2873, 1736 (C=O), 1703 (C=O), 1651, 1627, 1600, 1570, 1497, 1459, 1403, 1382, 1366, 1350, 1329, 1274, 1253, 1158, 1122, 1093, 1074, 1026, 902, 820, 764, 693, 464; HRMS *m/z* calc. for C₂₃H₃₃NNaO₅ [M+Na]: 426.2251; found: 426.2253 (σ = 0.50 ppm); HPLC Keto-enol tautomerism led to broad signals in the chromatograms and increased error bars. Accurate ee measurement was attained on the derived acetate (See below for data). Chiralpak AD-H; mobile phase: hexane:2-propanol (99:1 v/v); flow rate: 0.8 mL min⁻¹; retention times: major enantiomer – 4.5 min (70.9%), minor enantiomer – 12.2 min (29.1%), 42% ee; [α]_D²⁰ +120.2 (*c* = 1.0 in CHCl₃, 42% ee).

1-*tert*-Butyl 3-ethyl (S)-4-acetoxy-6-*tert*-butyl-2-ethyl-1,2-dihydroquinoline-1,3-dicarboxylate

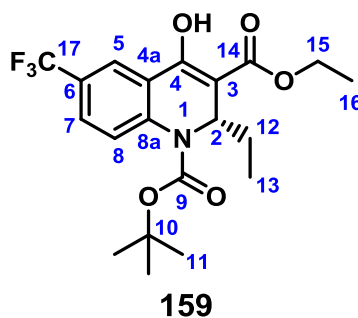


General procedure E was followed using the conjugate addition product **158** to afford the acetylated derivative; ¹H NMR (400 MHz, CDCl₃): δ_H 7.63 (br s, 1H, C⁸H), 7.41 (dd, *J* = 8.6, 2.4 Hz, 1H, C⁷H), 7.32 (d, *J* = 2.4 Hz, 1H, C⁵H), 5.54 (dd, *J* = 10.2, 4.3 Hz, 1H, C²H), 4.26 (q, *J* = 7.1, 2H, C¹⁵H₂), 2.40 (s, 3H, C¹⁸H₃), 1.55 (s, 9H, 3 × C¹¹H₃) overlapped by 1.63 – 1.47 (m, 2H, C¹²H₂), 1.35 (t, *J* = 7.1 Hz, C¹⁶H₃) overlapped by 1.32 (s, 9H, 3 × C²⁰H₃), 0.88 (t, *J* = 7.4 Hz, 3H, C¹³H₃).; HPLC Chiralpak AD-H; mobile phase: hexane:2-propanol (95:5 v/v); flow rate: 0.5 mL min⁻¹; retention times: major enantiomer – 9.6 min (65.0%), minor enantiomer – 12.2 min (35.0%), 30% ee. Only ¹H NMR data was collected for the compound to confirm structure prior to HPLC analysis.

HPLC chromatograms for racemic and enantioenriched **158** (enol, top traces) and derived acetate (lower traces):



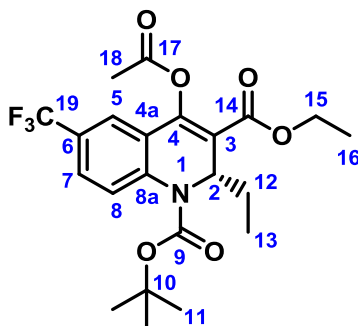
1-*tert*-Butyl 3-ethyl (S)-2-ethyl-4-hydroxy-6-trifluoromethyl-1,2-dihydroquinoline-1,3-dicarboxylate **159**



General procedure D was followed using the protected quinolone carboxylate **145** (53.3 mg, 0.138 mmol) and triethylaluminium (1.3 M in heptane) (0.27 mL, 0.351 mmol) to afford compound **159** as a colourless oil (40.8 mg, 0.098 mmol, 71%); ¹H NMR (500 MHz, CDCl₃): δ_H 12.10 (s, 1H, OH), 8.03 (d, *J* = 2.2 Hz, 1H, C⁵H), 7.78 (br d, *J* = 8.6 Hz, 1H, C⁸H), 7.63 (dd, *J* = 8.6, 2.2 Hz, 1H, C⁷H), 5.41 (dd, *J* = 9.6, 4.9 Hz, 1H, C²H), 4.41 – 4.28 (m, 2H, C¹⁵H₂), 1.56 (s, 9H, 3 × CH¹¹H₃) overlapped by 1.58 – 1.48 (m, 1H, C¹²H_AH_B), 1.39 (t, *J* = 7.1 Hz, 3H, C¹⁶H₃) overlapped by 1.42 – 1.36 (m, 1H, C¹²H_AH_B),

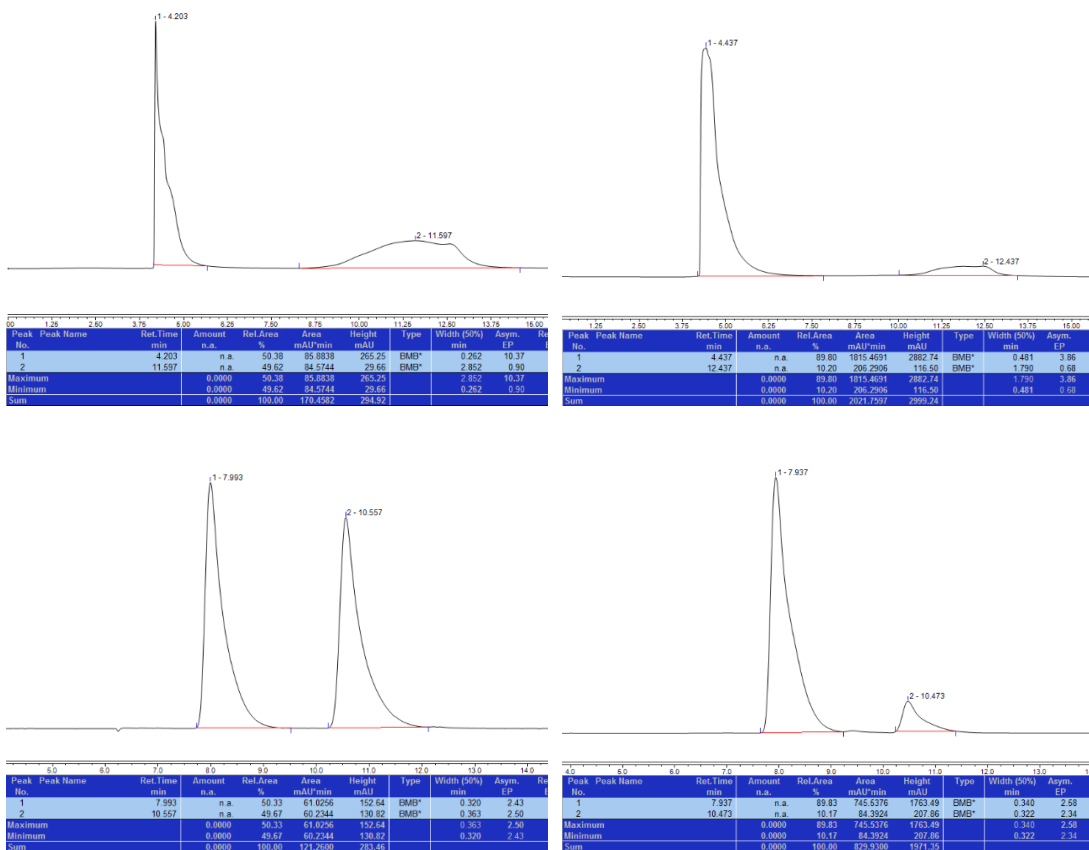
0.87 (t, $J = 7.4$ Hz, 3H, $C^{13}H_3$); ^{13}C { 1H } NMR (126 MHz, $CDCl_3$): δ_C 170.2 (C), 160.7 (C), 152.5 (C), 140.8 (C), 127.3 (q, $J = 3.6$ Hz, CH), 125.8 (q, $J = 32.8$ Hz, C), 125.1 (CH), 123.9 (q, $J = 271.9$ Hz), 123.2 (C), 121.65 (q, $J = 4.1$ Hz, CH), 101.5 (C), 82.3 (C), 61.1 (CH_2), 52.1 (CH), 28.2 (CH_3), 27.1 (CH_2), 14.2 (CH_3), 10.2 (CH_3); ^{19}F NMR (471 MHz, $CDCl_3$): δ_F -62.39 (3F); IR (ATR): ν_{max} 2972, 2934, 2877, 2858, 1714 (C=O), 1657, 1633, 1458, 1434, 1407, 1369, 1327, 1301, 1274, 1252, 1163, 1126, 1111, 1100, 1079, 1025, 909, 836, 765, 544; HRMS m/z calc. for $C_{20}H_{25}F_3NO_5$ [M+H]: 438.1499; found: 438.1505 ($\sigma = 1.30$ ppm); HPLC Keto-enol tautomerism led to broad signals in the chromatograms and increased error bars. Accurate ee measurement was attained on the derived acetate (See below for data). Chiralpak AD-H; mobile phase: hexane:2-propanol (99:1 v/v); flow rate: 0.8 mL min^{-1} ; retention times: major enantiomer – 4.4 min (89.8%), minor enantiomer – 12.4 min (10.2%), 80% ee; $[\alpha]_D^{20}$ +209.6 ($c = 1.0$ in $CHCl_3$, 80% ee).

1-*tert*-Butyl 3-ethyl (S)-4-acetoxy-2-ethyl-6-trifluoromethyl-1,2-dihydroquinoline-1,3-dicarboxylate

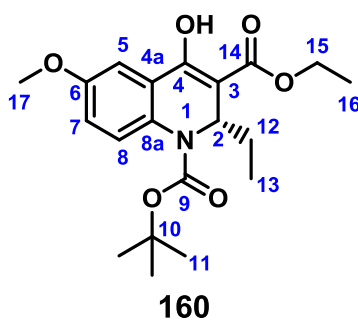


General procedure E was followed using the conjugate addition product **159** to the acetylated derivative; 1H NMR (400 MHz, $CDCl_3$): δ_H 7.87 (br d, $J = 8.6$ Hz, 1H, C^8H), 7.66 – 7.57 (m, 2H, C^5H , C^7H), 5.59 (dd, $J = 9.9, 4.4$ Hz, 1H, C^2H), 4.29 (q, $J = 7.1$ Hz, 1H, $C^{15}H_2$), 2.42 (s, 3H, $C^{18}H_3$), 1.66 (ddd, $J = 14.1, 7.4, 4.4$ Hz, 1H, $C^{12}H_AH_B$), 1.46 (ddd, $J = 14.1, 9.9, 7.4$ Hz, 1H, $C^{12}H_AH_B$), 1.36 (t, $J = 7.1$ Hz, 3H, $C^{16}H_3$), 0.89 (t, $J = 7.4$ Hz, 3H, $C^{13}H_3$); HPLC Chiralpak AD-H; mobile phase: hexane:2-propanol (95:5 v/v); flow rate: 0.5 mL min^{-1} ; retention times: major enantiomer – 7.9 min (89.8%), minor enantiomer – 10.5 min (10.2%), 80% ee. Only 1H NMR data was collected for the compound to confirm structure prior to HPLC analysis.

HPLC chromatograms for racemic and enantioenriched **159** (enol, top traces) and derived acetate (lower traces):



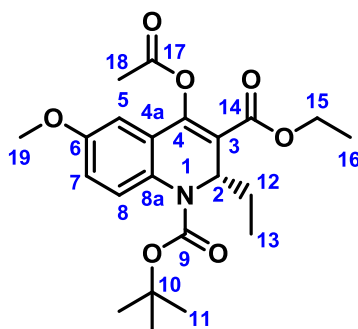
1-*tert*-Butyl 3-ethyl (S)-2-ethyl-4-hydroxy-6-methoxy-1,2-dihydroquinoline-1,3-dicarboxylate **160**



General procedure D was followed using the protected quinolone carboxylate **146** (48.0 mg, 0.138 mmol) and triethylaluminium (1.3 M in heptane) (0.27 mL, 0.351 mmol) to afford compound **160** as a colourless oil (24.5 mg, 0.065 mmol, 47%); ¹H NMR (400 MHz, CDCl₃): δ_H 12.16 (s, 1H, OH), 7.47 (br s, 1H, C⁸H), 7.28 (d, *J* = 3.0 Hz, 1H, C⁵H), 6.97 (dd, *J* = 9.0, 3.0 Hz, 1H, C⁷H), 5.36 (app br s, 1H, C²H), 4.41 – 4.26 (m, 2H, C¹⁵H₂), 3.86 (s, 3H, C¹⁷H₃), 1.53 (s, 9H, 3 × C¹¹H₃) overlapped by 1.57 – 1.45 (m, 1H, C¹²H_AH_B), 1.38 (t, *J* = 7.1 Hz, 3H, C¹⁶H₃) overlapped by 1.41 – 1.34 (m, 1H, C¹²H_AH_B), 0.87 (t, *J* = 7.4 Hz, 3H, C¹³H₃); ¹³C {¹H} NMR (101 MHz, CDCl₃): δ_C 170.6 (C), 162.1

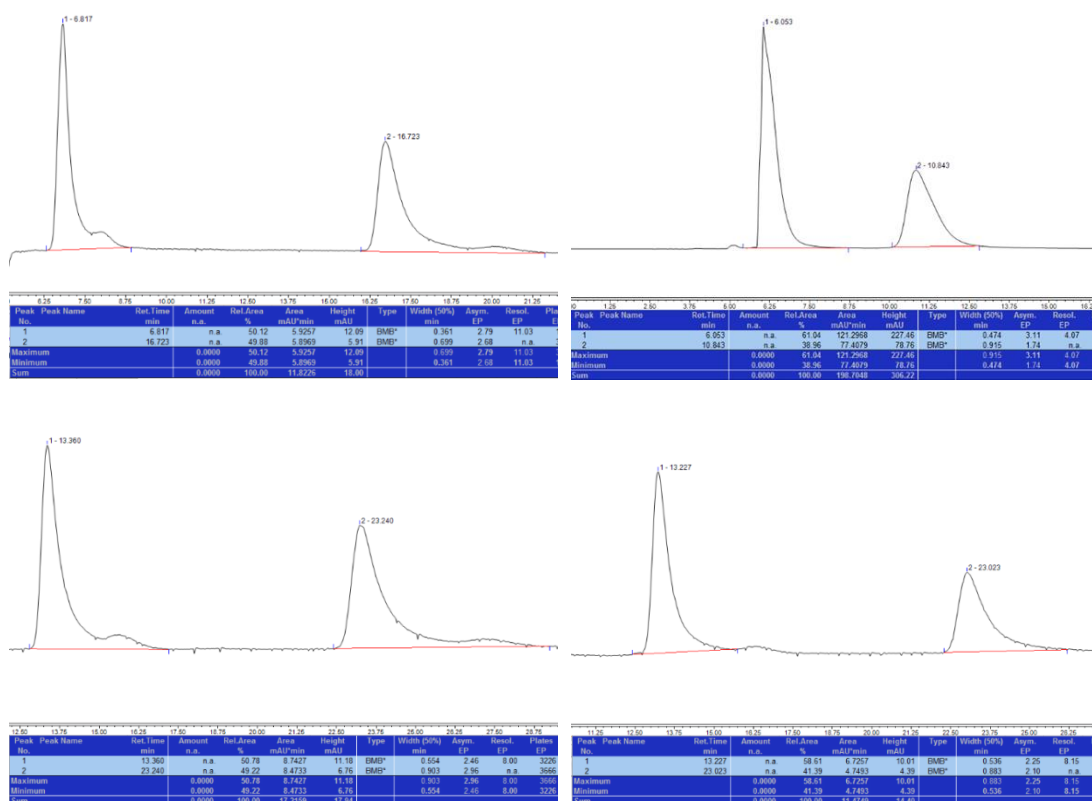
(C), 156.0 (C), 153.1 (C), 131.1 (C), 126.4 (CH), 124.0 (C), 117.8 (CH), 107.4 (CH), 101.3 (C), 81.2 (C), 60.8 (CH₂), 55.6 (CH₃), 51.8 (CH), 29.7 (CH₂), 28.3 (CH₃), 14.3 (CH₃), 10.3 (CH₃); **IR** (ATR): ν_{max} 2969, 2929, 2873, 2854, 1737 (C=O), 1702 (C=O), 1653, 1602, 1574, 1496, 1457, 1403, 1368, 1351, 1332, 1271, 1239, 1166, 1148, 1092, 1033, 818, 458, 409; **HRMS** m/z calc. for C₂₀H₂₇NNaO₆ [M+Na]: 400.1731; found: 400.1734 (σ = 0.80 ppm); **HPLC** Keto-enol tautomerism led to broad signals in the chromatograms and increased error bars. Accurate ee measurement was attained on the derived acetate (See below for data). Chiralpak AD-H; mobile phase: hexane:2-propanol (98:2 v/v); flow rate: 0.8 mL min⁻¹; retention times: major enantiomer – 6.9 min (61.0%), minor enantiomer – 10.8 min (39.0%), 22% ee; $[\alpha]_{\text{D}}^{20}$ +17.8 (c = 1.0 in CHCl₃, 22% ee).

1-tert-Butyl 3-ethyl (S)-4-acetoxy-2-ethyl-6-methoxy-1,2-dihydroquinoline-1,3-dicarboxylate

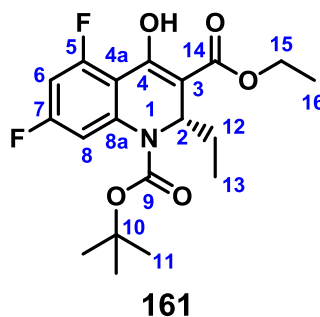


General procedure E was followed using the conjugate addition product **160** to the acetylated derivative; **¹H NMR** (400 MHz, CDCl₃): δ_{H} 7.64 (br s, 1H, C⁸H), 6.94 (dd, J = 8.9, 2.9 Hz, 1H, C⁷H), 6.86 (d, J = 2.9 Hz, 1H, C⁵H), 5.53 (app d, J = 8.9 Hz, 1H, C²H), 4.27 (q, J = 7.1 Hz, 2H, C¹⁵H₂), 3.83 (s, 3H, C¹⁹H₃), 2.39 (s, 3H, C¹⁸H₃), 1.54 (s, 9H, 3 x C¹¹H₃) overlapped by 1.57 – 1.45 (m, 2H, C¹²H₂), 1.36 (t, J = 7.2 Hz, 3H), 0.89 (t, J = 7.1 Hz, 3H); **HPLC** Chiralpak AD-H; mobile phase: hexane:2-propanol (95:5 v/v); flow rate: 0.5 mL min⁻¹; retention times: major enantiomer – 12.2 min (58.6%), minor enantiomer – 23.0 min (41.4%), 17% ee. Only ¹H NMR data was collected for the compound to confirm structure prior to HPLC analysis.

HPLC chromatograms for racemic and enantioenriched **160** (enol, top traces) and derived acetate (lower traces):



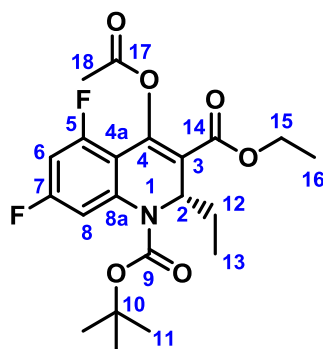
1-*tert*-Butyl 3-ethyl (S)-2-ethyl-5,7-difluoro-4-hydroxy-1,2-dihydroquinoline-1,3-dicarboxylate 161



General procedure D was followed using the protected quinolone carboxylate **147** (48.8 mg, 0.138 mmol) and triethylaluminium (1.3 M in heptane) (0.27 mL, 0.351 mmol) to afford compound **161** as a colourless oil (40.8 mg, 0.106 mmol, 77%); ¹H NMR (500 MHz, CDCl₃): δ_H 12.39 (s, 1H, OH), 7.28 (br d, *J* = 4.8 Hz, 1H, C⁸H), 6.65 (ddd, *J* = 11.2, 8.8, 2.5 Hz, 1H, C⁶H), 5.36 (dd, *J* = 9.5, 5.3 Hz, 1H, C²H), 4.40 – 4.27 (m, 2H, C¹⁵H₂), 1.55 (s, 9H, 3 × C¹¹H₃) overlapped by 1.57 – 1.46 (m, 1H, C¹²H_AH_B), 1.37 (t, *J* = 7.1 Hz, C¹⁶H₃) overlapped by 1.44 – 1.34 (m, 1H, C¹²H_AH_B), 0.86 (t, *J* = 7.4 Hz, 3H); ¹³C {¹H} NMR (126 MHz, CDCl₃): δ_C 170.2 (C), 163.7 (dd, *J* = 251.3, 14.7 Hz, C), 161.2 (C), 160.5 (dd, *J* = 260.2, 14.9 Hz, C), 152.2 (C), 141.0 (dd, *J* = 13.7, 6.4 Hz, C),

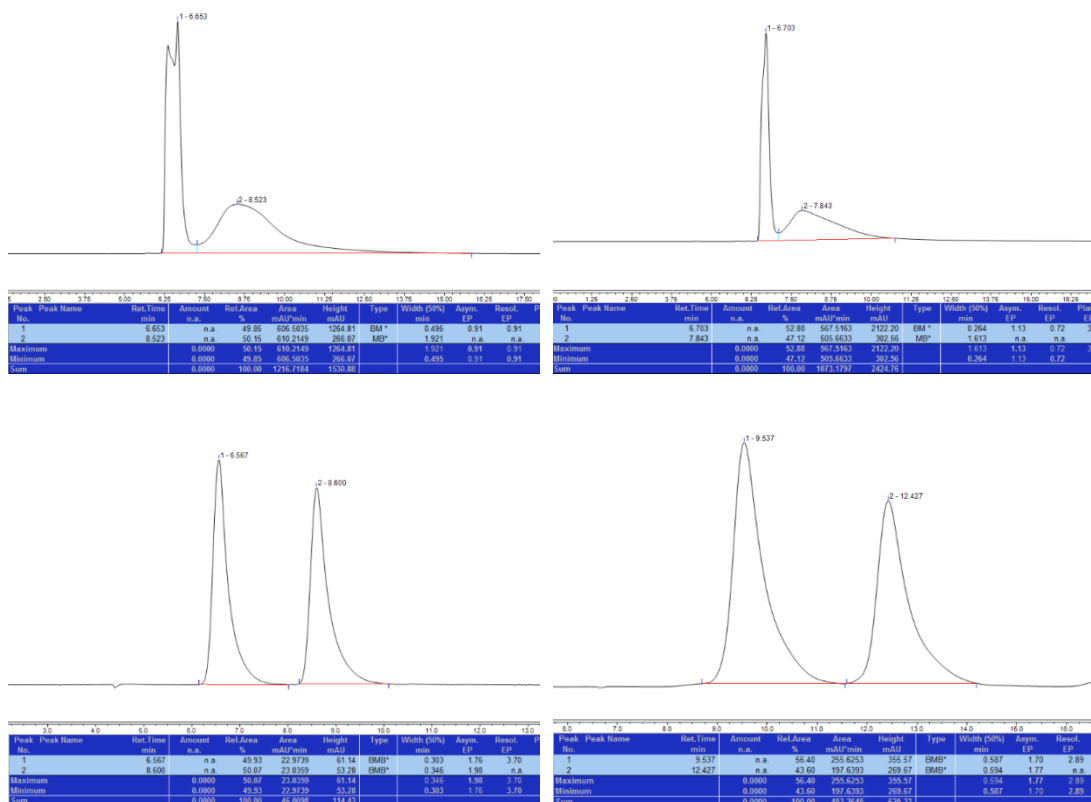
108.7(1) (app d, $J = 3.7$ Hz, C) overlapped by 108.7(0) (dd, $J = 26.0, 3.8$ Hz, CH), 100.8 (app t, $J = 26.2$ Hz, CH), 100.7 (C), 82.4 (C), 61.0 (CH₂), 52.0 (CH), 28.2 (CH₃), 26.3 (CH₂), 14.2 (CH₃), 10.2 (CH₃); ¹⁹F NMR (471 MHz, CDCl₃) δ_F -105.01 (1F), -107.69 (1F); IR (ATR): ν_{max} 2972, 2933, 2877, 2859, 1714 (C=O), 1653, 1628, 1580, 1448, 1410, 1370, 1311, 1281, 1255, 1151, 1121, 1024, 1008, 915, 852, 827, 764, 554, 528; HRMS ^{m/z} calc. for C₁₉H₂₃F₂NNaO₅ [M+Na]: 406.1436; found: 406.1435 (σ = 0.30 ppm); HPLC Keto-enol tautomerism led to broad signals in the chromatograms and increased error bars. Accurate ee measurement was attained on the derived acetate (See below for data). Chiralpak AD-H; mobile phase: hexane:2-propanol (99.5:0.5 v/v); flow rate: 0.8 mL min⁻¹; retention times: major enantiomer – 6.7 min (52.9%), minor enantiomer – 7.8 min (47.1%), 6% ee; [α]_D²⁰ +26.3 (c = 1.0 in CHCl₃, 6% ee).

1-tert-Butyl 3-ethyl (S)-4-acetoxy-2-ethyl-5,7-difluoro-1,2-dihydroquinoline-1,3-dicarboxylate

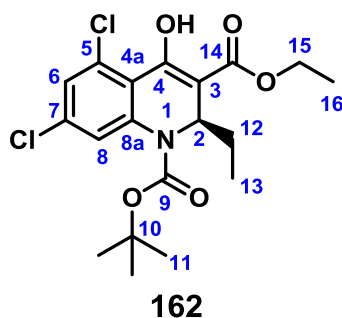


General procedure E was followed using the conjugate addition product **161** to afford the acetylated derivative; ¹H NMR (400 MHz, CDCl₃): δ_H 7.36 (br d, $J = 9.6$ Hz, 1H, C⁸H), 6.59 (ddd, $J = 11.9, 8.7, 2.5$ Hz, 1H, C⁶H), 5.54 (dd, $J = 9.9, 4.7$ Hz, 1H, C²H), 4.27 (q, $J = 7.1$ Hz, 2H, C¹⁵H₂), 2.31 (s, 3H, C¹⁸H₃), 1.66 (ddd, $J = 14.3, 7.2, 4.6$ Hz, 1H, C¹²H_AH_B), 1.57 (s, 9H, 3 × C¹³H₃), 1.49 (ddd, $J = 14.3, 9.9, 7.2$ Hz, 1H, C¹²H_AH_B), 1.35 (t, $J = 7.1$ Hz, 3H, C¹⁶H₃), 0.88 (t, $J = 7.2$ Hz, 3H, C¹³H₃); HPLC Chiralpak AD-H; mobile phase: hexane:2-propanol (98:2 v/v); flow rate: 0.5 mL min⁻¹; retention times: major enantiomer – 9.5 min (56.4%), minor enantiomer – 12.4 min (43.6%), 13% ee. Only ¹H NMR data was collected for the compound to confirm structure prior to HPLC analysis.

HPLC chromatograms for racemic and enantioenriched **161** (enol, top traces) and derived acetate (lower traces):

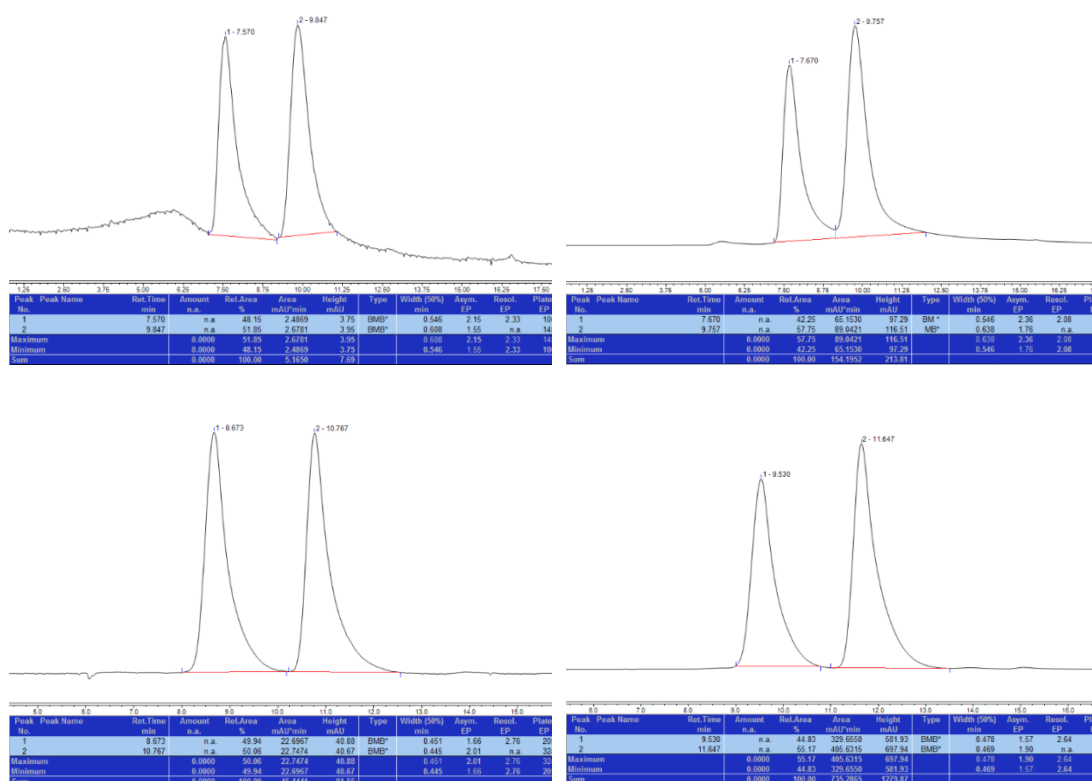


1-tert-Butyl 3-ethyl (R)-5,7-dichloro-2-ethyl-4-hydroxy-1,2-dihydroquinoline-1,3-dicarboxylate **162**

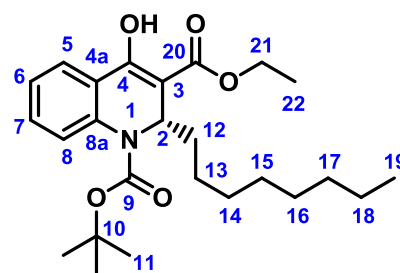


General procedure D was followed using the protected quinolone carboxylate **148** (53.4 mg, 0.138 mmol) and triethylaluminium (1.3 M in heptane) (0.27 mL, 0.351 mmol) to afford compound **162** as a colourless oil (42.6 mg, 0.102 mmol, 74%); ¹H NMR (500 MHz, CDCl₃): δ_H 12.61 (s, 1H, OH), 7.58 (br s, 1H, C⁸H), 7.23 (d, *J* = 2.0 Hz, 1H, C⁶H), 5.34 (dd, *J* = 9.8, 5.3 Hz, 1H, C²H) overlapped by occluded CH₂Cl₂ at 5.32 (s), 4.41 – 4.27 (m, 2H, C¹⁵H₂), 1.54 (s, 9H, 3 × C¹¹H₃) overlapped by 1.54 – 1.44 (m, 1H, C¹²H_AH_B), 1.38 (t, *J* = 7.1 Hz, 3H, C¹⁶H₃) overlapped by 1.41 – 1.31 (m, 1H, C¹²H_AH_B),

HPLC chromatograms for racemic and enantioenriched **162** (enol, top traces) and derived acetate (lower traces):



1-tert-Butyl 3-ethyl (S)-4-hydroxy-2-octyl-1,2-dihydroquinoline-1,3-dicarboxylate
165

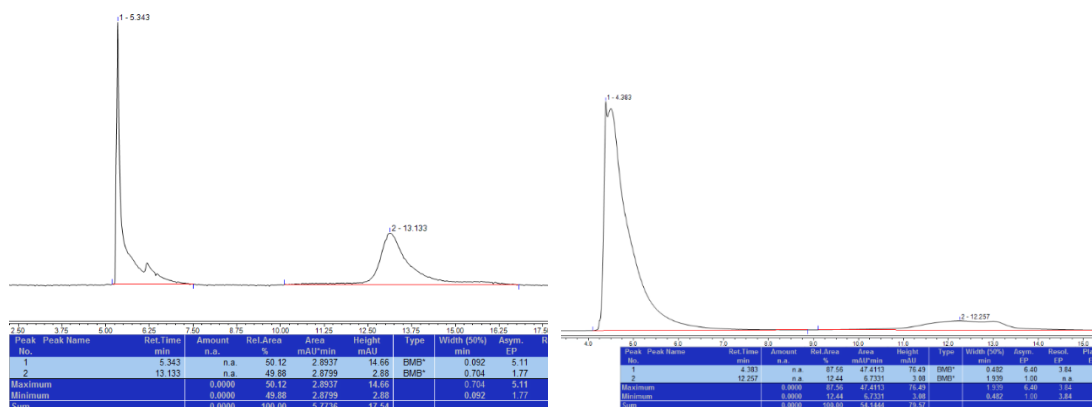


165

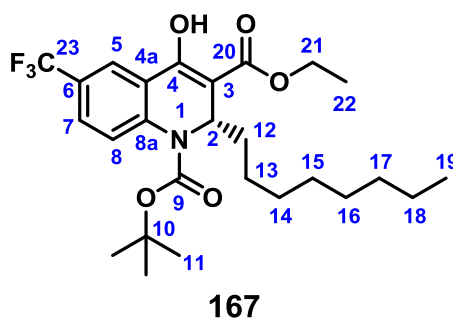
General procedure D was followed using the protected quinolone carboxylate **117** (73.6 mg, 0.232 mmol) and trioctylaluminium (0.478 M in hexanes) (1.2 mL, 0.574 mmol) to afford compound **165** as a colourless oil (63.8 mg, 0.148 mmol, 64%); ¹H NMR (400 MHz, CDCl₃): δ_H 12.08 (s, 1H, OH), 7.78 (dd, *J* = 7.7, 1.6 Hz, 1H, C⁵H), 7.61 (br s, 1H), 7.40 (ddd, *J* = 8.4, 7.5, 1.6 Hz, 1H, C⁷H), 7.18 (ddd, *J* = 7.7, 7.5, 1.1 Hz, 1H), 5.45 (t, *J* = 7.0 Hz, 1H), 4.42 – 4.25 (m, 2H), 1.54 (s, 9H), 1.38 (t, *J* = 7.1 Hz, 3H) overlapped by 1.44 – 1.14 (m, 14H), 0.89 (t, *J* = 6.7 Hz, 3H); ¹³C {¹H} NMR (101 MHz,

CDCl₃): δ_c 170.4 (C), 162.2 (C), 152.8 (C), 137.9 (C), 130.7 (CH), 125.2 (CH), 124.2 (CH), 123.9 (CH), 123.2 (C), 110.7 (C), 81.4 (C), 60.7 (CH₂), 50.4 (CH), 33.4 (CH₂), 31.9 (CH₂), 29.5 (CH₂), 29.2 (CH₂), 29.1 (CH₂), 28.3 (CH₃), 25.5 (CH₂), 22.7 (CH₂), 14.3 (CH₃), 14.1 (CH₃); **IR** (ATR): ν_{max} 2974, 2927, 2855, 1702 (C=O), 1651, 1623, 1568, 1487, 1455, 1402, 1367, 1350, 1327, 1273, 1234, 1143, 1091, 1022, 948, 853, 811, 763, 669, 601, 520, 458; **HRMS** *m/z* calc. for C₂₅H₃₇NNaO₅ [M+Na]: 454.2564; found: 454.2578 (σ = 3.30 ppm); **HPLC** Chiralpak AD-H; mobile phase: hexane:2-propanol (99:1 v/v); flow rate: 0.8 mL min⁻¹; retention times: major enantiomer – 4.4 min (87.6%), minor enantiomer – 12.3 min (12.4%), 75% ee; [α]_D²⁰ +216.0 (c = 1.0 in CHCl₃, 75% ee).

HPLC chromatograms for racemic **165** (left) and enantioenriched **165** (right):



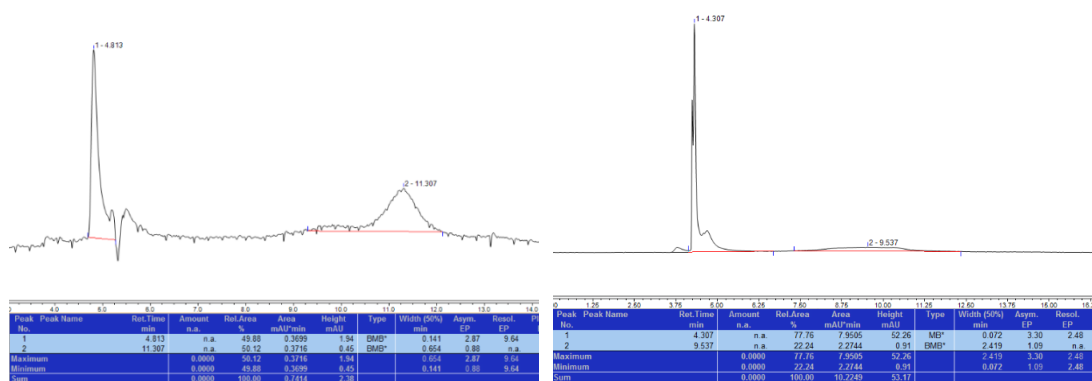
1-*tert*-Butyl 3-ethyl (*S*)-4-hydroxy-2-octyl-6-trifluoromethyl-1,2-dihydroquinoline-1,3-dicarboxylate **167**



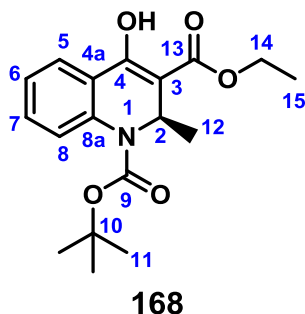
General procedure D was followed using the protected quinolone carboxylate **145** (77.5 mg, 0.200 mmol) and trioctylaluminium (0.478 M in hexanes) (1 mL, 0.478 mmol) to afford compound **167** as a colourless oil (72.3 mg, 0.145 mmol, 72%); ¹H NMR (400 MHz, CDCl₃): δ_H 12.06 (s, 1H, OH), 8.05 (d, *J* = 2.2 Hz, 1H, C⁵H), 7.77 (d, *J* = 7.5 Hz, 1H, C⁸H), 7.63 (dd, *J* = 8.8, 2.2 Hz, 1H, C⁷H), 5.48 (dd, *J* = 9.0, 5.1 Hz, 1H, C²H), 4.44

– 4.26 (2 × dq, $J = 12.1$ Hz, 7.1 Hz, 2H, C²¹H₂), 1.56 (s, 9H, 3 × C¹¹H₃), 1.43 – 1.36 (m, 5H, C¹²H₂, C²²H₃), 1.30 – 1.23 (m, 12H, C¹³H₂, C¹⁴H₂, C¹⁵H₂, C¹⁶H₂, C¹⁷H₂, C¹⁸H₂), 0.89 (t, $J = 6.7$ Hz, 3H, C¹⁹H₃); ¹³C {¹H} NMR (101 MHz, CDCl₃): δ_C 170.1 (C), 160.6 (C), 152.4 (C), 140.8 (C), 127.2 (q, $J = 3.7$ Hz, CH), 125.9 (q, $J = 32.9$ Hz, C), 125.3 (CH), 123.9 (q, $J = 271.7$ Hz, C), 123.3 (C), 121.6 (q, $J = 4.3$ Hz, CH), 101.8 (C), 82.3 (C), 61.1 (CH₂), 50.7 (CH), 33.8 (CH₂), 31.9 (CH₂), 29.5 (CH₂), 29.2 (CH₂), 29.1 (CH₂), 28.2 (CH₃), 25.5 (CH₂), 22.6 (CH₂), 14.2 (CH₃), 14.1 (CH₃); ¹⁹F NMR (376 MHz, CDCl₃): δ_F -62.4 (3F); IR (ATR): ν_{max} 2957, 2927, 2855, 1707 (C=O), 1653, 1630, 1569, 1456, 1433, 1404, 1382, 1368, 1325, 1272, 1238, 1147, 1097, 1022, 911, 811, 764, 677, 617, 541, 457; HRMS *m/z* calc. for C₂₆H₃₇F₃NO₅ [M+H]: 500.2610; found: 500.2618 (σ = 1.70 ppm); HPLC Chiralpak AD-H; mobile phase: hexane:2-propanol (99:1 v/v); flow rate: 0.8 mL min⁻¹; retention times: major enantiomer – 4.3 min (77.8%), minor enantiomer – 9.5 min (22.2%), 55% ee; [α]_D²⁰ +147.4 (c = 1.0 in CHCl₃, 55% ee).

HPLC chromatograms for racemic **167** (left) and enantioenriched **167** (right):

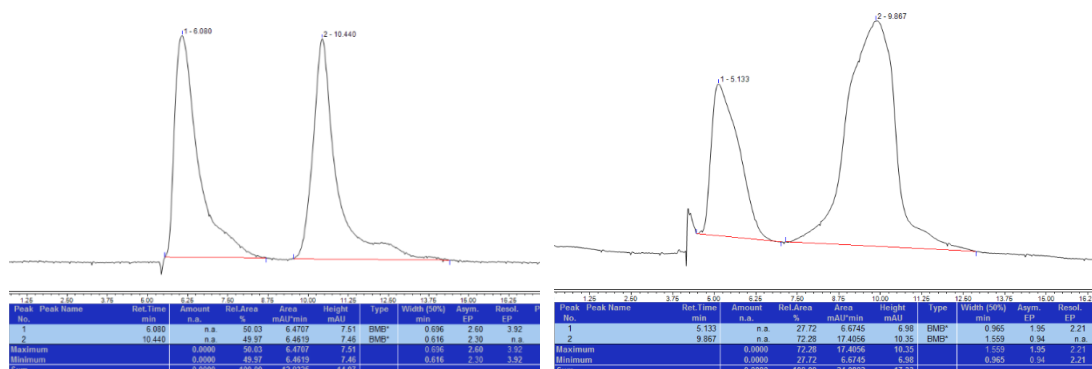


1-tert-Butyl 3-ethyl (R)-4-hydroxy-2-methyl-1,2-dihydroquinoline-1,3-dicarboxylate 168

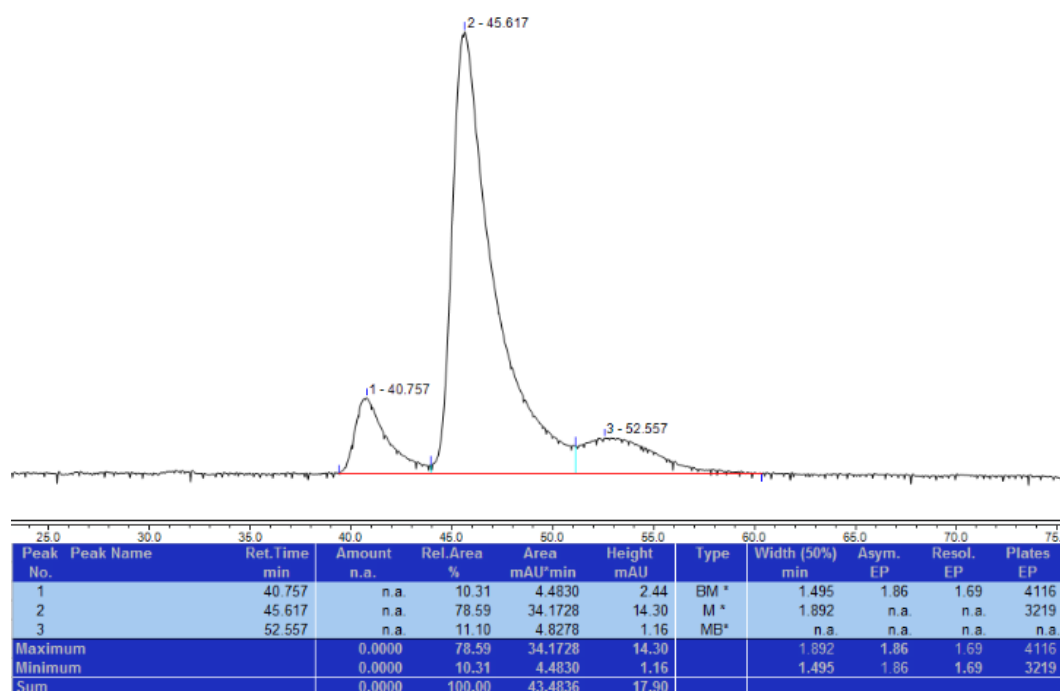


General procedure D was followed using the protected quinolone carboxylate **117** (190 mg, 0.600 mmol) and trimethylaluminium (2.0 M in hexanes) (0.75 mL, 1.50 mmol) to afford compound **168** as a colourless oil (122 mg, 0.366 mmol, 61%); ¹H NMR (400 MHz, CDCl₃): δ_H 12.09 (s, 1H, OH), 7.79 (dd, *J* = 7.7, 1.7 Hz, 1H, C⁵H), 7.61 (d, *J* = 8.3 Hz, 1H, C⁸H), 7.40 (ddd, *J* = 8.3, 7.4, 1.7 Hz, 1H, C⁷H), 7.18 (ddd, *J* = 7.7, 1.1 Hz, 1H, C⁶H), 5.55 (q, *J* = 6.6 Hz, 1H, C²H), 4.41 – 4.26 (m, 2H, C¹⁴H₂), 1.55 (s, 9H, 3 × C¹¹H₃), 1.38 (t, *J* = 7.1 Hz, 3H, C¹⁵H₃), 1.14 (d, *J* = 6.6 Hz, 3H, C¹²H₃); ¹³C {¹H} NMR (101 MHz, CDCl₃): δ_C 161.9 (C), 154.4 (C), 152.4 (C), 138.1 (C), 137.7 (C), 130.8 (CH), 124.7 (CH), 124.2 (CH), 123.7 (CH), 122.6 (C), 81.6 (C), 60.8 (CH₂), 47.0 (CH), 28.3 (CH₃), 19.2 (CH₃), 14.3 (CH₃); IR (ATR): ν_{max} 2976, 2928, 2870, 1698 (C=O), 1652, 1619, 1600, 1573, 1487, 1447, 1382, 1367, 1321, 1272, 1232, 1144, 1092, 1050, 1020, 948, 922, 851, 803, 753, 701, 667, 590, 492, 457; HRMS *m/z* calc. for C₁₈H₂₄NO₅ [M+H]: 334.1639; found: 334.1649 (σ = 3.00 ppm); HPLC Chiralpak AD-H; mobile phase: hexane:2-propanol (99:1 v/v); flow rate: 0.8 mL min⁻¹; retention times: major enantiomer – 9.9 min (72.3%), minor enantiomer – 5.1 min (27.7%), 45% ee; [α]_D²⁰ – 32.0 (*c* = 1.0 in CHCl₃, 45% ee).

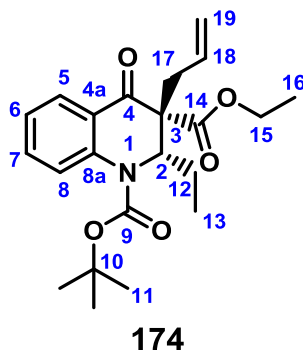
HPLC chromatograms for racemic **168** (left) and enantioenriched **168** (right):



HPLC chromatogram for **172**:



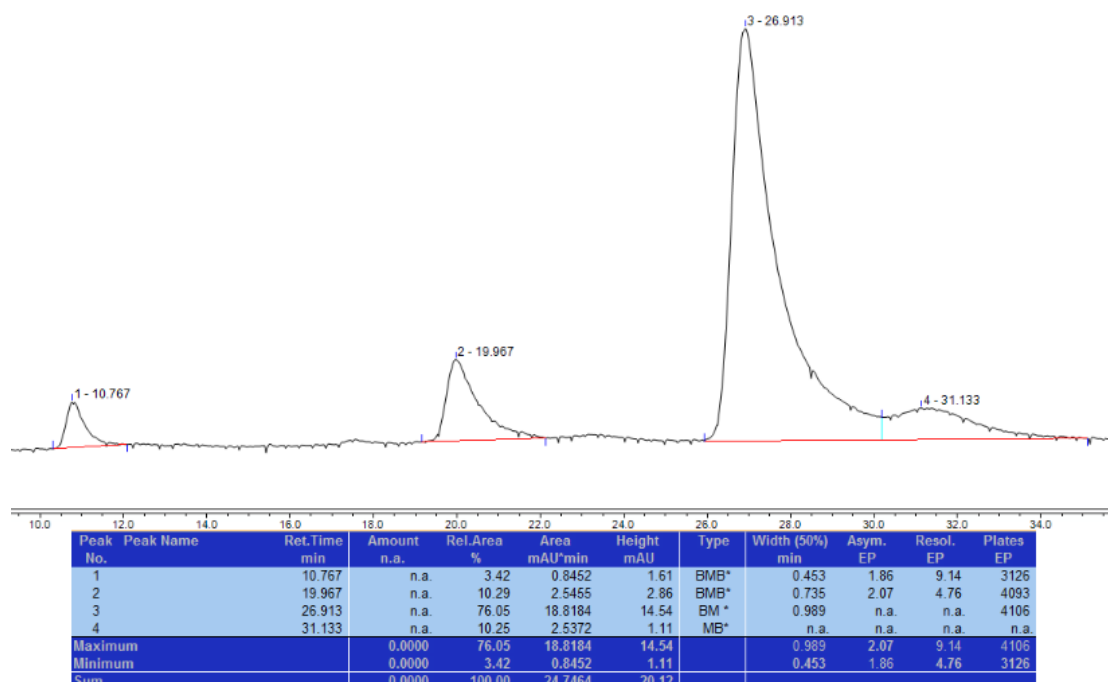
1-tert-Butyl 3-ethyl (S,R)-3-allyl-2-ethyl-2,3-dihydro-4(1H)-quinolone-1,3-dicarboxylate 174



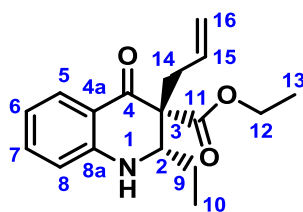
To a stirred solution of compound **121** (224 mg, 0.645 mmol) in CH_2Cl_2 (4.3 mL, 0.15 M solution) at $-78\text{ }^\circ\text{C}$ was added potassium hydroxide (145 mg, 2.58 mmol), tetrabutylammonium iodide (24 mg, 0.065 mmol) and allyl bromide (112 μL , 1.29 mmol). The reaction vessel was shielded from light to prevent decomposition of the tetrabutylammonium iodide and the suspension was allowed to warm slowly to r.t. whilst stirring over 18 h. The reaction mixture was partitioned between CH_2Cl_2 (10 mL) and H_2O (5 mL). The phases were separated and the aqueous phase was extracted with CH_2Cl_2 (3 \times 10 mL). The combined organic phases were dried (MgSO_4), concentrated *in vacuo* and purified by column chromatography (silica, CH_2Cl_2) to afford compound **174** as a colourless oil (203 mg, 0.524 mmol, 81%); $^1\text{H NMR}$ (400 MHz,

CDCl₃): δ_H 8.05 (dd, *J* = 7.9, 1.7 Hz, 1H, C⁵H), 7.79 (br d, *J* = 8.4 Hz, 1H, C⁸H), 7.55 (ddd, *J* = 8.4, 7.2, 1.7 Hz, 1H, C⁷H), 7.19 (ddd, *J* = 7.9, 7.2, 1.1 Hz, 1H, C⁶H), 5.77 (dddd, *J* = 17.3, 10.2, 7.3, 7.0 Hz, 1H, C¹⁸H), 5.12 – 5.03 (m, 2H, C¹⁹H₂), 4.85 (dd, *J* = 10.7, 4.8 Hz, 1H, C²H), 4.32 – 4.23 (2 × q, *J* = 7.1 Hz, 2H, C¹⁵H₂), 2.88 (dddd, *J* = 14.2, 7.0, 1.3, 1.3 Hz, 1H, C¹⁷H_AH_B), 2.60 (dddd, *J* = 14.2, 7.3, 1.2, 1.2 Hz, 1H, C¹⁷H_AH_B), 1.59 (s, 9H, 3 × C¹¹H₃) overlapped by 1.61 – 1.52 (m, 2H, C¹²H₂), 1.33 (t, *J* = 7.1 Hz, 3H, C¹⁶H₃), 0.88 (t, *J* = 7.3 Hz, 3H, C¹³H₃); ¹³C {¹H} NMR (101 MHz, CDCl₃): δ_C 190.0 (C), 169.4 (C), 153.6 (C), 139.9 (C), 134.2 (CH), 131.8 (CH), 127.9 (CH), 124.4 (CH), 124.3 (C), 124.0 (CH), 119.3 (CH₂), 82.4 (C), 63.0 (C), 61.4 (CH₂), 61.2 (CH), 38.7 (CH₂), 28.3 (CH₃), 22.3 (CH₂), 14.1 (CH₃), 10.6 (CH₃); IR (ATR): ν_{max} 3078, 2976, 2935, 2877, 1689 (C=O), 1600, 1479, 1459, 1367, 1332, 1253, 1218, 1154, 1127, 1078, 1013, 991, 923, 886, 758, 643, 582, 451; HRMS *m/z* calc. for C₂₂H₃₀NO₅ [M+H]: 388.2118; found: 388.2120 (σ = 0.30 ppm); HPLC Chiralpak AD-H; mobile phase: hexane:2-propanol (99:1 v/v); flow rate: 0.5 mL min⁻¹; retention times: major product (*S,R*)-**174** – 26.9 min (76.1%), minor *syn*-allylation product (*S,S*)-**174** – 31.1 min (10.3%), enantiomer of major product (*R,S*)-**174** – 20.0 min (10.3%), enantiomer of minor *syn*-allylation product (*R,R*)-**174** – 10.8 min (3.4%), 72% ee; [α]_D²⁰ +68.0 (*c* = 1.0 in CHCl₃, 72% ee).

HPLC chromatogram for **174**:



Ethyl (S,R)-3-allyl-2-ethyl-2,3-dihydro-4(1H)-quinolone-3-carboxylate **175**



175

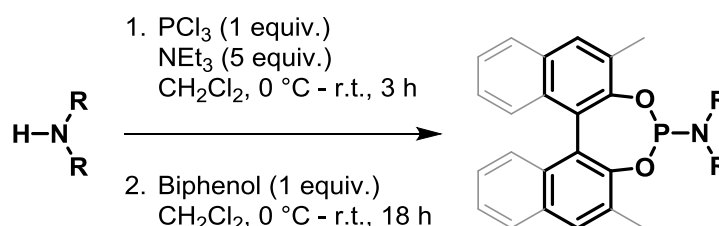
To a stirring solution of compound **174** (310 mg, 0.800 mmol) in CH₂Cl₂ (2.4 mL, 0.33 M solution) at r.t. was added trifluoroacetic acid (1.6 mL). The solution was stirred at r.t. for 24 h then diluted with CH₂Cl₂ (9.6 mL) and added slowly to a saturated aqueous solution of NaHCO₃ (12 mL). The aqueous phase was extracted with CH₂Cl₂ (3 × 12 mL). The combined organics were washed with H₂O (24 mL), dried (MgSO₄), concentrated *in vacuo* and purified by column chromatography (silica, CH₂Cl₂) to afford compound **175** as a bright yellow solid (198 mg, 0.689 mmol, 86%; 66% ee, 6.6:1 *dr*). The compound was recrystallized *via* dropwise addition of pentane to a saturated solution of compound **175** in Et₂O at r.t. to afford bright yellow needles (>99% ee, 10.5:1 *dr*); X-ray crystallographic analysis confirmed the displayed stereochemistry; **m.p.** 83-85 °C; **¹H NMR** (400 MHz, CDCl₃): δ_H 7.94 (dd, *J* = 8.0, 1.6 Hz, 1H, C⁵H), 7.33 (ddd, *J* = 8.2, 7.1, 1.6 Hz, 1H, C⁷H), 6.80 (td, *J* = 8.0, 7.1, 1.0 Hz, 1H, C⁶H), 6.70 (dd, *J* = 8.2, 1.0 Hz, 1H, C⁸H), 5.74 (dddd, *J* = 17.1, 10.2, 9.2, 5.4 Hz, 1H, C¹⁵H), 5.19 (ddd, *J* = 17.1, 1.7, 0.9 Hz, 1H, C¹⁶H_AH_B), 5.11 (ddd, *J* = 10.2, 1.7, 0.9 Hz, 1H, C¹⁶H_AH_B), 4.37 (s, 1H, NH), 4.14 (dq, *J* = 10.8, 7.1 Hz, 1H, C¹²H_AH_B), 4.05 (dq, *J* = 10.8, 7.1 Hz, 1H, C¹²H_AH_B), 3.47 (dd, *J* = 10.6, 2.3 Hz, 1H, C²H), 3.19 (ddt, *J* = 14.2, 5.5, 1.7 Hz, 1H, C¹⁴H_AH_B), 2.66 (dd, *J* = 14.2, 9.2 Hz, 1H, C¹⁴H_AH_B), 2.01 (ddd, *J* = 14.4, 7.5, 2.3 Hz, 1H, C⁹H_AH_B), 1.78 (ddd, *J* = 14.4, 10.6, 7.5 Hz, 1H, C⁹H_AH_B), 1.10 (t, *J* = 7.1 Hz, 3H, C¹³H₃), 1.07 (t, *J* = 7.5 Hz, 3H, C¹⁰H₃); **¹³C {¹H} NMR** (101 MHz, CDCl₃): δ_C 191.0 (C), 170.2 (C), 150.4 (C), 134.8 (CH), 133.1 (CH), 128.4 (CH), 119.8 (C), 118.9 (CH₂), 118.3 (CH), 115.5 (CH), 61.1 (CH₂), 60.0 (C), 59.6 (CH), 34.5 (CH₂), 21.6 (CH₂), 13.9 (CH₃), 11.2 (CH₃); **IR** (ATR): ν_{max} 3370, 3075, 2978, 2927, 1727 (C=O), 1661, 1638, 1608, 1505, 1484, 1464, 1435, 1388, 1344, 1307, 1258, 1222, 1203, 1158, 1111, 1093, 1048, 1031, 994, 921, 860, 781, 754, 650, 621, 529, 491, 444; **HRMS** *m/z* calc. for C₁₇H₂₂NO₃ [M+H]: 288.1594; found: 288.1599 (σ = 1.80 ppm); **HPLC** Keto-enol tautomerism led to broad signals in the chromatograms and increased error bars. Chiralpak AD-H; mobile phase: hexane:2-propanol (99:1 v/v); flow rate: 0.5 mL min⁻¹; retention times for purified sample: major product (S,R)-**175** – 24.7 min (73.1%), minor *syn*-allylation product (S,S)-**175** – 28.3 min (10.0%), enantiomer of major product

(*R,S*)-**175** – 20.6 min (13.6%), enantiomer of minor *syn*-allylation product (*R,R*)-**175** – 18.2 min (3.2%), 66% *ee*, 6.6:1 *dr*, retention times for recrystallized sample: major product (*S,R*)-**175** – 24.7 min (91.3%), minor *syn*-allylation product (*S,S*)-**175** – 28.2 min (8.7%), >99% *ee*, 10.5:1 *dr*, $[\alpha]_D^{20}$ purified sample: +14.4 (*c* = 1.0 in CHCl₃, 66% *ee*, 6.6:1 *dr*); recrystallized sample: +24.0 (*c* = 1.0 in CHCl₃, >99% *ee*, 10.5:1 *dr*).

HPLC chromatograms for racemic **175** (left) and enantioenriched **175** (right):

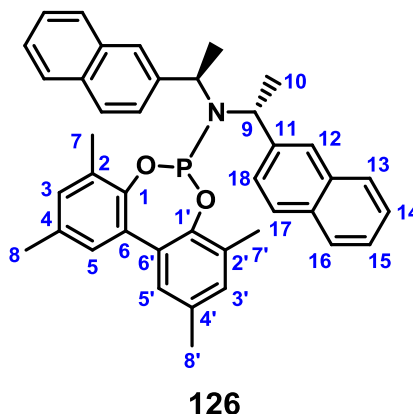


General procedures F for the synthesis of biphenol-phosphoramidite ligands 126 & 128-134



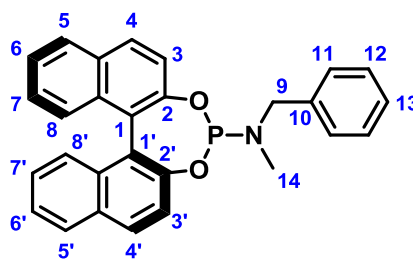
General procedure F: To a solution of amine (1 equiv.) and NEt₃ (5 equiv.) in CH₂Cl₂ (0.2 M solution) under argon at 0 °C was added PCl₃ (1 equiv.). The reaction mixture was warmed to rt and stirred under argon for 3 hours. The reaction mixture was then cooled to 0 °C and substituted biphenol (1 equiv.) was added (N.B. Exothermic reaction observed! Add across multiple portions to limit exotherm). The reaction mixture was warmed to rt and stirred under argon for 18 hours, after which the reaction mixture was partitioned between CH₂Cl₂ and water. The aqueous phase was then extracted with CH₂Cl₂. The combined organics were concentrated *in vacuo* to ~1-5 mL and the crude solution was eluted over silica gel (CH₂Cl₂) (N.B. 3 column volumes generally sufficient for complete elution of product) to afford the desired product. A number of the phosphoramidites have significant numbers of overlapping diastereotopic carbons making full assignment of the ¹³C data impractical in some cases, though attempts have been made and described.

2,4,8,10-Tetramethyl-*N,N*-bis((*R*)-1-(naphthalen-2-yl)ethyl)dibenzo[*d,f*][1,3,2]dioxaphosphepin-6-amine 126



General Procedure F was followed using 3,3',5,5'-tetramethyl-2,2'-biphenol (101.7 mg, 0.420 mmol), PCl_3 (37 μL , 0.424 mmol) and bis((*R*)-1-(naphthalen-2-yl)ethyl)amine (137 mg, 0.421 mmol) to afford compound **126** as an off-white solid (143 mg, 0.240 mmol, 57%); **m.p.** 71-73 °C; **^1H NMR** (400 MHz, CDCl_3): δ_{H} 7.97 – 7.75 (m, 1H, Ar-CH), 7.71 – 7.43 (m, 5H, 5 \times Ar-CH), 7.42 – 7.23 (m, 9H, 9 \times Ar-CH), 7.13 – 7.00 (m, 3H, 3 \times Ar-CH), 4.88 (s, 2H, 2 \times C⁹H), 2.53 (s, 2H, 2 \times [aliphatic-C]H), 2.36 (d, J = 8.7 Hz, 4H, 4 \times [aliphatic-C]H), 2.10 (s, 2H), 1.85 (d, J = 7.1 Hz, 4H, 4 \times [aliphatic-C]H), 1.56 (s, 6H, 2 \times C¹⁰H₃); rotamers seen in spectrum; **^{13}C { ^1H } NMR** (101 MHz, CDCl_3): δ_{C} 148.0 (d, J = 8.0 Hz, C), 147.1(3) (C), 147.1(1) (C), 140.9 (CH), 133.4 (CH), 133.0 (CH), 132.7 (CH), 132.3 (CH), 131.3 (d, J = 3.6 Hz, C), 131.1(6) (CH), 131.1 (C), 131.0 (CH), 130.2 (d, J = 1.5 Hz, C), 130.1 (d, J = 2.9 Hz, C), 129.3 (CH), 128.2 (CH), 128.2 (CH), 128.0 (C), 127.8 (CH), 127.6 (C), 127.3 (CH), 127.2 (CH), 126.8 (CH), 126.2 (CH), 126.0 (CH), 125.7 (C), 125.6 (CH), 125.5 (CH), 52.7 (d, J = 11.8 Hz, CH), 20.9 (CH₃), 20.8 (CH₃), 17.5 (CH₃), 16.5 (CH₃); **^{31}P { ^1H } NMR** (162 MHz, CDCl_3): δ_{P} 141.4; **IR** (ATR): ν_{max} 3054, 3027, 2973, 2928, 2878, 2852, 1732, 1574, 1490, 1458, 1361, 1331, 1228, 1211, 1111, 1063, 1027, 981, 942, 909, 863, 784, 722, 654, 610, 574, 523, 474, 420; **HRMS** m/z calc. for $\text{C}_{40}\text{H}_{39}\text{NO}_2\text{P}$ [M+H]: 596.2713; found: 596.2720 (σ = 1.20 ppm); **$[\alpha]_{\text{D}}^{20}$** +332.6 (c = 0.5 in CHCl_3).

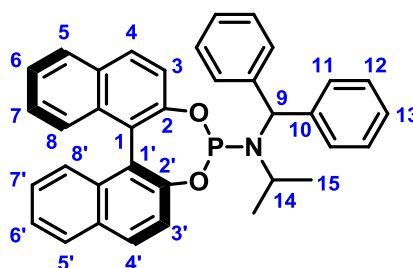
***N*-Benzyl-*N*-methyldinaphtho[2,1-*d*:1',2'-*f*][1,3,2]dioxaphosphepin-4-amine 128**



128

General Procedure F was followed using (*S*)-BINOL (286 mg, 1.00 mmol), PCl_3 (88 μL , 1.01 mmol) and *N*-methylbenzylamine (121 mg, 1.00 mmol) to afford compound **128** as a colourless solid (264 mg, 0.607 mmol, 61%); $^1\text{H NMR}$ (CDCl_3 , 400 MHz): δ_{H} 8.01 (d, $J = 8.8$ Hz, 1H, Ar-CH), 7.95 (d, $J = 8.2$ Hz, 1H, Ar-CH), 7.89 (d, $J = 7.3$ Hz, 1H, \times Ar-CH), 7.87 (d, $J = 9.1$ Hz, 1H, \times Ar-CH), 7.59 (dd, $J = 8.8$ Hz, 1H, \times Ar-CH), 7.47 – 7.35 (m, 7H, 7 \times Ar-CH), 7.34 – 7.25 (m, 5H, 5 \times Ar-CH), 4.38 (dd, $J = 15.0, 9.2$ Hz, 1H, $\text{C}^9\text{H}_\text{A}\text{H}_\text{B}$), 3.97 (t, $J = 15.0, 13.5$ Hz, 1H, $\text{C}^9\text{H}_\text{A}\text{H}_\text{B}$), 2.30 (d, $J = 6.4$ Hz, 3H, C^{14}H_3); $^1\text{H NMR}$ was consistent with previously recorded data for the compound.¹⁴¹

***N*-Benzhydryl-*N*-isopropyldinaphtho[2,1-*d*:1',2'-*f*][1,3,2]dioxaphosphepin-4-amine 129**

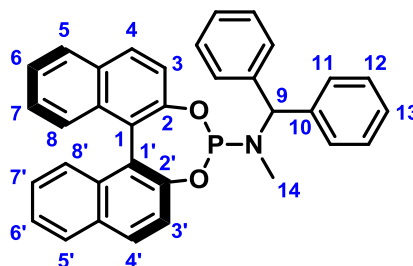


129

General Procedure F was followed using (*S*)-BINOL (286 mg, 1.00 mmol), PCl_3 (88 μL , 1.01 mmol) and *N*-isopropylbenzylamine (225 mg, 1.00 mmol) to afford compound **129** as a colourless solid (401 mg, 0.743 mmol, 74%); $^1\text{H NMR}$ (400 MHz, CDCl_3) δ_{H} 7.93 (d, $J = 8.8$ Hz, 1H, Ar-CH), 7.92 – 7.87 (m, 2H, 2 \times Ar-CH), 7.80 (d, $J = 8.8$ Hz, 1H, Ar-CH), 7.49 (d, $J = 7.2$ Hz, 2H, 2 \times Ar-CH), 7.46 – 7.39 (m, 6H, 6 \times Ar-CH), 7.39 – 7.31 (m, 6H, 6 \times Ar-CH), 7.31 – 7.20 (m, 4H, 4 \times Ar-CH), 5.73 (d, $J = 17.1$ Hz, 1H, C^9H), 3.60 (heptd, $J = 6.6, 4.6$ Hz, 1H, C^{14}H), 1.11 (d, $J = 6.6$ Hz, 3H, $\text{C}^{15\text{a}}\text{H}_3$), 0.99 (d, $J = 6.6$ Hz, 3H, $\text{C}^{15\text{b}}\text{H}_3$); $^1\text{H NMR}$ was consistent with previously recorded data for the compound.¹¹⁷

***N*-Benzhydryl-*N*-methyldinaphtho[2,1-*d*:1',2'-*f*][1,3,2]dioxaphosphepin-4-amine**

130

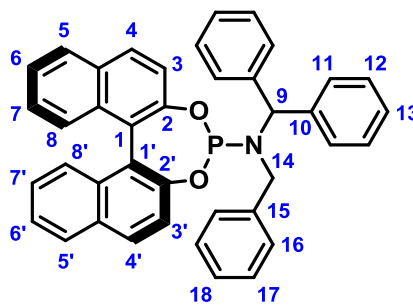


130

General Procedure F was followed using (*S*)-BINOL (1.12 g, 3.91 mmol), PCl_3 (0.34 mL, 3.90 mmol) and *N*-methylbenzhydrylamine (771 mg, 3.91 mmol) to afford compound **130** as an off-white solid (1.28 g, 2.50 mmol, 64%); **m.p.** 100-102 °C; **^1H NMR** (400 MHz, CDCl_3): δ_{H} 8.00 (d, $J = 8.7$ Hz, 1H, Ar-CH), 7.94 (dd, $J = 8.3, 1.2$ Hz, 1H, Ar-CH), 7.85 (dd, $J = 8.7, 1.2$ Hz, 1H, Ar-CH), 7.72 (d, $J = 8.8$ Hz, 1H, Ar-CH), 7.58 (d, $J = 8.8$ Hz, 1H, Ar-CH), 7.51 – 7.32 (m, 14H, 14 x Ar-CH), 7.27 – 7.23 (m, 2H, 2 x Ar-CH), 6.94 (d, $J = 8.7$ Hz, 1H, Ar-CH), 6.05 (d, $J = 10.9$ Hz, 1H, C⁹H), 2.14 (d, $J = 4.0$ Hz, 3H, C¹⁴H); **^{13}C { $^1\text{H}}$ NMR** (101 MHz, CDCl_3): δ_{C} 150.2 (d, $J = 5.5$ Hz, C), 149.4 (CH), 140.1 (d, $J = 3.7$ Hz, C), 139.7 (d, $J = 7.2$ Hz, C), 132.9 (CH), 132.6 (CH), 131.4 (CH), 130.7 (CH), 130.3 (CH), 129.9 (CH), 129.8 (CH), 128.5 (CH), 128.4 (CH), 128.3 (CH), 128.2 (CH), 127.6 (CH), 127.2 (CH), 127.1 (CH), 127.0 (CH), 126.1 (CH), 126.0 (CH), 124.8 (CH), 124.6 (CH), 124.0 (d, $J = 5.1$ Hz, C), 122.6 (d, $J = 2.0$ Hz, C), 122.2 (CH), 121.8 (CH), 65.3 (d, $J = 45.3$ Hz, CH), 28.96 (CH₃); **^{31}P { $^1\text{H}}$ NMR** (162 MHz, CDCl_3): δ_{P} 148.7; **IR** (ATR): ν_{max} 3054, 3027, 2970, 2937, 1739, 1619, 1589, 1493, 1462, 1431, 1364, 1327, 1231, 1203, 1141, 1071, 1031, 979, 940, 864, 819, 800, 779, 747, 727, 696, 681, 626, 599, 575, 556, 541, 523, 481, 465, 417; **HRMS** m/z calc. for $\text{C}_{34}\text{H}_{27}\text{NO}_2\text{P}$ [M+H]: 512.1774; found: 512.1773 ($\sigma = 0.20$ ppm); **$[\alpha]_{\text{D}}^{20}$** +151.0 ($c = 0.5$ in CHCl_3).

***N*-Benzhydryl-*N*-benzylidinaphtho[2,1-*d*:1',2'-*f*][1,3,2]dioxaphosphepin-4-amine**

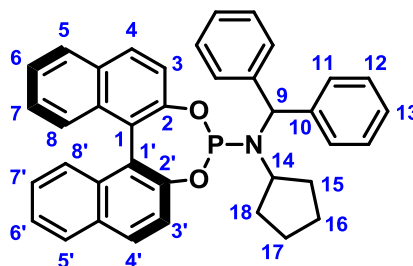
131



131

General Procedure F was followed using (*S*)-BINOL (244 mg, 0.852 mmol), PCl_3 (74 μL , 0.848 mmol) and *N*-benzylbenzhydrylamine (233 mg, 0.852 mmol) to afford compound **131** as an off-white solid (356 mg, 0.606 mmol, 71%); **m.p.** 122-124 °C; **^1H NMR** (400 MHz, CDCl_3): δ_{H} 7.95 (d, $J = 8.8$ Hz, 1H, Ar-CH), 7.91 (d, $J = 8.4$ Hz, 2H, 2 \times Ar-CH), 7.86 – 7.83 (m, 1H, Ar-CH), 7.81 (d, $J = 8.9$ Hz, 1H, Ar-CH), 7.68 – 7.62 (m, 2H, 2 \times Ar-CH), 7.60 – 7.51 (m, 3H, 3 \times Ar-CH), 7.47 (dt, $J = 7.3, 1.9, 1.3$ Hz, 1H), 7.41 (ddd, $J = 8.1, 6.6, 1.3$ Hz, 1H, Ar-CH), 7.39 – 7.34 (m, 2H, 2 \times Ar-CH), 7.34 – 7.29 (m, 7H, 7 \times Ar-CH), 7.28 – 7.20 (m, 5H, 5 \times Ar-CH), 7.18 – 7.12 (m, 2H, 2 \times Ar-CH), 5.29 (d, $J = 16.7$ Hz, 1H, C^9H), 4.17 (dd, $J = 14.6, 1.8$ Hz, 1H, $\text{C}^{14}\text{H}_\text{A}\text{H}_\text{B}$), 3.34 (dd, $J = 14.6, 1.8$ Hz, 1H, $\text{C}^{14}\text{H}_\text{A}\text{H}_\text{B}$); **^{13}C { ^1H } NMR** (101 MHz, CDCl_3): δ_{C} 150.4 (d, $J = 5.7$ Hz, C), 149.5 (CH), 140.6 (d, $J = 8.7$ Hz, C), 140.3 (CH), 138.3 (CH), 132.8 (C), 132.6 (C), 131.4 (CH), 130.6 (CH), 130.2 (CH), 130.1 (CH), 129.4 (CH), 129.4 (CH), 129.3 (CH), 129.2 (CH), 129.2 (CH), 128.7 (CH), 128.4 (CH), 128.3 (CH), 128.3 (CH), 128.2 (CH), 127.8 (CH), 127.4 (CH), 127.3 (CH), 127.1 (CH), 127.0 (CH), 126.1 (CH), 126.0 (CH), 124.8 (CH), 124.6 (CH), 124.1 (d, $J = 8.7$ Hz, C), 122.46, 122.4 (d, $J = 1.0$ Hz, C), 121.9 (CH), 65.0 (d, $J = 26.9$ Hz, CH), 49.6 (d, $J = 3.5$ Hz); **^{31}P { ^1H } NMR** (162 MHz, CDCl_3): δ_{P} 142.6; **IR** (ATR): ν_{max} 3056, 3027, 2970, 2925, 2851, 1739, 1588, 1493, 1453, 1360, 1326, 1227, 1202, 1155, 1097, 1062, 1028, 981, 940, 911, 864, 818, 787, 745, 693, 679, 624, 605, 574, 551, 523, 470, 415; **HRMS** m/z calc. for $\text{C}_{40}\text{H}_{31}\text{NO}_2\text{P}$ [$\text{M}+\text{H}$]: 588.2087; found: 588.2081 ($\sigma = 1.10$ ppm); **$[\alpha]_{\text{D}}^{20}$** +193.7 ($c = 0.5$ in CHCl_3).

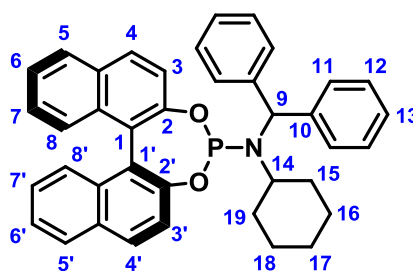
N*-Benzhydryl-*N*-cyclopentylidinaphtho[2,1-*d*:1',2'-*f*][1,3,2]dioxaphosphepin-4-amine **132*



132

General Procedure F was followed using (*S*)-BINOL (286 mg, 1.00 mmol), PCl_3 (88 μL , 1.01 mmol) and *N*-cyclopentylbenzhydrylamine (251 mg, 1.00 mmol) to afford compound **132** as a colourless solid (442 mg, 0.781 mmol, 78%); $^1\text{H NMR}$ (CDCl_3 , 400 MHz): δ_{H} 7.96 (d, $J = 8.8$ Hz, 1H, Ar-CH), 7.91 (dd, $J = 8.0, 1.2$ Hz, 1H, Ar-CH), 7.84 (dd, $J = 8.3, 1.5$ Hz, 1H, Ar-CH), 7.62 (d, $J = 8.8$ Hz, 1H, Ar-CH), 7.49 (dd, $J = 8.8, 0.9$ Hz, 1H, Ar-CH), 7.46 – 7.32 (m, 8H, 8 \times Ar-CH), 7.32 – 7.26 (m, 6H, 6 \times Ar-CH), 7.24 (dd, $J = 6.7, 1.4$ Hz, 2H, 2 \times Ar-CH), 7.05 (d, $J = 8.8$ Hz, 1H, Ar-CH), 5.70 (d, $J = 12.3$ Hz, 1H, C°H), 3.60 (app h, $J = 8.8$ Hz, 1H, C^{14}H), 1.97 – 1.73 (m, 2H, 2 \times [*aliphatic*]-CH), 1.40 – 1.31 (m, 3H, 3 \times [*aliphatic*]-CH), 1.23 – 1.11 (m, 3H, 3 \times [*aliphatic*]-CH); $^1\text{H NMR}$ was consistent with previously recorded data for the compound.¹²⁰

N*-Benzhydryl-*N*-cyclohexylidinaphtho[2,1-*d*:1',2'-*f*][1,3,2]dioxaphosphepin-4-amine **133*

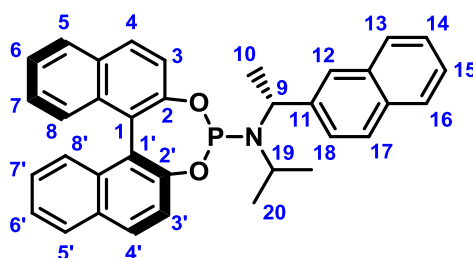


133

General Procedure F was followed using (*S*)-BINOL (716 mg, 2.50 mmol), PCl_3 (220 μL , 2.52 mmol) and *N*-cyclohexylbenzhydrylamine (664 mg, 2.50 mmol) to afford compound **133** as a colourless solid (1.24 g, 2.14 mmol, 86%); $^1\text{H NMR}$ (CDCl_3 , 400 MHz): δ_{H} 7.93 (d, $J = 8.8$ Hz, 1H, Ar-CH), 7.91 – 7.86 (m, 2H, 2 \times Ar-CH), 7.77 (d, $J = 8.8$ Hz, 1H, Ar-CH), 7.48 (d, $J = 7.3$ Hz, 2H, 2 \times Ar-CH), 7.45 – 7.36 (m, 6H, 6 \times Ar-CH), 7.36 – 7.26 (m, 9H, 9 \times Ar-CH), 7.22 (ddd, $J = 8.5, 6.7, 1.3$ Hz, 1H, Ar-CH), 5.75

(d, $J = 16.6$ Hz, 1H, C⁹H), 2.99 (ddt, $J = 14.9, 11.4, 3.3$ Hz, 1H, C¹⁴H), 1.78 (d, $J = 12.4$ Hz, 1H, [aliphatic]-CH), 1.63 – 1.29 (m, 5H, 5 × [aliphatic]-CH), 0.97 – 0.83 (m, 2H, 2 × [aliphatic]-CH), 0.71 – 0.55 (m, 2H, 2 × [aliphatic]-CH); ¹H NMR was consistent with previously recorded data for the compound.¹²⁰

N*-isopropyl-*N*-((*R*)-1-(naphthalen-2-yl)ethyl)dinaphtho[2,1-*d*:1',2'-*f*][1,3,2]dioxaphosphepin-4-amine **134*



134

General Procedure F was followed using (*S*)-BINOL (544 mg, 1.90 mmol), PCl₃ (165 μL, 0.190 mmol) and *N*-isopropyl-*N*-((*R*)-1-(naphthalen-2-yl)ethyl)amine (405 mg, 1.90 mmol) to afford compound **134** as an off-white solid (633 mg, 1.20 mmol, 63%); **m.p.** 167-169 °C; ¹H NMR (400 MHz, CDCl₃) δ_H 8.02 (d, $J = 8.7$ Hz, 1H, Ar-CH), 7.98 – 7.90 (m, 3H, 3 × Ar-CH), 7.87 – 7.78 (m, 4H, 4 × Ar-CH), 7.75 (dd, $J = 8.5, 1.9$ Hz, 1H, Ar-CH), 7.62 (dd, $J = 8.8, 1.0$ Hz, 1H, Ar-CH), 7.58 (d, $J = 8.8$ Hz, 1H, Ar-CH), 7.51 – 7.38 (m, 5H, 5 × Ar-CH), 7.32 (d, $J = 8.4$ Hz, 1H, Ar-CH), 7.28 – 7.22 (m, 2H, Ar-CH), 4.72 (app p, $J = 7.3$ Hz, 1H, C⁹H), 3.35 (app hept, $J = 6.8$ Hz, 1H, C¹⁹H), 1.71 (d, $J = 6.8$ Hz, 3H, C¹⁸H₃), 1.43 (d, $J = 6.8$ Hz, 3H, C²⁰H₃), 1.00 (d, $J = 7.3$ Hz, 3H, C¹⁰H₃); ¹³C {¹H} NMR (101 MHz, CDCl₃) δ_C 150.3 (d, $J = 7.3$ Hz, C), 150.0 (C), 141.4 (C), 133.1 (C), 132.9 (C), 132.8 (C), 132.5 (C), 131.5 (C), 130.6 (C), 130.4 (CH), 129.5 (CH), 128.4 (CH), 128.2 (CH), 128.0 (CH), 127.7 (CH), 127.6 (CH), 127.2 (CH), 127.2 (CH), 127.1 (CH), 126.1 (CH), 126.0 (CH), 125.9 (CH), 125.7 (CH), 125.5 (CH), 124.8 (CH), 124.5 (CH), , 124.1 (d, $J = 5.1$ Hz, C), 122.5(1) (CH), 122.4(8) (CH), 121.92 (C), 51.7 (d, $J = 7.3$ Hz, CH), 46.1 (d, $J = 17.2$ Hz, CH), 25.7 (d, $J = 8.8$ Hz, CH₃), 24.6 (d, $J = 10.6$ Hz, CH₃), 21.29 (CH₃); ³¹P {¹H} NMR (162 MHz, CDCl₃): δ_P 147.6; **IR** (ATR): ν_{max} 3051, 2967, 2928, 2867, 1618, 1589, 1504, 1461, 1430, 1362, 1326, 1270, 1230, 1203, 1149, 1126, 1102, 1069, 1041, 984, 942, 854, 818, 788, 746, 696, 678, 656, 624, 593, 555, 524, 506, 474, 416; **HRMS** ^{m/z} calc. for C₃₅H₃₁NO₂P [M+H]: 528.2087; found: 528.2090 (σ = 0.60 ppm); [α]_D²⁰ +235.0 (c = 0.5 in CHCl₃).

4 References

- (1) Michael, A. *Am. Chem. J.* **1887**, 9, 274.
- (2) Conrad, M.; Guthzeit, M. *Ber. Dtsch. Che. Ges.* **1884**, 17, 1185.
- (3) Frankland, E. *Liebigs Ann. Chem.* **1849**, 71, 171.
- (4) Hallwachs, W.; Schafarik, A. *Liebigs Ann. Chem.* **1859**, 109, 206.
- (5) Barbier, P. *Compt. Rend.* **1899**, 128, 110.
- (6) Grignard, V. *Compt. Rend.* **1900**, 130, 1322.
- (7) Kharasch, M. S.; Tawney, P. O. *J. Am. Chem. Soc.* **1941**, 63, 2308.
- (8) Gilman, H.; Jones, R. G.; Woods, L. A. *J. Org. Chem.* **1952**, 17, 1630.
- (9) Normant, J. F. *Synthesis (Stuttg.)* **1972**, 1972, 63.
- (10) Ahn, K.-H.; Klassen, R. B.; Lippard, S. J. *Organometallics* **1990**, 9, 3178.
- (11) Mandoli, A.; Calamante, M.; Feringa, B. L.; Salvadori, P. *Tetrahedron: Asymmetry* **2003**, 14 (23), 3647.
- (12) Feringa, B. L.; Badorrey, R.; Peña, D.; Harutyunyan, S. R.; Minnaard, A. J. *P. Natl. Acad. Sci. USA* **2004**, 101, 5834.
- (13) Alexakis, A.; Albrow, V.; Biswas, K.; D'Augustin, M.; Prieto, O.; Woodward, S. *Chem. Comm.* **2005**, 3, 2843.
- (14) Blackmond, D. G. *Angew.* **2005**, 44, 4302.
- (15) Alexakis, A.; Bäckvall, J. E.; Krause, N.; Pàmies, O.; Diéguez, M. *Chem. Rev.* **2008**, 108, 2796.
- (16) Jerphagnon, T.; Pizzuti, M. G.; Minnaard, A. J.; Feringa, B. L. *Chem. Soc. Rev.* **2009**, 38, 1039.
- (17) Bertz, S. H.; Hardin, R. A.; Heavey, T. J.; Ogle, C. A. *Angew. Chem. Int. Ed.* **2013**, 52, 10250.

- (18) Krause, N.; Wagner, R.; Gerold, A. *J. Am. Chem. Soc.* **1994**, *116*, 381.
- (19) Uerdingen, M.; Krause, N. *Tetrahedron* **2000**, *56*, 2799.
- (20) Bertz, S. H.; Cope, S.; Murphy, M.; Ogle, C. A.; Taylor, B. J. *J. Am. Chem. Soc.* **2007**, *129*, 7208.
- (21) Bertz, S. H.; Cope, S.; Dorton, D.; Murphy, M.; Ogle, C. A. *Angew. Chem. Int. Ed.* **2007**, *46*, 7082.
- (22) Bartholomew, E. R.; Bertz, S. H.; Cope, S.; Dorton, D. C.; Murphy, M.; Ogle, C. A. *Chem. Comm.* **2008**, *44*, 1176.
- (23) Bartholomew, E. R.; Bertz, S. H.; Cope, S. K.; Murphy, M. D.; Ogle, C. A.; Thomas, A. A. *Chem. Comm.* **2010**, *46*, 1253.
- (24) Bertz, S. H.; Murphy, M. D.; Ogle, C. A.; Thomas, A. A. *Chem. Comm.* **2010**, *46*, 1255.
- (25) Bertz, S. H.; Hardin, R. A.; Murphy, M. D.; Ogle, C. A.; Richter, J. D.; Thomas, A. A. *J. Am. Chem. Soc.* **2012**, *134*, 9557.
- (26) Chang, H. C.; Lo, F. C.; Liu, W. C.; Lin, T. H.; Liaw, W. F.; Kuo, T. S.; Lee, W. Z. *Inorg. Chem.* **2015**, *54*, 5527.
- (27) Hannigan, S. F.; Lum, J. S.; Bacon, J. W.; Moore, C.; Golen, J. A.; Rheingold, A. L.; Doerrer, L. H. *Organometallics* **2013**, *32*, 3429.
- (28) Casitas, A.; King, A. E.; Parella, T.; Costas, M.; Stahl, S. S.; Ribas, X. *Chem. Sci.* **2010**, *1*, 326.
- (29) Kitamura, M.; Miki, T.; Nakano, K.; Noyori, R. *B. Chem. Soc. Jpn.* **2000**, *73*, 999.
- (30) Pfretzschner, T.; Kleemann, L.; Janza, B.; Harms, K.; Schrader, T. *Chem.-Eur. J.* **2004**, *10*, 6048.
- (31) Krauss, S. R.; Smith, S. G. *J. Am. Chem. Soc.* **1981**, *103*, 141.
- (32) Canisius, J.; Gerold, A.; Krause, N. *Angew. Chem. Int. Ed.* **1999**, *38*, 1644.

- (33) Harutyunyan, S. R.; López, F.; Browne, W. R.; Correa, A.; Peña, D.; Badorrey, R.; Meetsma, A.; Minnaard, A. J.; Feringa, B. L. *J. Am. Chem. Soc.* **2006**, *128*, 9103.
- (34) Smith, M. B.; Becker, W. E. *Tetrahedron* **1966**, *22*, 3027.
- (35) Benn, B. R.; Lehmkuhl, H.; Mehler, K.; Rufinska, A. *Angew. Chem. Int. Ed.* **1984**, *23*, 534.
- (36) López, F.; Harutyunyan, S. R.; Meetsma, A.; Minnaard, A. J.; Feringa, B. L. *Angew. Chem. Int. Ed.* **2005**, *44*, 2752.
- (37) Zhang, H.; Gschwind, R. M. *Angew. Chem. Int. Ed.* **2006**, *45*, 6391.
- (38) Zhang, H.; Gschwind, R. M. *Chem.-Eur. J.* **2007**, *13*, 6691.
- (39) Schober, K.; Zhang, H.; Gschwind, R. M. *J. Am. Chem. Soc.* **2008**, *130*, 12310.
- (40) Gschwind, R. M. *Chem. Rev.* **2008**, *108*, 3029.
- (41) Rekowski, F. Von; Koch, C.; Gschwind, R. M. In *NMR Spectroscopic Aspects. In Copper-Catalyzed Asymmetric Synthesis*; Alexakis, A., Krause, N., Woodward, S., Eds.; Wiley-VCH: Weinheim, Germany, 2014; pp 353–373.
- (42) Von Rekowski, F.; Koch, C.; Gschwind, R. M. *J. Am. Chem. Soc.* **2014**, *136*, 11389.
- (43) Thaler, T.; Haag, B.; Gavryushin, A.; Schober, K.; Hartmann, E.; Gschwind, R. M.; Zipse, H.; Mayer, P.; Knochel, P. *Nat. Chem.* **2010**, *2*, 125.
- (44) Teichert, J. F.; Feringa, B. L. *Angew. Chem. Int. Ed.* **2010**, *49*, 2486.
- (45) Girard, C.; Kagan, H. B. *Angew. Chem. Int. Ed.* **1998**, *37*, 2922.
- (46) Chai, J.-D.; Head-Gordon, M. *Phys. Chem. Chem. Phys.* **2008**, *10*, 6615.
- (47) Dolg, M.; Wedig, U.; Stoll, H.; Preuss, H. *J. Chem. Phys.* **1987**, *86*, 866.
- (48) Molteni, R.; Bertermann, R.; Edkins, K.; Steffen, A. *Chem. Comm.* **2016**, *52*, 5019.

- (49) Leshner, G. Y.; Froelich, E. J.; Gruett, M. D.; Bailey, J. H.; Brundage, R. P. *J. Med. Chem.* **1962**, *5*, 1063.
- (50) Hooper, D. C. *Drugs* **1999**, *58*, Suppl.2: 6.
- (51) Andersson, M. I.; MacGowan, A. P. *J. Antimicrob. Chemoth.* **2003**, *51*, S1: 1.
- (52) Heeb, S.; Fletcher, M. P.; Chhabra, S. R.; Diggle, S. P.; Williams, P.; Cámara, M. *FEMS Microbiol. Rev.* **2011**, *35*, 247.
- (53) Green, G. M.; Oliphant, C. M. *Am. Fam. Physician* **2002**, *65*, 455.
- (54) Lee, K. H.; Yi, X.; Yang, Z.-Y.; Peng, X.; Hackl, T.; Hamel, E.; Mauger, A.; Wu, J.-H. *J. Med. Chem.* **2001**, *44*, 3932.
- (55) Andriole, V. T. *Eur. J. Clin. Microbiol. Infec. Dis.* **1991**, *10*, 342.
- (56) Ivanov, D. V.; Budanov, S. V. *Antibiot. Khimioter.* **2006**, *51*, 29.
- (57) MacDougall, C.; Guglielmo, B. J.; Maselli, J.; Gonzales, R. *Emerg. Infect. Dis.* **2005**, *11*, 380.
- (58) Chang, Y. H.; Kim, S. H.; Young, K. K. *Bioorg. Med. Chem. Lett* **1997**, *7*, 1875.
- (59) Biswas, N. R.; Verma, K.; Gupta, S. K.; Velpandian, T. In *Clinical Ophthalmology: Contemporary Perspectives*, eds. A. K. Gupta and V. Krishna, Elsevier India, 9th Ed.; pp 111–112.
- (60) Domagala, J. M. *J. Antimicrob. Chemoth.* **1994**, *33*, 685.
- (61) Zhanel, G. G.; Ennis, K.; Vercaigne, L.; Walkty, A.; Gin, A. S.; Embil, J.; Smith, H.; Hoban, D. J. *Drugs* **2002**, *62*, 13.
- (62) Conrad, M.; Limpach, L. *Chem. Ber.* **1887**, *20*, 944.
- (63) Gould, R. G.; Jacobs, W. A. *J. Am. Chem. Soc.* **1939**, *61*, 2890.
- (64) Camps, R. *Chem. Ber.* **1899**, *22*, 3228.
- (65) Combes, A. *Bull. Soc. Chim. Fr.* **1888**, *49*, 89.

- (66) Niementowski, S. v. *Chem. Ber.* **1894**, 27, 1394.
- (67) Staskun, B. *J. Org. Chem.* **1964**, 29, 1153.
- (68) Hu, W.; Lin, J. P.; Song, L. R.; Long, Y. Q. *Org. Lett.* **2015**, 17, 1268.
- (69) Yadav, A. K.; Sharma, G. R.; Dhakad, P.; Yadav, T. *Tetrahedron Lett.* **2012**, 53, 859.
- (70) Tois, J.; Vahermo, M.; Koskinen, A. *Tetrahedron Lett.* **2005**, 46, 735.
- (71) Åkerbladh, L.; Nordeman, P.; Wejdemar, M.; Odell, L. R.; Larhed, M. *J. Org. Chem.* **2015**, 80, 1464.
- (72) Jones, C. P.; Anderson, K. W.; Buchwald, S. L. *J. Org. Chem.* **2007**, 72, 7968.
- (73) Shi, P.; Wang, L.; Chen, K.; Wang, J.; Zhu, J. *Org. Lett.* **2017**, 19, 2418.
- (74) Yu, M. J. *J. Cheminformatics* **2013**, 5, 1.
- (75) Barker, A.; Kettle, J. G.; Nowak, T.; Pease, J. E. *Drug Discov. Today* **2013**, 18, 298.
- (76) Dandapani, S.; Marcaurelle, L. A. *Nat. Chem. Biol.* **2010**, 6, 861.
- (77) Medina-Franco, J. L. *Drug Dev. Res.* **2012**, 73, 430.
- (78) López-Vallejo, F.; Giulianotti, M. A.; Houghten, R. A.; Medina-Franco, J. L. *Drug Discov. Today* **2012**, 17, 718.
- (79) McNally, A.; Prier, C. K.; MacMillan, D. W. C. *Science* **2011**, 334, 1114.
- (80) Anderson, K. W.; Tepe, J. J. *Tetrahedron* **2002**, 58, 8475.
- (81) Li, J.; Jin, L.; Yu, C.; Weike, S. *J. Chem. Res.* **2009**, 3, 170.
- (82) Chelghoum, M.; Bahnous, M.; Bouraiou, A.; Bouacida, S.; Belfaitah, A. *Tetrahedron Lett.* **2012**, 53, 4059.
- (83) Okamoto, N.; Sueda, T.; Yanada, R. *J. Org. Chem.* **2014**, 79, 9854.

- (84) Minami, H.; Okamoto, N.; Sueda, T.; Sakaguchi, T.; Ishikura, M.; Yanada, R. *Tetrahedron Lett.* **2017**, *58*, 4277.
- (85) Saito, A.; Kasai, J.; Odaira, Y.; Fukaya, H.; Hanzawa, Y. *J. Org. Chem.* **2009**, *74*, 5644.
- (86) Park, C. M.; Choi, J. I.; Choi, J. H.; Kim, S. Y.; Park, W. K.; Seong, C. M. *Bioorg. Med. Chem. Lett* **2011**, *21*, 698.
- (87) Saito, K.; Moriya, Y.; Akiyama, T. *Org. Lett.* **2015**, *17*, 3202.
- (88) Cheng, S.; Zhao, L.; Yu, S. *Adv. Synth. Catal.* **2014**, *356*, 982.
- (89) Rueping, M.; Moreth, S. A.; Bolte, M. *Z. Naturforsch.* **2012**, *67*, 1021.
- (90) Liu, X.; Lu, Y. *Org. Lett.* **2010**, *12*, 5592.
- (91) Kanagaraj, K.; Pitchumani, K. *J. Org. Chem.* **2013**, *78*, 744.
- (92) Jeong, Y.; Lim, S. M.; Hong, S. *Bioorg. Med. Chem. Lett* **2015**, *25*, 5186.
- (93) Kiely, J. S.; Huang, S.; Lesheski, L. E. *J. Heterocycl. Chem.* **1989**, *26*, 1675.
- (94) Giorgi-Renault, S.; Husson, H.-P.; Clémencin-Le Guillou, C.; Quirion, J.-C. *Tetrahedron Lett.* **1997**, *38*, 1037.
- (95) Beifuss, U.; Schniske, U.; Feder, G. *Tetrahedron* **2001**, *57*, 1005.
- (96) Beifuss, U.; Ledderhose, S. *Synlett* **1997**, *3*, 313.
- (97) Bichovski, P.; Haas, T. M.; Keller, M.; Streuff, J. *Org. Biomol. Chem.* **2016**, *14*, 5673.
- (98) Bichovski, P.; Haas, T. M.; Kratzert, D.; Streuff, J. *Chem.-Eur. J.* **2015**, *21*, 2339.
- (99) Shintani, R.; Yamagami, T.; Kimura, T.; Hayashi, T. *Org. Lett.* **2005**, *7*, 5317.
- (100) Zhang, X.; Chen, J.; Han, F.; Cun, L.; Liao, J. *Eur. J. Org. Chem.* **2011**, 1443.
- (101) Holder, J. C.; Marziale, A. N.; Gatti, M.; Mao, B.; Stoltz, B. M. *Chem.-Eur. J.*

2013, 19, 74.

- (102) Pappoppula, M.; Aponick, A. *Angew. Chem. Int. Ed.* **2015**, 54, 15827.
- (103) Brown, M. K.; Degrado, S. J.; Hoveyda, A. H. *Angew. Chem. Int. Ed.* **2005**, 44, 5306.
- (104) Tang, X.; Blake, A. J.; Lewis, W.; Woodward, S. *Tetrahedron-Asymmetr.* **2009**, 20, 1881.
- (105) Teichert, J. F.; Feringa, B. L. *Chem. Comm.* **2011**, 47, 2679.
- (106) Vila, C.; Hornillos, V.; Fañanás-Mastral, M.; Feringa, B. L. *Chem. Comm.* **2013**, 49, 5933.
- (107) Pàmies, O.; Net, G.; Ruiz, A.; Claver, C.; Woodward, S. *Tetrahedron Asymmetr.* **2000**, 11, 871.
- (108) Börner, C.; Dennis, M. R.; Sinn, E.; Woodward, S. *Eur. J. Org. Chem.* **2001**, 2435.
- (109) Fraser, P. K.; Woodward, S. *Chem.-Eur. J.* **2003**, 9, 776.
- (110) Mata, Y.; Diéguez, M.; Pàmies, O.; Biswas, K.; Woodward, S. *Tetrahedron Asymmetr.* **2007**, 18, 1613.
- (111) Mata, Y.; Diéguez, M.; Pàmies, O.; Woodward, S. *J. Organomet. Chem.* **2007**, 692, 4315.
- (112) Biswas, K.; Woodward, S. *Tetrahedron Asymmetr.* **2008**, 19, 1702.
- (113) Robert, T.; Velder, J.; Schmalz, H. G. *Angew. Chem. Int. Ed.* **2008**, 47, 7718.
- (114) Selwood, D.; Hobbs, A. Agents For Use in the Treatment of Cardiovascular and Inflammatory Diseases Structurally Based on 4(1H)-Quinolone, European Patent 3145914, 2016.
- (115) Brown, M. F. Antibiotic Quinolones and derivatives, US Patent 6080757, 1997.
- (116) Roth, P. M. C.; Sidera, M.; Maksymowicz, R. M.; Fletcher, S. P. *Nat. Protoc.* **2014**, 9, 104.

- (117) Sidera, M.; Roth, P. M. C.; Maksymowicz, R. M.; Fletcher, S. P. *Angew. Chemie - Int. Ed.* **2013**, *52* (31), 7995.
- (118) Maciver, E. E.; Maksymowicz, R. M.; Wilkinson, N.; Roth, P. M. C.; Fletcher, S. P. *Org. Lett.* **2014**, *16* (12), 3288.
- (119) Termath, A. O.; Sebode, H.; Schlundt, W.; Stemmler, R. T.; Netscher, T.; Bonrath, W.; Schmalz, H. G. *Chem. - A Eur. J.* **2014**, *20* (38), 12051.
- (120) Fletcher, S. P.; Maksymowicz, R. M.; Roth, P. M. C.; Portela, M. S. Catalysts, Ligands and Use Thereof, World Patent 170642, 2014.
- (121) Barton, D. H. R.; Lester, D. J.; Motherwell, W. B.; Barros Papoula, M. T. *J. Chem. Soc. Chem. Comm.* **1980**, *8*, 246.
- (122) Fillion, E.; Wilsily, A. *J. Am. Chem. Soc.* **2006**, *128* (9), 2774.
- (123) Uhl, W. *Coord. Chem. Rev.* **2008**, *252*, 1540.
- (124) Arnold, L. A.; Imbos, R.; Mandoli, A.; De Vries, A. H. M.; Naasz, R.; Feringa, B. L. *Tetrahedron* **2000**, *56*, 2865.
- (125) Gilman, H.; Cartledge, F. K. *J. Org. Chem.* **1964**, *2*, 447.
- (126) Billo, E. J. In *Excel for Chemists: A Comprehensive Guide, 3rd Ed.*, John Wiley & Sons, Inc., New York, 2011.
- (127) Hernández, S.; Moreno, I.; San Martín, R.; Herrero, M. T.; Domínguez, E. *Org. Biomol. Chem.* **2011**, *9*, 2251.
- (128) Bogányi, B.; Kámán, J. *Tetrahedron* **2013**, *69*, 9512.
- (129) Li, M.; Li, L.; Ge, H. *Adv. Synth. Catal.* **2010**, *352*, 2445.
- (130) Davie, B. J.; Valant, C.; White, J. M.; Sexton, P. M.; Capuano, B.; Christopoulos, A.; Scammells, P. J. *J. Med. Chem.* **2014**, *57*, 5405.
- (131) Eaton, P. E.; Carlson, G. R.; Lee, J. T. *J. Org. Chem.* **1973**, *38*, 4071.
- (132) Niedermeier, S.; Singethan, K.; Rohrer, S. G.; Matz, M.; Kossner, M.; Diederich, S.; Maisner, A.; Schmitz, J.; Hiltensperger, G.; Baumann, K.;

- Holzgrabe, U.; Schneider-Schaulies, J. *J. Med. Chem.* **2009**, *52*, 4257.
- (133) Stern, E.; Muccioli, G. G.; Bosier, B.; Hamtiaux, L.; Millet, R.; Poupaert, J. H.; Hénichart, J.-P.; Depreux, P.; Goossens, J.-F.; Lambert, D. M. *J. Med. Chem.* **2007**, *50*, 5471.
- (134) Lager, E.; Andersson, P.; Nilsson, J.; Petersson, I.; Østergaard Nielsen, E.; Nielsen, M.; Sterner, O.; Liljefors, T. *J. Med. Chem.* **2006**, *49*, 2526.
- (135) Billaud, E. M. F.; Maisonia-Besset, A.; Rbah-Vidal, L.; Vidal, A.; Besse, S.; Béquignat, J.-B.; Decombat, C.; Degoul, F.; Audin, L.; Deloye, J.-B.; Dollé, F.; Kuhnast, B.; Madelmont, J.-C.; Tarrit, S.; Galmier, M.-J.; Borel, M.; Auzeloux, P.; Miot-Noirault, E.; Chezal, J.-M. *Eur. J. Med. Chem.* **2015**, *92*, 818.
- (136) Chen, Y.-L.; Zacharias, J.; Vince, R.; Geraghty, R. J.; Wang, Z. *Bioorg. Med. Chem.* **2012**, *20*, 4790.
- (137) El-Essawy, F. A.; El-Sayed, W. A. *J. Heterocycl. Chem.* **2013**, *50*, E1.
- (138) Bodor, N. S. Amino acids containing dihydropyridine ring systems for site-specific delivery of peptides to the brain, US Patent 4888427, 1989.
- (139) Podányi, B.; Keresztúri, G.; Vasvári-Debreczy, L.; Hermeecz, I.; Tóth, G. *Magn. Reson. Chem.* **1996**, *34*, 972.
- (140) López Rivilli, M. J.; Moyano, E. L.; Yranzo, G. I. *Tetrahedron Lett.* **2010**, *51*, 478.
- (141) Peña, D.; Minnaard, A. J.; de Vries, J. G.; Feringa, B. L. *J. Am. Chem. Soc.* **2002**, *124*, 14552.